Oxidative stress induced alterations during aging: Quantifying the metabolic changes associated with aging and oxidative stress

Dissertation
zur Erlangung des Grades
des Doktors der Naturwissenschaften
der Naturwissenschaftlich-Technischen Fakultät
der Universität des Saarlandes

Von

Richa Garg

Saarbrücken

2016

Tag des Kolloquiums:	17.08.2017
Dekan:	Univ.-Prof. Dr. rer. nat. Guido Kickelbick
Berichterstatter:	Prof. Dr. Elmar Heinzle
	Prof. Dr. Rita Bernhardt
Vorsitz:	Prof. Dr. Gerd Kohring
Akad. Mitarbeiter:	Dr.-Ing. Michael Kohlstedt

“Everything is theoretically impossible, until it is done”.

Robert A. Heinlein

“Somewhere, something incredible is waiting to be known.”

Carl Sagan

Acknowledgments

First of all, I would like to express by deepest gratitude to Prof. Elmar Heinzle for offering me the opportunity to work on this project. I would like to thank him for supervising my work and helping me in the analysis of my data. He has been a great advisor and encouragement for me to accomplish my thesis. I would like to thank Dr. Fozia Noor for supervision and helpful advice related to lab work and experimental planning. I would like to acknowledge the financial support from the German Federal Ministry of Education and Research (BMBF). I am grateful to our project partner Pharmacelsus GmbH for performing cell isolation from rats and carrying out CYP enzyme measurements. I am also thankful to our project partner Insilico Biotechnology for providing modeling support. I am very thankful to Prof. Rita Bernhardt for agreeing to review this thesis. I would like to thank my colleagues Inês, Christian, Yeda, Daniel, Malina and Averina for fruitful discussions about my work and providing support in the lab. I want to thank, especially, Michel Fritz for the support and help with different analytics. I would like to thank Dr. Susanne Kohring for general help and for organizing and coordinating the administrative work. I am thankful to the entire Technsiche Biochemie group for numerous discussions and support. I am especially thankful to my friends Inês, Juhi and Mittul for being a constant support during my stay here in Saarbrücken. I have enjoyed a lot our coffee talks and hang outs in the city. Many thanks go to my partner Mayank for his support, encouragement and belief in me. I would like to express my deepest gratitude to my parents who have supported and encouraged me in every step of the way in the last 4 years.

Table of Contents

Abstract……1

1. General introduction – Aging 3

2. Material and Methods 30

3. Establishment of oxidative stress and anti-oxidant conditions 43

4. Separation of differentially aged hepatocytes from Wistar and Sprague Dawley rats based on quantitative analysis of metabolism 50

5. A 2-D monolayer culture to compare metabolic changes associated with aging in primary rat hepatocytes. 62

6. Quantitative characterization of oxidative stress effects on metabolism of differentially aged primary rat hepatocytes 82

7. Quercetin treatment affects metabolite rates in middle age primary rat hepatocytes exposed to oxidative stress 106

8. Summary and future prospects 130

9. Bibliography 136

Supplementary Material……154

Abstract

This thesis focused on investigating the role of oxidative stress on the extracellular metabolic changes during aging in rat hepatocytes. We characterized the metabolic rates of two commonly used strains of experimental rats: Sprague-Dawley (SD) and Wistar. Higher uptake rates of amino acids were observed for SD rat hepatocytes suggesting their hypermetabolic state in comparison to Wistar hepatocytes. Further experiments were performed with SD rat hepatocytes. Old (24 months) and middle (6 months) age hepatocytes showed differences based on their metabolite rates. Hepatocytes from old age rats were more sensitive to *in vitro* culture conditions as seen by their decreased cell viability, CYP activity, increased AST and LDH leakage. The consumption rates of various amino acids were higher for middle age rat hepatocytes indicating faster metabolisation of these amino acids. Old age hepatocytes were observed to be more sensitive towards hydrogen peroxide induced oxidative stress as indicated by higher intracellular ROS, AST and LDH values. The H_2O_2 stressed cells consumed more amino acids than control cells showing increased cellular demands under stress. Lastly, we observed that middle age hepatocytes were more susceptible towards quercetin, an anti-oxidant treatment as seen by the changes in their metabolite profile. Thus, we could identify metabolic changes associated with oxidative stress during aging.

Zusammenfassung

Diese Arbeit beschäftigt sich mit dem Einfluss von oxidativem Stress auf extrazelluläre metabolische Veränderungen bei der Alterung von Rattenhepatocyten. Es wurden metabolische Raten zweier Laborrattenstämme, Sprague-Dawley (SD) und Wistar, charakterisiert. Bei SD Rattenhepatocyten wurden höhere Aminosäure-Aufnahmeraten als bei Wistar Hepatocyten gemessen. Alle weiteren Untersuchungen wurden mit SD Rattenhepatocyten durchgeführt. Es wurden Unterschiede in den metabolischen Raten von Hepatocyten alter (24 Monate) und mittelalter (6 Monate) Ratten beobachtet. Hepatocyten alter Tiere reagierten empfindlicher auf die *in vitro* Kultivierung, was an Hand verringerter Viabilität und CYP Aktivität sowie erhöhter AST und LDH Aktivität zu sehen war. In Zellen mittelalter Ratten wurden einige Aminosäuren schneller verbraucht was eine schnellere Metabolisierung dieser Aminosäuren anzeigt. Hepatocyten alter Tiere reagierten empfindlicher auf oxidativem Stress durch Wasserstoffperoxid (H_2O_2) Behandlung, was anhand erhöhter intrazellulärer ROS, AST und LDH Werte festgestellt wurde. Die H_2O_2 behandelten Zellen zeigten erhöhten Aminosäure-Verbrauch aufgrund der erhöhten zellulären Anforderungen unter Stress. Wie am metabolischen Profil erkennbar, reagierten Zellen mittelalter Ratten empfindlicher auf Quercetinbehandlung. So konnten wir während der Alterung metabolischen Veränderungen im Zusammenhang mit oxidativem Stress.

1. General introduction – Aging

There has been a progressive interest in the underlying mechanism of aging. The basic chemical processes of aging were first explained by Harman in 1954, in his **free radical theory of aging** (Harman, 1956). He integrated the results from electron spin resonance (ESR) study (Commoner et al., 1954), post-Hiroshima studies of radiation damage (Hempelmann and Hoffman, 1953), Fenton's findings (Fenton, 1894), and contemporary theories regarding mechanisms for the oxidation of organic compounds and dismutation of hydrogen peroxide by iron salts (Uri, 1952) to propose that physiological iron and other metals would cause reactive oxygen species (ROS) formation in the cell via Haber–Weiss chemistry as a by-product of normal redox reactions. The ROS would damage nearby cells and tissues and these deleterious changes tend to accumulate with progressing age. He postulated that damage to cellular macromolecules via free radical production in aerobic organisms is a major determinant of life span. He defined aging as the progressive accumulation of diverse deleterious changes in cells and tissues with advancing age that increase the risk of disease and death.

It was later discovered that ROS, some of which are not free radicals, can lead to the accumulation of oxidative damage to cellular constituents. Thus, a more modern version of this tenet is the **"oxidative stress theory"** of aging, which says that increases in ROS accompany aging, leading to functional alterations, pathological conditions, and even death (Hagen, 2005) .

1.1. Theories of Aging

In recent years many other theories related to aging and ROS have been proposed. One such theory is the **"mitochondrial theory of aging"**, which hypothesizes that mitochondria are the critical component in control of aging. It is proposed that electrons leaking from the electron transport chain (ETC) produce ROS and these molecules can then damage ETC components and mitochondrial DNA, leading to further increases in intracellular ROS levels and a decline in mitochondrial function. An increase in mitochondrial damage with age has been shown by various studies (Wallace, 2005; Hagen et al., 2004).

The next theory is the **"cellular senescence theory of aging"** which emphasizes the importance of cellular signal responses to stress and damage (Beauséjour et al., 2003)

Another theory to gain attention is the **"molecular inflammatory theory of aging"**, which postulates the activation of redox sensitive transcriptional factors by age related oxidative stress. This causes the upregulation of pro-inflammatory gene expression. As a result, various pro-inflammatory molecules are generated, leading to inflammation processes in various tissues and organs. This inflammatory cascade is exaggerated during aging and has been linked with many age- associated pathologies, such as cancer, various cardiovascular diseases, arthritis, and several neurodegenerative diseases (Chung et al., 2006).

Several other theories of aging have been proposed in the past years like **"Programmed longevity"** - which defines aging as a result of sequential switching on and off of certain genes (Davidovic et al., 2010), "**Endocrine theory"** – where hormones control the pace of aging (Heemst, 2010), **"Immunological theory"** – which holds that the immune system is programmed to decline over time leading to detrimental age related changes (Cornelius 1972), **"Wear and tear theory"** - Cells and tissues have vital parts that wear out resulting in aging (Rose, 1988), **"Rate of living theory"** – emphasizing the rate of organism's oxygen basal metabolism, leading to shorten its life span (Brys et al., 2007), **"Cross – Linking theory"** – damage to bodily processes due to accumulation of cross-linked proteins (Diggs, 2008), **"Somatic DNA damage theory"** – which stresses the role of continuous DNA damage in aging (Rose, 1988), **"Telomere Shortening theory"** – where telomeres have experimentally been shown to shorten with each successive cell division leading to cell death and progressive decay in the maintenance of organ homeostasis with aging (Campisi, 2000). Aging cannot be accounted by any one of these single theories (Kregel and Zhang, 2007). Despite of years of investigation there is lot of scope left to elucidate the role of ROS in aging mechanisms. The focus of this research has been to study the effect of oxidative stress on aging and metabolic changes on induction of oxidative stress in non-aged and aged hepatocytes from rats. The introduction will focus mainly on the oxidative stress / free radical theory of aging, as this formed the basis of this project work.

1.2. Basics of ROS

Oxygen is the major electron sink in biological systems. Its molecular structure permits the uptake of electrons to form a number of partially reduced oxygen species, known as reactive oxygen species (ROS) such as such as hypochlorite ion, **hydroxyl radical, superoxide anion, hydrogen peroxide** (Dröge, 2002). The most reactive and therefore potentially hazardous, oxygen derived radical is the hydroxyl radical (HO•). ROS such as hydrogen peroxide are often relatively stable. In aerobic organisms, more than 95% of the oxygen is reduced to water through electron transport chain in mitochondria (Riley, 1994). Sometimes there is leakage of electrons, resulting in the formation of superoxide radical (O_2^{-} •) and after addition of a second electron to O_2^{-} at physiologic pH gives rise to hydrogen peroxide (H_2O_2). It is reduced to water (H_2O) by catalase and hydroxyl radical (HO•) by transition metals, particularly iron and copper (Castro and Freeman, 2001).

$$H_2O_2 \xrightarrow{Fe^{II}} HO\bullet + HO\bullet$$
$$H_2O_2 \xrightarrow{\text{Catalase}} H_2O + 1/2\ O_2 \qquad (1)$$

Reaction 1: Cleavage of hydrogen peroxide (H_2O_2) to hydroxyl radical (HO•) catalyzed by iron (Fe^{II}) and to water (H_2O) and molecular oxygen (O_2) via catalase.

1.3. Production of ROS

The source of ROS in cells may be classified as intrinsic or extrinsic.

Intrinsic sources include physiological processes associated with mitochondrial respiration, the metabolism of peroxisomes, the NADPH oxidase system of leucocytes, cytochrome P450 oxidase and the enzymatic synthesis of nitric oxide.

1.3.1. Mitochondrial electron transport chain

In eukaryotic cells, mitochondria are thought to be the largest contributors to intracellular oxidant production. Mitochondria generate ATP in an oxygen-dependent manner, during which the flow of electrons down the respiratory chain eventually culminates at complex IV with the reduction of molecular oxygen to water. Throughout this process, molecular oxygen can also undergo a one-electron reduction to generate a superoxide anion (Holmström and Finkel, 2014; Murphy, 2009). The production of mitochondrial superoxide radicals occurs primarily at two discrete points in the electron transport chain, namely at complex I (NADH

dehydrogenase) and at complex III (ubiquinone–cytochrome *c* reductase). Under normal metabolic conditions, complex III is the main site of ROS production.

With respect to human aging, the Achilles' heel of this elegant system lies in the formation of the free radical semiquinone anion species (Q^{-}•) that occurs as an intermediate in the regeneration of coenzyme Q. Once formed, Q^{-}• can readily and non-enzymatically transfer electrons to molecular oxygen with the subsequent generation of a superoxide radical (Holmström and Finkel, 2014). Thus, this basal metabolism leads to accumulation of ROS and hence oxidative stress with aging. This is also the basis for the "Rate of living theory".

1.3.2. NADPH oxidases.

In addition to mitochondria, another important intracellular source of ROS is the family of NADPH oxidases. This family, now collectively known as NOX enzymes, was first described in the context of neutrophils. Neutrophils are activated by various inflammatory mediators and produce a large amount of ROS as part of their essential role in host defense. In particular, these cells can internalize microorganisms by phagocytosis and then inactivate these microorganisms by a combination of ROS and secreted enzymes within a specialized compartment known as the phagosome (Holmström and Finkel, 2014; Westervelt and Ley, 1999)

1.3.3. Cytochrome P450 oxidase

The membrane-bound microsomal monooxygenase system (MMO) localized in the endoplasmic reticulum (ER) of most animal tissues catalyzes the oxygenation of a wide variety of exogenous and endogenous compounds. It contains cytochromes P450 (CYP), which are heme-thiolate proteins, as the terminal oxidases. The highest content of MMO components is found in liver cells (Zangar et al., 2004).

A significant portion of the activated oxygen is released from the activity of this enzyme. The first branch leading to the production of a ROS is the release of superoxide anion radical due to decay of the oxy-complex of P450. The second ROS-producing branch is the reverse of the peroxide shunt, which is the protonation of the peroxicytochrome P450 with the formation of hydrogen peroxide. Electrons are transferred from NADPH through electron carriers to the P450 for monooxygenation of substrate. Continuous production of ROS during the CYP activity is an inevitable result of NADPH consumption by microsomal P450 both in the presence and in the absence of substrates. Even in the absence of any substrates, the

microsomal electron-transfer chain continues to oxidize NADPH and produce ROS (Zangar et al., 2004).

1.3.4. Peroxisomes

Mammalian peroxisomes play a key role in various metabolic pathways, including fatty acid α- and β-oxidation, ether-phospholipid biosynthesis, glyoxylate metabolism, amino acid catabolism, polyamine oxidation, and the oxidative part of the pentose phosphate pathway (Wanders and Waterham, 2006). Many of the enzymes participating in these pathways generate specific ROS or reactive nitrogen species (RNS) as byproducts of their normal catalytic function (Table 1-1). Peroxisomes in rat liver may be responsible for as much as 20% of the oxygen consumption and 35% of the H_2O_2 production (Boveris et al., 1972)

Table 1-1 Human peroxisomal enzymes that produce ROS/RNS as byproducts of their normal catalytic activity (Fransen et al., 2012)

Name	ROS/RNS	Localization
Acyl-CoA oxidase 1	H_2O_2	PO
Acyl-CoA oxidase 2	H_2O_2	PO
Acyl-CoA oxidase 3	H_2O_2	PO
D-amino acid oxidase	H_2O_2	PO
D-aspartate oxidase	H_2O_2	PO
L-pipecolic acid oxidase	H_2O_2	PO
L-α-hydroxyacid oxidase 1	H_2O_2	PO
L-α-hydroxyacid oxidase 2	H_2O_2	PO
Polyamine oxidase	H_2O_2	PO
Xanthine oxidase	H_2O_2, NO•, $O_2•^-$	PO/C/MT
Inducible nitric oxide synthase	NO•, $O_2•^-$	C/PO

C, cytosol; MT, mitochondria; PO, peroxisomes

1.4. Extrinsic sources of ROS

Besides the ROS generation that occurs naturally in the body, humans are constantly exposed to environmental stimuli in the form of ionizing and UV radiation, smog, tobacco smoke, heat shock, inflammation and certain compounds referred to as redox cycling agents, which include some pesticides, certain medications used for cancer treatment contributing to ROS production. (Ermak and Davies, 2002)

1.5. Oxidative stress and its consequences

Oxidative stress reflects an imbalance between production of ROS and a biological system's inability to readily counteract it. Oxidative stress disturbs the redox balance of the cells. The

burden of ROS production is largely counteracted by an intricate antioxidant defense system that includes the enzymatic scavengers superoxide dismutase (SOD), catalase and glutathione peroxidase. A variety of other non-enzymatic, low molecular mass molecules are important in scavenging ROS. These include ascorbate, pyruvate, flavonoids, carotenoids and perhaps most importantly, glutathione, which is present in millimolar concentrations within cells (Castro and Freeman, 2001). Consequences of this stress include modification to cellular proteins, lipids and DNA.

Different amino acids in protein differ in their sensitivity to interactions with ROS. For example, the amino acids cysteine, methionine, and histidine are especially sensitive to attack and oxidation by the hydroxyl radical. Thus, enzymes in which these amino acids are located at the active site will become inactivated by interaction with ROS. Also, the ROS induced oxidation of proteins can lead to changes in the proteins three dimensional structure as well as to fragmentation, aggregation, or cross–linking of the proteins. Finally, protein oxidation often will make the marked protein more susceptible to degradation by cellular systems responsible for eliminating damaged proteins from the cell (Berlett, 1997).

The polyunsaturated fatty acids present in the membrane phospholipids are particularly sensitive to attack by hydroxyl radicals and other oxidants. A single hydroxyl radical can result in the peroxidation of many polyunsaturated fatty acid molecules because the reactions involved in this process are part of a cyclic chain reaction. In addition to damaging cells by destroying membranes, lipid peroxidation can result in the formation of reactive products that themselves can react with and damage proteins and DNA. The complete degradation (i.e., peroxidation) of lipids is a hallmark of oxidative damage. (Niki et al., 2005)

The highly reactive hydroxyl radical reacts with DNA by addition to double bonds of DNA bases and by abstraction of an H atom from the methyl group of thymine and each of the C-H bonds of 2′-deoxyribose (Barzilai and Yamamoto, 2004). Other ways in which ROS can cause DNA damage include strand breaks, removal of nucleotides, and a variety of modifications of the organic bases of the nucleotides. Although cells have developed repair mechanisms to correct naturally occurring changes in the DNA, additional or excessive changes caused by ROS can lead to permanent changes with potentially detrimental effects for the cell (Wu, 2004).

1.6. Beneficial effects of ROS in cell signaling

We have seen until now the detrimental effects of ROS. But, ROS in small amounts plays an important role in various vital cellular processes, gene regulatory and cell signaling pathways (Schrader and Fahimi, 2006). NO and H_2O_2 are membrane permeable, diffusible molecules, which are less-reactive and longer-lived than OH•, thus being best suited for intra- and even intercellular signaling (Dröge, 2002). They are released by phagocytes as part of the immune defense system (Westervelt and Ley, 1999). Apoptosis is a special form of programmed cell death that plays an indispensable role in the development and homeostasis of multicellular organisms. An increase in cellular ROS production is often observed in apoptotic processes triggered by various stimuli including APO-1/Fas/ CD95 ligands. They also induce cell death through induction of TNF-α in tumor cells (O'Donnell et al., 1995). Controlled changes in the adhesive properties of cells and tissues play an important role in many biological processes. The adherence of leukocytes to endothelial cells is also induced by ROS (Roy et al., 1998). There are various examples of growth factors, cytokines, or other ligands that trigger ROS production in non-phagocytic cells through their corresponding membrane receptors. Such ROS production can mediate a positive feedback effect on signal transduction from these receptors since intracellular signaling is often enhanced by ROS or by a pro-oxidative shift of the intracellular thiol/disulfide redox state. The role of ROS has been demonstrated for nerve growth factor (NGF) signaling in neuronal cells (Suzukawa et al., 2000), for epidermal growth factor (EGF) signaling in human epidermoid carcinoma cells (Bae et al., 1997). ROS plays a role in the regulation of Insulin Receptor Kinase activity. In intact cells high concentrations of hydrogen peroxide in the order of 1 mM induce insulin like effects in the absence of insulin (Hayes and Lockwood, 1987). These effects were found to involve the insulin-independent tyrosine phosphorylation of the insulin receptor β-chain. NF- κB, a ubiquitous transcription factor present in the cytosol of mammalian cells, is typically present as an inactive heterodimer protein. ROS activates NF-κB by causing the release of the inhibitory subunit, via phosphorylation of IκB. Activated NF-κB then migrates into the nucleus, binds to DNA, and activates expression of several target genes encoding cytokines, acute phase proteins, inducible nitric oxide synthase, growth factors, adhesion molecules, and cytokine receptors (Castro et al., 2001). All these positive effects of ROS at physiological concentrations have been summarized in detail in the review of Wulf Dröge (Dröge, 2002). However increase in concentrations of ROS beyond a certain limit leads to cellular damage.

To combat this excessive production of ROS, cells are equipped with various antioxidant defenses. These defenses can be enzymatic or non-enzymatic.

1.7. Anti-oxidant defenses

1.7.1. Enzymatic defenses

Enzymes involved in the elimination of ROS include superoxide dismutases (SODs), catalase, and glutathione peroxidase.

1.7.1.1. Superoxide Dismutase (SOD)

SODs catalyze rapid removal of superoxide radicals via conversion of superoxide to hydrogen peroxide and water (reaction 2). They were originally discovered by McCord & Fridovich in 1969. They are classified based on their metal co-factor namely, copper/zinc (Cu/ZnSOD), manganese (MnSOD) and iron (FeSOD). Experimentally, these three different types can be identified by their differential sensitivities to KCN and H_2O_2. Cu/ZnSOD is characterized as being sensitive to both H_2O_2 and KCN, FeSOD is sensitive to H_2O_2 only, and MnSOD is resistant to both the inhibitors. Eukaryotes contain mainly Cu/ZnSOD (Bowler et al., 1992).

$$O_2\bullet^- + O_2\bullet^- + 2H^+ \rightarrow O_2 + H_2O_2 \qquad (2)$$

Reaction 2: The conversion of superoxide ions to molecular oxygen and peroxide by superoxide dismutase

1.7.1.2. Catalase

Catalase is an iron containing enzyme found primarily in peroxisomes. It serves to detoxify hydrogen peroxide and various other molecules. One way that catalase eliminates hydrogen peroxide is by catalyzing a reaction between two hydrogen peroxide molecules, resulting in the formation of water and O_2. In addition, it promotes the interaction of hydrogen peroxide with compounds that can serve as hydrogen donors so that the hydrogen peroxide can be converted to one molecule of water, and the reduced donor becomes oxidized (a process sometimes called the peroxidatic activity of catalase). This enzyme contains a heme in its active site responsible for its catalytic activity (Michiels et al., 1994). Overexpression of catalase in cytosolic or mitochondrial compartments protects HepG2 cells against oxidative injury (Bai et al., 1999)

$$2H_2O_2 \rightarrow 2H_2O + O_2 \qquad (3)$$

Reaction 3: Breakdown of two hydrogen peroxide molecules into water and oxygen by catalase

1.7.1.3. Glutathione peroxidase (Gpx)

Glutathione peroxidase (80 kDa) is a selenoprotein (Se - Gpx). It is a tetrameric enzyme with four identical subunits of around 22 kDa, each of them containing one atom of selenium as a selenocysteine involved in the catalytic activity (Michiels et al., 1994). It causes the reduction of hydroperoxides using GSH, protecting mammalian cells against oxidative damage. In fact, glutathione metabolism is one of the most essential anti-oxidative defense mechanisms (Rikans and Hornbrook, 1997)

$$ROOH + 2GSH \rightarrow ROH + GSSG + H_2O \quad (4)$$

Reaction 4: Reduction of lipid hydroperoxides to their corresponding alcohols along with oxidation of glutathione (GSH) to glutathione disulfide (GSSG) by glutathione peroxidase.

There are five Gpx isoenzymes found in mammals. Although their expression is ubiquitous, the levels of each isoform vary depending on the tissue type (Matés et al., 1999)

1.7.2. Non enzymatic anti-oxidant defenses

GSH is one of the most important non-enzymatic anti-oxidants found in cells. It is a ubiquitous tripeptide, γ-glutamylcysteinyl glycine, found in most plants, microorganisms, and all mammalian tissues. Glutathione exists in the thiol reduced (GSH) and disulfide-oxidized (GSSG) forms (Hwang et al., 1992). Eukaryotic cells have three major reservoirs of GSH. Almost 90% of cellular GSH are in the cytosol, 10% in the mitochondria, and a small percentage in the endoplasmic reticulum. Cytosolic GSH in the rat liver turns over rapidly with a half-life of 2 - 3 hours. (DeLeve and Kaplowitz, 1991)

The endogenously produced hydrogen peroxide is reduced by GSH in the presence of selenium-dependent GSH peroxidase **(**Figure 1-1**).** As a result, GSH is oxidized to GSSG, which in turn is reduced back to GSH by GSSG reductase at the expense of NADPH, forming a redox cycle (Lu, 1999).

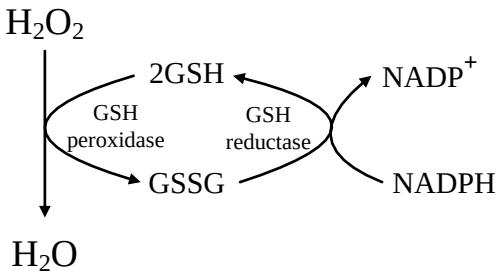

Figure 1-1 Hydrogen peroxide generated as a result of aerobic metabolism, is metabolized by GSH in the presence of GSH peroxidase in cytosol. To maintain the cellular redox equilibrium, GSSG is reduced back to GSH by GSSG reductase at the expense of NADPH, thereby forming a redox cycle.

GSH is synthesized from precursor amino acids in the cytosol of virtually all cells (DeLeve and Kaplowitz, 1991). The synthesis of GSH from its constituent amino acids, L-glutamate, L-cysteine, and L-glycine, involves two ATP-requiring enzymatic steps:

L-glutamate + L-cysteine + ATP → γ-glutamyl-L-cysteine + ADP + Pi (1)

γ-glutamyl-L-cysteine + L-glycine + ATP → GSH + ADP + Pi (2)

The first step of GSH biosynthesis is rate-limiting and catalyzed by γ-glutamylcysteine synthetase (GCS), which exhibits an absolute requirement for either Mg^{2+} or Mn^{2+}. The second step in the synthesis of GSH is catalyzed by GSH synthetase (Lu, 1999). The GSH pool is tightly linked to glucose metabolism through the pentose phosphate pathway (PPP), as this pathway generates the NADPH that is necessary to maintain GSH in a reduced form (Holmström and Finkel, 2014).

Liver has one of the highest organ contents of GSH. It is unique in two aspects of GSH synthesis. Firstly, hepatocytes have the unique ability to convert methionine to cysteine through the transsulfuration pathway. Secondly, the rate of GSH biosynthesis in the hepatocyte is balanced by its rate of export into plasma, bile, and mitochondria via distinct GSH transport systems. The mitochondrial GSH transporter maintains the GSH pool in the mitochondria which cannot biosynthesize GSH. It is selectively impaired in rats fed alcohol or under oxidative stress (Lu et al., 1996).

There are many other nonenzymatic antioxidants present in the cells, most prominent being vitamin E (α–tocopherol) and vitamin C (ascorbate). Vitamin E is a major antioxidant found in the lipid phase of membranes and acts as a powerful terminator of lipid peroxidation.

During this process vitamin E radical is formed, from which vitamin E can be regenerated in a reaction involving GSH and ascorbate. (Wu, 2004)

1.8. Role of oxidative stress in aging

Aging is a physiologic state in which a progressive decline of organ functions is accompanied with the development of age-related diseases. Since the free radical theory of aging was proposed by D Haman in 1956, a lot of research has been done in support of this theory where increase in oxidative damage on various cellular macromolecules with age has been shown. In this section, the past research in this area is reviewed.

1.8.1. DNA, Protein and Lipid oxidation

As explained in the previous section, excessive ROS production leads to lipid, protein and DNA damage. First studies describing the increase of isoprostane levels, a product of lipid peroxidation, in blood of old Sprague-Dawley rats were published in 2001 (Roberts and Reckelhoff, 2001). After that other studies were made to show age related increase in F2-isoprostane levels in the blood and other tissues (e.g., liver and kidney) of male F344 rats (Bokov et al., 2004). Most important form of protein oxidation, carbonylation was shown to be increased after 60 years of age in cultured human fibroblasts, aged rat liver and human lens (Oliver et al., 1987). Stadtman *et al*. proposed the role of protein oxidation in the development of various diseases during the aging process (Stadtman et al., 1992). The carbonyl content was also reportedly increased with age in rhesus monkey (Zainal et al., 2000). Goswami *et al*. (Goswami et al., 2006) proposed the role of oxidative stress-mediated protein aggregation in the neuronal death in several forms of aging-related neurodegenerative diseases. DNA damage due to accumulation of ROS with aging was first published in 1990's. 8-oxo-2-deoxyguanosine (oxo8dG) is the oxidative by-product of DNA damage (Richter et al., 1988). Ames laboratory reported approx. 2 fold increase in oxo8dG levels in the nDNA isolated from liver, kidney and intestine of male rats between 2 and 24 months. They also observed its level increased in mtDNA in liver from aged rats (Ames et al., 1993). Since then various studies have been made to demonstrate that the oxo8dG lesion increases significantly with age in nDNA in all the major tissues of rats and mice (Bokov et al., 2004). These studies show evidence of increasing cellular damage during aging by accumulating reactive oxygen species.

1.8.2. Apoptosis

Apoptosis or programmed cell death is executed via two major signaling pathways, the intrinsic and extrinsic pathways, in either caspase-dependent or caspase-independent manners. ROS and ROS-modulated molecules participate in both intrinsic and extrinsic apoptotic pathways (Matsuzawa and Ichijo, 2005). Age associated increases in apoptosis have been observed in several physiological systems, including the human immune system, human hair follicle, and rat skeletal muscle (Aggarwal and Gupta, 1999).

1.8.3. Autophagy

Autophagy is a housekeeping system for cells and a major pathway for the degradation and recycling of damaged cellular components to ensure cell survival under stress conditions, such as nutrition deprivation (Mortimore and Pösö 1987). Reports have shown excessive activation of autophagy leading to cell death in neurons, suggesting their role in aging-related neurodegenerative diseases (Fortun et al., 2006). The regulation of autophagy is not yet completely understood. Although there is evidence suggesting that aging related increases in ROS production can result in elevated oxidative damage to proteins, including lysosomal proteins and proteins in autophagic pathways (Butler and Bahr, 2006).

1.8.4. Cellular senescence

Senescence or irreversible growth arrest was first observed in cultured primary cells that ceased proliferation after a finite number of divisions (Toussaint et al., 2002). There are many evidences in the literature showing the role of oxidative stress leading to arrest in cell growth. Two tumor suppressor proteins that are involved in cell cycle regulation, p53 and Rb protein, play central roles in the molecular mechanisms of cellular senescence. Evidence has shown that both p53 and Rb protein are activated when cells are in a senescent state, while inactivation of these two proteins prevents senescence of human lung fibroblasts (Kulju and Lehman, 1995) and allows senescent cells to resume proliferation (Gire et al., 1998). Telomere shortening, acting through a pathway involving p53, is one of the well documented triggers for cellular senescence. ROS can cause DNA damage and also accelerate telomere shortening (Bar-Or et al., 2001). A recent study indicated telomere shortening is exponentially increased with age in skin fibroblasts of primates (Herbig et al., 2006). Exogenous treatment with hydrogen peroxide or inhibition of antioxidant enzymes initiates premature senescence in human fibroblasts (Blander et al., 2003). Senescence is routinely observed in cells grown in a high ambient oxygen concentration, while the proliferation life span of cells is extended when they were grown under physiologically relevant low oxygen tension (Chen et al., 1995).

Therefore, developing a better understanding of the molecular mechanisms of cellular senescence may provide some insight into the biology of aging and potential sites for therapeutic interventions (Kregel and Zhang, 2007).

1.9. Alteration in cellular stress response pathways due to aging

Various researches suggest that longevity depends on the ability of the organism to cope with extrinsic or intrinsic stressors (Kirkwood and Austad, 2000). Compromised stress responses are linked to the onset of many age-related diseases. Stress is broadly defined as a noxious factor either physical, chemical or biological, which triggers a series of cellular and systemic events, resulting in restoration of cellular and organismal homeostasis. To cope with conditions of stress, organisms have developed a wide range of sophisticated stress response mechanisms, acting at the cellular or organelle-specific level. Exposure to mild stress activates cellular homeodynamic mechanisms, without mounting a comprehensive stress response, which better prepares the organism against stronger insults and promotes long-term survival. This phenomenon is known as hormesis (Rattan, 2008). In this section various cellular stress response pathways activated during aging are briefly overviewed.

1.9.1. Heat shock response

Heat, oxidative and osmotic stress, heavy metals and proteasome inhibitors induce a highly conserved, programmed gene expression leading to selective transcription and translation of heat shock proteins (HSPs) (Morimoto, 2008). They are regulated by a set of heat shock transcription factors (HSFs). The mammalian HSF family consists of four members of HSF (HSF1-4). Activation of heat shock response is a complex process that involves trimerization and translocation of HSF1 to the nucleus, where it binds to heat shock elements within the promoters of heat shock genes. HSF1 undergoes multiple post-translational regulatory modifications such as phosphorylation, sumoylation and acetylation (Kourtis and Tavernarakis, 2011). Aging is associated with elevated expression of HSP genes, in the absence of other external stressors suggesting that aging generates intrinsic stress signals leading to altered gene expression (Muller et al., 2007). The effectiveness of heat shock response following acute extrinsic stress deteriorates with age. This is due to signaling defects leading to HSF1 activation (Heydari et al., 2000). While detailed analysis of the heat shock response pathway steps affected by aging is still incomplete, it is becoming clear that protein aggregation leading to HSF inactivation is characterized by age-dependent progression (Kourtis and Tavernarakis, 2011).

1.9.2. Ubiquitin-proteasome system (UPS)

UPS is the main proteolytic mechanism, responsible for the degradation of damaged proteins and the turnover of most cytosolic and nuclear proteins. This process is very important to maintain the protein turnover in cells. The process of protein degradation by the UPS involves two steps: tagging of the protein with a polyubiquitin chain and the degradation of the tagged protein by the proteasome (Ciechanover, 2005). Aging is accompanied by accumulation of damaged and modified proteins due to deterioration of cellular quality control mechanisms. The role of increasing oxidative stress with ageing has been already emphasized in the previous section. In the presence of moderate oxidant concentrations, proteasomal degradation increases, whereas higher oxidation levels lead to proteolytic inhibition (Ding et al., 2006). Decline in proteasome activity with age has been observed in many tissues as reviewed by Conconi *et al*. (Conconi et al., 1996).

1.9.3. Insulin/IGF1 signaling and mTOR pathway

The best characterized metabolic pathways leading to aging are the insulin-like growth factor (IGF-1) signaling pathway and the mammalian target of rapamycin (mTOR) pathway. The insulin/IGF-1 signaling pathway plays an essential role in the regulation of various cellular activities such as lipid and carbohydrate metabolism, gene expression, cell differentiation, growth and survival. It is highly conserved across species and is best characterized to study the longevity of species (Kenyon, 2010). Suppressing the insulin/IGF-1 signaling pathway has been shown to increase lifespan and delay aging process in species ranging from *C. elegans* (Wolkow et al. 2000), yeast (Fabrizio et al. 2001) to rodents (Holzenberger et al. 2003). One possible mechanism by which reducing the signaling through this pathway increases life span is through alterations in cell proliferation and apoptosis, which would decrease the incidence of cancer in animals (Hursting et al., 2003). Additionally, reducing insulin/IGF-1 signaling may alter the sensitivity of the animals to oxidative stress and reducing the accumulation of oxidative damage (Richardson et al., 2004). Inhibition of TOR leads to inhibition of proliferation in mammalian cells and other immunosuppressive properties. In the presence of nutrients and growth stimuli the activity of TOR is upregulated stimulating growth. Under nutrient limiting conditions TOR is downregulated and further downregulates general protein synthesis, upregulates macroautophagy and activates several stress-responsive transcription factors. These mechanisms have been extensively reviewed (Wullschleger et al., 2006). Partial inhibition of TOR function in yeast, worms, and flies have been shown to significantly increase the life span of these organisms, possibly by mimicking calorie restriction (reviewed

in Martin et al., 2004). There is a lot of work going on to study the detailed mechanisms behind the role of these pathways in aging.

1.10. Summarizing role of oxidative stress in aging

As noted in preceding sections, aging is linked to an increase in ROS generation and oxidative damage. In addition, many types of stressors, such as hyperthermia (Zhang et al., 2003) and hypoxia (Blomgren and Hagberg, 2006), have been associated with an increased production of prooxidants and induction of oxidative stress. For instance, repeated heat challenge produced extensive injury in the liver of older rats, whereas young rats tolerate the stress very well. In the old cohort, this injury pattern was associated with increases in steady-state levels of ROS and substantial oxidative damage to hepatocellular macromolecules (e.g., lipids, DNA), along with alterations in intracellular redox status and aberrant activation of stress-response transcription factors (Zhang et al., 2003). These data demonstrate that young animals can more effectively cope with oxidative stress in response to environmental challenge. In contrast, in older animals, a decline in cellular redox potential, along with exaggerated ROS generation, lead to extensive oxidative damage and alterations in intracellular signal transduction. One possible integrative scenario by which ROS and oxidative stress could contribute to aging is proposed in Figure 1-2. As illustrated in this figure, the aging process involves multifaceted changes that are affected by both exogenous conditions and endogenous factors at molecular, cellular, tissue, organ, and systemic levels. Aging effects are revealed first at molecular levels and include the accumulation of macromolecular damage and changes in signal transduction pathways. These alterations subsequently impact on cellular responses, such as organelle dysfunction, inflammation, cell proliferation, survival, and death. Eventually, dysfunction is manifested at systemic levels, which would likely include a decline in organ function, reduced stress tolerance, frailty, increased incidence of diseases, and death that are hallmarks of aging (Kregel and Zhang, 2007). Developing a clearer understanding of the underlying mechanisms of aging would help to understand age related diseases and improving quality of life.

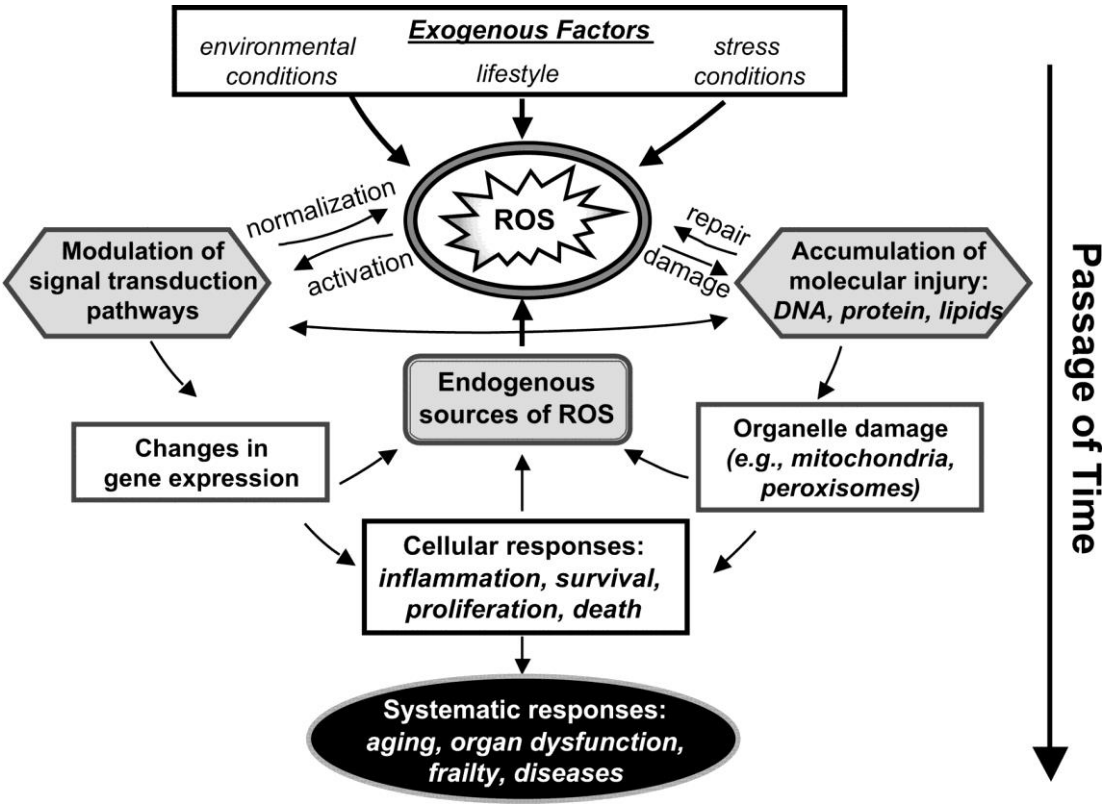

Figure 1-2 A schematic summary of proposed mechanisms by which ROS and oxidative stress could contribute to the process of aging (Kregel and Zhang, 2007).

1.11. Metabolism studies associated with aging

As reviewed in above section, aging encompasses a variety of bodily changes. Theories have been proposed to explain aging through telomere shortening, mitochondrial dysfunction, accumulation of oxidative stress, uncontrolled inflammation, and hormone dysregulation. Not one but a combination of these mechanisms is needed to explain the complex phenomenon of aging. Thus, researchers have now looked toward systems biology approaches to study causes and consequences of aging at genome, transcriptome, proteome and metabolome levels (Hood et al., 2004). This helps us to understand the complex interactions between these components to get a complete picture of the network behavior. Studies in genomics, transcriptomics and proteomics can explain the changes happening at gene and protein level. However, metabolome is the furthest down the line from gene to function and is most characteristic of the entire physiological state (Figure 1-3). Therefore, changes in the metabolome provide the most important representation of the characteristic decline in body functions with age (Soltow et al., 2010).

There are several biological databases like KEGG, Metabolights, Reactome etc. detailing the complete metabolic networks dealing with genome, biological pathways specific to the organelle and the organism.

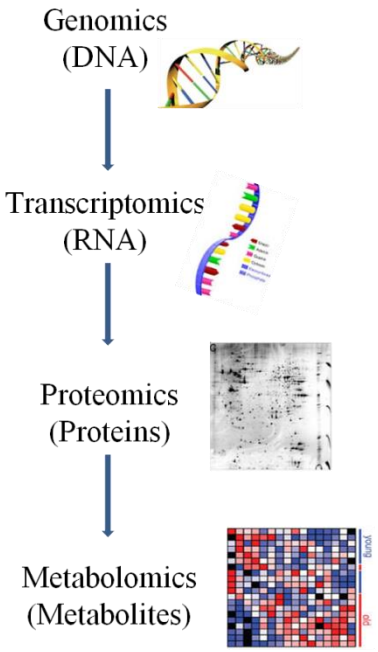

Figure 1-3 The central dogma of life studied with "-omics" technologies

Metabolomics aims at identifying simultaneously numerous low-molecular weight compounds called metabolites from biological samples like blood, plasma, urine etc. Metabolites such as amino acids, lipids, organic acids, peptides etc. represent intermediate and end products of metabolic pathways that rapidly reflect physiological dysfunctions and may mirror early stages of a pathological process (Valde, 2013). The level of metabolites is determined by the concentration of enzymes and regulatory processes inside the cells such as the regulation of transcription, translation and protein-protein interactions. Network reconstruction based on metabolomic data would provide a structured framework to systematically integrate and analyze datasets which would represent the molecular phenotype of a cell or organism in response to the genetic or environmental factors (Mo et al., 2009). This network can be converted into a predictive model that enables *in silico* simulations of allowable network states in order to analyze network metabolic capabilities under different environmental and genetic conditions (Becker et al., 2007).

First step in metabolomics is sampling of metabolites. Metabolites can be extracellular or intracellular depending on the method of collection (Figure 1-4).

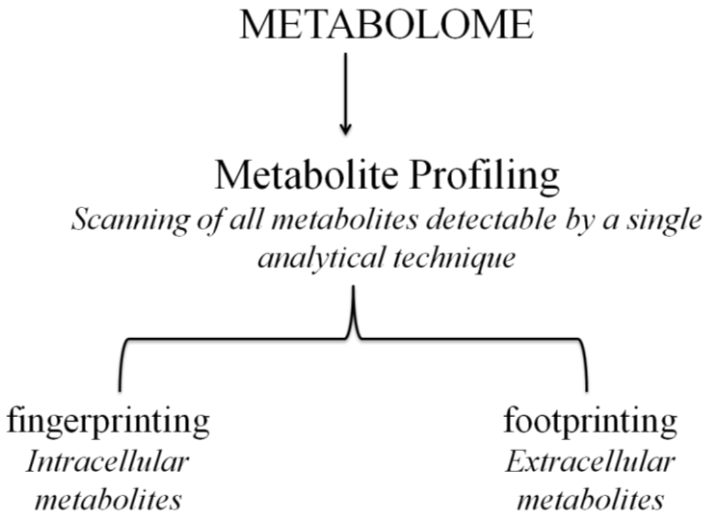

Figure 1-4 Metabolome analysis (adapted from Villas-Boas et al., 2007)

Intracellular metabolites (metabolic fingerprinting), are extracted from cells or tissues. Cell membrane is made permeable to an extracting agent, such as an organic solvent, or through freeze-thaw cycles thus releasing intracellular metabolites. Thus a broad range of polar metabolites are extracted, while maintaining the samples at low temperature to avoid chemical degradation of heat sensitive metabolites.

The analysis of the extracellular metabolites (metabolic footprinting) is achieved by profiling the level of metabolites secreted into the extracellular culture medium by cells without disrupting the cells. Every metabolite detected in the medium is either a compound secreted by the cell or part of the initial medium composition. Thus, using this technique production and consumption of specific metabolites can be easily determined, which reflects the internal metabolic state of the cells and its composition varies in response to genetic or experimental perturbations due to changes in intracellular pathway activities involved in the production and utilization of extracellular metabolites (Kell et al., 2005). Extracellular metabolites can be collected from *in vitro* cell culture or directly from animals *(in vivo)* analyzing their urine, plasma or blood.

Detection of hundreds of metabolites simultaneously has been made possible through development of many modern analytical platforms like GC (gas-chromatography), HPLC

(high performance liquid chromatography), mass spectrometry and NMR (nuclear magnetic resonance). However, no single analytic platform can be applied to detect all metabolites in samples owing to the complexity of metabolome. The combined use of these techniques has led to major advancements in this field (Zhang et al., 2012).

Once metabolic composition is determined, data reduction techniques can be used to elucidate patterns and connections. In many studies, like evaluating drug-toxicity and some disease models, the metabolites of interest are not known *a priori*. Thus, methods with no prior assumptions are the most favored choice for data evaluation. The most common of these methods includes principal component analysis (PCA) which can efficiently reduce the dimensions of a dataset to a few which explain the greatest variation (Nicholson and Wilson, 2003). Another method to determine metabolite changes due to culture conditions is through calculation of specific rates for each metabolite over time. These could also be used for PCA to determine patterns in data reflecting metabolite changes in response to experimental perturbations.

The next step followed by determination of metabolite rates is metabolic flux analysis. Variations in metabolic fluxes can provide insight into the intracellular pathway activities related to metabolite secretion. The result is a flux map that shows the distribution of anabolic and catabolic fluxes over the metabolic network. Based on such a flux map or a comparison of different flux maps, system-wide cellular physiology can be analyzed, and consequently metabolic engineering strategies at a systems-level can be designed for manipulation of cellular pathways. Figure 1-5 details the process of metabolism analysis through integration of metabolic data.

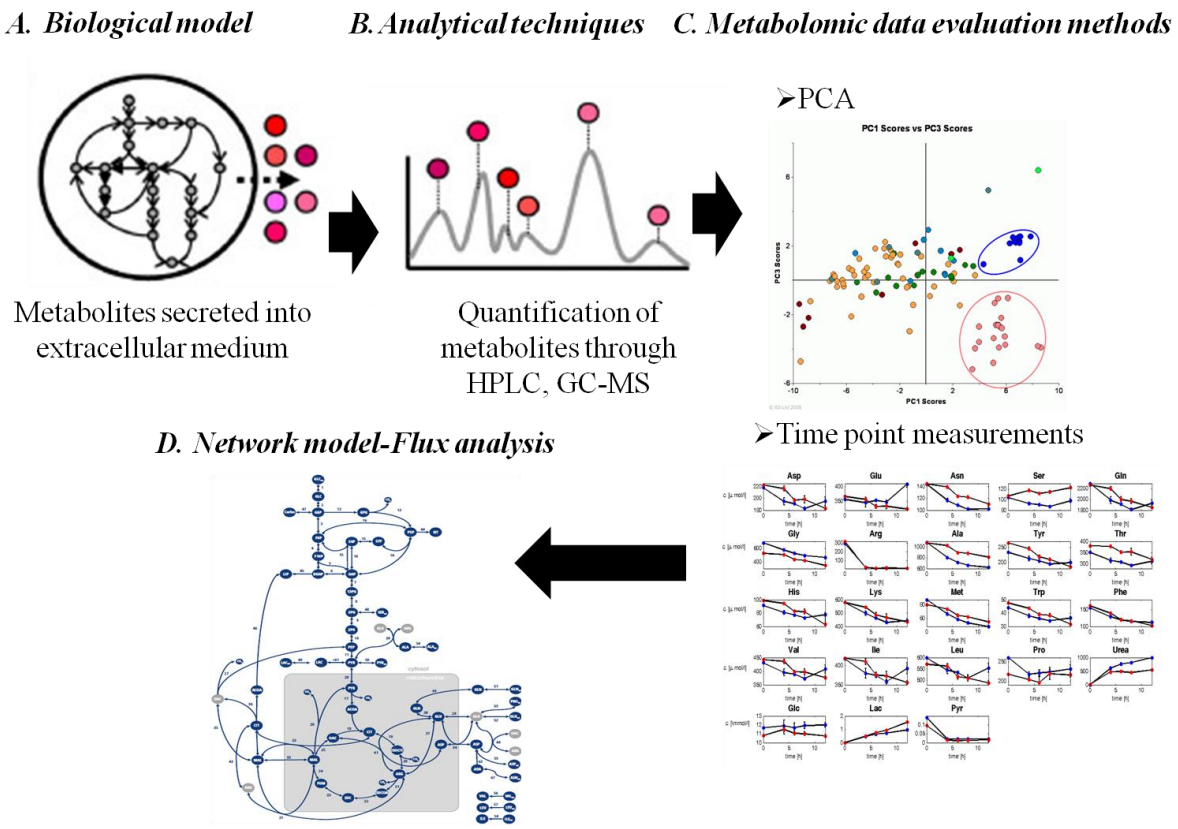

Figure 1-5 Schematic workflow of metabolome analysis through integration of extracellular metabolite data (A) Extracellular metabolite secreted into medium from cultured cells are (B) Metabolites are detected and quantified through various analytical techniques like HPLC; GC-MS (C) Metabolomic data is evaluated through statistical data techniques like PCA and determination of metabolite rates over time (D) Integration of metabolite data to determine intracellular metabolite fluxes to reveal a intracellular flux map (adapted from Mo et al., 2009).

1.12. *In vivo* models for aging studies

1.12.1. Humans

A large scale metabolomic study was carried out to screen 280 metabolites in 6000 individuals aged between 17 and 85 to determine the metabolomic markers of aging. C-glycosyl tryptophan (C-glytr) was particularly interesting in this study, as this modified amino acid showed marked difference in blood samples from young and old age groups. However, this metabolite was higher among donors with high blood pressure, low bone mass, and low lung function. More studies are however required related to understand the mechanism of action of this metabolite (Valde, 2013).

A large scale study based on metabolomics in humans was carried out by Berger *et al*., (Berger et al., 2007). They evaluated the effects of aging on 270 human subjects through analysis of 432 compounds in the plasma metabolome. They found that age affected the level of almost 100 metabolites measured via mass spectrometry. They observed increased TCA intermediates, creatine, essential/non-essential amino acids, urea, ornithine and polyamines with increased age. Compounds related to fat metabolism, including fatty acids, carnitine, betahydroxybutyrate, cholesterol and glycocholate, were higher in persons of 51–65 years. Dehydroepiandrosterone (DHEA, a proposed anti-aging androgen) levels were lower in this older age group; whereas markers of oxidative stress including oxoproline, hippurate and 3, 4-dihydroxybenzoate were higher. Xenobiotics (e.g. caffeine) were increased in older subjects, which may be related to P450 metabolism (Berger et al., 2007)

These findings indicate that aging clearly controls alterations in human metabolic pathways, and underline the potential of MS-based metabolomic techniques to detect a large number of age-perturbed metabolites in humans.

1.12.2. Rodents

Various studies in rats have been done to identify different age related metabolites. These studies have been done in plasma or urine of rats. William *et al*. (Williams et al., 2005) used HPLC-TOF-MS to look at the effects of age on the profile of metabolites in the urine of male Wistar rats. Samples were collected every 2 weeks from 4 to 20 weeks of age. Significant differences were seen in the data between 4 weeks, 6 weeks and rest of the age groups. While the majority of the metabolites contributing to the clustering (based on PLS loading weights) were not identified, at least one metabolite which increased across all age groups was identified as carnitine, pointing to perturbations in lipid metabolism with increased age.

Schnackenberg *et al*. (Schnackenberg et al., 2007) investigated age-related changes in the urinary metabolic profile of Sprague – Dawley rats. The authors were able to distinguish 25-day, 40-day, and 80-day-old rats. They identified hippuric acid, a kynurenic acid salt, ferulic acid sulfate, and suberic acid as metabolites that increased with advancing age. It was also noted that the concentrations of several Krebs cycle intermediates including fumarate, oxaloacetate and trans-aconitate as well as acetate and pyruvate were decreased in the aged rats, possibly indicating alterations in mitochondrial activity.

Lu *et al*. (Lu et al., 2008) studied metabolites in the blood plasma of spontaneously hypertensive rats. The concentrations of several fatty acids, including linoleic acid, oleic acid, and hexadecanoic acid, were observed to increase with age (10 – 18 weeks) in the spontaneously hypertensive rats, and decrease in the control rats pointing to changes in lipid metabolism with age.

Another study relevant to studying the identification of metabolites in aging and thereby determining the biomarkers of aging was carried out by Houtkooper *et al*. (Houtkooper et al. 2011b). They showed impaired mitochondrial function, changes in the insulin and mTOR signaling pathways with age through measurement of various metabolites in signaling, enzymes and genes. They measured various amino acid and fatty acid metabolites in blood and plasma from liver and muscle in a bid to identify biomarkers of aging. In both liver and muscle, increased breakdown of glycogen, increased lactate and reduced glycolysis intermediates were seen. This suggested altered glycogen and glucose metabolism in aged mice. They also studied the effect of aging on fatty acid metabolism. An increased flux in fatty acid oxidation pathway was reported due to the presence of high amount of free fatty acids in aged mice.

Collectively, these studies show that MS-based metabolomics can be used to detect overall age related changes in the metabolome of rodents. Various other studies related to aging in *C. elegans*, *D. melanogaster*, dogs have been reviewed by Mishur *et al*. (Mishur and Rea, 2012). These studies show the importance of metabolomics in studying molecular and metabolic changes associated with aging. It is expected that in the near future it will become possible to tell from an individual's "metabolomic profile" the extent of their biological aging. Continued research in this area will help in disease prevention and treatment for age-related diseases (Ana, 2013).

In vivo research in humans is expensive and difficult to perform accurately. Extracellular metabolites are usually measured in blood or urine. Liver samples (tissue or cells) for aging studies from differently aged groups are hard to obtain. For reproducible datasets, large numbers of samples are required which may not be available due to ethical and cost constraints. As described above, metabolites in rats have been mostly measured in blood, plasma or urine. Intracellular studies have been done with liver tissue extracts. This involves killing of the whole rat which increases the overall cost of the studies as higher number of rats are needed to carry out experiments. *In vitro* culture of hepatocytes has evolved to be the most

direct way to study liver function to test novel drug candidates. Figure 1-6 summarizes the various *in vitro* and *in vivo* methods for metabolomic analysis.

1.12.3. *In vitro* cell culture model – primary rat hepatocytes

Fresh primary hepatocytes are considered the gold standard for studying liver function and drug metabolism *in vitro*. Freshly isolated hepatocytes can express most of the functions of the intact liver like phase I metabolizing enzyme cytochrome - P450 (CYP) and transport proteins organized in a physiologically relevant context and regulated via cellular processes that occur within the liver *in vivo* (e.g., nuclear hormone-mediated xenosensors). An appropriate *in vitro* model has many advantages such as the reduction of animal assays, saving time when evaluating new drug candidates or the development of safer drugs. Due to these advantages freshly isolated rat hepatocytes cultured as 2-D monolayer were used for the experiments. They were cultured on collagen prepared from rat tail tendons. The use of collagen as an extracellular matrix (ECM) and affinity of PRH to collagen has been shown in various studies (Bissell et al., 1986).

Primary hepatocytes do not proliferate *in vitro* and therefore need to be freshly isolated for each experiment. Rats are a very common source of primary hepatocytes, with 100 to 400 million cells routinely isolated from each animal liver with more than 70% viability. There has been considerable improvement in the past years in the process of hepatocyte isolations. The first technique for large-scale preparation of isolated hepatocytes was described in 1953 and involved perfusion of rat liver under pressure with a Ca^{2+} free solution containing a chelating agent. Various modifications of this technique were used in the next decades. The successful preparation of intact isolated hepatocytes by collagenase treatment of liver was achieved in 1967, followed by the development of two-step enzymatic digestion technique established by Seglen (Seglen, 1976) This process allowed for the isolation of relatively pure population of cells with high viability. Since then, it has been widely used with slight modifications for isolation of primary hepatocytes (Berry et al., 1997).

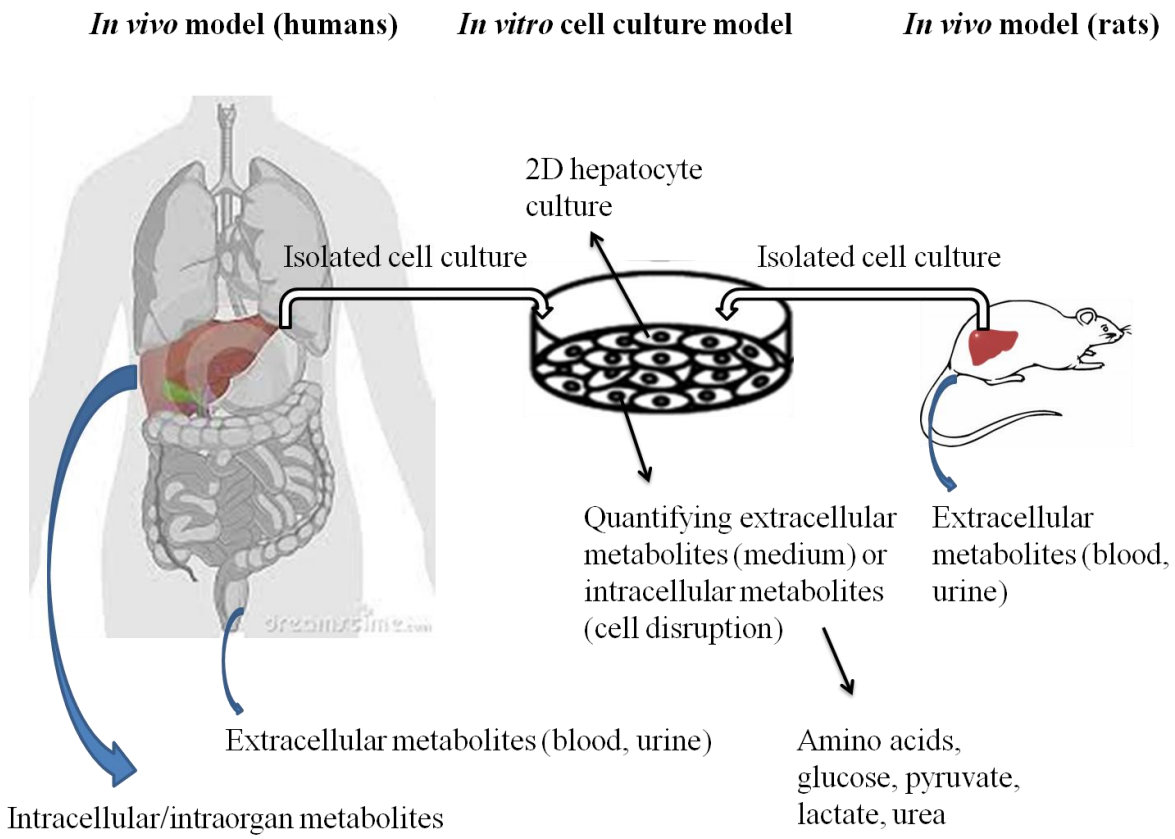

Figure 1-6 *In vivo* and *in vitro* methods for aging studies. Extracellular metabolites are measured in blood or urine from humans or rodents. Intracellular metabolites can be measured *in vivo* in liver tissue. 2D cell culture involves isolation of hepatocytes from liver tissues and quantification of extra or intracellular metabolites in medium or through cell disruption respectively.

1.13. Liver as a model for aging

Liver is a vital organ in our body responsible for many functions like carbohydrate metabolism, glucose homeostasis, drug metabolism through cytochrome P450 enzyme, protein and fatty acid metabolism, synthesis and degradation of amino acids as well as bile secretion. This is also the organ in our body with the highest ability to regenerate. Hepatocytes make up to 60% of the total liver cells. Other cell types present in the liver are Kupffer, stellate and sinusoidal endothelial cells (Malarkey et al., 2005).

The percentage of deaths due to liver disease increases dramatically in humans beyond the age of 45 years. According to the statistics from the United States Department of Health, liver diseases cause a substantial loss in potential lifespan prior to 75 years of age. It has been reviewed extensively in literature that elderly are more prone to liver diseases (Schmucker, 2005). Hence, comes the natural question as to how is liver affected during aging. Due to

aging, liver shows many morphological and physiological changes. These changes have been extensively studied and reviewed (Schmucker, 1998; Schmucker, 2005; Stell et al., 2003)

There is a decrease in the size and mass of liver with senescence in humans and rodents (Wynne et al., 1989). There is reduced hepatic blood flow, increase in the number of dense bodies such as secondary lysosomes, residual bodies, lipofuscin in rodents and human hepatocytes (Schmucker, 1998). Aging in liver in humans is associated with larger hepatocyte size, increase in polyploidy and binuclear index. Increase in nuclear ploidy was also seen in rodent livers (Carriere, 1967). Aging in rodents and humans is also associated with an increase in individual mitochondria volume and a decline in their number. Aging also makes liver mitochondria more susceptible to injury and leads to its impaired function. Mitochondrial membrane potential is also impaired with age which could affect mitochondrial protein synthesis (Sastre et al., 1996). There is a loss of cytochrome P450 enzymes with age as seen in rats and humans affecting phase I of drug metabolism. This was due to the decline in the cytochrome P450 microsomal monooxygenase enzyme system (MMO). These changes were more significant in males in comparison to females (Disposition and Woodhouse, 1992). The rate of liver regeneration, rather than the regenerative capacity, is diminished in the elderly. Aged livers regenerate but they take longer than the younger ones**.** There is inhibition of hepatocyte proliferation and cell cycle genes with age (Schmucker and Sanchez, 2011). There is also evidence of telomere shortening with age which may compromise hepatic regeneration (Schmucker, 2005). Many liver functions such as hepatic enzymes AST, LDH, HDL cholesterol, bilirubin are maintained in the elderly. Although, bile acid synthesis is reduced with age (Schmucker, 1998).

Zhang *et al*. compared the anti-oxidative capacity of hepatocytes from old and young rats through heating rats *in vivo* (Zhang et al., 2003). Old rats showed extensive hepatic injury with 24 h of heat stress in comparison to younger ones. Thus, it was concluded that old age rats have less effective protection against oxidative injury in comparison to younger rats. It was indeed shown through various studies that hepatic antioxidant defenses decrease with age. Aged rat liver shows higher production of ROS and is more sensitive to oxidative stress injury then younger rat hepatocytes (Bejma et al., 2000). Frith *et al*. (Frith et al., 2009) showed that aged liver had decreased superoxide dismutase levels. There are also various studies showing age dependent decline in the induction of heat-shock response or stress proteins following injury (as reviewed in Chapter 6).

Thus, aging in liver is associated with many changes at physiological levels. It is also sensitive to oxidative stress injury. This is the reason for taking liver as a model for this project.

1.14. Aims and outline of the thesis

The work of this thesis was part of the BMBF funded "OXISYS" project - the role of oxidative injury in aging and its therapeutic implications. This project aimed to study the metabolic changes associated with aging and oxidative stress in a 2-D monolayer culture of hepatocytes isolated from 6 (middle age) and 24 months (old age) old rats. When the project was started there was already a lot of work done in describing age associated processes and the cellular pathways altered during aging. Changes in liver due to aging had been studied in isolated liver perfusion models or in *in vivo* studies (Mishur and Rea, 2012; Nevedomskaya et al., 2010; Williams et al., 2005). The effect of heat stress on metabolism (Biljana et al., 2013; Ippolito et al., 2014) and synthesis of heat shock proteins has also been described (Hall et al., 2000; Oberley et al., 2008; Zhang et al., 2003). However, a detailed analysis of changes in the extracellular metabolites of freshly isolated hepatocytes from differentially aged rats has not been done before. Also, the effect of external oxidative stress through heat and hydrogen peroxide on metabolite changes has not been seen before. We chose heat stress as firstly it is a chemically non-invasive way to induce oxidative stress. Thus, it can be done safely also *in vivo*. Secondly, old age rats have been shown to be sensitive towards heat stress (Zhang et al., 2003). Hydrogen peroxide on the other hand is a strong free radical generator of reactive oxygen species (ROS) in cell culture experiments. Another part of the project dealt with investigating the effect of quercetin, a naturally available flavonoid on the stressed hepatocytes. In chapter 2 of this thesis, various methods established for culture of hepatocytes on collagen and their enrichment via Percoll are described. Various assays developed during this work, like cell counting, ROS, cytochrome P450 activity (CYP) and glutathione (GSH) assay are described in detail. Chapter 3 describes the development of heat and hydrogen peroxide stress conditions. It also shows the optimization of quercetin concentration for further experiments. Wistar and Sprague-Dawley rats are two of the most commonly used strains of rat in labs. The rates of extracellular metabolites in the hepatocytes from these two rats in both middle and old age groups are characterized in chapter 4. Further chapters deal with experiments done with hepatocytes isolated from Sprague-Dawley (SD) rats. In chapter 5, extracellular metabolite rates of hepatocytes isolated from old and middle age rats was

characterized based on the measurement of amino acids, glucose, lactate, pyruvate, urea and other liver specific parameters like AST, LDH, CYP activity and albumin levels. In chapter 6, the effect of oxidative stress on hepatocytes isolated from old age rats was observed. Old and middle age rat hepatocytes were exposed to oxidative stress through heat and hydrogen peroxide. Metabolic changes and effect on liver specific parameters was investigated. Lastly, chapter 7 describes effects of the commonly used flavonoid quercetin on stressed middle and old age hepatocytes. Again changes in extracellular metabolite rates have been investigated. In chapter 8, overall summary of the thesis work and possible future work that can be done are discussed. In this project principal component analysis (PCA) has been used to emphasize variation and bring out patterns in data. The metabolic changes were studied via analysis of the 19 amino acids, glucose, lactate, pyruvate and urea. These were measured using an HPLC based method. The response of aged hepatocytes to these oxidative stress and anti-oxidant treatment could be used to establish a metabolic model of aging and develop therapeutic interventions to counteract oxidative stress associated damage in aged liver cells.

2. Material and Methods

2.1. Cell isolation

Primary rat hepatocytes were isolated by Pharmacelsus GmbH from heparinised old (23 months) and middle age (6 months) male Wistar (weighing 200 - 300 g, purchased from Janvier, Le Genest-St-Isle, France) or Sprague – Dawley rats (weighing 400 - 500 g purchased from Harlan laboratories Inc., Indianapolis, IN, USA) as previously reported (Noor et al., 2009).

2.2. Percoll enrichment

Hepatocytes isolated from rats were treated with percoll to remove non-parenchymal cells like Kupffer cells and sinusoidal endothelial cells. Percoll consists of colloidal silica particles of 15 – 30 nm diameter (23% w/w in water), which have been coated with polyvinylpyrrolidone (PVP). Due to its heterogeneity in particle size, sedimentation occurs at different rates, separating hepatocytes from other cells. The living cells settle at the bottom and the dead cells form an upper layer which is carefully removed via aspiration.

20 ml of a 25% Percoll solution (Easycoll, Biochrom, Berlin, Germany) diluted with phosphate buffered saline (PBS) was overlaid with the cell suspension (max. 35×10^6 viable cells in a volume of 5 ml) and centrifuged at 1,000 × g for 20 min at 25 °C (Labofuge 400 R, Thermo Scientific, Schwerte, Germany). The supernatant was discarded and the pellet was resuspended in 50 ml PBS and centrifuged (50 × g; 5 min; 25 °C). After removing the supernatant, the pellet was resuspended in Williams Medium E (PAN Biotech, Aidenbach, Germany) (amino acid composition of the medium is shown in Table 2-1) supplemented with 15 mM HEPES (cc-pro, Oberdorla, Germany), 1% penicillin/streptomycin (cc-pro), 50 µg/ml gentamycin (cc-pro), 10% fetal calf serum (FCS) from PAA Laboratories, Pasching, Austria, 1.4 µM hydrocortison (Sigma-Aldrich, Steinheim, Germany) and 1 µM insulin (cc-pro). The concentration of amino acids, glucose and sodium pyruvate present in the medium is described in Table 2-1. The cell number and viability were determined using trypan blue staining (Invitrogen, Darmstadt, Germany). In all cases, the seeding cell viability was between 75 - 80%.

2.3. Cell cultivation

Primary rat hepatocytes were seeded at a density of 1 million cells per well in 2 ml Williams Medium E (supplemented as described above) in 6 - well plates (Greiner BioOne GmbH, Frickenhausen, Germany) to determine extracellular metabolites, enzymatic activity (AST, LDH), albumin and GSH. For CYP and ROS assays cells were plated at a density of 150,000 cells per well in collagen coated 24 well plates. The plates were coated with rat tail collagen (Roche, Mannheim, Germany) at a concentration of ~ 7.5 µg/cm^2. After 4 hours of adherence, the medium was removed and the wells were washed with PBS at 37 °C to remove dead / unattached cells. To each well, 2 ml or 500 µl of Williams Medium E (supplemented as described above except FCS) was added in 6 or 24 - well plates respectively. The cells were incubated overnight at 37 °C with 5% CO_2 in a humidified incubator. Next day before starting the experiments, cells were washed with pre - warmed PBS. For oxidative stress experiments, cells were exposed to heat stress at 42 °C for one hour and 2 mM hydrogen peroxide for one hour in parallel plates followed by time point measurements. In another set of experiments with quercetin, cells were incubated with 50 µM quercetin (Sigma-Aldrich, Steinheim, Germany) for 4 hours followed by oxidative stress treatment with heat and hydrogen peroxide. For labeling experiments, cells were cultured with 50% [U-$^{13}C_6$] glucose (11 mM) and 50% [U-$^{13}C_5$] glutamine (2 mM). The medium was changed after 12 hours. Cells were cultivated for 2 days after isolation. Cell number, metabolite measurements, enzymatic assays (AST, LDH, CYP) and albumin were measured in the extracellular supernatant at 12 h and 24 h. CYP assay was carried out at 3 h and 12 h after stress induction. Intracellular GSH and ROS were measured at 1 h, 5 h and 24 h.

Table 2-1 Composition of Williams medium E used for cultivation of PRH

Amino acids	µM
Alanine	1010.10
Arginine (free base)	287.03
Asparagine H_2O	133.23
Aspartat	225.39
Cysteine (free acid)	330.14
Glutamate	302.45
Glutamine	1997.95
Glycine	666.05
Histidine (free base)	96.67
Isoleucine	381.18
Leucine	571.78
Lysine-HCl	478.87
Methionine	100.53
Phenylalanine	151.34
Proline	260.58
Serine	95.16
Threonine	335.80
Tryptophan	48.96
Tyrosine 2Na 2 H_2O	191.69
Valine	426.80
Glucose	11101.24
Pyruvat-Na	227.17

2.4. Determination of viable cell number

2.4.1. Trypan blue staining

Cell sample was diluted with trypan blue (Invitrogen, Karlsruhe, Germany) and counted in a hemocytometer. Viable cells excluded the stain whereas, non-viable are stained blue.

2.4.2. Calcein AM staining

Viable cell number was determined with Calcein AM (Tebu-bio, Offenbach, Germany) dissolved in dimethyl sulfoxide as described by Priesnitz *et al*. (Priesnitz et al. 2014).

Principle

Calcein AM (Calcein acetoxymethyl ester) is an acetomethoxy derivative of calcein and is passively transported into the cells. Intracellular esterases cleave off the acetomethoxy group resulting in the generation of green fluorescent calcein which is kept inside the living cells (Figure 2-1). Since the esterases are only active in viable cells, the fluorescence is observed in viable cells allowing an easy distinction between dead and viable cells (Bratosin et al. 2005).

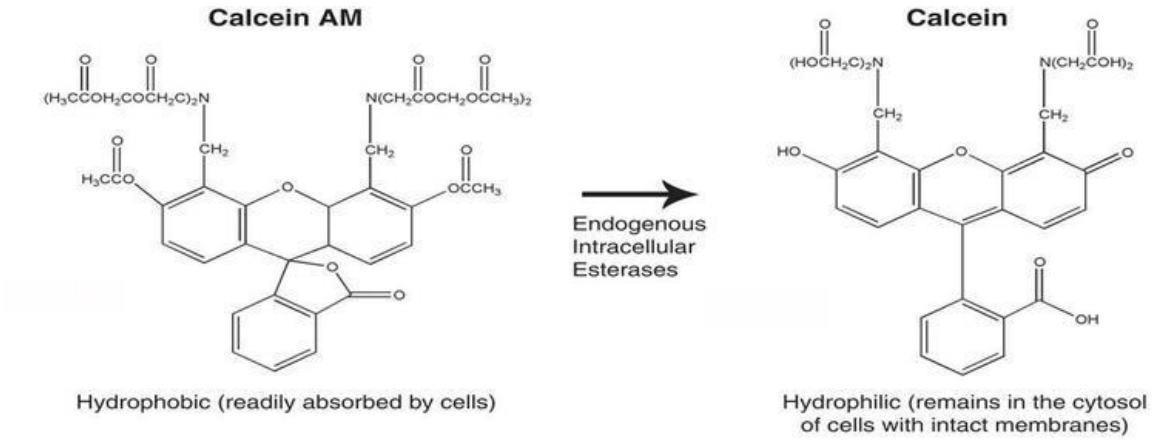

Figure 2-1 The conversion of hydrophobic calcein AM to the hydrophilic and fluorescent complex calcein by endogenous intracellular esterases present in viable hepatocytes

The cells were stained for 10 min with Calcein AM (1 mg/ml in dimethyl sulfoxide) in Williams Medium E in a final concentration of 4 µg/ml. After washing twice with 1 ml PBS to remove unbound dye, 1 ml of Williams Medium E was added and fluorescence pictures (excitation/emission: 495 nm/515 nm) of 12 spots in each well were recorded. Bright-field pictures of three of these spots were also recorded. The cell number in the bright-field pictures was counted manually and related to the fluorescence stained area of the picture of the same spot. The stained area of every fluorescence picture was determined using ImageJ (http://rsb.info.nih.gov/ij/). The average cell size was estimated by dividing the fluorescence stained area by the manually counted cell number. This was done separately for all three spots in each well. The exact cell number in the remaining 9 spots was obtained by dividing the stained area of each spot by the average cell size in each respective well. Taking the mean cell numbers per spot and extrapolation to the area of the well, the viable cell number per well was

determined. The scheme described in Figure 2-2 explains this procedure (Priesnitz et al., 2014).

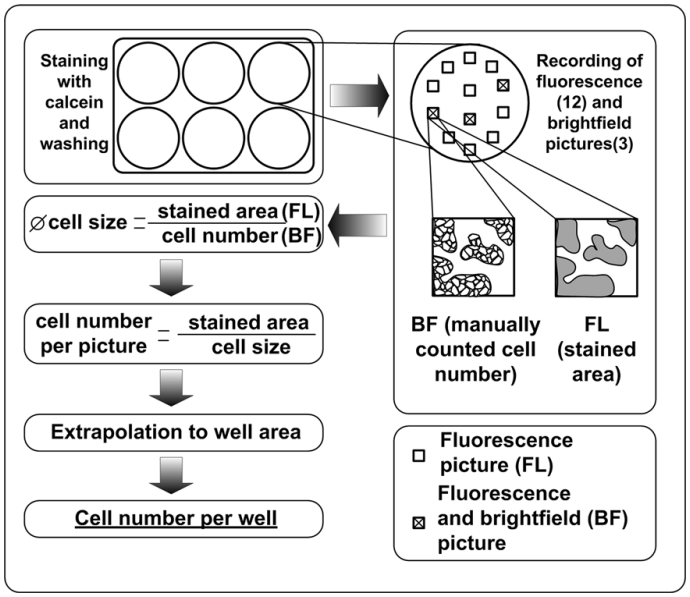

Figure 2-2 Experimental procedure for the determination of the viable cell number per well in a 6-well-plate using Calcein AM staining (Priesnitz et al., 2014)

2.4.3. Cell viability with protein content

Cell numbers from 100,000 to 300,000 were seeded in a 24 well plate for middle and old age PRH. They were washed with PBS followed by cell lysis for 10 min with 75 µl of cell lytic M (Sigma-Aldrich, Steinheim, Germany). The cells were collected in pre-chilled Eppendorf tubes. The lysed cells were centrifuged at 13,000 × g, 10 min, 4 °C to pellet the cellular debris. The protein containing supernatant was removed to a chilled Eppendorf tube and frozen at -20 °C for Bradford test (Bradford, 1976). A calibration curve between cell number and intracellular protein content was made to determine the cell number in case of CYP and ROS assays.

Figure 2-3 shows the calibration curve between cell number and protein content for middle and old age hepatocytes. The regression coefficient of this graph was 80% for middle age and 90% for old age PRH.

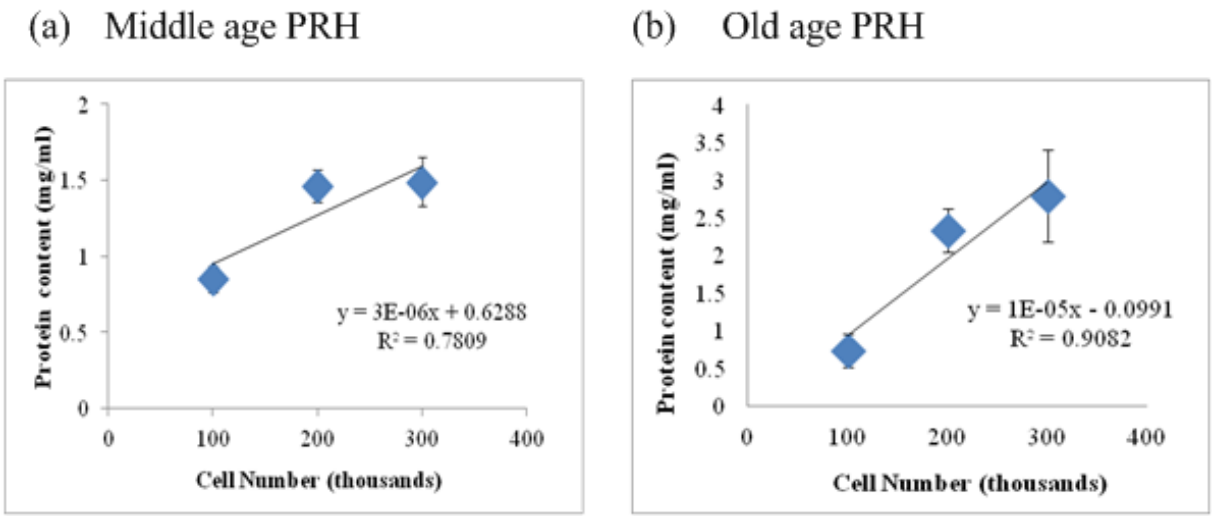

Figure 2-3 : Protein content as measured with Bradford test for different cell numbers in (a) middle age PRH (b) old age PRH

Following equations were used for determination of cell number:

$$Cell\ Number\ (Middle\ age\ PRH) = \frac{\left(Protein\ content\ \left(\frac{mg}{ml}\right) - 0.6288\left(\frac{mg}{ml}\right)\right)}{3 * 10^{-6}(\frac{mg}{ml} * cell\ number)}$$

$$Cell\ Number\ (Old\ age\ PRH) = \frac{\left(Protein\ content\ \left(\frac{mg}{ml}\right) + 0.0991\left(\frac{mg}{ml}\right)\right)}{1 * 10^{-5}\left(\frac{mg}{ml} * cell\ number\right)}$$

2.5. Quantification of metabolites in medium and supernatants

Glucose, pyruvate and lactate in the medium supernatants were quantified using high performance liquid-chromatography (HPLC) (Kontron Instruments, Neufahrn, Germany). After separation using an Aminex HPX 87H ion exchange column (300 × 7.8 mm, Bio-Rad, Hercules, CA, USA) at 60 °C with an isocratic flow rate of 0.8 ml per min of 7 mM H_2SO_4 as the mobile phase, compounds were detected via the refractive index (glucose) or UV absorption at 210 nm (lactate and pyruvate).

Quantification of amino acids was performed with an HPLC method as described previously (Krömer et al., 2005). Briefly, quantification was carried out using HPLC (Agilent 1100

series, Agilent technologies, Germany) with a C18 RP-column (Gemini® 5u C18 110A, 150 mm × 4.6 mm, Phenomenex, Germany) at 40 °C. A gradient separation was carried out (Eluent 1: 40 mM Na_2HPO_4, pH 7.8; Eluent 2: methanol, acetonitrile, water 45:45:10 (v/v)) with a flow rate of 1 ml/min. Primary amino acids were derivatized by pre-column derivatization using *ortho*-phthalaldehyde (OPA) (Agilent, Germany) (excitation wavelength: 330 nm; emission wavelength: 450 nm). Proline, a secondary amino acid, was derivatized using 9-fluorenylmethylchloroformate (FMOC) (Agilent, Germany) (excitation wavelength: 266 nm, emission wavelength: 305 nm).

Urea was quantified using an HPLC method as described previously (Clark et al., 2007).

2.5.1. Analysis of isotopomer labeling patterns

The scope of metabolomics could be enhanced by associating it with mass isotopomer analysis, which allows identification of labeling patterns of metabolites, pointing to unknown reactions and/or regulatory mechanisms (Fridman and Pichersky, 2005).

GC-MS is widely used for measurement of labeling pattern of metabolites from the tracer studies. The organism of interest is hereby cultivated on a substrate, specifically labeled on certain positions with a stable isotope, mainly ^{13}C. The labeling patterns of metabolites formed at different time points during cultivation are then measured with GC-MS. GC-MS can resolve single *mass isotopomers* of a compound differing by the number of labeled atoms and thus allows the measurement of mass isotopomer distributions. Mass isotopomers differ in the number of heavy atoms in their molecules, resulting in different molecular weights. The mass isotopomer distribution of a compound can be obtained from the analysis of an ion cluster, which contains the intact carbon skeleton of the analyte. Similarly mass isotopomer distributions can be determined for certain parts of an analyte considering appropriate fragment ions containing only parts of its carbon skeleton (Wittmann, 2007). The mass isotopomer distribution can be used to calculate the average ^{13}C enrichment of a molecule, called *molar enrichment* (Kelleher, 1999) or *summed fractional labeling* (Christensen and Nielsen, 1999) via the weighted sum of mass isotopomer fractions.

PRH were cultured with 50% [U-$^{13}C_6$] glucose (11 mM) and 50% [U-$^{13}C_5$] glutamine (2 mM) and labeling in mass isotopomers of glucose, glutamine and lactate were determined with gas chromatography – mass spectrometer (GC-MS).

Mass isotopomers of glucose

Glucose was derivatised with (N,O-Bis(trimethylsilyl)trifluoracetamid) BSTFA to form volatile trimethylsilyl (TMS) derivatives which are measured by GC-MS. Two mass isotopomers of glucose were measured: m/z = 319 and m/z = 160 which represent labeling in carbons C - 3,4,5,6 and C - 1,2 respectively (Figure 2-4) (Laine and Sweeley, 1971).

(a)

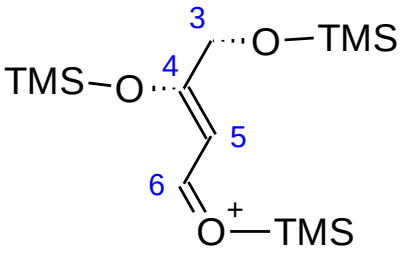

Molecular Formula = $C_{13}H_{31}O_3Si_3$
Formula Weight = 319

(b)

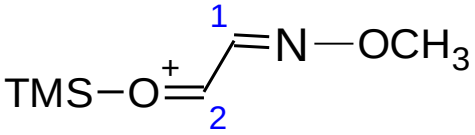

Molecular Formula = $C_6H_{14}NO_2Si$
Formula Weight = 160

Figure 2-4 Mass isotopomers (a) m/z = 319 (b) m/z = 160 of trimethylsilyl (TMS) derivatives of glucose

Silylated mass isoptopomer fragment ions of glutamine and lactate derivatives were measured at monoisotopic peaks of m/z 431 (Wittmann et al., 2002) and m/z 261 (Nicolae et al., 2014) respectively.

Sample preparation

For determination of labeling patterns of lactate and glutamine, 50 µl of supernatants were lyophilized, dissolved in 50 µl N,N-dimethylformamide (0.1% pyridine) and incubated at 80 °C for 30 min. 50 µl N-methyl-N-t-butyldimethylsilyl-trifluoro-acetamide (MBDSTFA) was added followed by another incubation at 80 °C for 30 min for derivatization of metabolites into corresponding dimethylt-butylsilyl derivatives. For determination of the labeling pattern of glucose, lyophilized supernatants were dissolved in 50 µl pyridine containing 6.3 mg/ml methoxyamine hydrochloride and incubated for 30 min at 80 °C. 50 µl N,O-bis(trimethylsilyl)trifluoracetamid (BSTFA) (Macherey-Nagel, Düren, Deutschland) was

added and the mixture was further incubated at 80 °C for 20 min for derivatization into the methoxyamine-trimethylsilyl derivative. Derivatized samples were centrifuged at 13000 × g for 5 min at 4 °C and supernatants transferred into fresh glass vials with micro inlets. They were diluted 1:50 with 1:1 solution of BSTFA and methoxyamine solution before injection.

GC - MS measurements

Extracellular ^{13}C - labeling dynamics were analyzed by gas chromatography mass spectrometry (GC - MS). The GC - MS measurements were carried out on a GC (HP 6890, Hewlett Packard, Paolo Alto, CA, USA) equipped with an HP5MS capillary column (5% phenyl-methyl-siloxane diphenylpolysiloxane, 30 m × 0.25 mm × 0.25 µm, Agilent Technologies, Waldbronn, Germany), electron impact ionization at 70 eV, and a quadrupole detector (Agilent Technologies). The injection volume was 1 µl (7683B Autosampler, Agilent, Waldbronn, Germany; PTV-Injektor, Gerstel, Mühlheim a. d. Ruhr, Germany). Helium was used as carrier gas at a flow rate of 1.1 ml/min for analysis of lactate and glutamine derivatives or 1.1 ml/min for glucose derivatives. The following temperature gradient was applied for lactate and glutamine analysis: 135 °C for 7 min, 10 °C/min up to 162 °C, 7 °C/min up to 170 °C, 10 °C/min up to 325 °C, 325 °C for 2.5 min; inlet temperature: 140 °C and heating with 720 °C/min up to 320 °C; interface temperature 320 °C; quadrupole temperature 150 °C. The temperature gradient for glucose analysis was as follows: 160 °C for 1 min, 20 °C/min up to 320 °C ; inlet temperature: from 160 °C to 280 °C heating with 720 °C/min ; interface temperature 320 °C; quadrupole temperature 150 °C.

Data analysis

After identification of metabolites in the scan mode using the NIST data bank, quantification of labeling enrichment was done in SIM (single ion monitoring) using the following unique fragments containing the complete carbon skeleton of metabolites: glutamine 431, lactate 261, glucose 319, 160. Mass isotopomer distributions were corrected for naturally occurring isotopes using the method of Yang *et al*. (Yang et al., 2009)

2.6. Cytochrome P450 activity assay

The functional enzyme activity test for CYP1A2, CYP2B6, CYP2C9 and CYP3A4 was performed in a cassette approach, based on enzyme reactions. Samples were taken 3 h after incubation with the cocktail of CYP substrates. The enzyme substrates, their test

concentrations and the products used for the quantification of the enzyme reactions are summarized in Table 2-2.

Table 2-2 Substrates, products and metabolizing enzymes used for cytochrome P450 activity assay

Substrate	Product	Enzyme	Substrate concentration (µM)
Phenacetin	Acetaminophen	CYP1A2	26
Bupropion	Hydroxybupropion	CYP2B6	100
Diclofenac	4-Hydroxydiclofenac	CYP2C9	9
Midazolam	1-Hydroxymidazolam	CYP3A4	3

The LC-MS method of detection for the enzymes have been described by Mueller *et al*., 2011 (Mueller et al., 2011). The enzyme activities were measured by Pharmacelsus GmbH. The CYP activities were normalized to cell number determined via protein content (see Sec 2.4.3).

2.7. AST and LDH activities

The activity of liver-specific aspartate aminotransferase (AST) in the culture supernatant was determined using a kinetic UV assay kit (Hitado, Möhnesee-Delecke, Germany) according to the manufacturer's instructions. The activity of lactate dehydrogenase (LDH) in the culture supernatant was determined using a colorimetric enzymatic assay kit (Cytotoxicity Detection Kit; Roche, Grenzach, Germany). For both a dilution series of standard serum (NobiCal-Multi, Hitado, Möhnesee-Delecke, Germany) was measured in parallel for quantification. The enzyme values were normalized to cell number determined via Calcein AM.

2.8. Albumin assay

Albumin concentration was determined via an enzyme-linked immunosorbent assay (ELISA; Albuwell II; Exocell, Philadelphia, USA) performed according to the manufacturer's instructions. The values were normalized to cell number determined via Calcein AM.

2.9. Intracellular GSH assay

GSH assay was adapted from the protocol of Rahman *et al*. (Rahman et al., 2006).

Principle

Reduced Glutathione (GSH) reacts with 5,5´-dithiobis-(2-nitrobenzoic acid) (DTNB) to form a mixed disulfide and free TNB, which can be measured spectrophotometrically at 412 nm. The rate of the TNB formation thereby is proportional to the concentration of GSH in the sample. During the recycling assay, oxidized GSH (GSSG) is reduced by GSH reductase (GR) in the presence of NADPH (Figure 2-5). Therefore, the determined GSH concentration represents total GSH in the sample, i.e. the sum of reduced and oxidized GSH.

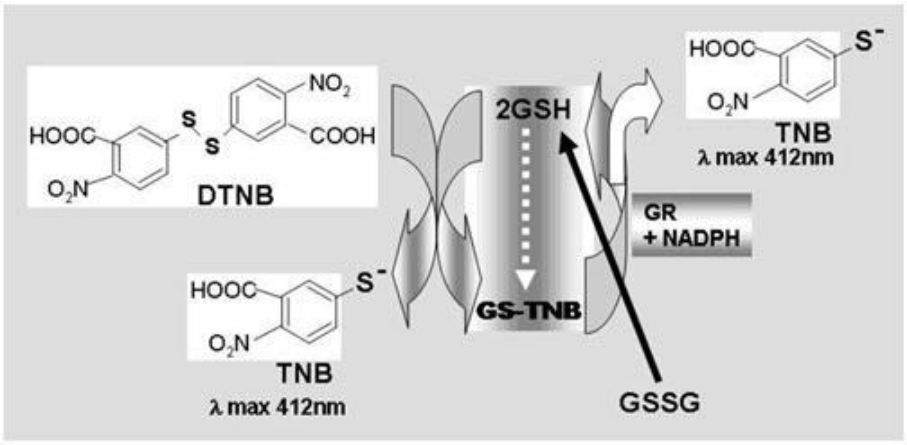

Figure 2-5 Schematic representation of the glutathione recycling assay for the quantitative determination of total cellular glutathione (Rahman et al., 2006)

The cell layer was washed once with 2 ml cold PBS, scraped, resuspended in 1 ml cold PBS and transferred into a pre-chilled Eppendorf tube. They were centrifuged at 1000 × g / 5 min / 4 °C. Supernatant was discarded and pellets were resuspended in 100 µl of 3% Metaphosphoric acid (Sigma-Aldrich, Steinheim, Germany). The pellets were frozen, thawed and centrifuged again at 3000 × g / 10 min / 4 °C. The supernatant was used for GSH determination and pellets were used for protein measurement with the Bradford assay. Equal volumes of 1.7 mM 5, 5'-dithiobis-(2-nitrobenzoic acid) (DTNB) (Sigma-Aldrich, Steinheim, Germany) and 5 - 10 units of glutathione reductase (GR) (Sigma-Aldrich, Steinheim, Germany) solution were mixed. 120 µl of this mixture was added to each well. This plate was incubated for 30 seconds to allow for initial conversion of GSSG to GSH and then 60 µl of

0.8 mM NADPH was added. Absorbance was immediately measured at 412 nm in a micro titer plate reader (5 cycles, every 30 s). The rate of GSH conversion was determined. GSH values of the samples were calculated by using a linear regression of the standard curve. GSH values were expressed as nmol per mg protein.

2.10. Intracellular ROS assay

Principle

The method for detection of ROS with 2´, 7´-dichlorofluorescin diacetate (DCFH-DA) was adapted from Aliá *et al*. (Alia et al. 2005). When applied to intact cells, the non-ionic, non-polar DCFH-DA crosses cell membranes and is hydrolyzed enzymatically by intracellular esterases to non-fluorescent DCFH. In the presence of ROS, DCFH is oxidized to highly fluorescent dichlorofluorescein (DCF) which can be read on a fluorescent microplate reader (Figure 2-6). This intracellular DCF fluorescence is used as an index to quantify the overall oxidative stress in cells (LeBel et al., 1992).

Assay procedure

10 µM DCFH-DA (Sigma-Aldrich, Steinheim, Germany) was added to the wells in the dark for 30 min at 37 °C. Then the cells were washed twice with serum free medium followed by treatment at different conditions. For heat stress the plates were put in a humidified incubator (5% CO_2) at 41, 42 or 44 °C. It took approximately 30 minutes to reach the temperature (Figure 3-2) and the respective temperatures were maintained for 30 minutes. For cells to be treated with hydrogen peroxide, it was added to the cells after incubation with DCFH-DA. Plates were read in a fluorescent microplate reader at excitation wavelength of 485 nm and emission wavelength of 530 nm. Intracellular ROS was measured at 1, 5 and 24 hour. The values were normalized to cell number measured via protein content (see Sec 2.4.3).

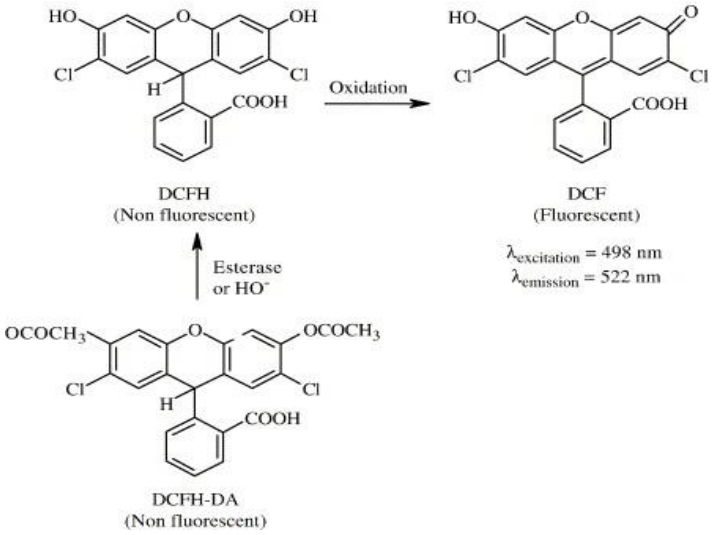

Figure 2-6 Mechanism of detection of ROS or RNS. 2,7-dichlorodihydrofluorescein diacetate (DCFH-DA) de-esterification to 2,7-dichlorodihydrofluorescein (DCFH), and further oxidation to fluorescent 2,7-dichlorofluorescein (DCF) by ROS and RNS (Gomes et al., 2005)

3. Establishment of oxidative stress and anti-oxidant conditions

Hepatocytes isolated from middle and old age rats were exposed to oxidative stress through heat and hydrogen peroxide. To counteract oxidative stress, cells were pretreated with N-acetyl cysteine (NAC) or the commonly available flavonoid quercetin. This chapter focuses on establishment of these conditions for carrying out the experiments.

3.1. Hydrogen peroxide toxicity and heat stress temperature

Hepatocytes from old age male Sprague-Dawley rats were seeded in collagen coated 24 well plates at a density of 150,000 cells / well in WME supplemented with 10% FCS for 3 - 4 hours to adhere. The medium was then changed to WME without FCS and cells were cultured overnight at 37 °C with 5% CO_2 in a humidified incubator.

1 Next day hepatocytes were exposed to different concentrations of hydrogen peroxide (1, 2, 4, 6, 8, 12 mM) for one hour. Intracellular ROS was measured at 1 h and 24 h after treatment. Cell viability was determined via sulforhodamine B dye as described in literature (Vichai and Kirtikara, 2006). Hepatocytes exposed to 1 and 2 mM hydrogen peroxide were almost 90% viable in comparison to controls. A continuous decrease in cell viability with increasing peroxide concentrations was observed (Figure 3-1a). Hepatocytes exposed to 2 mM hydrogen peroxide showed slightly higher intracellular ROS in comparison to cells exposed to 1 mM hydrogen peroxide (Figure 3-1b). It has been seen in previous studies that primary hepatocytes are able to maintain cell viability without necrosis or apoptosis at concentrations up to 2 mM (Rosa et al. 2006). Hence this concentration of hydrogen peroxide was chosen for the further experiments.

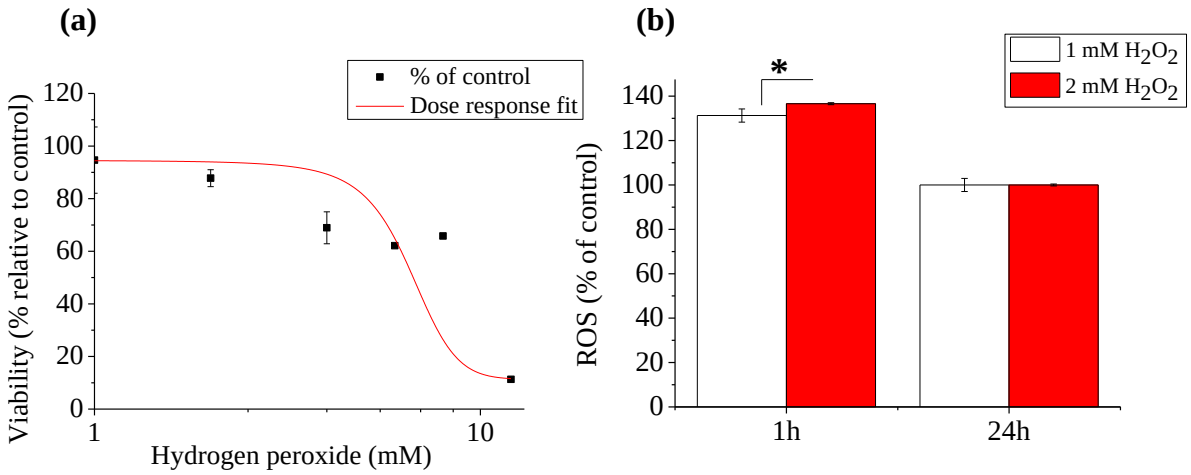

Figure 3-1 (a) Dose response curve for different concentrations of hydrogen peroxide (H_2O_2) with respect to untreated old age SD PRH. PRH were treated for one hour with different concentrations of H_2O_2 and viability was measured after 24 hours (b) Intracellular ROS measured 1 and 24 h after H_2O_2 stress with respect to untreated old age PRH. * indicate significance at $p < 0.05$.

2 After overnight culture PRH were exposed to heat stress at 41 °C, 42 °C and 44 °C for 30 minutes in a separate incubator. Increase in temperature within the wells was monitored with a PT-100 sensor. When the wells reached at particular temperature, it was maintained for 30 minutes and then allowed to cool down to 37 °C. The time required to reach the corresponding temperatures in the wells as measured with a sensor as shown in Figure 3-2. It took 18, 28 and 34 minutes to reach 41, 42 and 44 °C temperatures respectively in the well. For heat stress, these set-point temperatures were maintained for 30 minutes followed by a gradual decrease to 37 °C. However, these temperatures could not be exactly maintained in the plates (Figure 3-2). They tend to increase by 0.3 to 0.5 °C during these 30 minutes. In summary, the total incubation time for 41 °C was 50 minutes and 60 minutes for 42 °C and 44 °C.

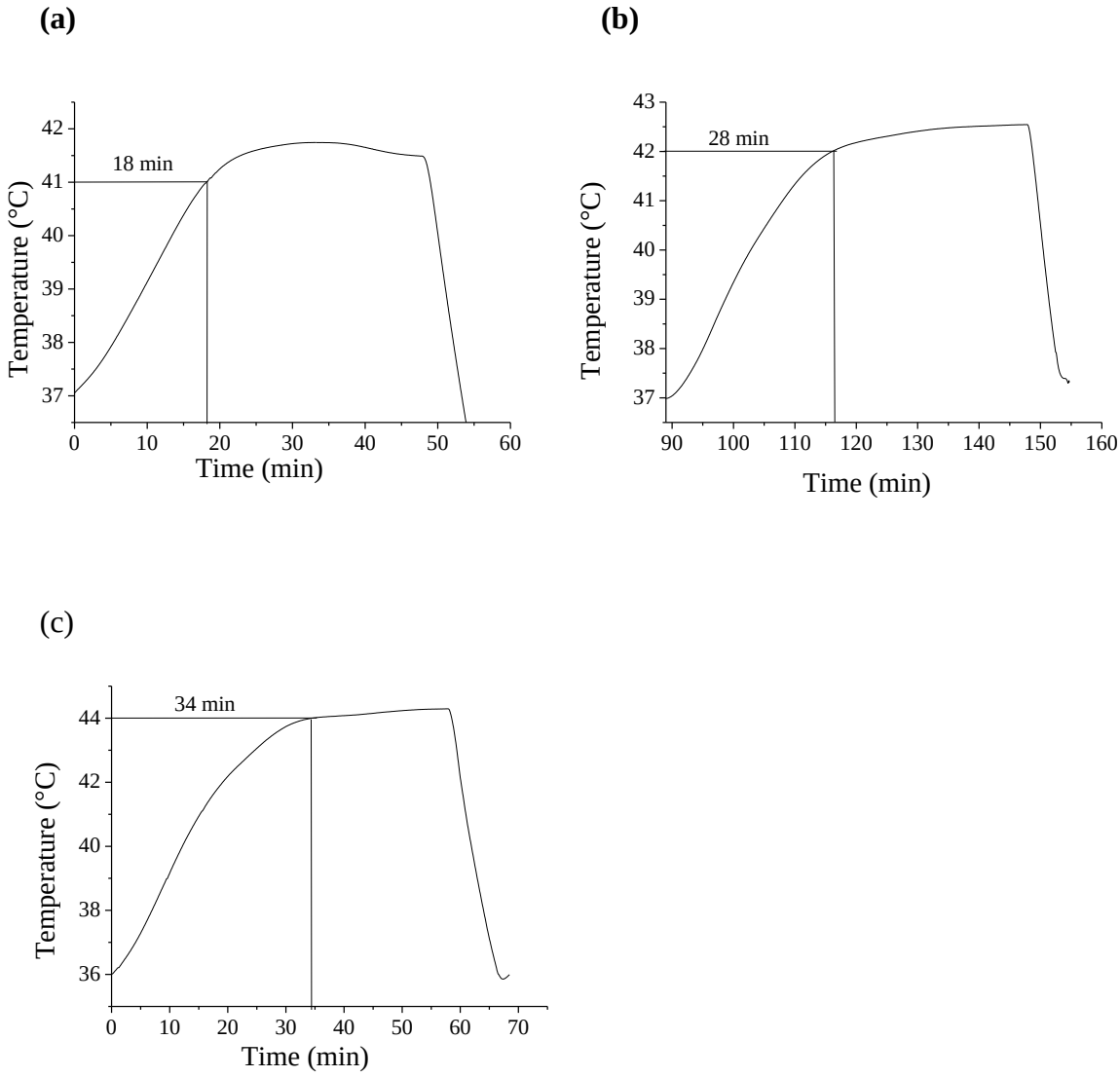

Figure 3-2 PRH were heated at (a) 41 °C (b) 42°C (c) 44 °C in a humidified incubator. The starting temperature of the seeded well was 36 – 37 °C. Time required to increase the temperature was measured with the help of a PT-100 temperature sensor fixed into the plate. It took 18, 28 and 34 minutes to reach the temperatures of 41, 42 and 44 °C respectively in the wells. These set-point temperatures were maintained for 30 minutes followed by a gradual decrease to 37 °C.

Cell number was determined via intracellular protein content (see Sec 2.4.3) at 1 and 24 hour after heat stress. Intracellular ROS was measured at 1 h and 24 h after heat stress. There was a 10% decrease in cell viability for PRH exposed to 44 °C with respect to control PRH (at 37 °C). No significant change in viability was observed for hepatocytes exposed to 41 or 42 °C (Figure 3-3a). Intracellular ROS was significantly increased but was the same as control hepatocytes at 44 °C in comparison to 41 °C and 42 °C. At 42 °C intracellular ROS values were higher in comparison to 41 °C at 1 hour. Although the values for ROS due to heat stress

are lower than for control PRH at 37 °C (Figure 3-3b). It is possible that at higher than normal *in vivo* temperatures, the metabolic pathways like mitochondrial respiratory chain are affected leading to lower ROS generation. It has been shown before that at high temperatures like 44 °C, there is apoptosis in hepatocytes and there are extreme effects on protein expression (Li et al., 2012; Schamhart et al., 1984). Thus, we did not consider this temperature for heat stress. For heat stress experiments, PRH were exposed to 42 °C for 30 minutes as it corresponds to physiologic temperatures which can be accomplished *in vivo* without killing the rats.

(a) **(b)**

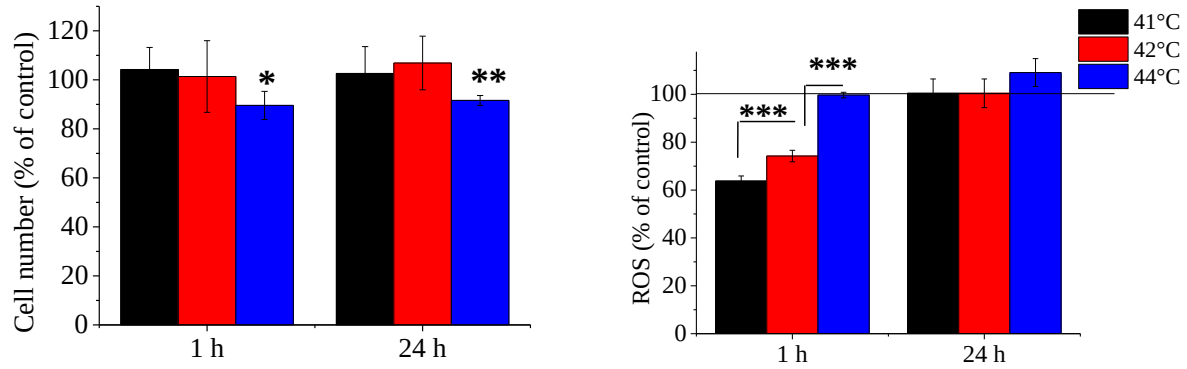

Figure 3-3 (a) Cell viability determined via protein content and (b) Intracellular ROS was measured 1 and 24 h after heat stress for old age PRH with respect to control PRH at 37 °C. *, **, *** indicate significance at $p < 0.05$, $p < 0.01$ and $p < 0.001$, respectively.

However, in a second experiment, intracellular ROS was measured during the time of heat exposure. It was seen that intracellular ROS during the time of heat stress at 42 °C (0.5 h) was significantly higher than control PRH (at 37 °C). These values came down to control levels at 1, 5 and 24 hours after heat stress (Figure 3-4).

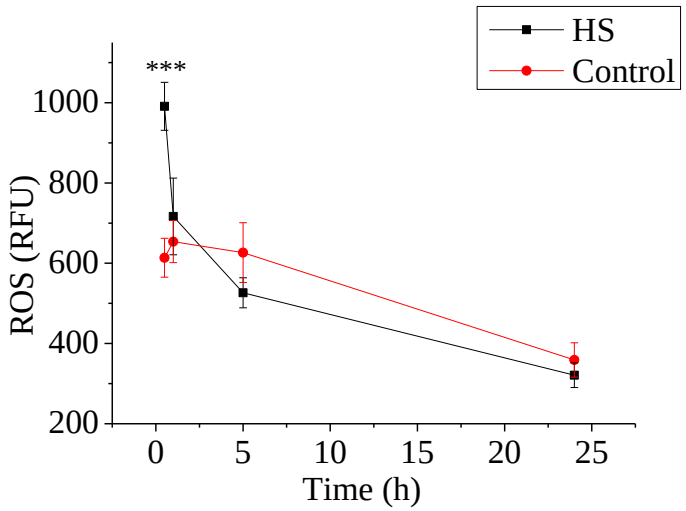

Figure 3-4 Intracellular ROS measured for control old age PRH (at 37 °C) during the time of heat stress at 42 °C (0.5 h) and 1, 5, 24 h after heat stress. *** indicate significance at $p < 0.001$. RFU – relative fluorescence units

This shows that free radicals are generated during heat stress but cells are able to remove this stress with time and hence we observe lower ROS levels at later time points. In a previous *in vivo* study by Zhang et al. (Zhang et al., 2003), liver samples isolated from heat stressed old age rats showed higher ROS levels up to 6 hours after heating. However, this study shows that life time of reactive oxygen species is much lower in *in vitro* culture and cells are able to neutralize this stress through various intracellular anti-oxidant mechanisms.

3.2. N-acetylcysteine (NAC) and quercetin as an anti-oxidant

NAC plays an important role in regulating the oxidant/antioxidant balance in cells and also prevents the decrease in GSH activity. Pre-treatment rather than co-treatment of hepatocytes with NAC was shown to counteract toxicity in hepatocytes exposed to stress via fluoride (Pawłowska-Góral et al., 2013), acetaminophen (Bajt et al., 2004) and *N*-methyl-α-methyldopamine (Carvalho et al., 2004). There was a study where no significant difference between before and co-adding of NAC against the statins induced cytotoxicity in freshly isolated rat hepatocytes (Abdoli et al., 2014). A naturally occurring flavonoid present in many plants, was reported to have many beneficial effects on human health, e.g., anti-tumor, anti-inflammatory, and antioxidant activity (Middleton et al., 2000). Hepatocytes were pre-treated with quercetin for 4 hours at a concentration of 50 µM based on a study from Liu et al. (Liu et al., 2010). In this study, a 2 – 4 hour pre-treatment of rat hepatocytes with quercetin followed

by ethanol exposure was able to reduce the cytotoxic effects of ethanol. Thus, we chose to pre-treat the hepatocytes with querectin and NAC followed by exposure to oxidative stress.

Hepatocytes from middle age Wistar rats were seeded in collagen coated 96 well plates at a density of 30,000 cells / well in WME supplemented with 10% FCS for 3 - 4 hours to adhere. The medium was then changed to WME without FCS and cells were cultured overnight at 37 °C with 5% CO_2 in a humidified incubator. Next day PRH were pre-treated with different concentrations of NAC (0.5 – 8 mM) for 4 hours followed by heat stress treatment. Intracellular ROS was measured after 1 and 5 h. No significant reduction in intracellular ROS was observed due to different concentrations of NAC (Figure 3-5). High concentrations of NAC have been shown to be toxic to liver cells in previous studies (Estrela et al. 1983). Thus, 0.5 mM concentration of NAC was chosen to compare its effect with quercetin.

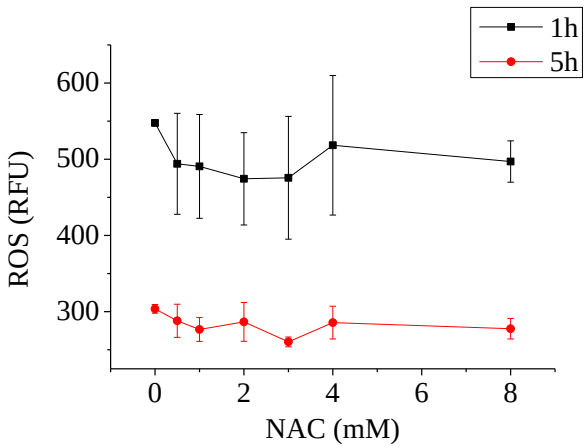

Figure 3-5 Intracellular ROS measured for middle age Wistar PRH pre-treated with various NAC concentrations (0 – 8 mM), followed by exposure to heat stress. ROS was measured 1 and 5 h after heat stress.

Significant reduction in intracellular ROS at 1 and 5 h was observed for PRH pre-treated with 50 µM quercetin for 4 hours followed by exposure to heat and hydrogen peroxide stress (Figure 3-6a). PRH pre-treated with NAC however showed no changes in ROS in comparison to untreated PRH (Figure 3-6b). Thus for metabolite analysis, hepatocytes were pre-treated with quercetin at a concentration of 50 µM for 4 hours.

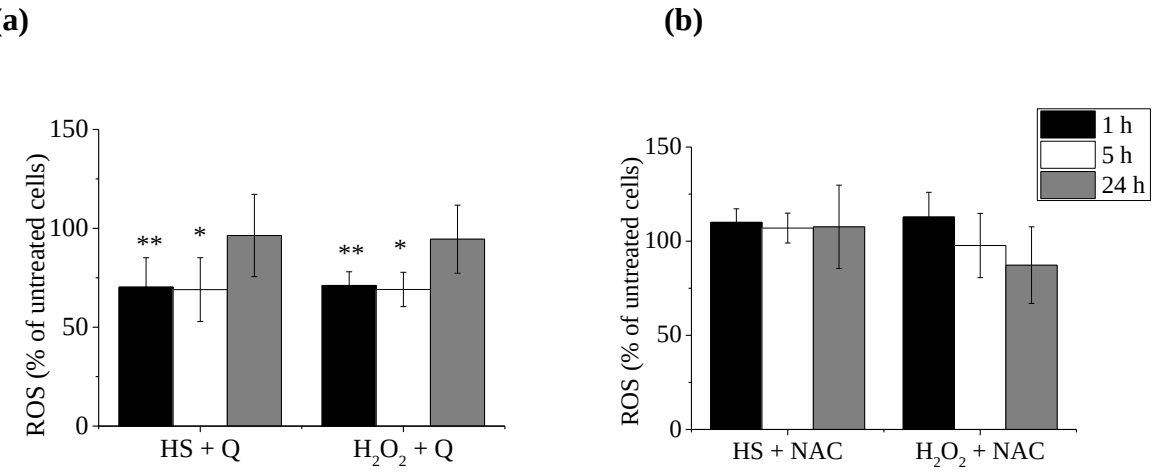

Figure 3-6 Intracellular ROS measured at 1, 5 and 24 hours for middle age Wistar PRH pre-treated with (a) 50 µM quercetin (b) 0.5 mM NAC followed by exposure to heat stress. *, **, *** indicate significance at $p < 0.05$, $p < 0.01$ and $p < 0.001$, respectively. Q – quercetin.

In summary, for oxidative stress, middle and old age PRH were exposed to heat stress through incubation at 42 °C for one hour and to 2 mM hydrogen peroxide for one hour. At these conditions, cell viability was more than 90% and there was generation of intracellular ROS. Quercetin was chosen as antioxidant as it leads to significant reduction in intracellular ROS. For further experiments, PRH were pre-treated with 50 µM quercetin for 4 hours followed by oxidative stress treatment.

4. Separation of differentially aged hepatocytes from Wistar and Sprague Dawley rats based on quantitative analysis of metabolism

Abstract

Sprague–Dawley (SD) and Wistar rats are the most commonly used experimental rats. They have similar genetic background, and are considered interchangeable in practical researches. In this study, we aim to identify the metabolic similarities of Wistar and SD rat hepatocytes from middle and old age groups. Metabolites like amino acids, glucose, lactate and urea were measured in the supernatants at 12 and 24 h by HPLC. Their uptake and production rates from 0 – 12 and 12 – 24 h were normalized to cell number. We could identify systematic metabolic differences between Wistar and SD rat hepatocytes from middle and old age groups. SD rat hepatocytes showed higher uptake rate of amino acids and production rates of glucose and urea. These results suggest that SD rat hepatocytes utilize amino acids at faster rates for intracellular metabolism or proteins synthesis in comparison to Wistar rat hepatocytes. Based on these results, we suggest that a careful selection of animal strain for metabolic studies and result interpretation should be made.

Introduction

Rats are the most commonly used laboratory animals for research owing to their many physiologic and anatomic similarities to human, easy maintenance, short life span and gestation period. Wistar and Sprague – Dawley (SD) are the two most commonly used outbred strains in the laboratory. Wistar rats are preferentially used in Europe and SD rats are generally preferred in the US (Zmarowski et al., 2012).

Strain differences between SD and Wistar rats are already known to exist regarding food intake, growth rate, hormone levels (Kühn et al., 1983), cholesterol and bile acid metabolism (Uchida et al., 1978) and tumor genesis (Kubatka et al., 2002). A GC-MS based urinary metabolic study revealed differences between the two rats under fasting, fed and ethanol exposure conditions (Gao et al., 2011). Both these strains show differences in expression of CYP 450 1A and 3A enzymes (Kishida et al., 2008). Such differences could be due to genetic modification (Holmes et al., 2000), age (Plumb et al. 2005), stress (Wang et al. 2007; 2009) or gut microflora (Wikoff et al. 2009). Differential performance of these rat strains have been observed in neurotoxicity (Zmarowski et al., 2012) and drug toxicity (Garcia-Lopez et al., 1996; Hart et al., 1982; Riley et al., 2000) studies.

Such variation in the test animals needs to be taken into account in routine toxicity testing as it could provide additional information on mechanisms and possible human responses to the test drugs. The possibility of using a multi-strain experimental design in toxicity testing is now beginning to be taken more seriously by some toxicologists. Shellaberger *et al.* (Shellabarger et al., 1978) observed differences in mammary tumor induction according to the sensitivity of different rat strains. Shirai *et al.* (Shirai et al., 1990) observed strain differences in susceptibility to the development of prostate tumors following treatment with carcinogen 3,2'-dimethyl-4-aminobiphenyl (DMAB). Festing *et al.* (Festing et al., 2001) also saw strain differences in haematological response to antibiotic chloramphenicol succinate in mice. Thus, in animal studies it is important to account for strain differences for optimum result analysis.

In this study hepatocytes from SD and Wistar rats from two different age groups (6 and 24 months) were compared based on their extracellular metabolic profile over a course of 24 hours. These results could be useful in selecting the rat strain for aging associated metabolic changes.

4.1. Experimental Design

Freshly isolated primary rat hepatocytes (PRH) from old (23 months) and middle age (6 months) male Wistar (weighing 200 - 300 g, purchased from Janvier, Le Genest-St-Isle, France) and Sprague – Dawley rats (weighing 400 - 500 g purchased from Harlan Laboratories Inc., Indianapolis, IN, USA) (N = 2) were enriched with Percoll followed by overnight culture in Williams Medium E. Next day, extracellular supernatants were collected at 12 and 24 hours for measurement of amino acids, glucose, lactate, pyruvate and urea. Cell number was determined with Calcein AM at 12 and 24 hours of cell cultivation. The experimental design for this study is shown below:

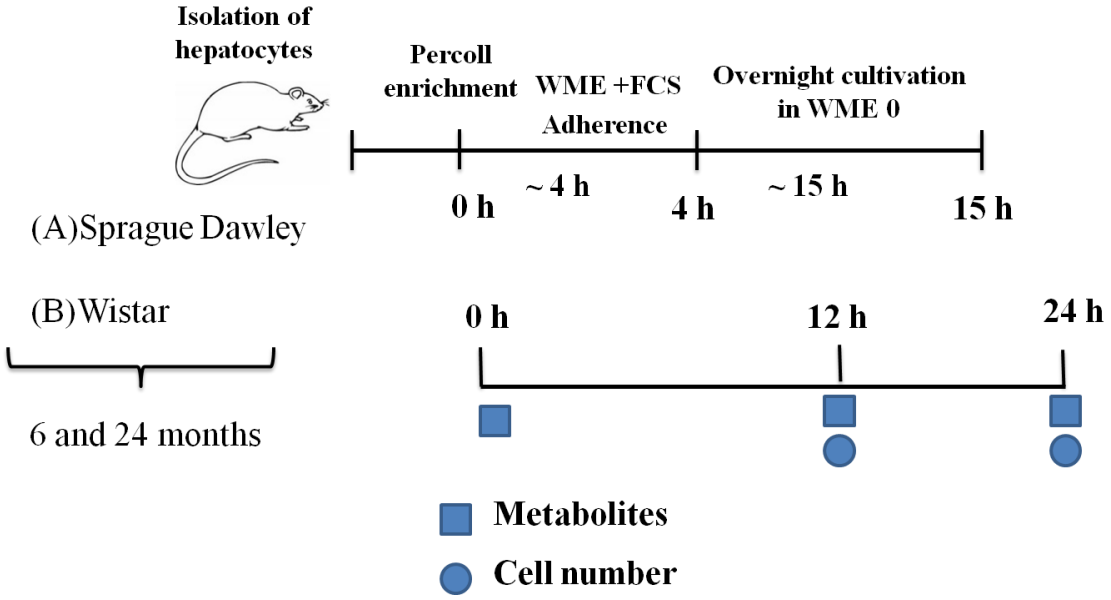

Figure 4-1 Experimental design to compare the metabolite changes in hepatocytes isolated from 6 and 24 month old Wistar and Sprague Dawley (SD) rats. Hepatocytes were enriched with Percoll and cultured overnight in William medium E (WME) with medium change at 12 hours. After overnight culture, extracellular supernatants were collected at 12 and 24 hour for measurement of metabolites by HPLC. Cell viability was determined via Calcein AM at 12 and 24 hour. The upper part refers to cell preparation; the lower part refers to sample collection at various time points.

4.2. Calculation of extracellular rates

The following equation was used for the calculation of substrate consumption and product formation rates:

$$r = \frac{(C_{r,t2} - C_{r,t1}) * V_w}{\Delta t * \text{Cell Number}_{t2}} \qquad \text{Eq (4.1)}$$

where, r is the specific consumption or production rate (fmol/cell/h). $C_{r,t2}$ is concentration measured at 12 h and $C_{r,t1}$ is measured at 0 h for 0 -12 h time interval, $C_{r,t2}$ is concentration measured at 24 h and $C_{r,t1}$ measured at 12 h for 12 - 24 h time interval, V_w is the volume of the culture well and Δt is the time difference, Cell Number_{t2} is living cell number at 12 h or 24 h.

The uptake and consumption rate of metabolites for 0 – 12 h and 12 – 24 h was compared between middle (Eq. 4.2) and old (Eq. 4.3) age hepatocytes from SD and Wistar rats through calculation of fold difference as shown below:

$$f_{MA} = \frac{r_{SD,MA}}{r_{W,MA}} \qquad \text{Eq (4.2)}$$

where, f_{MA} is the fold difference in metabolite consumption or production rate for middle age PRH, $r_{SD,MA}$ is the specific consumption or production rate of metabolite in middle age SD rat PRH and $r_{W,MA}$ is the specific consumption or production rate of metabolite in middle age Wistar rat PRH. This fold difference was calculated for 0 – 12 h and 12 – 24 h.

$$f_{OA} = \frac{r_{SD,OA}}{r_{W,OA}} \qquad \text{Eq (4.3)}$$

where, f_{OA} is the fold difference in metabolite consumption or production rate for old age PRH, $r_{SD,OA}$ is the specific consumption or production rate of metabolite in old age SD rat PRH and $r_{W,OA}$ is the specific consumption or production rate of metabolite in old age Wistar rat PRH. This fold difference was calculated for 0 – 12 h and 12 – 24 h.

4.3. Statistical analysis

PRH used in this work were isolated from 2 middle and 2 old age rats from Sprague-Dawley and Wistar rat strains (N = 2). For each rat there were three biological replicates. Thus, n = 6 for each experiment.

An unpaired Student's t-test and Principal Component Analysis (PCA) was performed using MatLab 2012b (MathWorks, Nattick, MA, USA). PCA emphasizes the variation and brings out strong patterns in a dataset. It transforms the data in the original coordinate system to new coordinates called principal components. The first principal component (PC1) represents the maximum variance in the data. The second principal component (PC2) accounts for the second highest variation in the dataset. For a 3-D visualization, the third principal component (PC3) is used to represent remaining variation. PCA plot was made with normalized metabolite rates. Z-score (in-built MatLab PCA routine) was used for data normalization. Z-score is defined as, $z_i = \frac{x_i - \mu}{\sigma}$ where, x_i is a particular measurement, μ is the mean of all the measurements, and σ is the standard deviation of all the measurements. Outliers in samples can be observed using this method.

In the unpaired Student's t-test, differences between two measurements are considered significant at $p < 0.001$, $p < 0.01$ and $p < 0.05$.

4.4. Results

4.4.1. Cell Viability of old and middle age Wistar and SD rat hepatocytes

The viability of middle (MA) and old age (OA) Wistar (W) and Sprague-Dawley (SD) rat hepatocytes cultivated for 24 hours with medium change at 12 hours is depicted in Figure 4-2. Hepatocytes from Wistar rats showed significantly higher viability in comparison to SD rats for both age groups at 12 and 24 hours. Overall, there was no significant change in viability from 12 to 24 hours for both types of rat hepatocytes.

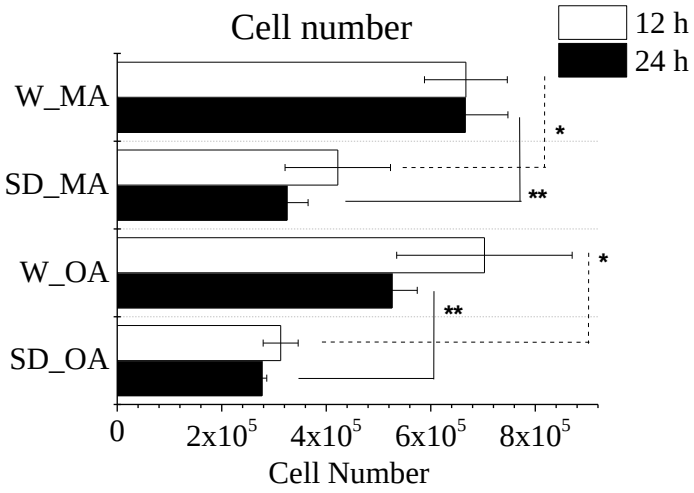

Figure 4-2 Viability of middle age (MA) and old age (OA) PRH from male Wistar (W) and Sprague Dawley (SD) rats determined via Calcein AM at 12 and 24 hours of cultivation. Error bars indicate standard deviations (N =2, n = 6). *, **, *** indicate significance at $p < 0.05$, $p < 0.01$ and $p < 0.001$, respectively.

4.4.2. HPLC analysis of extracellular metabolites

Extracellular concentrations of amino acids, glucose, lactate, pyruvate and urea were quantified and uptake/secretion rates were calculated (according to Eq. 4.1). Amino acid concentrations in the supernatants were quantified and compared with concentrations in fresh medium. To compare the systematic metabolic variations between the two strains of rats, a PCA was done with the metabolite rates normalized to Z-score. 90% confidence ellipses were drawn to show the separation of PRH isolated from SD and Wistar rats (Figure 4-3a), and the clusters of middle and old age hepatocytes from the two types of rats (Figure 4-3b). A clear separation was observed in PC1 and PC2 scores plot between SD and Wistar rat hepatocytes during the 0 – 12 h and 12 – 24 h of cultivation (Figure 4-3a). PC1 and PC2 accounted for 42.1% and 23.8% variation respectively. The middle and old age hepatocytes at 0 - 12 h and 12 - 24 h from Wistar rats, although clustered closely, showed overlapping between the two

age groups (Figure 4-3b). Old age hepatocytes from the two SD rats overlapped with the middle age SD rat hepatocytes. Middle age SD hepatocytes showed more separation between 0 – 12 h and 12 – 24 h time points in comparison to old age hepatocytes which were more closely clustered (Figure 4-3b)

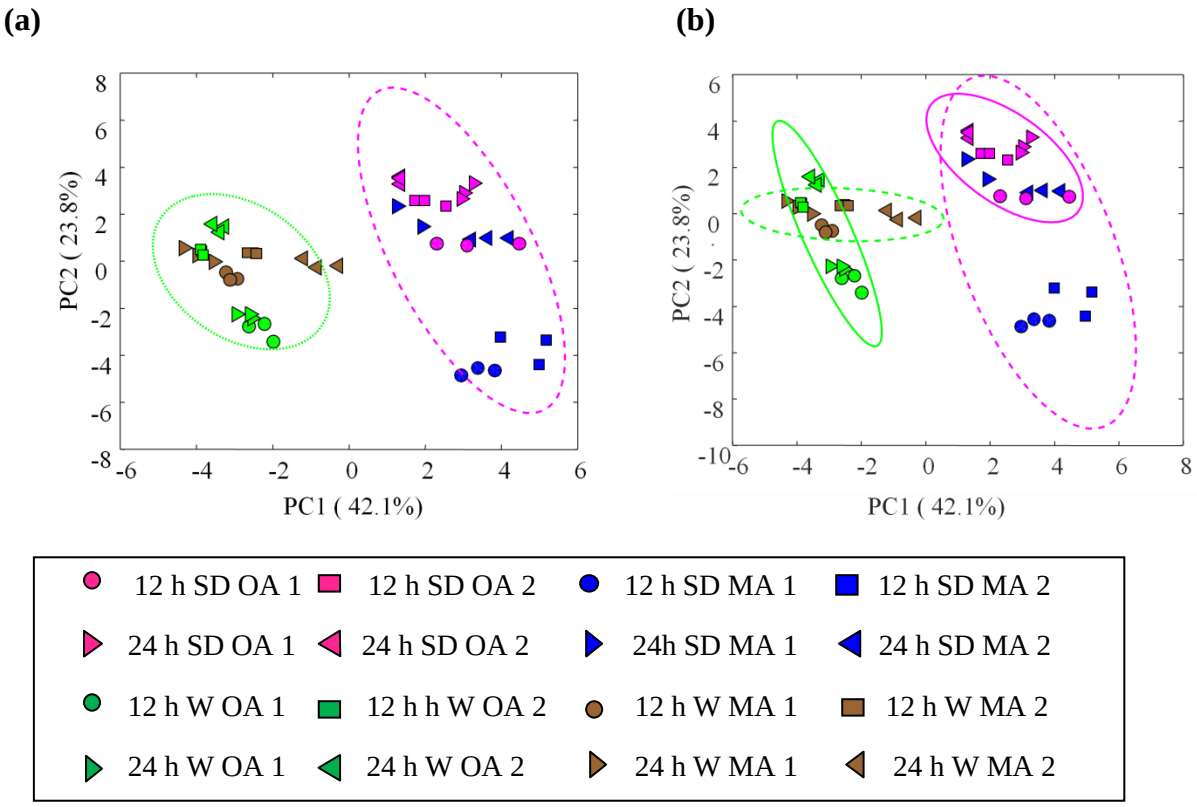

Figure 4-3 PCA scores of specific metabolite rates (measured as fmol/cell/h) of PRH isolated from the two middle age (MA) and old age (OA) SD and Wistar rats (N = 2, n = 6) during 0 – 12 and 12 – 24 hours of cultivation. The data has been normalized according to the Z-score. (a) 90% confidence ellipses show the clusters for SD (pink line) and Wistar rats (green line) (b) 90% confidence ellipses shows the clusters of MA (dashed line) and OA (solid line) hepatocytes from SD and Wistar rats.

Figure 4-4 shows loadings of PC1 and PC2 for the PCA plot shown above. PC1 accounted for maximum variation in the data for both the time intervals. The loadings plot represents the summary of the variables that contributes to the patterns in the score plot. The higher the loading of a particular variable onto a principal component, the more it contributes to that PC. In Figure 4-4, all amino acids except Ile, Val, Asp and Pro have significant Z-scores in PC1 which contribute towards the separation of SD and Wistar rat hepatocytes. The metabolites which show most significant changes in their uptake rates are summarized in Figure 4-5.

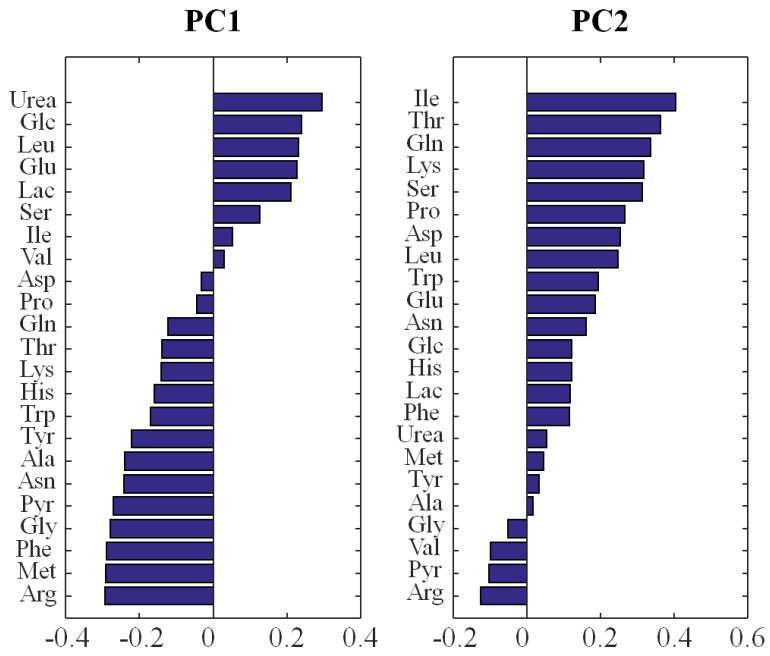

Figure 4-4 Loadings for PC1 and PC2 for middle age and old age Sprague Dawley and Wistar rats during 0 – 12 h and 12 – 24 h.

Figure 4-5a,b summarizes the significantly different fold difference of specific uptake and production rates of metabolites between middle and old age SD and Wistar PRH for 0 – 12 and 12 – 24 h (calculated according to Eq. 4.2 and 4.3). A fold difference greater or less than 1 indicates higher or lower consumption or production rate of a metabolite for SD PRH. A negative fold difference is due to production of the specific amino acid by SD PRH. Most metabolites showed a higher uptake rate by SD PRH in comparison to Wistar PRH. During 0 – 12 h significantly higher uptake rate of various essential amino acids like His, Lys, Met, Phe, Thr and Trp was observed for middle age SD PRH than for Wistar PRH. There was an almost 2 fold higher uptake of non-essential amino acids like Gln, Asn and Gly by SD PRH. Branched chain amino acids like Val, Leu and Ile were produced by SD PRH and consumed by Wistar PRH (see Supplementary Tables S8, S9). During 12 – 24 h, higher consumption rate of only a few non-essential amino acids like Gly, Arg and Tyr was observed for middle age SD rat PRH. Overall, during the first 12 hours of culture, middle age SD PRH showed significantly higher uptake of amino acids in comparison to Wistar PRH (Figure 4-5a).

Again, most metabolites showed higher uptake rates in old age SD PRH than Wistar PRH. Old age SD rat hepatocytes showed significantly higher uptake rates of essential amino acids Phe and Met throughout 24 hours of cultivation. Branched chain amino acids Leu and Ile

were produced by old age SD PRH and consumed by Wistar PRH, hence a negative fold difference in their uptake rates was observed (see Supplementary Tables S10, S11). Other non-essential amino acids like Asn, Gly, Ala, Arg showed almost 2 fold higher uptake during 0 – 12 h and 12 – 24 h in old age SD PRH in comparison to Wistar PRH. Overall, higher uptake rates for certain essential and non-essential amino acids were seen for old age SD PRH (Figure 4-5b) than Wistar PRH.

Organic acids like glucose, lactate and pyruvate were measured during the two phases of cell cultivation. Significantly higher production of glucose was observed for middle and old age SD PRH in comparison to Wistar PRH. Old age Wistar rat hepatocytes showed glucose consumption from 12 - 24 h in comparison to SD rat PRH, hence we see a negative fold difference. 3 - 5 fold higher consumption rate of pyruvate was also observed for SD PRH. There were no changes in lactate production between the two strains of middle age PRH. However, old age SD PRH showed 2 fold higher lactate production during 0 – 12 h and 12 – 24 h in comparison to Wistar PRH. Urea production as a measure of liver function was also measured. SD rat hepatocytes from middle and old age groups showed 2 fold higher urea production than Wistar PRH.

Overall, we could observe a clear separation of SD and Wistar rat hepatocytes for both middle and old age groups in a PCA analysis with the normalized uptake and production rates of metabolites (Figure 4-3a).

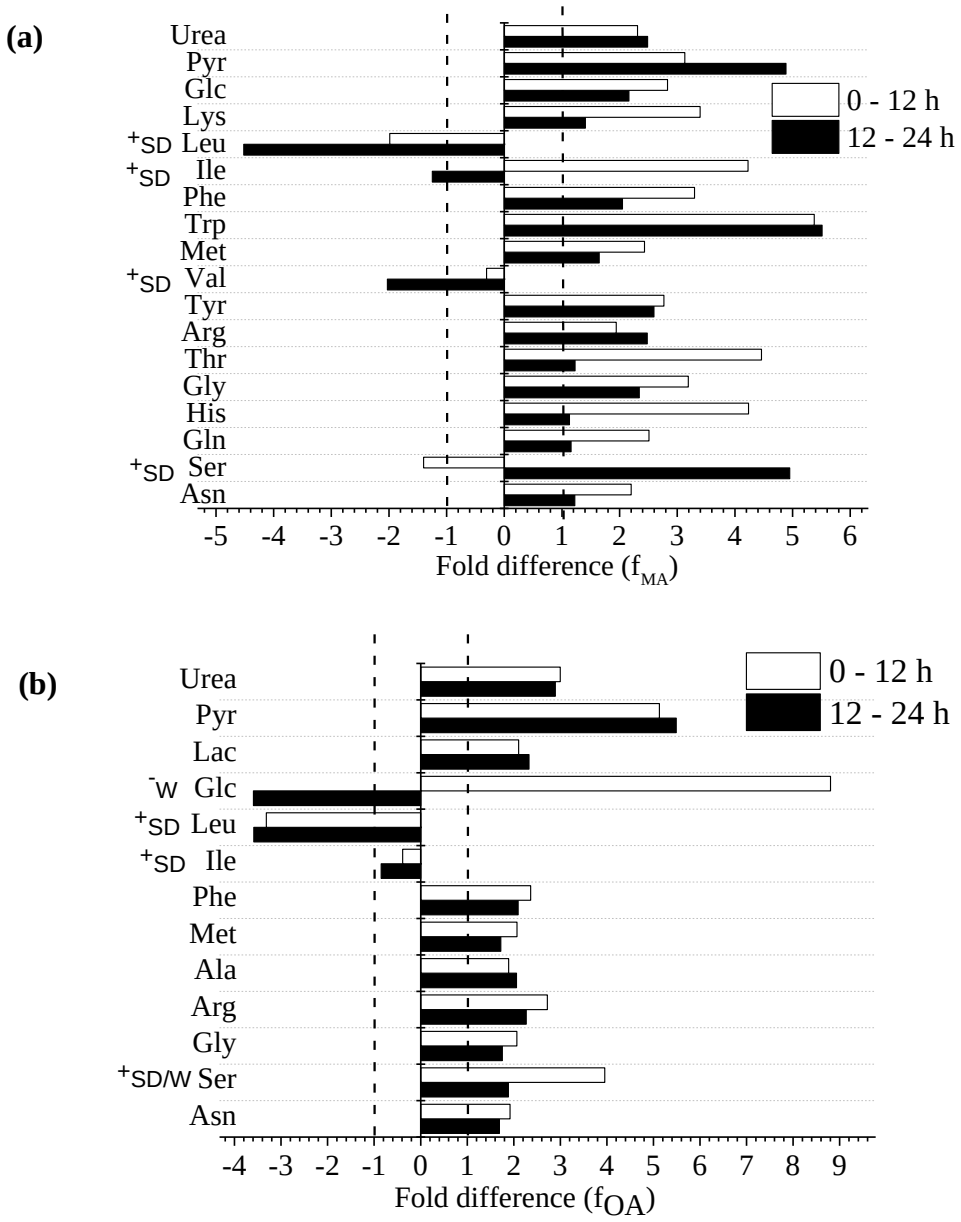

Figure 4-5 Fold difference of specific uptake and production rates (measured as fmol/cell/h) of metabolites measured in extracellular supernatants during 0 – 12 h and 12 – 24 h for (a) middle age (MA) and (b) old age (OA) SD and Wistar PRH (N = 2, n = 6). Fold differences were calculated according to Eq. 4.2 and 4.3. $f_{MA} > 1$ (dashed line) or $f_{OA} > 1$ (dashed line) indicates higher uptake rate for SD PRH. Only metabolites where uptake and production rates were significantly changed are shown here. In middle age PRH, negative values for amino acid rates are seen for Ser, Val, Leu and Ile due to their production by SD rat hepatocytes and consumption by Wistar rat hepatocytes. In old age PRH, negative values for Leu and Ile rates are due to their production by SD rat hepatocytes and consumption by Wistar rat hepatocytes. Ser is produced by both strains of rats. All other amino acids are consumed by both types of PRH. Glucose is produced by both types of PRH except for Wistar old age rat from 12 - 24 h. Thus, a negative fold difference is seen. $+_{SD}$ indicates production rate of amino acid by SD PRH, $-_{W}$ indicates consumption rate of amino acid by Wistar (W) PRH, $+_{SD/W}$ indicates production rate of Ser for both SD and Wistar PRH. Original data is shown in supplementary Tables S8, S9, S10 and S11.

4.5. Discussion

Metabolic rates of hepatocytes isolated from the two commonly used rat strains in scientific research - Sprague - Dawley (SD) and Wistar (W) were compared. Middle and old age PRH from both these strains were compared.

A distinct separation of Wistar and SD rat hepatocytes was observed in the PCA scores plot based on specific uptake and production rates of metabolites (normalized to Z-score). This difference was apparent for both middle (6 months) and old age (23 months) groups (Figure 4-3). In addition to leucine (produced by SD PRH and consumed by Wistar PRH), glucose and lactate production played a major role in the separation of the clusters of samples from these two types of rats (Figure 4-4). This indicates differences in the energy metabolism between SD and Wistar rats. In addition, SD rats showed time dependent differences with the middle age samples clustering more with the old age samples at 24 h. This indicates that isolated hepatocytes from the SD rats are more susceptible to stress of *in vitro* culture with time, regardless if they are isolated from adult or old age rats. There were no clear differences in the corresponding cultures of Wistar rats.

As seen in figure 4-5, except for Wistar OA PRH at 24 h, glucose is produced by both SD and Wistar rat hepatocytes (Figure 4-5). Estimating the glucose that can be produced from glycogen by considering published values for glycogen (Baqué et al. 1996, Schudt et al. 1979) and protein (Engelmann et al. 1981) content, we conclude that the amount of glucose produced was higher than that which could be produced by glycogen degradation. In all these cases, gluconeogenesis seems to be contributing to the glucose release. This argument is supported by the fact that there is consumption of most glucogenic amino acids such as alanine, glycine, glutamine, asparagine, aspartate, histidine and arginine.

Release of urea which is produced during amino acid catabolism was significantly higher in SD PRH in comparison to Wistar PRH (Figure 4-5). This is in line with higher consumption of amino acids and subsequent detoxification of ammonia generated by amino acid degradation through the urea cycle.

These results clearly show the metabolic differences in the hepatocytes isolated from these two rat strains. These differences are significant in rats from both middle and old age groups as well. Our study clearly shows that for performing aging associated studies, the choice of

the rat strain should be a matter of concern in order to accomplish the most optimal and reproducible results. For the further experiments in this thesis, hepatocytes from SD rats were used as old age Wistar rats were unavailable. However, from the above results we can say that the metabolite results related to aging studies are not inter-changeable between different strains of rats.

5. A 2-D monolayer culture to compare metabolic changes associated with aging in primary rat hepatocytes.

Abstract

This work focuses on investigating amino acid metabolism in hepatocytes isolated from old and middle age rats to identify metabolic changes associated with aging. This in turn would provide data for the development of metabolic models to identify age associated metabolic biomarkers. Several *in vivo* studies in the past have identified age related changes in the liver (Mishur and Rea, 2012; Nevedomskaya et al., 2010; Williams et al., 2005). However, our study quantifies extracellular metabolites in freshly isolated hepatocytes from 6 and 24 month old rats cultured as 2-D monolayer. Hepatocytes isolated from both age groups of rats were cultured for 24 hours and various metabolites were measured for time intervals 0 - 12 h and 12 -24 h. Hepatocytes isolated from old age rats showed higher release of the marker enzymes of liver damage like aspartate transaminase (AST) and lactate dehydrogenase (LDH), decrease in cell viability, albumin production, intracellular glutathione (GSH) and cytochrome P450 (CYP) activity. A PCA score analysis of the specific uptake and consumption rates of amino acids, glucose, lactate, pyruvate and urea was done to identify differences in the metabolism of the two types of rat hepatocytes. During 0 -12 h, the rates of middle and old age rats were clearly separated in the PCA plot. However, from 12 – 24 h, there was some overlap in the two groups and old age rats showed high individual variation. Old age rats generally showed higher glucose production from 0 – 12 h and high lactate production throughout 24 hours of cell cultivation suggesting differences in glucose metabolism. The consumption rates of various essential and non-essential amino acids was higher for middle age rat hepatocytes in comparison to old age ones. From these results we could see that old age hepatocytes are more sensitive to stress related to cell isolation and *in vitro* cultivation in comparison to middle age hepatocytes. PCA analysis and metabolite uptake rates could shed light on differential amino acid metabolism between old and middle age rats. Middle age hepatocytes metabolize amino acids at faster rates than old age hepatocytes.

Introduction

Aging is an inevitable part of life which comes with all types of physical and mental ailment. Several common processes are suggested to contribute to aging, including DNA damage, accumulation of reactive oxygen species (ROS), and general metabolic dysfunction (Houtkooper et al., 2011). Metabolites are furthest down the line from gene to function and are most characteristic of the organism phenotype. Cataloging changes in metabolites over time would provide a wonderful tool to study age associated changes (Mishur and Rea, 2012).

Metabolomic studies of aging have been carried out in various organisms like *C. elegans*, Drosophila, rodents and humans based on the identification of metabolites associated with age (Mishur and Rea, 2012). These studies have been mostly carried out using blood, plasma, urinary or tissue extracts from differently aged organisms.

Experimental work using rats to identify age related metabolites was limited to plasma or urine as they are easy to obtain in a non-life threatening manner. In a study by Nevedomskaya *et al.* (Nevedomskaya et al., 2010), differences in the urinary metabolome of wild type versus accelerated-aging mice were observed. N-acetylspermidine, a compound involved in the processes of cell growth and differentiation and lysine, which is associated with calcium absorption and bone health were the major compounds contributing to the differences between the two mice. Using ^{1}H NMR, urine samples from aged rats showed that creatinine, amino acids, and fatty acids increased with age whereas, glucose, myoinositol (Williams et al., 2005), succinate, and other Krebs- cycle intermediates decrease with age (Schnackenberg et al., 2007). Another study of aging using HPLC–MS was performed to characterize the metabolites in the serum of 4, 10, 18, and 24-month-old rats. The rats could be grouped based on the levels of carnosine, cholesterol, and various fatty acids among other unidentified metabolites (Yan et al. 2009). Houtkooper *et al*. (Houtkooper et al. 2011) characterized various plasma metabolites in mice of different age groups. They observed that lipid and glucose metabolism pathways were affected in liver and muscles of mice. Son et al. (Son et al., 2012) carried out a metabolomic analysis in the liver extracts from tissues of differently aged groups of rats through ultra-performance liquid chromatography - quadrupole-time-of-flight mass spectrometry (UPLC−Q-TOFMS). Rats were significantly separated with increasing age, except those aged between 6 and 12 months. Metabolites showing clear differences were: lipid metabolites (glycerol-3-phosphate, linolenic acid, lysophosphatidylcholines [lysoPCs]), energy metabolism intermediates (betaine, carnitine,

acylcarnitines, creatine, pantothenic acid), nucleic acid metabolites (inosine, xanthosine, uracil, hypoxanthine, xanthine), and tyrosine. These metabolome studies suggest that aging might be related with mitochondrial dysfunction and lipid and glucose dysmetabolism.

Although these studies validate the use of metabolomics to study aging, to the best of our knowledge there has been no *in vitro* hepatic metabolic studies in 2-D cell culture to characterize aging in rat hepatocytes. Therefore in this study, we characterize metabolic rates of freshly isolated hepatocytes from 6 and 24 months old Sprague - Dawley rats cultured as monolayer through HPLC and GC-MS techniques.

5.1. Experimental Design

Freshly isolated primary rat hepatocytes (PRH) from old (23 months) and middle age (6 months) male Sprague – Dawley rats (N = 3) were enriched with Percoll followed by overnight culture in Williams Medium E. Next day, cells were incubated with labeled medium (50% [U-$^{13}C_6$] glc and 50% [U-$^{13}C_5$] gln) followed by collection of extracellular supernatants at various time points for metabolite analysis and measurement of other end point parameters. The experimental scheme is shown below:

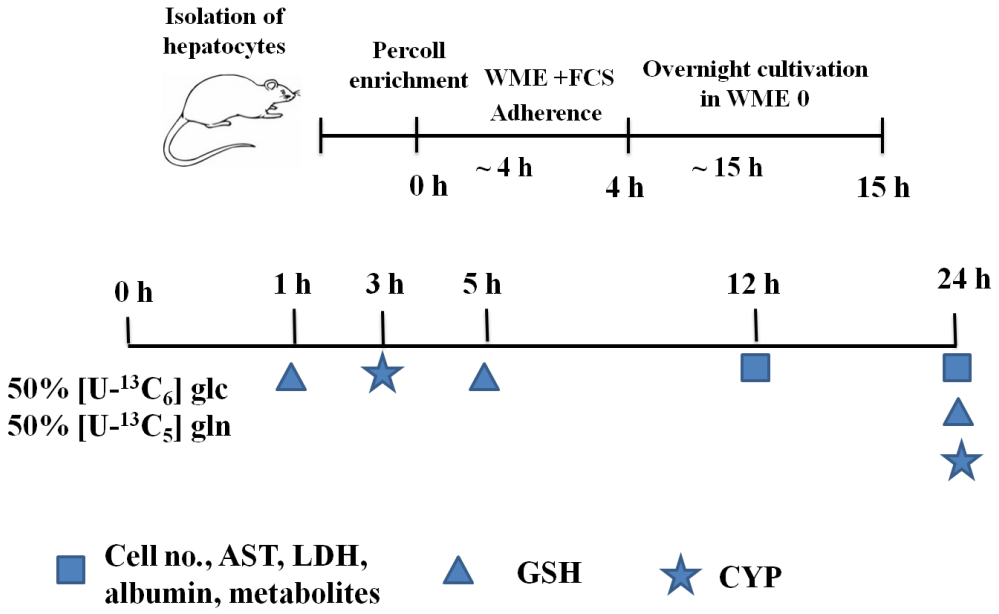

Figure 5-1 Experimental design to study the effect of aging on various biochemical parameters and metabolite levels for old (23 months) and middle (6 months) age Sprague Dawley rat hepatocytes. Symbols indicate time points of sampling. The upper part refers to cell preparation; the lower part refers to experiments at various time points.

5.2. Calculation of extracellular rates

The following equation was used for the calculation of substrate consumption and product formation rates of amino acids, glucose, lactate, pyruvate, urea, AST, LDH and albumin:

$$r = \frac{(C_{r,t2} - C_{r,t1}) * V_w}{\Delta t * \text{Cell Number}_{t2}} \qquad \text{Eq (4.1)}$$

where, r is the specific consumption or production rate (fmol/cell/h). $C_{r,t2}$ is concentration measured at 12 h and $C_{r,t1}$ is measured at 0 h for 0 -12 h time interval, $C_{r,t2}$ is concentration

measured at 24 h and $C_{r,t1}$ measured at 12 h for 12 - 24 h time interval, V_w is the volume of the culture well and Δt is the time difference, Cell Number_{t2} is living cell number at 12 h or 24 h.

5.3. Statistical analysis

The experiments were carried out in 3 middle age (MA) and 3 old age (OA) rats (N = 3), with 3 biological replicates from each rat (n = 9). An unpaired Student's t-test and principal component analysis (PCA) was performed using MatLab 2012b® (MathWorks, Nattick, MA, USA). Differences between two measurements were considered significant at $p < 0.001$, $p < 0.01$ and $p < 0.05$. Data for uptake or production rate of amino acid, urea, glucose, lactate and pyruvate was normalized by Z-score for PCA analysis (in-built MatLab routine) (See details of PCA analysis in Sec 4.3).

5.4. Isotopic studies

Middle and old age PRH were cultured with a mixture of 50% [U-$^{13}C_6$] glucose (11 mM) and 50% [U-$^{13}C_5$] glutamine (2 mM) and labeling in mass isotopomers of glucose, glutamine and lactate were determined with gas chromatography – mass spectrometer (GC-MS). We wanted to investigate simultaneously both the central carbon metabolism and TCA cycle anaplerosis. Mixture of [U-$^{13}C_6$] glucose and [U-$^{13}C_5$] glutamine has been commonly used to distinguish these two branches of metabolism, respectively (Chokkathukalam et al., 2014). When using a labeling mixture of two different uniformly labeled substrates, only 50% of each pools should be enriched to prevent saturation of the metabolic pools with ^{13}C which would prevent distinction of the relative activity of different pathways.

5.5. Results

5.5.1. Effect of aging on viability and cellular parameters

Freshly isolated hepatocytes from middle and old age rats were cultured for 24 hours. Cellular parameters like AST, LDH enzyme activities and albumin production were measured for time intervals 0 - 12 h and 12 - 24 h. Old age hepatocytes showed 15% and 6% lower cell viability at 12 h and 24 h respectively in comparison to middle age hepatocytes (Figure 5-2a). Cellular injury was measured in terms of release of liver specific enzymes AST and LDH. There was almost a 2 fold increase in AST release accompanied by a 10 fold increase in LDH during the two phases by old age PRH in comparison to middle age PRH (Figure 5-2c,d). Another parameter measured for liver function is albumin production. Middle age hepatocytes showed 2 fold and 4 fold higher albumin production at 12 and 24 h respectively in comparison to old age PRH (Figure 5-2b).

5.5.2. GSH depletion due to aging

Intracellular GSH, a measure of oxidative stress in cells, was measured at 1, 5 and 24 h for both old and middle age PRH. Middle age hepatocytes showed about 2 fold higher intracellular GSH levels at the 3 time points (Figure 5-3).

5.5.3. Influence of aging on liver specific drug metabolizing CYP450 activity

To assess liver-specific drug-metabolizing function, CYP 450 activity assay was performed at 3 h and 24 h of cultivation that is, metabolizing capacities at an early phase and at the end of the culture. Activities of CYP1A2, CYP2C9, CYP2B6 and CYP3A4 in terms of product formation rates are shown in Figure 5-4. In general, CYP activities at 24 hours were lower than at 3 hours. Old age hepatocytes showed significantly lower CYP activity in comparison to middle age cells. There was no significant difference in activity of CYP2C9 at 3 hours between old and middle age PRH.

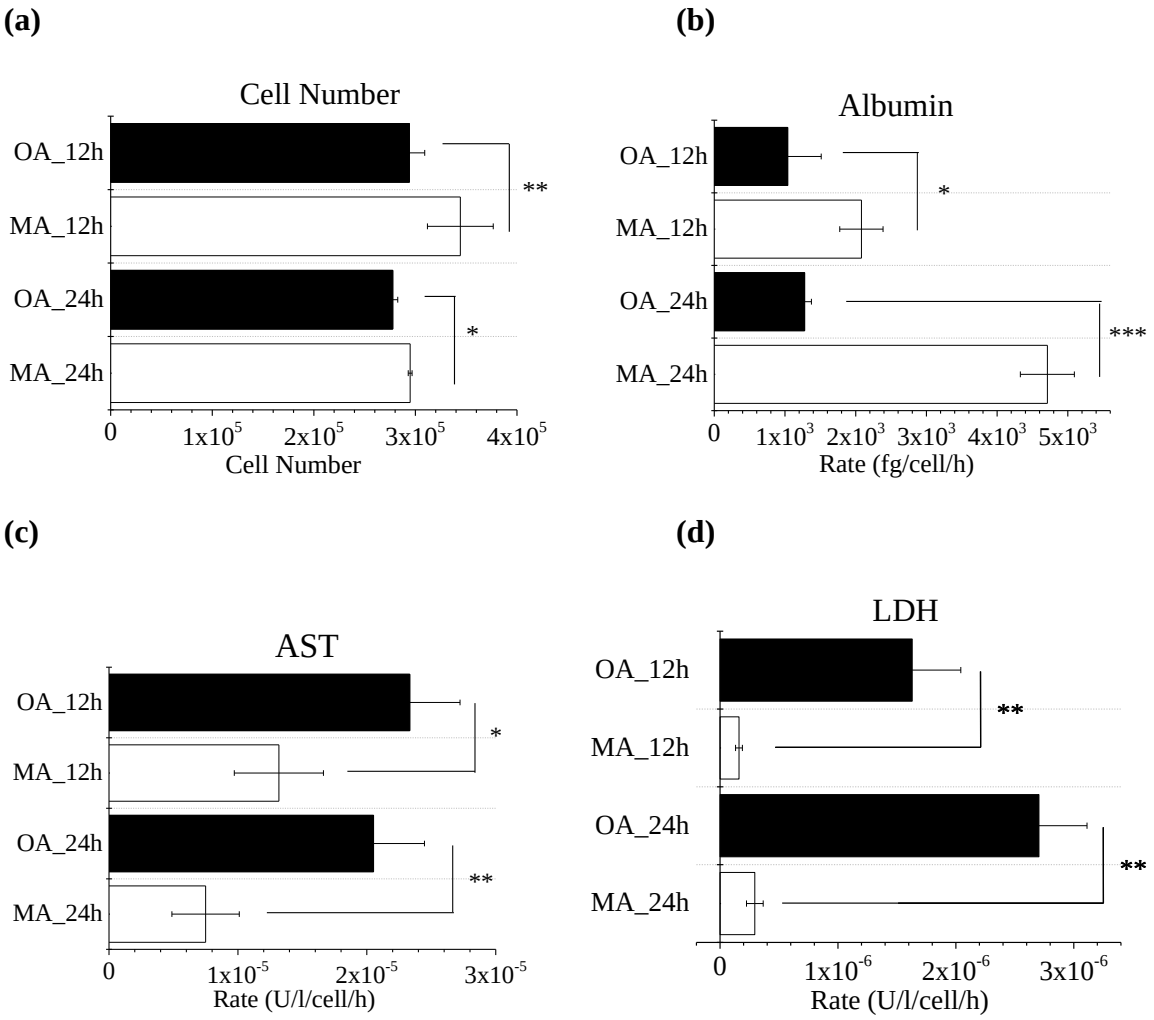

Figure 5-2 (a) Cell number at 12 and 24 h measured through Calcein AM (b) Rate of albumin production (c) AST activity and (d) LDH activity measured for 0 – 12 h and 12 – 24 h for middle age (MA) and old age (OA) PRH. Significance is determined through Student's t- test. *, **, *** indicate significance at $p < 0.05$, $p < 0.01$ and $p < 0.001$, respectively. All values are related to cell number determined by Calcein AM. Error bars indicate standard deviations (N = 3, n = 9). AST, aspartate transaminase; LDH, lactate dehydrogenase.

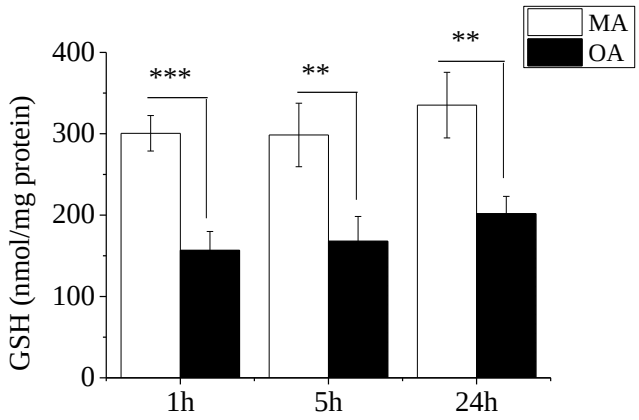

Figure 5-3 Intracellular GSH measured at 1, 5 and 24 h for middle age (MA) and old age (OA) PRH. Significance is determined through Student's t- test. *, **, *** indicate significance at $p < 0.05$, $p < 0.01$ and $p < 0.001$, respectively. The values were normalized to intracellular protein content. Error bars indicate standard deviations (N = 3, n = 9). GSH, Glutathione

5.5.4. Analysis of metabolic changes due to aging

The metabolites amino acids, glucose, lactate, pyruvate and urea were measured in the initial medium and the subsequent extracellular supernatants at 12 and 24 hour of cell culture. The uptake or production rates of these metabolites were determined (according to Eq. 4.1) for 0 – 12 h and 12 – 24 h. A 3-D plot of the scores of the three most significant factors of PCA using Z-score is shown for middle age and old age PRH for 0 – 12 and 12 – 24 h. One of the middle age rats at 12 hour was a clear outlier in comparison to the other rats as shown by the PCA analysis (Figure 5-5). It showed significant differences in uptake rates of amino acids Asn, Ser, Gln and Ala from 0 – 12 h in comparison to the hepatocytes from other two rats (see also supplementary Table S1b). Hence this outlier was removed for further analysis.

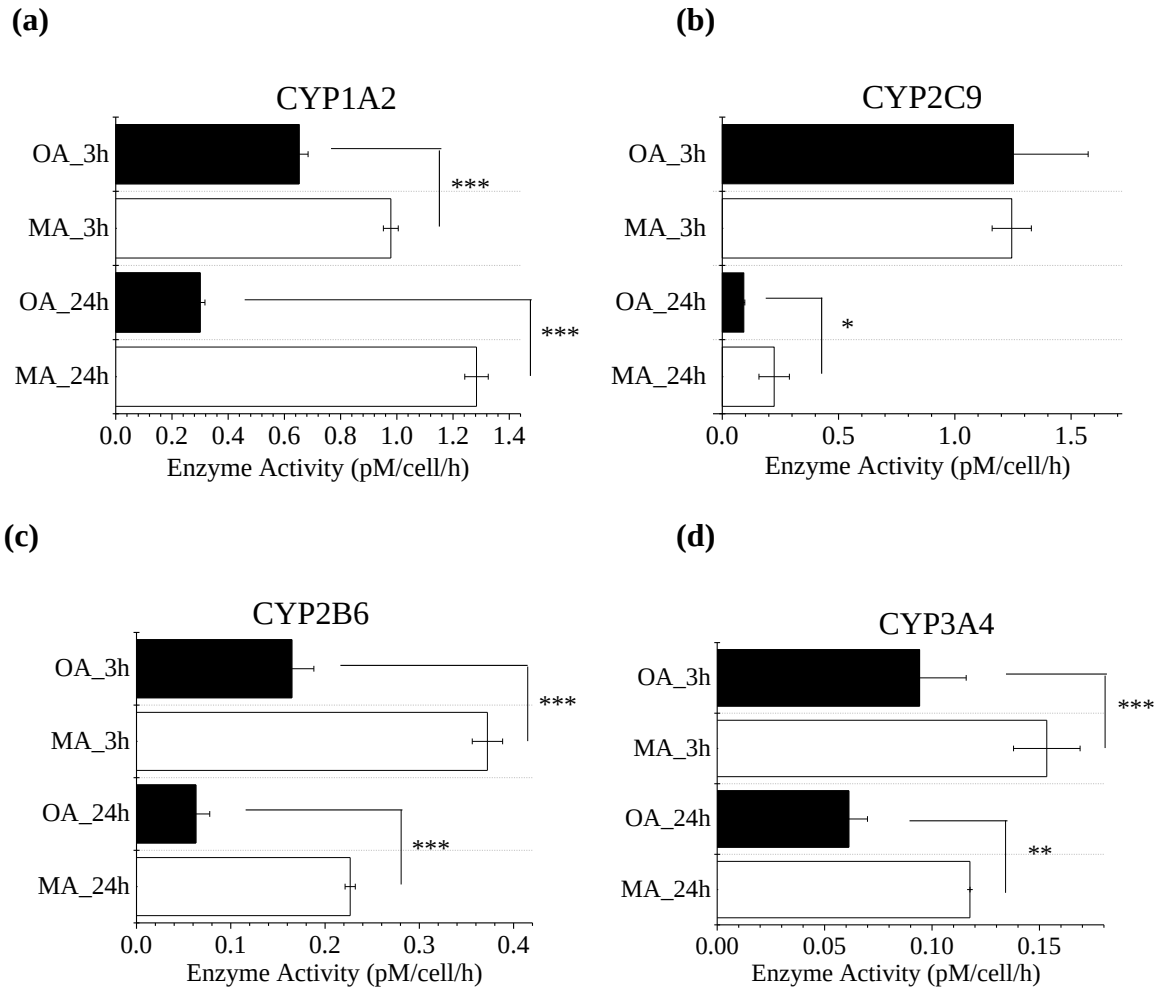

Figure 5-4 CYP enzyme activities of (a) CYP1A2 (b) CYP2C9 (c) CYP2B6 (d) CYP3A4 measured for middle age (MA) and old age (OA) PRH at 3 h and 24 h. Significance is determined through Student's t- test. *, **, *** indicate significance at $p < 0.05$, $p < 0.01$ and $p < 0.001$, respectively. The values were normalized to cell concentration determined via protein content (Bradford test). Error bars indicate standard deviations (N = 3, n = 9).

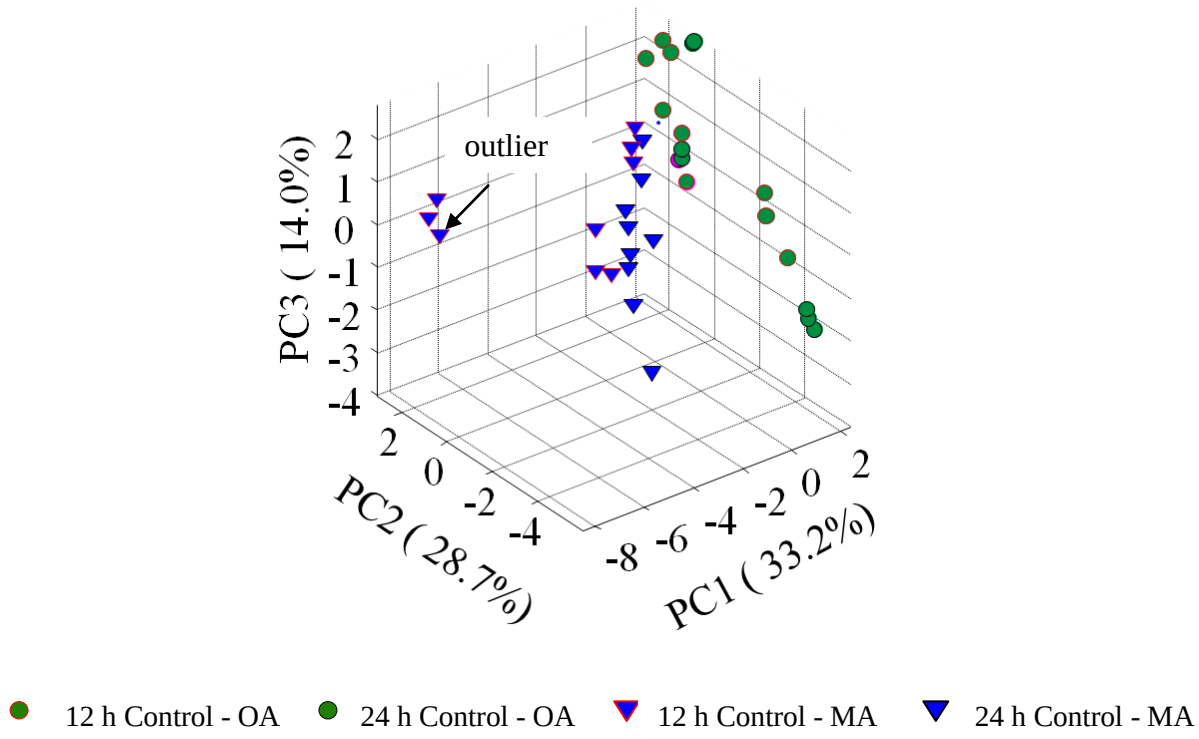

Figure 5-5 PCA scores of specific rates of amino acids, glucose, lactate, pyruvate and urea (in fmol/cell/h) measured during 0 – 12 and 12 – 24 h (N = 3, n = 9) of middle (MA) and old age (OA) PRH. The data has been normalized to Z-score (MatLab pca routine). Metabolite rates during 0 – 12 h for one of the middle age rat (n = 3) is an outlier in comparison to other data points.

In a 2-D PCA plot 90% confidence ellipses show separation of hepatocytes isolated from middle and old age PRH based on the uptake or production rates of metabolites. Separate clusters for middle and old age PRH are observed during 0 - 12 hours. PC1 and PC2 accounted for 45% and 28.5% variation respectively (Figure 5-6a). During 12 - 24 h hepatocytes from the three individual old age rats showed separation among each other as compared to middle age PRH which were more closely grouped (Figure 5-6b). PC1 shows 54.3% variation and PC2 shows 22.6% of the variation. There was slight overlapping in the ellipses of middle and old age PRH for 12 – 24 h.

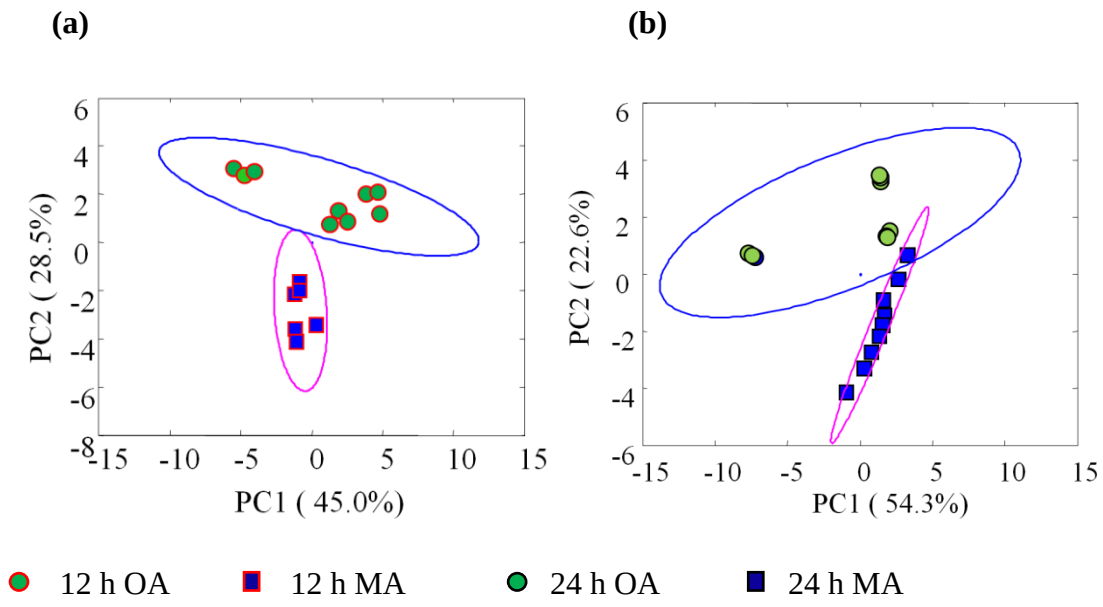

Figure 5-6 PCA scores of specific metabolite rates (measured as fmol/cell/h) of PRH isolated from middle age (MA) and old age (OA) SD rats (N = 3, n = 9) during (a) 0 – 12 and (b) 12 – 24 h. One of the middle age PRH samples for 0 – 12 h has been removed as it was an outlier in comparison to PRH from the other two middle age rats. The data has been normalized according to the Z-score (MatLab pca routine). 90% confidence ellipses show the clusters for old and middle age PRH at 0 – 12 h and 12 – 24 h.

Supplementary Figure S1 shows loadings of PC1 and PC2 at 12 and 24 hours. PC1 accounted for maximum variation in the data for both the time intervals. We see that all amino acids except Thr, and Pro have significant loadings in PC1 which contribute towards the separation of middle and old age hepatocytes. The most significant changes in uptake rates of amino acids are summarized in Figure 5-7.

Specific uptake and production rates of metabolites were analyzed leading to the PCA separation of old and middle age PRH. 19 proteinogenic amino acids (contained in the culture medium) were measured at 12 and 24 hours of cultivation. Fig. 5-7a, b summarizes the specific rates of amino acids which showed significant differences among the two groups during 0 – 12 and 12 – 24 h. Ala, Gly and Gln were the most consumed amino acids. Consumption of all essential amino acids was observed except for Val, Leu and Ile. All non-essential amino acids were consumed except for Ser and Pro at 12 – 24 h. Middle age PRH showed significant increase in uptake of essential amino acids like Thr, Met, Phe, Ile. There was also higher uptake of other amino acids like Gln, Asn and Pro. Old age PRH showed significantly higher production of Ser and Leu. During 12 – 24 h middle age PRH again showed significantly higher consumption of essential amino acids like Thr, Lys and Val.

Higher uptake of other non-essential amino acids like Ala, Gly and Tyr was also observed. Pro and Leu were produced in significant amounts by old age PRH. We could see that these amino acids contribute towards separation of middle and old age PRH from the PC1 loadings in Figure 5-7. Overall, middle age PRH showed higher consumption rate of various amino acids as compared to old age PRH.

Organic acids like glucose, lactate and pyruvate were measured during the two phases of cell cultivation (Figure 5-8a, b). There was significantly higher production of glucose and lactate from 0 – 12 h. From 12 – 24 h, no differences in glucose production were observed whereas, lactate showed significantly higher production in old age PRH. Pyruvate was consumed throughout the cultivation. Urea production as a measure of liver function was also measured. Middle age PRH showed significantly higher production of urea from 12 – 24 h.

5.5.5. Mass Isotopomer Results

Mass isotopomer fragments of glutamine, glucose - which are the major substrate for cells - and lactate - which is formed from pyruvate during glycolysis were measured for both middle and old age PRH (Figure 5-9, 5-10). Cells were cultivated with a mixture of 50% [U-$^{13}C_6$] glucose (11 mM) and 50% [U-$^{13}C_5$] glutamine (2 mM) for 24 hours. From 0 to 24 h there was a decrease in the m+5 (uniformly labeled) and increase in the m + 0 (unlabeled) mass isotopomer fragment of glutamine. The other mass isotopomers m+1, m+2 and m+3 were also present from 0 to 24 h for both middle and old age PRH. There was a decrease in the unlabelled (m+0) lactate fragment and an increase in the fully labeled m+3 lactate fragment from 0 to 24 h for both PRH. Old age PRH showed, actually, an increase of almost 6% in the m+3 mass isotopomer at 12 hours. m+1 and m+2 mass isotopomers of lactate were also observed. Two fragments of glucose were measured: m/z = 319 and m/z = 160 which keep the carbons C3, C4, C5, C6 and C1, C2 of the parent ion of glucose, respectively (Laine and Sweeley, 1971). For both PRH there was a decrease of the fully labeled mass isotopomers (m+4 and m+2) of the fragments of glucose and increase of its unlabelled mass isotopomer fragment (m+0) from 0 to 24 h. Differently labeled mass isotopomers m+1, m+2, m+3 and m+4 were also observed for the fragment 319 m/z.

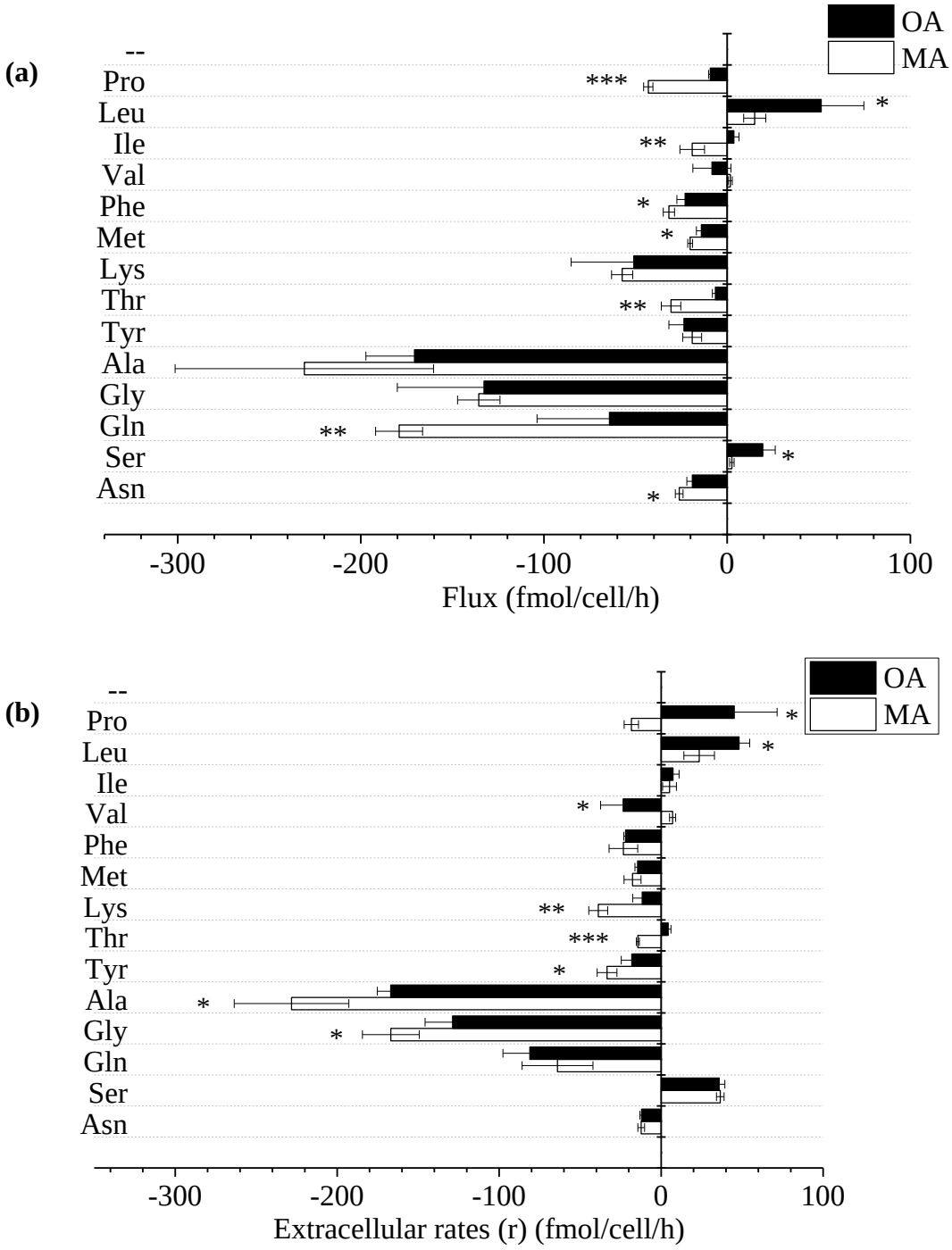

Figure 5-7 Specific uptake and production rates of amino acids measured in extracellular supernatants during (a) 0 – 12 h (b) 12 – 24 h for middle age (MA) and old age (OA) PRH (calculated according to Eq. 4.1). Uptake rates have negative values and production rates have positive values. Significance is determined through Student's t- test. *, **, *** indicate significance at $p < 0.05$, $p < 0.01$ and $p < 0.001$, respectively. The concentration of metabolites was normalized to cell number determined via Calcein AM. Error bars indicate standard deviations (N = 3, n = 9).

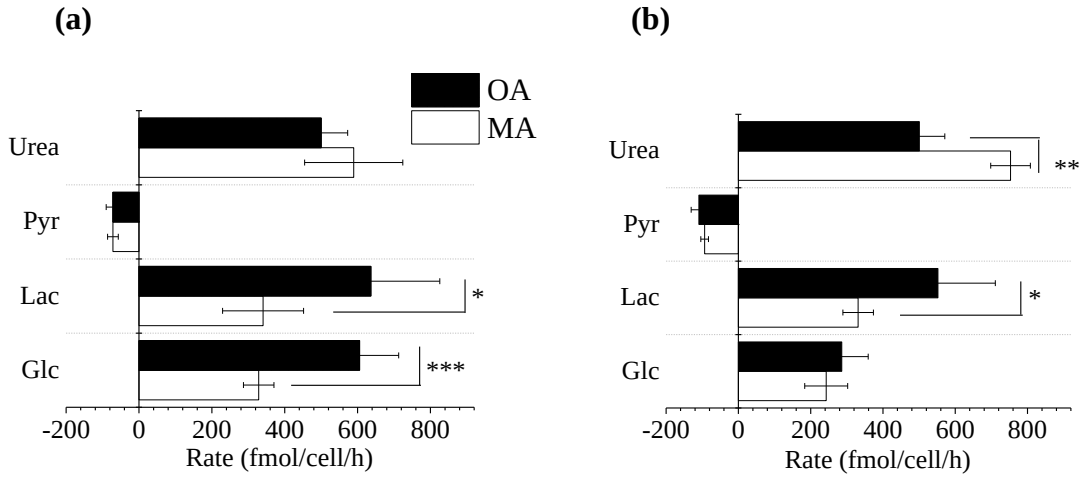

Figure 5-8 Specific uptake and production rates of glucose, lactate, pyruvate and urea measured in extracellular supernatants during (a) 0 – 12 h (b) 12 – 24 h for middle age (MA) and old age (OA) PRH (calculated according to Eq. 4.1). Uptake rates have negative values and production rates have positive values. Significance is determined through Student's t- test. *, **, *** indicate significance at $p < 0.05$, $p < 0.01$ and $p < 0.001$, respectively. The concentration of metabolites was normalized to cell number determined via Calcein AM. Error bars indicate standard deviations (N = 3, n = 9).

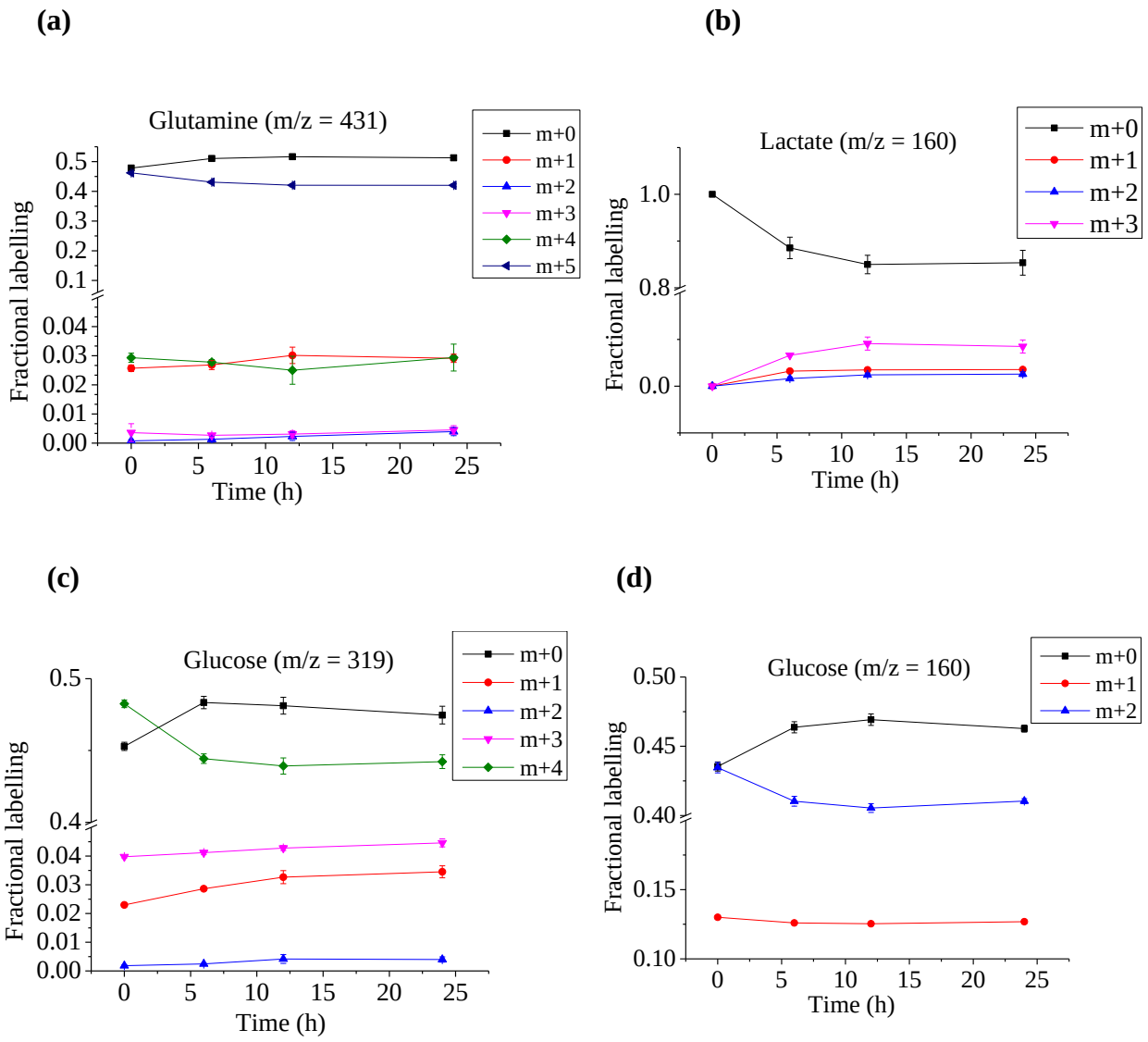

Figure 5-9 Middle age PRH were cultured with a mixture of 50% [U-$^{13}C_6$] glucose (11 mM) and 50% [U-$^{13}C_5$] glutamine (2 mM). Mass isotopomer labeling of (a) Glutamine ^{13}C-mass isotopomer fragment 431 (b) Lactate ^{13}C-mass isotopomer fragment 160 (c) Glucose mass isotopomer fragment 319 (d) Glucose mass isotopomer fragment 160 was measured for middle age PRH at 0, 6, 12 and 24 h. m + 0 - unlabelled fragment, m + 1 - One carbon labeled fragment, m + 2 - two carbon labeled fragment, m + 3 - three carbon labeled, m + 4 - four carbon labeled and m + 5 - five carbon labeled fragment. Error bars indicate standard deviations (N = 3, n = 9).

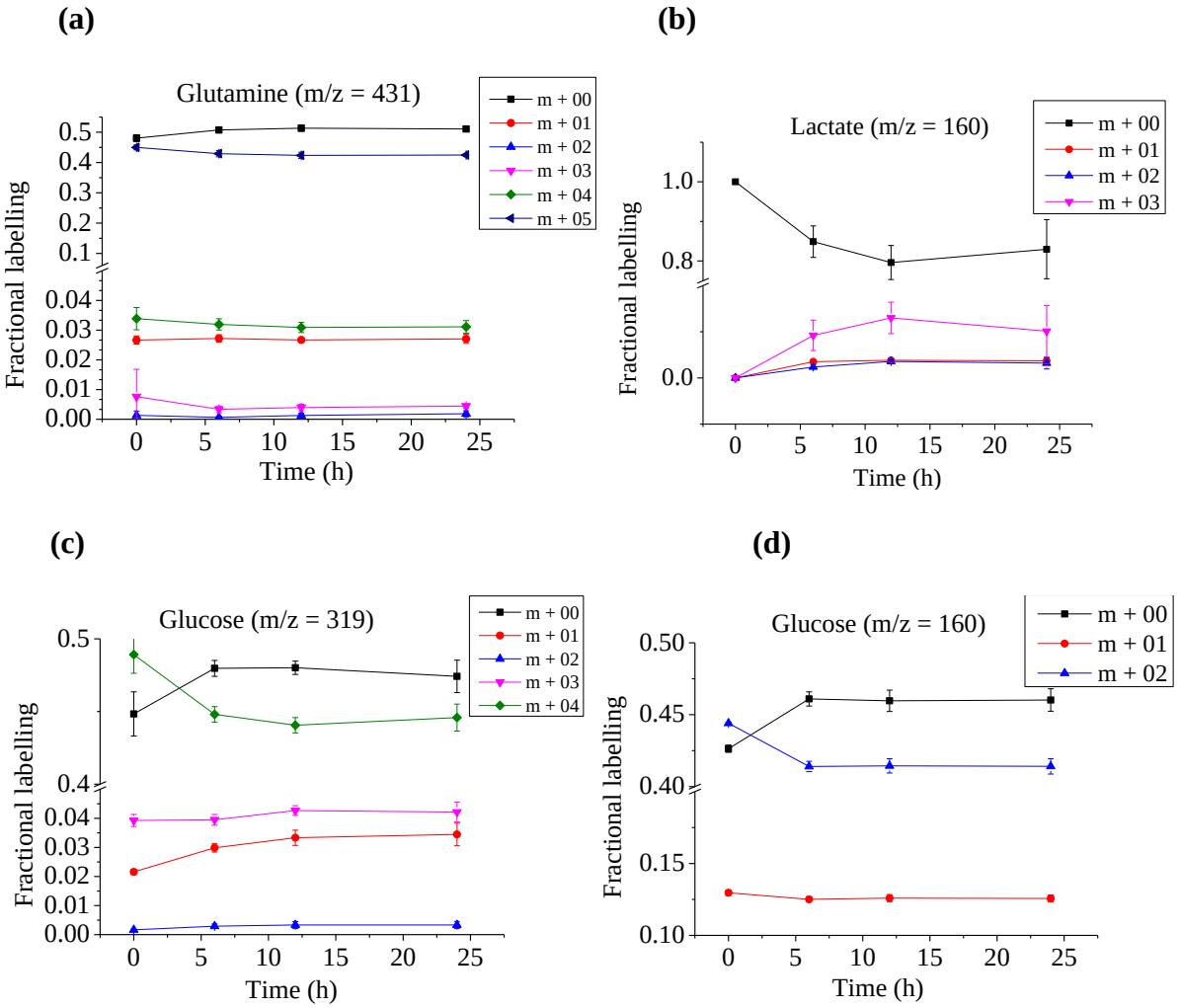

Figure 5-10 Old age PRH were cultured with a mixture of 50% [U-$^{13}C_6$] glucose (11 mM) and 50% [U-$^{13}C_5$] glutamine (2 mM). Mass isotopomer labeling of (a) Glutamine ^{13}C-mass isotopomer fragment 431 (b) Lactate ^{13}C-mass isotopomer fragment 160 (c) Glucose mass isotopomer fragment 319 (d) Glucose mass isotopomer fragment 160 was measured for old age PRH at 0, 6, 12 and 24 h. m + 0 - unlabelled fragment, m + 1 - One carbon labeled fragment, m + 2 - two carbon labeled fragment, m + 3 -three carbon labeled, m + 4 - four carbon labeled and m + 5 - five carbon labeled fragment. Error bars indicate standard deviations (N = 3, n = 9).

5.6. Discussion

In this work, freshly isolated hepatocytes (PRH) from 6 and 24 month old male Sprague-Dawley rats were cultured in 2-D monolayer to study the biochemical and metabolic changes associated with aging. Our work focused specifically on liver as it is shown to be susceptible to age related changes such as mitochondrial dysfunction (Sastre et al., 1996), increased ROS production (Yen et al., 1994) or delayed regeneration after injury (Schmucker and Sanchez, 2011).

The hepatocytes were cultured for 24 hours with a mixture of 50% [U-$^{13}C_6$] glucose (11 mM) and 50% [U-$^{13}C_5$] glutamine (2 mM). The use of labeled substrates contributes to a further elucidation of metabolism. The mass isotopomer distribution of metabolites of interest elucidates the fraction of those metabolic pools that originates from the metabolism of the labeled substrates. Labeling in lactate, glucose and glutamine was measured during the 24 hours of cultivation. The metabolic changes during the two cultivation phases 0 - 12 h and 12 - 24 h were compared between middle (MA) (6 months) and old (OA) (24 months) age hepatocytes.

AST, LDH and albumin were measured as a marker for liver cell function. Old age PRH showed a decrease in cell viability accompanied by lower albumin production and increase in release of AST and LDH enzymes (Figure 5-2). Old age rats have been shown to be more sensitive towards collagenase disruption of liver and cell isolation (Shenvi et al., 2008). This could lead to lower viability of cells and release of AST, LDH enzymes indicative of cell damage. Lower albumin production has also been observed in studies with elderly patients (Kitani, 1992). Low intracellular GSH in old age PRH (Figure 5-3) again shows the sensitivity of hepatocytes to isolation and culture conditions. Zhang *et al*. (Zhang *et al*., 2003) has also shown lower anti-oxidant capacity of liver in old age rats. Lower activity of CYP 450 isoforms for old age PRH was observed in comparison to middle age PRH (Figure 5-4). CYP3A4, the major isoform involved in the metabolism of a large number of xenobiotics in the liver showed almost 50% lower activity on day 2. CYP1A2, another enzyme found mainly in liver showed significant decrease in levels from day 1 to day 2 for old age hepatocytes in comparison to middle age hepatocytes. This is another consequence of aging as previously seen in studies with elderly patients (Sotaniemi et al. 1997). Urea which is a marker of intracellular ammonia detoxification showed lower production during 12 - 24 h for old age

hepatocytes (Figure 5-8). Lower urea levels due to aging have been observed previously in an isolated perfused liver model (Schmucker, 2005).

A clear separation of middle and old age hepatocytes in a 2-D PCA scores plot based on their metabolite profile was observed for the first 12 hours of cultivation (Figure 5-6). 90% confidence ellipses showed distinct clusters for both middle and old age PRH. During 12 - 24 hours, the individual old age rats tend to differ from each other and there was a slight overlapping of the ellipses. PC1 showed the maximum variation in the data. From PC1 and PC2 loadings (Figure 5-7) we could observe proportions of various amino acids which contributed to the differences between the hepatocytes. Significant differences in uptake rates of some of these amino acids between old and middle age hepatocytes have been summarized in Figure 5-7. The uptake of various essential and non-essential amino acids like Thr, Lys, Val, Met Phe, Gln, Asn, Pro, Gly, Ala in middle age hepatocytes increased from 0 - 12 h and 12 – 24 h. These amino acids are utilized by cells as anaplerotic substrates and for protein synthesis. Thus, we could say that middle age rats metabolize amino acids faster than old age rats. In a study by Schnackenberg *et al.* (Schnackenberg et al., 2007) the urine of differently aged rat hepatocytes showed decrease in Krebs cycle intermediates with age. This is in accordance with our results where lower uptake rates of amino acids for old age hepatocytes are observed and hence a probable decrease in intracellular metabolism. However, intracellular metabolites need to be measured to confirm this hypothesis.

Labeling in the major substrate glutamine was measured for 24 hours for both middle and old age PRH. There was a decrease in the fully labeled (m+5) mass isoptopomer of the glutamine fragment and 1 - 2% increase in the m +0, m+1, m+2, m+ 3 and m+ 4 mass isotopomers from 0 – 24 h (Figure 5-9, 5-10). This shows that, apart from net uptake, there is also secretion of glutamine by hepatocytes. In the initial medium glutamine is 50% fully labeled and 50% unlabeled. The presence of multilabeled (m+1, m+2, m+3 and m+4) mass isotopomers indicate that some of the extracellular glutamine was produced intracellularly and secreted. As the multilabeled mass isotopomers were not provided in the initial medium, they can only come from the carbon rearrangements taking place as labeled substrates (glucose and/or glutamine) are metabolized. It has been reported previously that hepatocytes restricted to the distal end of pericentral zone (comprising ~6% of the total hepatocyte population) show the expression of glutamine synthetase (Brosnan and Brosnan, 2009) which could be responsible for glutamine synthesis from its precursors in the intermediary metabolism.

Secretion of essential amino acids like Val, Leu and Ile was observed. Previous studies have reported that secretion of these amino acids in primary hepatocytes occurs due to protein degradation (Crane and Miller, 1977). Leucine forms 11% of the liver protein in comparison to valine and isoleucine which form only 6% and 3% respectively (Judah and Nicholls, 1971). This could be the reason for higher production of leucine in comparison to valine and isoleucine. The observation that the mass isotopomer distribution of these amino acids resembled precisely the natural isotopic distribution, confirms that the source of these amino acids is protein degradation and not any production from intermediary metabolism (see Supplementary Table S7).

A net glucose production was observed for both types of PRH (Figure 5-9). It can be produced either through gluconeogenesis or through glycogen degradation. Increase in the unlabelled mass isotopomer (m+0) of glucose from 0 to 24 hours shows that glycogen breakdown yields glucose which has also been observed previously for rat hepatocytes (Mueller et al., 2011). A 2 - 3 % increase in mass isotopomers m+1, m+2, m+3, m+4 of glucose shows that gluconeogenesis is also active in these cells (Figure 5-9, 5-10) as, these isotopic distribution results from the carbon rearrangement taking place as labeled substrates are metabolized. Hence glucose production in these cells is the result of both gluconeogenesis and glycogenolysis. The average weight of middle age rats was 450 g and average weight of old age rats was 550 g. Thus, old age rats may have more glycogen deposits leading to higher glucose production during the first 12 hours of culture. Higher glycogen breakdown along with elevated glycolysis has been seen in the liver extracts of old mice by Houtkooper et al. (Houtkooper et al., 2011). This suggests their increased need of energy in comparison to middle age hepatocytes during cell culture.

Simultaneous lactate production was seen for both old and middle age PRH (Figure 5-8). Increase in fully labeled (m+3) mass isotopomer of lactate suggests its continuous production from pyruvate via glycolysis in both hepatocytes. Old age hepatocyte showed 3 - 4% higher relative abundance of m+3 mass isotopomer which is in accordance to the higher secretion rates (Figure 5-9, 5-10). Significantly higher production of lactate by old age hepatocytes suggests higher rate of glycolysis in these cells. This shows that old age hepatocytes differ from their younger counterparts significantly with respect to carbohydrate metabolism.

In summary, differences in middle and old age PRH based on their extracellular metabolite profiles were observed in this study. Middle age PRH showed higher uptake of essential and non-essential amino acids which could be utilized for intracellular metabolism or protein synthesis in cells. Old age PRH were more sensitive to *in vitro* culture conditions in comparison to middle age hepatocytes as seen by their lower cell viability, intracellular GSH, CYP activity and increased AST and LDH values. Previous metabolite studies related to aging have been done in liver tissues, in plasma, blood or urine of differently aged rats. This is the first study to compare age associated metabolic changes in a 2-D *in vitro* hepatocyte model. *In vitro* culture offers many advantages over *in vivo* methods such as better control of experimental conditions and larger data collection with lesser rats. This suggests the usefulness of this work.

6. Quantitative characterization of oxidative stress effects on metabolism of differentially aged primary rat hepatocytes

Abstract

Age related diseases may be associated with increasing oxidative stress due to accumulating free radicals. Metabolic analysis of these aging related changes could help in development of various therapeutic manipulations towards a healthier aging process. Primary rat hepatocytes isolated from 6 and 24 month old male Sprague-Dawley rats were exposed to oxidative stress via hydrogen peroxide (2 mM for 1 h) and heat (42 °C for 1 h). The parameters: cell viability, lactate dehydrogenase (LDH), aspartate transaminase (AST), glutathione (GSH), reactive oxygen species (ROS), cytochrome P450 (CYP), amino acids, glucose, lactate and pyruvate were measured for 0 – 12 h and 12 – 24 h time interval. Hepatocytes from old age rats showed reduced cell viability, CYP activity, significant increase in AST and LDH values and higher intracellular ROS and GSH levels due to hydrogen peroxide stress. There was significantly higher uptake of amino acids due to hydrogen peroxide stress. Also glucose consumption was observed suggesting increased energy demand under oxidative stress. There was a small increase in AST and LDH and decrease in cell viability due to heat stress in old age hepatocytes. Control and hydrogen peroxide stressed hepatocytes from old age rats were clearly separated in a 2-D PCA scores plot based on their metabolite profiles. However, no significant separation due to heat stress was observed. Heat stress and hydrogen peroxide treatment did not induce any changes in the extracellular metabolic rates in hepatocytes isolated from middle age rats. These results indicate that, old age hepatocytes are more susceptible to metabolic changes due to oxidative stress generated via hydrogen peroxide than hepatocytes from middle age rats. Furthermore, oxidative stress during aging leads to increased utilization of amino acids for various intracellular processes. It was also shown that, hepatocytes *in vitro* are robust to heat stress irrespective of the age of the rats.

Introduction

The dynamics and the underlying mechanisms of aging processes in humans are largely unclear. Reactive oxygen species (ROS) play a major role in the aging process as presented in "free radical theory of aging" (Harman, 1956). Over the past decades, a number of studies have shown an age related increase in oxidative damage to lipids, proteins and DNA. These studies have been extensively reviewed (Bokov et al., 2004). The most common intracellular sources of ROS in eukaryotic cells are the mitochondrial respiratory chain, microsomal cytochrome P450 enzymes, flavoprotein oxidases and peroxisomal fatty acid metabolism (Chance et al., 1979). External environmental factors such as heat, UV radiation, smoke and chemical compounds also cause ROS production (Ermak and Davies, 2002).

A better understanding of ROS-induced alterations could help to identify potential therapeutic targets for manipulation of aging processes. Along with an increase in free radical production and oxidative damage, one of the consequences of aging is a decrease in stress tolerance at both cellular and whole-organism levels. It was observed in a range of animal studies that upon exposure to heat stress, aged rats display increased morphological damage at cellular and tissue levels, along with elevated levels of reactive oxygen species (ROS) production, substantial oxidative damage, and an associated increase in mortality rate (Zhang et al., 2003).

Exposure to heat stress can lead to two types of responses in organisms: Heat shock response (Hsr) and heat acclimation (Moseley, 1997). Hsr response leads to the induction of heat shock proteins (Hsps) which minimizes cell damage. This leads to development of transient thermo tolerance in cells. Acclimation on the other hand is a slowly developing response caused by chronic exposure to moderate heat (Horowitz, 1998). However, severe exposure to heat can cause heat stroke and lead to cell death if cellular defense mechanisms cannot cope with stress. Rectal temperatures (Trs) of typical patients with heat stroke are higher than 40 °C (Ando et al., 1997). Heat stress may lead to generation of metal ions (mainly Fe^{2+}/Fe^{3+}) forming H_2O_2, which is further cleaved to the extremely reactive OH• radical causing oxidative stress (Zhao et al., 2006). It increases lipid peroxidation (LPO), damage to proteins and DNA (Davidson and Schiestl, 2001). Acute and chronic heating of cells and tissues induces alterations in nuclear and cytoskeletal structures, decrease in mitotic figures in the epithelium and somites, disruption of neural and vascular basal membranes, increase in apoptosis, and inhibition of natural cell-mediated immunity (Katschinski et al., 2000).

Several studies have been done in the past to show the decrease in the organism's ability to tolerate heat stress with age (Hall et al., 2000; Oberley et al., 2008; Zhang et al., 2003). One of the earliest studies done to show the impact of heat induced liver injury in old rats was done by Hall et al. (Hall et al., 2000). They observed a reduced expression of HSP70 in the old age rats subjected to heat stress at 41 °C for 30 min during a 48 hr recovery period. The liver of older rats also showed extensive zone-specific liver injury in comparison to the younger ones. Zhang et al., (Zhang et al., 2003) established a 2 day heating protocol where livers from old and young rats were exposed to heating on 2 consecutive days and liver samples were obtained at several time points during the 24 hours. Liver samples from old age rats showed widespread liver injury including sinusoidal congestion, monocyte infiltration, hepatocellular vacuolization, and widespread necrosis. The younger rats could recover from injury in 24 hours. Liver from old rats also showed increased steady state levels of ROS and prolonged hepatic oxidative damage to lipids and DNA. Liver of heat stressed old rats also showed lower GSH/GSSH ratio indicating an oxidized environment in the liver with aging. Significant changes in the liver carbohydrate metabolism due to heat stress have also been studied before (Biljana et al., 2013). Heat stress has been shown to influence various metabolic pathways such as glutathione metabolism, TCA cycle, urea cycle/creatine metabolism, pyrimidine and purine degradation in the plasma of a conscious rat (Ippolito et al., 2014**).** A study on mouse hepatocytes where the mice were systematically heated to 40, 42, 44 and 46 °C showed the impact of heat stress on expression levels of Hsp 70, Pcna – a marker for cell proliferation, CYP enzymes, Bax - pro-apototic and Bcl2 – anti-apoptotic factors. It was shown that heat stress at a lower temperature of 40 °C promotes hepatocyte proliferation and improves the metabolic efficiency in mouse liver while heat stress at higher temperatures (44 °C, 46 °C) inhibits hepatocyte proliferation, promotes hepatocyte apoptosis and induces hepatocyte necrosis. Heat stress not only affects liver but also other organs such as kidney and central nervous system (Ando et al., 1997). Thus, it could be observed that old age rats are sensitive to heat stress and it results in many intracellular changes. It also results in generation of free radicals (Zhang et al., 2003) associated with an increased production of prooxidants and induction of oxidative stress.

Hydrogen peroxide causes oxidative stress in cells via direct generation of intracellular reactive oxygen species (ROS). It is produced in eukaryotic cells mainly during mitochondrial respiration (Perry et al., 2010), drug metabolism by cytochrome P450 (Chance et al., 1979) and through phagocytic oxidases by stimulated phagocytic cells (Giorgio et al., 2007). It is the

most frequently used compound for inducing short term oxidative stress in cell culture experiments (Imlay and Linn 1988).

In an *in vivo* study, age dependent effects of hydrogen peroxide were investigated. It was shown that old hepatocytes were more sensitive to H_2O_2 treatment as compared to their younger counterparts as determined through various parameters like apoptosis, DNA fragmentation and decreased activation of cell survival pathways like ARK and Akt (Ikeyama et al., 2002). Normally in cells, H_2O_2 functions as a signaling molecule in the intracellular propagation of both physiological and oncogenic growth signals. An increase in intracellular H_2O_2 is seen during induction of cell proliferation by several growth factors (such as EGF, PDGF, nerve growth factor (NGF) and insulin (Finkel, 2000). It mediates angiogenic signaling and has been implicated in the so-called angiogenic switch, which allows non-invasive and poorly vascularized tumors to become highly invasive and angiogenic (through direct activation of the transcription factor hypoxia-inducible factor (HIF) (North et al., 2005). H_2O_2 is a direct and potent inducer of apoptosis. The dual character of H_2O_2 as a mediator of growth and apoptosis suggests specificity in its biological activity. Specific activity of hydrogen peroxide depends on the amount and the intracellular site of its production. Its continuous production can affect cell death and proliferation which are ultimately the determinants of life span. Therefore, in a way it plays a role in determination of life span and hence aging (Giorgio et al., 2007).

Hepatocytes degrade H_2O_2 by at least two pathways. Firstly, via glutathione peroxidase and GSH to yield water and GSSG or secondly, via catalase in peroxisomes to yield water and molecular oxygen. Previous studies using both isolated perfused liver (Oshino et al., 1975) and suspensions of isolated hepatocytes (Jones et al., 1978) suggested that the relative contributions of catalase and glutathione peroxidase to the catabolism of endogenously generated H_2O_2 depend on both the intracellular location and rate of its formation. Hydrogen peroxide generated at a relatively low rate in the endoplasmic reticulum was predominantly metabolized by glutathione peroxidase (Starke and Farber, 1985).

One of the primary aims of this project was to analyze the quantitative effects of oxidative stress associated with aging based on the analyses of the metabolite rates in primary rat hepatocytes isolated from middle (6 months) and old age (24 months) rats. Oxidative stress

was induced through exposure to heat stress and hydrogen peroxide stress. At 42 °C hepatocytes showed 90% viability and intracellular ROS generation (see Sec 3.1). This temperature can be applied *in vivo* without killing rats (El-rahim et al., 2012). Temperatures like 44°C and above, have been demonstrated to cause apoptosis in hepatocytes and effect protein expression (Li et al., 2012; Schamhart et al., 1984).

Hydrogen peroxide is a commonly used free radical inducer in cell culture experiments. Cells exposed to 2 mM hydrogen peroxide showed higher intracellular ROS than untreated control cells and 90% viability (see Sec 3.1). In previous experiments with primary hepatocytes, it was seen that cells were able to maintain viability without necrosis or apoptosis at concentrations up to 2 mM (Rosa et al. 2006). Thus, these conditions were used to generate oxidative stress in hepatocytes.

Various endpoint markers like amino acids, glucose, lactate, pyruvate and liver specific parameters like AST (aspartate transaminase), LDH (lactate dehydrogenase), urea, albumin and CYP450 enzymes were measured in control and stressed hepatocytes for 0 – 12 h and 12 – 24 h time interval. Sampling was done at 0, 12 and 24 hours. Markers of oxidative stress such as intracellular ROS and reduced glutathione concentration were also evaluated.

Previous studies (as reviewed above) to observe the effect of oxidative stress in aging have been done *in vivo*, with analysis of plasma, urine and tissue extracts. To our knowledge there have not been any studies to see the differential effects of oxidative stress directly on hepatocytes isolated from old age rats. The results from this study could be useful to build a metabolic model to analyze intracellular metabolism and characterize changes in hepatocyte metabolism due to age associated oxidative stress and predict potential biomarkers associated with ROS injury in aging.

6.1. Experimental Design

Freshly isolated primary rat hepatocytes (PRH) from old (23 months) and middle age (6 months) male Sprague – Dawley rats (N = 3) were enriched with Percoll followed by overnight culture in Williams Medium E. Next day, cells were exposed to heat and hydrogen peroxide stress followed by collection of extracellular supernatants at various time points for metabolite analysis and measurement of other parameters. The experimental scheme is shown below:

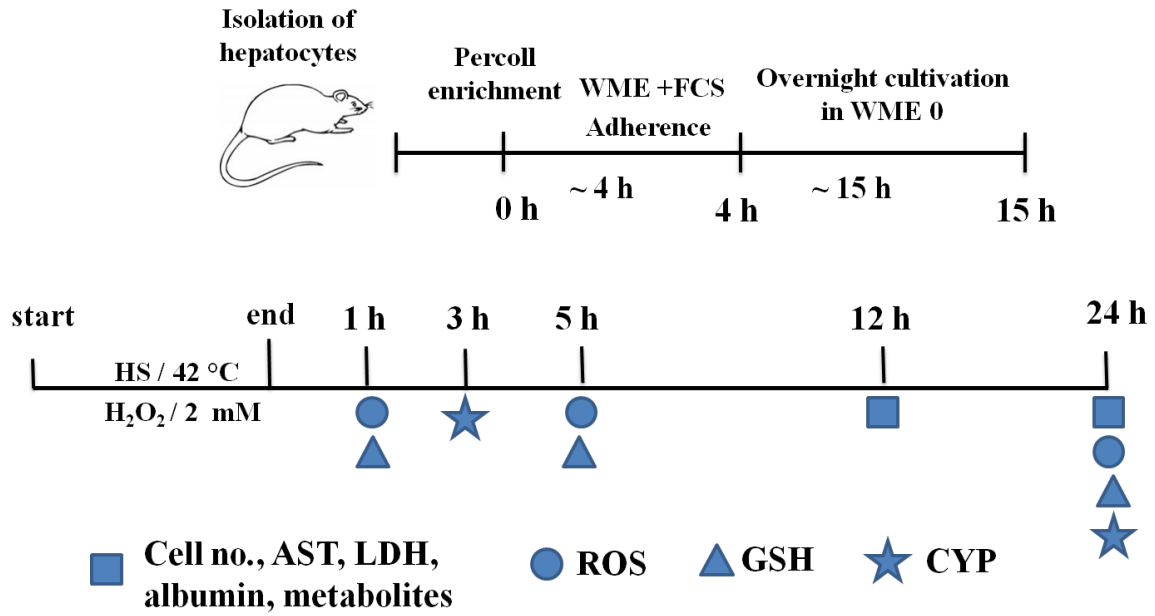

Figure 6-1 Experimental design to study the effect of oxidative stress (due to heat and hydrogen peroxide) on various biochemical parameters and metabolite levels in PRH isolated from old (23 months) and middle (6 months) age rats. Symbols indicate time points of sampling. HS – heat stress, H_2O_2 – hydrogen peroxide stress. The upper part refers to cell preparation; the lower part refers to stress experiments.

6.2. Calculation of extracellular rates

The following equation was used for the calculation of substrate consumption and product formation rates of amino acids, glucose, lactate, pyruvate, urea, AST, LDH and albumin:

$$r = \frac{(C_{r,t2} - C_{r,t1}) * V_w}{\Delta t * \text{Cell Number}_{t2}} \qquad \text{Eq (4.1)}$$

where, r is the specific consumption or production rate (fmol/cell/h). $C_{r,t2}$ is concentration measured at 12 h and $C_{r,t1}$ is measured at 0 h for 0 -12 h time interval, $C_{r,t2}$ is concentration measured at 24 h and $C_{r,t1}$ measured at 12 h for 12 - 24 h time interval, V_w is the volume of the culture well and Δt is the time difference, Cell Number_{t2} is living cell number at 12 h or 24 h.

r > 0 signifies production of a metabolite and r < 0 signifies consumption of the metabolite.

6.3. Statistical analysis

The experiments were carried out in hepatocytes isolated from 3 middle and 3 old age rats (N = 3), with 3 biological replicates (n = 9) in each. The results have been presented as fold change of various parameters (metabolite rates, enzyme activities of AST, LDH, CYP450, cell viability, and intracellular ROS, GSH and albumin production) in heat (HS) or hydrogen peroxide stress (H_2O_2) hepatocytes and control hepatocytes (cont) from middle and old age rats.

$$R_{HS} = \frac{r_{HS}}{r_{cont}} \qquad \text{Eq 6.1}$$

$$R_{H_2O_2} = \frac{r_{H_2O_2}}{r_{cont}} \qquad \text{Eq 6.2}$$

where, R is the ratio of the uptake or the production rate of the respective metabolite or cellular parameter of HS (r_{HS}) or H_2O_2 stressed hepatocytes ($r_{H_2O_2}$) with respect to control hepatocytes (r_{cont}). A negative value of R represents change in the direction of the respective metabolic rate for stressed hepatocytes in comparison to control hepatocytes.

An unpaired Student's t-test and principal component analysis (PCA) was performed using MatLab 2012b® (MathWorks, Nattick, MA, USA). Differences between two measurements were considered significant at $p < 0.001$, $p < 0.01$ and $p < 0.05$. Data for uptake or production rate of amino acid, urea, glucose, lactate and pyruvate was normalized by Z-score for PCA analysis (in-built MatLab routine) (See details of PCA analysis in Sec 4.3).

6.4. Results

6.4.1. Damaging effect of heat and hydrogen peroxide stress on old age PRH

Changes in cell viability, rate of albumin production, rate of enzymatic activity of AST, LDH for middle and old age PRH after exposure to heat (42 °C / 1 h) and hydrogen peroxide stress (2 mM / 1 h) with respect to control PRH were measured for, 0 - 12 h and 12 - 24 h time interval (using Eqs. 6.1 and 6.2). A 10% decrease in cell viability was seen for old age PRH exposed to HS and H_2O_2 stress during 12 - 24 h (Figure 6-2a). From 0 – 12 h, a 10% decrease in albumin production was seen for old age PRH exposed to H_2O_2. Whereas, middle age PRH showed an almost 30% decrease throughout 24 hours (Figure 6-2b). A significant increase in liver specific AST and LDH activity was observed for H_2O_2 stressed old age PRH from 12 - 24 h. Heat stress lead to only 3 – 5% increase in enzyme activity (Figure 6-2c,d).

6.4.2. Intracellular ROS and GSH production due to oxidative stress in old age PRH

The fold changes in intracellular ROS and GSH as markers of oxidative stress were measured for PRH stressed with heat (HS) and H_2O_2 and compared to control PRH after 1, 5 and 24 h. Old age hepatocytes showed an almost 50% increase in ROS at 1 h accompanied by an increase in GSH at 1 and 5 hours for H_2O_2 exposed cells. The values came down to control levels at 24 hours. Middle age PRH showed no significant changes in ROS or GSH. There was no significant increase in ROS values for heat stress in old and middle age PRH. Heat stressed old age PRH showed no significant change in GSH values at 1 and 24 hours (Figure 6-3).

However, as discussed in Sec. 3.1, old age hepatocytes showed increase in ROS during the time of heat exposure. It came down to control levels as soon as the heat stress exposure was over.

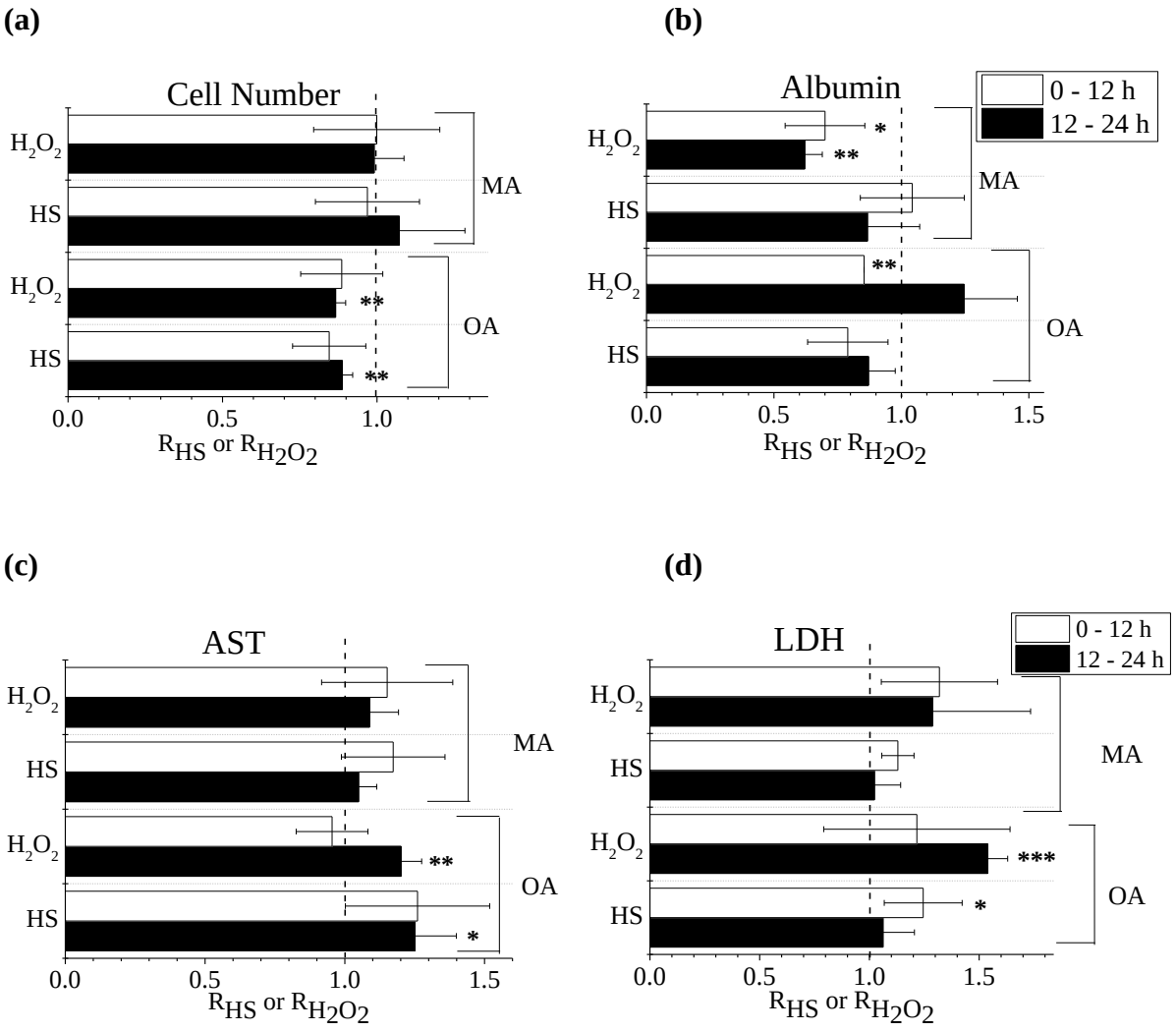

Figure 6-2 Ratio of responses of heat stress (HS) $\mathbf{R_{HS}}$ and hydrogen peroxide stress (H_2O_2) $\mathbf{R_{H_2O_2}}$ to control PRH (calculated according to Eq. 6.1 and 6.2) in (a) cell number at 12 and 24 h (b) albumin production (c) AST (d) LDH activity for 0 – 12 and 12 – 24 h for middle age (MA) and old age (OA) PRH. *, **, *** indicate significance at $p < 0.05$, $p < 0.01$ and $p < 0.001$ respectively compared to control hepatocytes (R = 1, dashed line). All values are specific ratios related to cell number determined by Calcein AM. Error bars indicate standard deviations (N = 3, n = 9). AST, aspartate transaminase; LDH, lactate dehydrogenase (measured as U/l/cell/h); albumin (measured as fg/cell/h). Original data is shown in supplementary Tables S5 and S6.

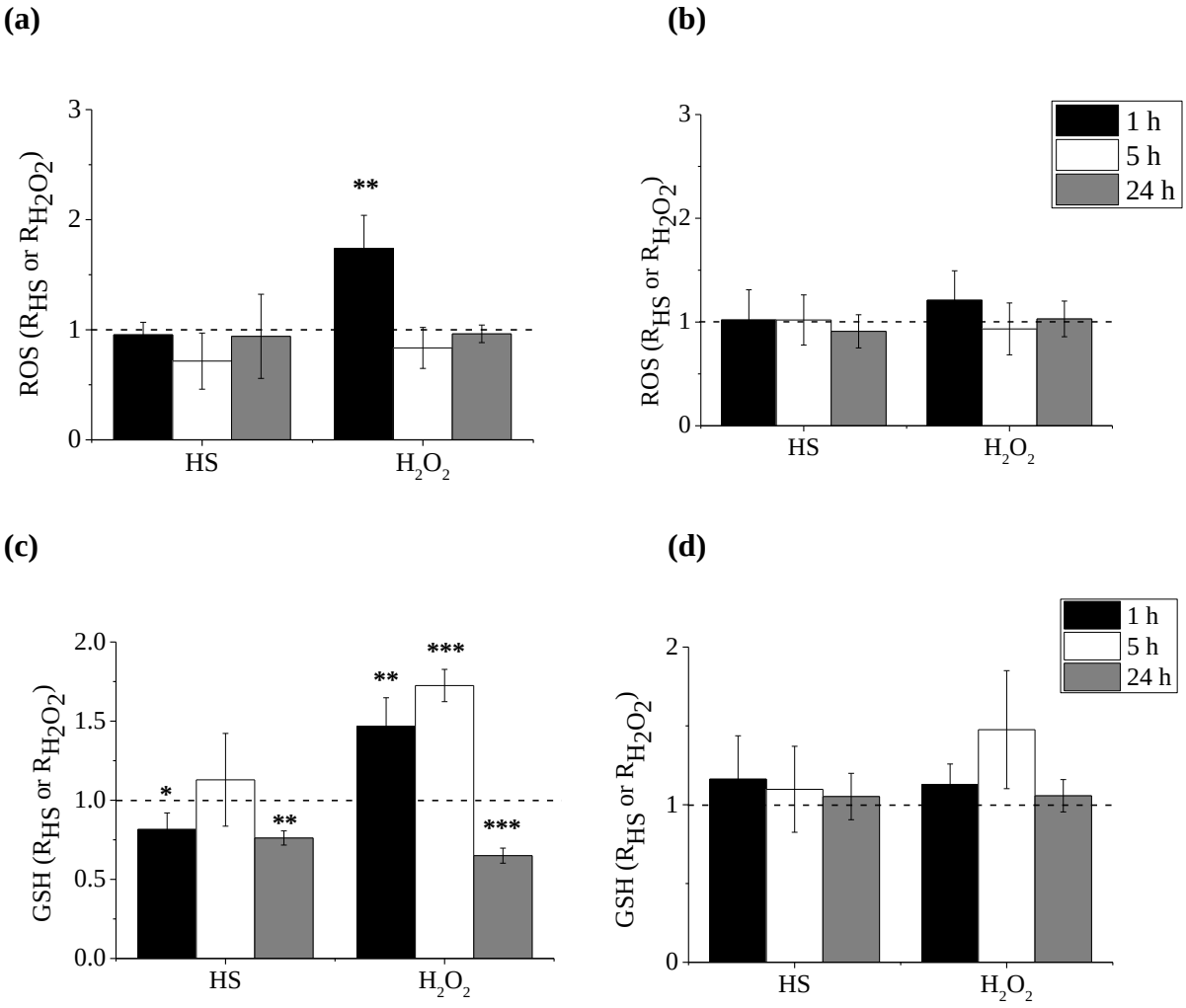

Figure 6-3 Ratio of responses of heat stress (HS) $\mathbf{R_{HS}}$ and hydrogen peroxide stress (H_2O_2) $\mathbf{R_{H_2O_2}}$ to control PRH (calculated according to Eq. 6.1 and 6.2) in (a) ROS (c) GSH in old age PRH (b) ROS (d) GSH in middle age PRH at 1, 5 and 24 h. *, **, *** indicate significance at $p < 0.05$, $p < 0.01$ and $p < 0.001$ respectively compared to control hepatocytes (R = 1, dashed line). All values are specific ratios related to cell number determined via protein content. Error bars indicate standard deviations (N = 3, n = 9). ROS, reactive oxygen species (measured as RFU/cell); GSH, reduced glutathione (measured as nmol/mg protein). Original data is shown in supplementary Tables S5 and S6.

6.4.3. Effect of oxidative stress on CYP 450 activity

To assess liver-specific drug-metabolizing function, a CYP 450 activity assay was performed at 3 h and 24 h of cultivation i.e. its metabolizing capacities in the early phase and at the end of the culture. Ratios of activities of the investigated CYP isoform after 3 h assay time for HS and H_2O_2 stressed to control hepatocytes isolated from old and middle age rats (according to Eq 6.1 and 6.2) are shown in Figure 6-4. Hepatocytes isolated from middle age rats exposed to HS and H_2O_2 stress show significant decrease in activity of CYP enzymes as compared to control PRH. Old age hepatocytes exposed to H_2O_2 stress showed significantly lower activity

of CYP1A2, CYP2C9, CYP2B6 and CYP3A4 enzymes whereas HS hepatocytes showed significantly lower activities for CYP1A2 and CYP2C9 at 24 hours.

6.4.4. Metabolite analysis due to heat stress in old and middle age PRH

Amino acids, glucose, lactate, pyruvate and urea were measured in the extracellular supernatants at 12 and 24 hour of cell culture for control and heat stress hepatocytes. The uptake or production rates of these metabolites were determined (according to Eq. 4.1) for 0 – 12 h and 12 – 24 h. A 2-D plot of the scores of the two most significant factors of PCA using Z-score was made for control and heat stressed middle and old age PRH at 0 - 12 and 12 - 24 h. Hepatocytes from one of the middle age rats at 12 hour was a clear outlier in comparison to the hepatocytes from the other two rats (Figure 6-5a). It showed significant differences in uptake rates of amino acids Asn, Ser, Gln and Ala from 0 – 12 h in comparison to the hepatocytes from other two rats (see supplementary Table S1b). Hence this outlier was removed to obtain another PCA plot (Figure 6-5b). In this plot a clear separation of middle and old age PRH with respect of uptake or production rates of metabolites under control and heat stress conditions was observed. The variation shown by PC1 (45.7%) and PC2 (18.1%) was also improved after removing this outlier. Hepatocytes from the three old age rats showed generally significant variations among themselves.

A 2-D PCA plot of PC1 and PC2 was made separately for old and middle age PRH under control and heat stress conditions. The hepatocytes from the three individual old age rats showed more individual variations than separation based on heat stress (Figure 6-6a). 90% confidence ellipses show the clusters three old age rats for both control (blue) and heat stressed (green) hepatocytes. On the other hand, hepatocytes from the three middle age rats were more closely grouped (Figure 6-6b). However no separation due to heat stress was observed.

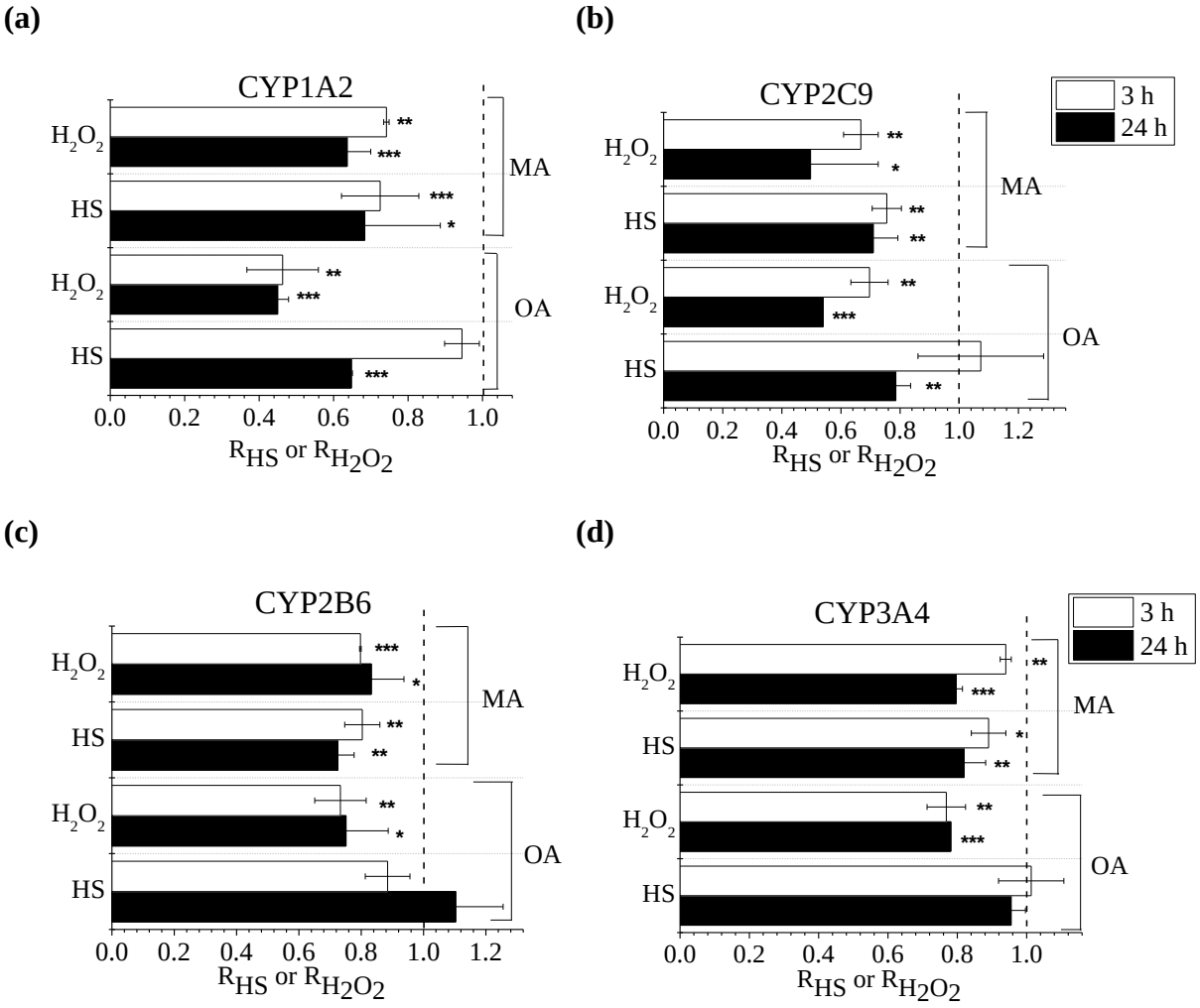

Figure 6-4 Ratio of responses of heat stress (HS) $\mathbf{R_{HS}}$ and hydrogen peroxide stress (H_2O_2) $\mathbf{R_{H_2O_2}}$ to control PRH (calculated according to Eq. 6.1 and 6.2) in CYP enzyme activities (a) CYP1A2 (b) CYP2C9 (c) CYP2B6 (d) CYP3A4 at 3 and 24 h for middle age (MA) and old age (OA) PRH. *, **, *** indicate significance at $p < 0.05$, $p < 0.01$ and $p < 0.001$ respectively compared to control hepatocytes (R = 1, dashed line). All values are specific ratios related to cell number determined via protein content. Error bars indicate standard deviations (N = 3, n = 9). CYP, cytochrome P450 (measured as pM/cell/h). Original data is shown in supplementary Tables S5 and S6.

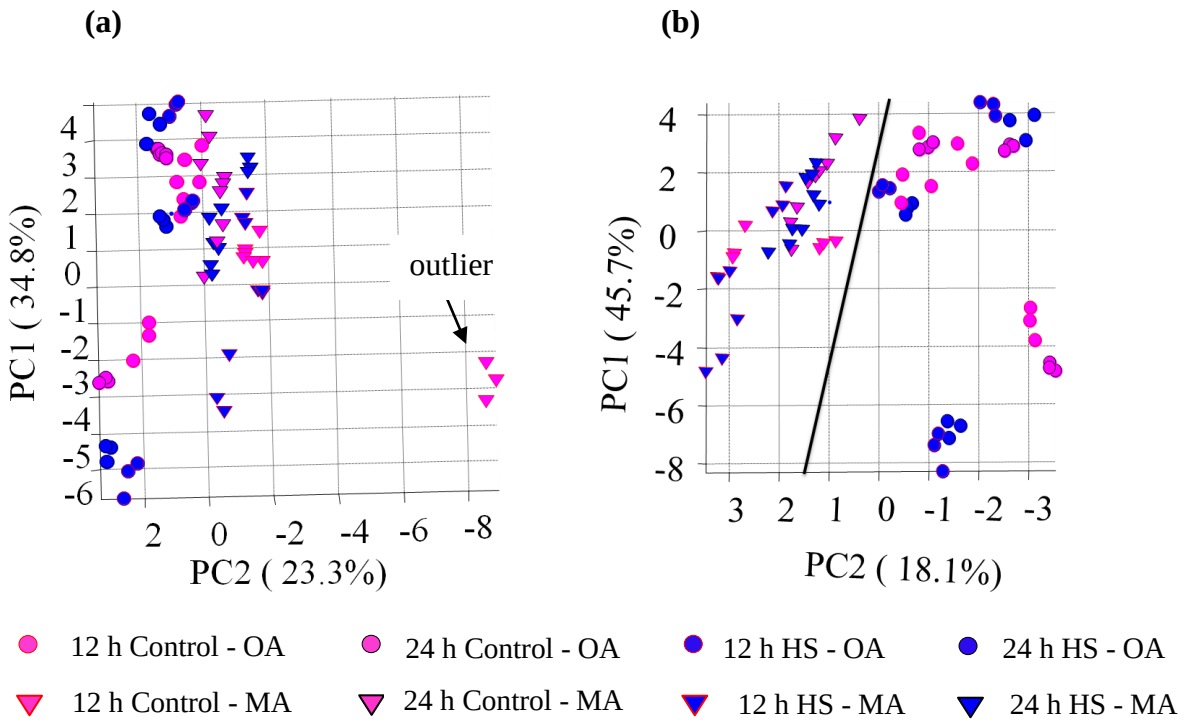

Figure 6-5 PCA of metabolic rates after heat stress (a) PCA scores of specific rates of amino acids, glucose, lactate, pyruvate and urea (in fmol/cell/h) measured during 0 – 12 and 12 – 24 h (N = 3, n = 9) of middle (MA) and old age (OA) PRH exposed to heat stress (HS). The data has been normalized according to the Z-score (MatLab pca routine). (b) Metabolite rates during 0 – 12 h for one of the control middle age rat (n = 3) is an outlier in comparison to other data points. This outlier has been removed to generate a second PCA plot showing separation of middle (triangle) and old (circle) age PRH along PC1 and PC2. Original data in supplementary Tables S1,S2,S3,S4.

Heat stress and control PCA plots of the three individual middle and old age rats were made to see if there were any differences due to heat stress. However overlaps in clusters of control and heat stress data was observed for both the rats (supplemetary Figure S2 and S3).

This signifies that heat stress in hepatocytes isolated from old and middle age rats does not result in significant changes in the metabolite profiles of hepatocytes.

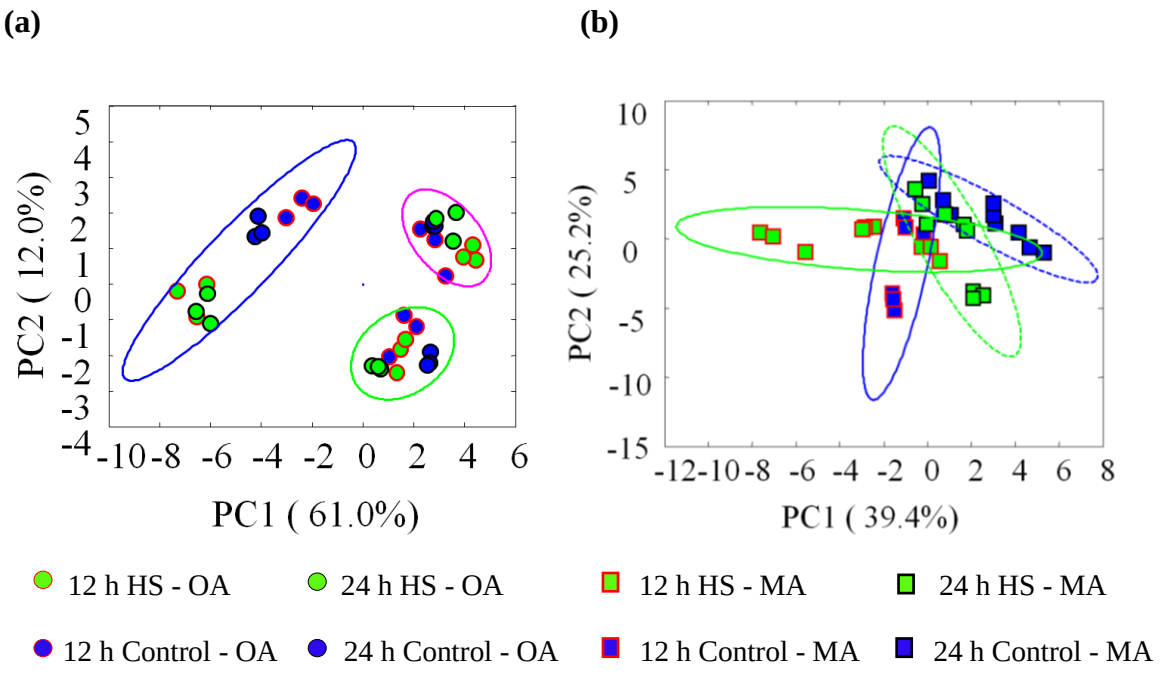

Figure 6-6 PCA scores of specific metabolite rates (measured as fmol/cell/h) for heat stress (HS) and control (C) PRH isolated from (a) old age (OA) and (b) middle age (MA) SD rats for 0 – 12 h and 12 – 24 h (N = 3, n = 9) time interval. The data has been normalized according to the Z-score (MatLab pca routine). (a) 90% confidence ellipses show the clusters of individual old age rats for control and heat stress (b) 90% confidence ellipses show the clusters of control and heat stressed middle age PRH at 0 – 12 (solid line) and 12 – 24 h (dashed line). Outliers for control MA PRH at 12 h (n =3) have been left out in this PCA plot.

6.4.5. Effect of hydrogen peroxide stress on aged hepatocytes

A 3-D plot of the scores of the three most significant factors of PCA using Z-score was made for control and hydrogen peroxide stress in middle and old age PRH at 0 – 12 and 12 – 24 h. The variation shown by PC1, PC2 and PC3 was 32%, 26.4%, and 14.5% respectively. One of the middle age rats under control and hydrogen peroxide stress at 12 hours was a clear outlier in comparison to other rats (Figure 6-7a). This is the same rat as before (see Sec 5.4.4) which shows significant differences in uptake rates of amino acids Asn, Ser, Gln and Ala during 0 – 12 h for control and hydrogen peroxide groups in comparison to the other two rats (see supplementary Table S1b). Hence this outlier was removed to obtain another PCA plot (Figure 6-7b). In this plot a clear separation of middle and old age rats with respect to metabolite uptake or production rates under control and hydrogen peroxide stress conditions was observed. PC1, PC2 and PC3 accounted for maximum variation of 44.7%, 16.9% and

11.9% respectively. The hepatocytes from the three old age rats showed higher variation among each other in comparison to middle age rats.

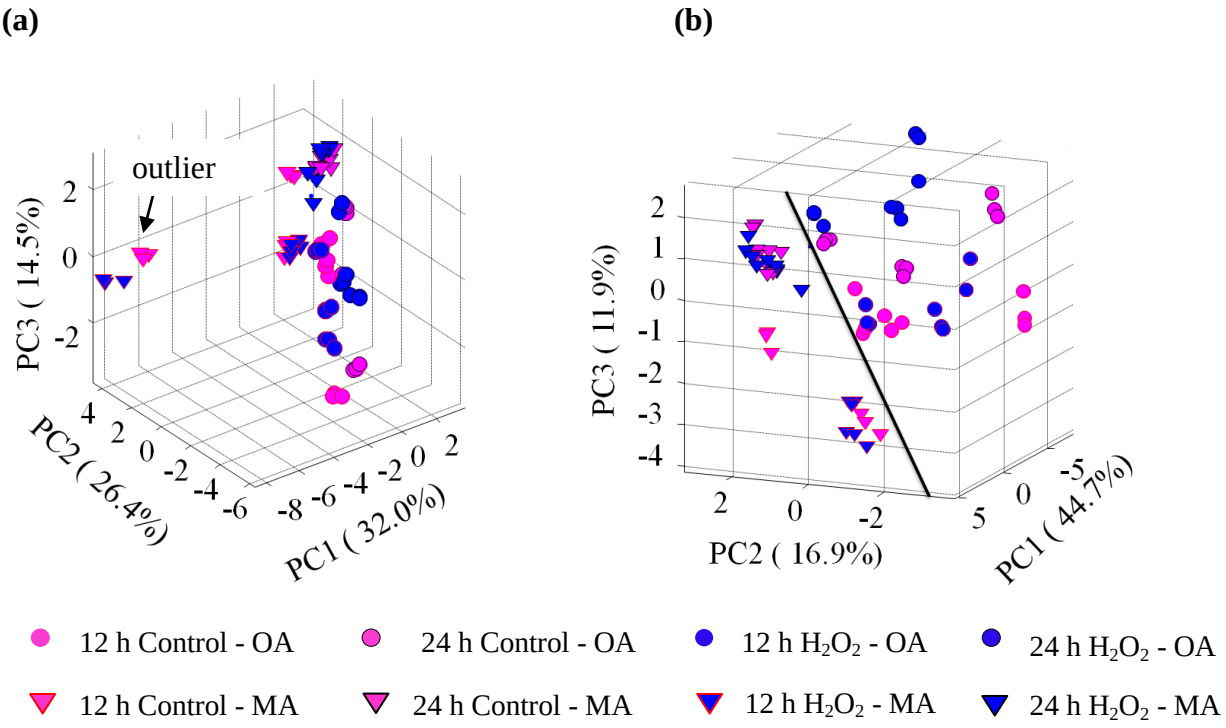

Figure 6-7 PCA of metabolic rates after hydrogen peroxide stress (a) PCA scores of specific rates of amino acids, glucose, lactate, pyruvate and urea (in fmol/cell/h) measured during 0 – 12 and 12 – 24 h (N = 3, n = 9) of middle (MA) and old age (OA) PRH exposed to hydrogen peroxide stress (H_2O_2). The data has been normalized according to the Z-score (MatLab pca routine). (b) Metabolite rates during 0 – 12 h of one middle age rat (n = 3) under control and H_2O_2 stress is an outlier in comparison to other data points. This outlier has been removed to generate a second PCA plot showing separation of middle (triangle) and old (circle) age PRH along PC1, PC2, and PC3. Original data in supplementary Tables S1,S2,S3,S4.

A separate PCA analysis was done for old and middle age PRH under control and hydrogen peroxide stress conditions. The three individual old age rats showed some separation due to hydrogen peroxide stress but due to high individual variations a clear separation due to hydrogen peroxide stress could not be observed (Figure 6-8a). 90% confidence ellipses show the clusters of three old age rats for control (blue) and H_2O_2 (green) stress hepatocytes. Hepatocytes from the three middle age rats were more closely grouped (Figure 6-8b). However no separation due to hydrogen peroxide stress was observed

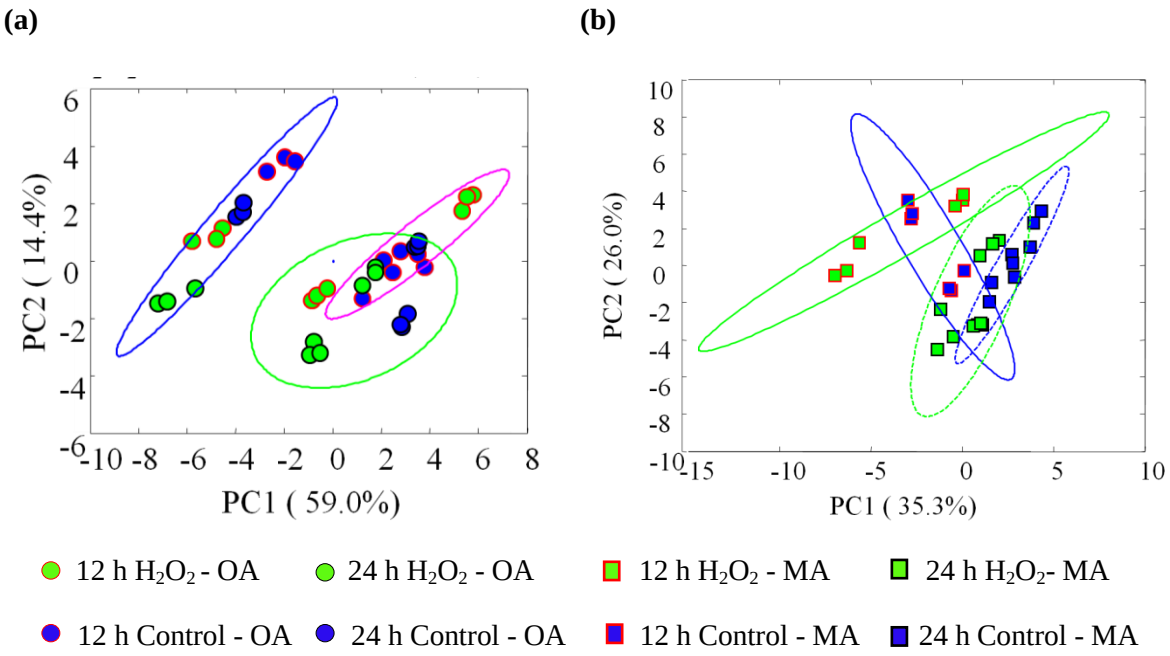

Figure 6-8 PCA scores of specific metabolite rates (measured as fmol/cell/h) for hydrogen peroxide stress (H_2O_2) and control (C) PRH isolated from (a) old age (OA) and (b) middle age (MA) SD rats during 0 – 12 and 12 – 24 h (N = 3, n = 9). The data has been normalized according to the Z-score (MatLab pca routine). (a) 90% confidence ellipses show the clusters of individual old age rats for control and hydrogen peroxide stress (b) 90% confidence ellipses show the clusters of control and hydrogen peroxide stressed middle age PRH at 0 – 12 (solid line) and 12 – 24 h (dashed line). Outliers for control and H_2O_2 stress MA PRH at 12 h (n =3) have been left out in this PCA plot.

A separate PCA analysis was carried out for the three individual old age rats under control and hydrogen peroxide stress conditions (Fig 6-9a,b,c). In this case a clear separation between control (blue) and H_2O_2 stress (green) hepatocytes was observed. 90% confidence ellipses identified separate clusters due to H_2O_2 stress.

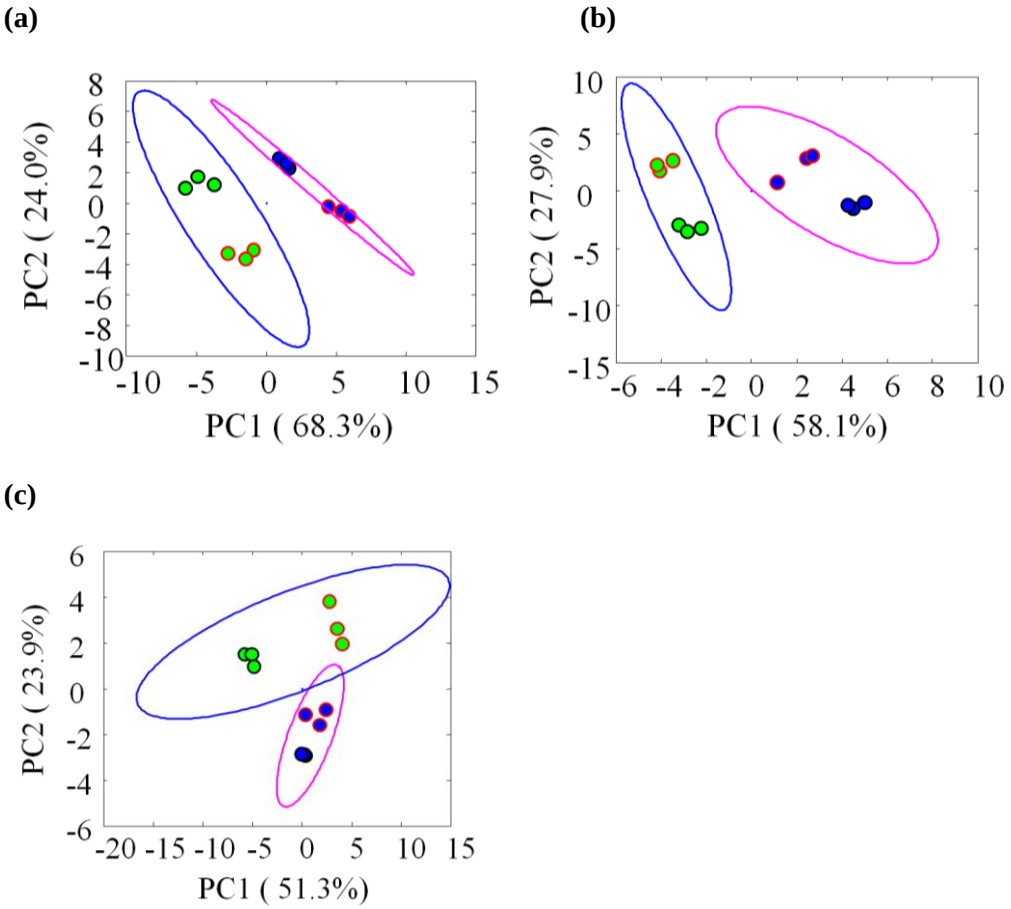

Figure 6-9 PCA scores of hydrogen peroxide (H_2O_2) stress and control (C) hepatocytes isolated from (a) old age (OA) rat 1 (b) old age (OA) rat 2 and (c) old age (OA) rat 3 during 0 – 12 and 12 – 24 hour. The data has been normalized according to the Z-score (MatLab pca routine). 90% confidence ellipses show the clusters for control (pink line) and hydrogen peroxide stress (blue line) cells. Loadings for the PC1 and PC2 are shown in supplementary Figure S4.

Supplementary Fig S4 shows loadings of PC1 and PC2 of control and hydrogen peroxide stressed old age hepatocytes from the three old age rats. PC1 accounted for maximum variation in the data. All the amino acids showed significant loadings to the separation of H_2O_2 stress and control old age PRH. Amino acids showing most significant differences in the uptake or production rates due to hydrogen peroxide stress are shown in Figure 6-11.

On the other hand, a separate PCA plot of the three middle age rats showed overlaps in clusters of control and H_2O_2 stressed PRH (Figure 6-10 a,b,c). These results indicate that middle age hepatocytes are more robust to heat and hydrogen peroxide stress than old age

hepatocytes. Uptake and production rates of amino acids and glucose in hepatocytes isolated from old age rats are susceptible to changes due to hydrogen peroxide stress.

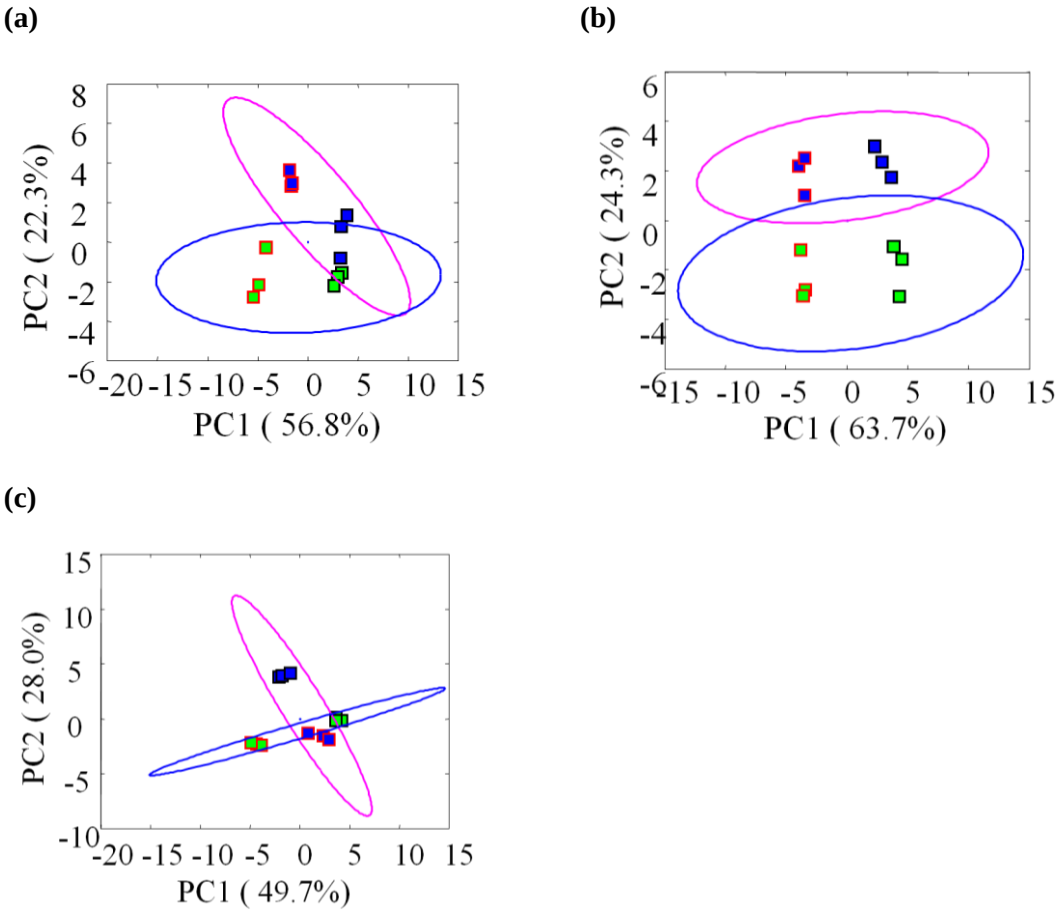

Figure 6-10 PCA scores of hydrogen peroxide (H_2O_2) stress and control (C) hepatocytes isolated from (a) middle age (MA) rat 1 (b) middle age (MA) rat 2 and (c) middle age (MA) rat 3 during 0 – 12 and 12 – 24 hour. The data has been normalized according to the Z-score (MatLab pca routine). 90% confidence ellipses show the clusters for control (pink line) and hydrogen peroxide stress (blue line) cells.

Figure 6-11 summarizes the ratios of specific uptake and production rates of hydrogen peroxide stress to control old age PRH (calculated according to Eq. 6.2) which change significantly due to stress for 0 – 12 h and 12 – 24 h time interval. Only the amino acids where there is a significant change in rates due to H_2O_2 stress i.e. $R_{H_2O_2} > 1$ or < 1 have been shown. There was a significantly higher consumption of essential amino acids Phe and Met. All non-essential amino acids were consumed except for Ser which showed production. Lower production rate of Ser was observed from 0 – 12 h. Major substrate glutamine showed significantly higher uptake rates for hydrogen peroxide stress cells throughout 24 hours of

cultivation. Other non-essential amino acids like His and Ala, were taken up significantly during the first 12 hours of stress. During 12 – 24 h there was significant uptake of many more amino acids like Lys, Phe, Met and other non-essential amino acids feeding TCA cycle like Tyr, Ala, Gly, His and Asn.

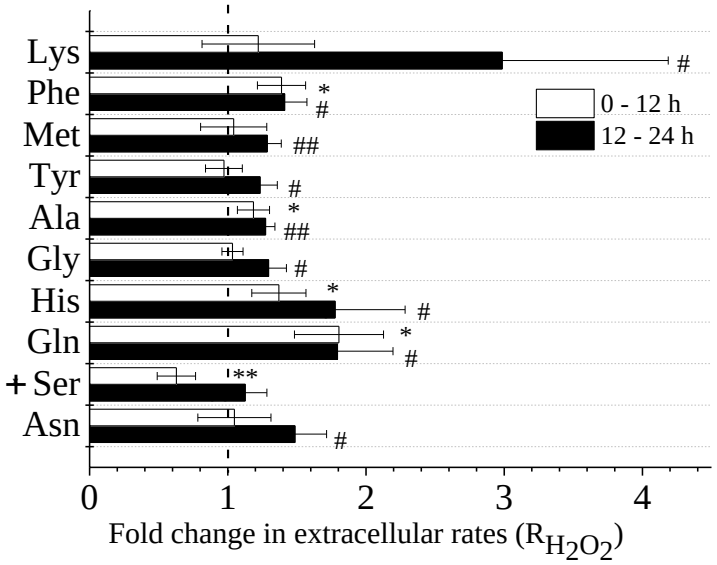

Figure 6-11 Ratio of specific uptake and production rates (measured as fmol/cell/h) of amino acids for hydrogen peroxide (H_2O_2) ($\mathbf{R_{H_2O_2}}$) to control old age PRH (calculated according to Eq. 6.2) measured in extracellular supernatants for 0 – 12 h and 12 – 24 h time interval. *, **, *** indicate significance during 0 – 12 h at $p < 0.05$, $p < 0.01$ and $p < 0.001$ respectively compared to control hepatocytes (R = 1). # represents significance during 12 - 24 h compared to control hepatocytes (R = 1, dashed line). The concentration of metabolites was normalized to cell number determined via Calcein AM. Error bars indicate standard deviations (N = 3, n = 9). All the amino acids were consumed except for Ser which was produced by both control and H_2O_2 stressed PRH at 12 h and 24 h (+ represents production). Original data is shown in supplementary Tables S3, S4.

6.4.6. Effect of oxidative stress on glucose, lactate, pyruvate and urea levels

Consumption of glucose was measured for 0 – 12 h and 12 – 24 h time intervals. Again, here flux ratios for heat stress (R_{HS}) or H_2O_2 ($R_{H_2O_2}$) stress were calculated with respect to control PRH. H_2O_2 stressed middle age PRH showed significantly higher glucose production from 0 – 12 h which decreased from 12 -24 h. HS PRH also showed significantly lower glucose production from 12- 24 h in comparison to first 12 hours. Control old age PRH showed glucose production (see Chapter 5, Figure 5-8a,b) whereas stressed old age PRH showed glucose consumption (see supplementary table S4). Thus a negative fold change for glucose consumption rate was observed (Figure 6-12a). However, for one of the old age PRH there glucose was produced under stress. Thus, high standard deviations were observed. Both types

of PRH produced lactate throughout 24 hours. There was no significant change due to stress (Figure 6-12b). Pyruvate was consumed by both types of PRH. A 5% increase in pyruvate consumption was observed for middle age PRH under H_2O_2 stress from 12 – 24 hours (Figure 6-12c). Urea production as a measure of liver function did not change (Figure 6-12d).

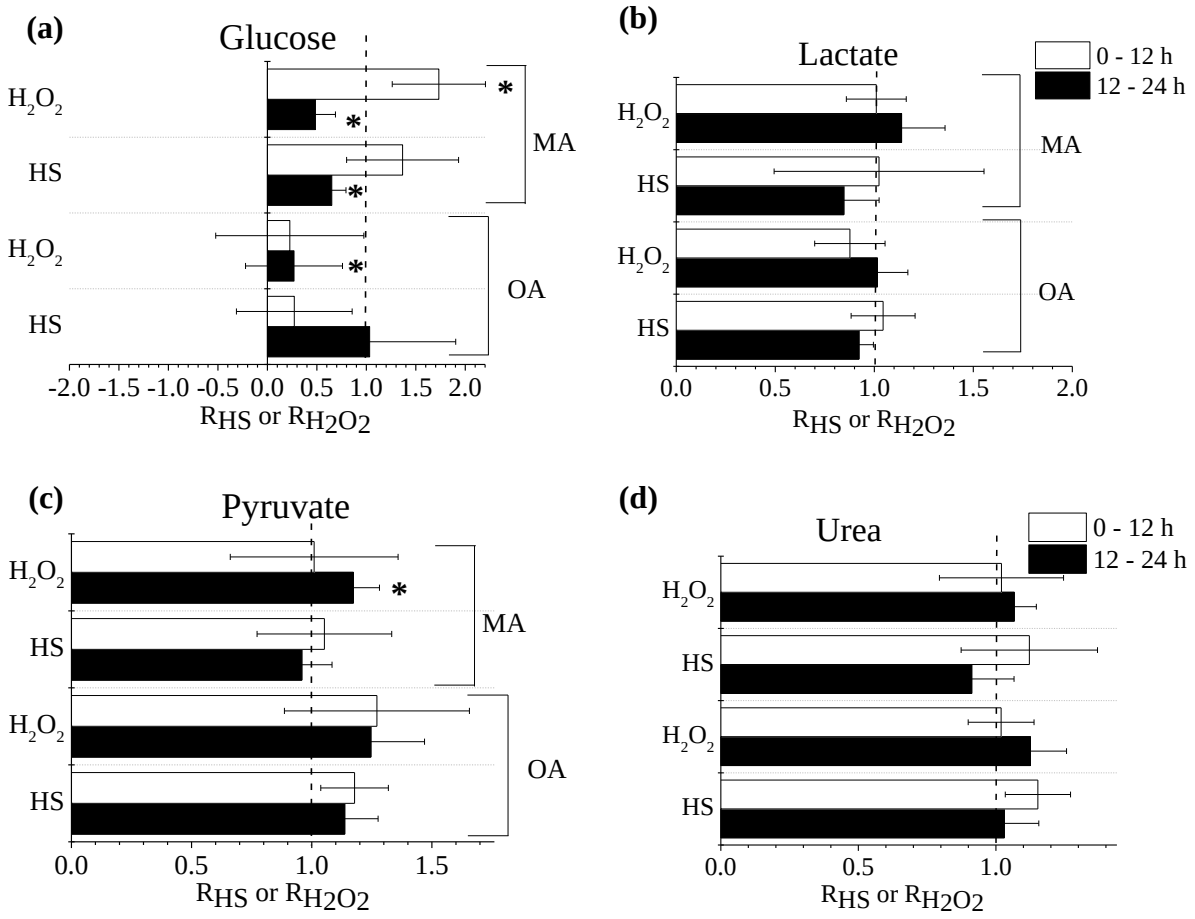

Figure 6-12 Ratio of specific uptake and production rates (measured as fmol/cell/h) of (a) glucose (b) lactate (c) pyruvate and (d) urea for heat stress (HS) ($\mathbf{R_{HS}}$) and hydrogen peroxide stress (H_2O_2) ($\mathbf{R_{H_2O_2}}$) PRH to control PRH (calculated according to Eq. 6.1 and 6.2) measured in extracellular supernatants from 0 – 12 h and 12 – 24 h for middle age (MA) and old age (OA) PRH. Glucose is always produced by control old age PRH. Negative values indicate glucose consumption due to stress in old age PRH. *, **, *** indicate significance at $p < 0.05$, $p < 0.01$ and $p < 0.001$ respectively compared to control hepatocytes (R = 1, dashed line). The concentration of metabolites was normalized to cell number determined via Calcein AM. Error bars indicate standard deviations (N = 3, n = 9). Original data is shown in supplementary Tables S1, S2, S3, S4.

6.5. Discussion

In this work, we investigated the effect of heat and hydrogen peroxide stress on the extracellular metabolism of hepatocytes isolated from aged rats. To this end, hepatocytes from old and middle age rats were isolated and cultivated for 24 hours following oxidative stress. Changes in metabolites and various biochemical parameters were analyzed during 0 – 12 and 12 – 24 h to study the impact of aging on stress tolerance. Studies related to heat stress on the liver metabolism have been done *in vivo* analyzing plasma or liver extracts (Zhang et al., 2003; Biljana et al., 2013; Ippolito et al., 2014). The age dependent effect of hydrogen peroxide stress was studied on various cellular pathways (Ikeyama et al., 2002). To the best of our knowledge, there have been no studies distinctly differentiating the effect of oxidative stress due to both heat and hydrogen peroxide stress on the metabolism of hepatocytes isolated from differently aged rats.

Hepatocytes were exposed to 42 °C for one hour and 2 mM hydrogen peroxide for one hour followed by metabolite analysis. This temperature and concentration of hydrogen peroxide were chosen as there was increased intracellular ROS with 90% cell viability (see Sec 3.1).

Old age PRH showed lower cell number accompanied by increase in AST and LDH during 12 – 24 h (Figure 6-2). Thus, old age hepatocytes tend to become leaky or damaged due to stress. These parameters remain unchanged for middle age PRH indicating their resistance to the stress. Another parameter to measure liver function is albumin production (Figure 6-2). Middle age PRH unlike old age PRH showed significant decrease in albumin production due to hydrogen peroxide stress. Middle age hepatocytes show almost 2-3 fold higher albumin production, thus we see a noticeable effect on albumin. But, old age PRH showed low albumin production in comparison (see chapter 5, Figure 5-2) and thus we could not observe significant variation with stress treatment. However, in case of hydrogen peroxide stress, a decrease in albumin was still observed during the first 12 hours of cultivation indicating the susceptibility of old age hepatocytes to hydrogen peroxide stress.

The susceptibility of old age PRH to hydrogen peroxide stress could be further seen in the values of intracellular ROS (Figure 6-3): Old age PRH exposed to hydrogen peroxide stress showed higher ROS one hour after the exposure. Correspondingly an increase in GSH was observed to counteract this stress. Heat stress did not result in higher ROS generation. However, in previous experiments we observed that ROS are generated during the time cells

are exposed to heat stress and it comes down to basal levels after the stress is over (Figure 3-4). This suggests that free radicals are generated due to heat stress but they have lower life time in *in vitro* hepatocyte culture as compared to when rats are heated followed by liver isolation (as seen in an *in vivo* study by Zhang et al., 2003). Middle age PRH showed no changes in intracellular ROS or GSH due to oxidative stress (Figure 6-3). These results show the susceptibility of old age hepatocytes towards hydrogen peroxide treatment.

The CYP activity assay showed that all investigated CYP enzymes were active during the whole cultivation. CYP activity was affected for both middle and old age PRH exposed to oxidative stress (Figure 6-4). However, CYP1A2 and CYP3A4, the major isoforms involved in drug metabolism showed significantly lower activity for old age PRH exposed to hydrogen peroxide stress in comparison to middle age PRH. The decrease was also more significant in comparison to old age PRH exposed to heat stress. The activity of CYP2C9 and CYP2B6 was also significantly reduced for hydrogen peroxide stress old age PRH. This again shows the susceptibility of old age PRH towards hydrogen peroxide stress in comparison to heat stress and also compared to stressed middle age PRH.

Middle and old age PRH were distinctly separated in a 2-D (Figure 6-5) and 3-D (Figure 6-7) PCA plot made from the normalized specific uptake and production rates of amino acids, glucose, lactate, pyruvate and urea measured for heat and hydrogen peroxide stressed hepatocytes. However, no separation was observed due to heat stress in hepatocytes isolated from old age or middle age rats (Figure 6-6).

On the other hand, old age PRH showed distinct separation in 2-D PCA plot based on their metabolite profiles between hydrogen peroxide stress and control cells (Figure 6-9). This difference was noticeable in separate analysis made for each rat. Old rats tend to show a higher variance in metabolite levels as compared to middle age PRH. This is expected as they stay longer in cages and their differential feeding habits could cause this variation (fed *ad libitum*).

For hydrogen peroxide stressed cells, there was increased uptake of major substrate glutamine and various other essential and non-essential amino acids like Asn, His, Gly, Thr, Ala, Met, Phe and Pro. These amino acids are metabolized in intracellular metabolic pathways like glycolysis and TCA cycle. They could also be used for intracellular protein synthesis and cell maintenance. Thus, we could say that hydrogen peroxide stress leads to increased cellular

demands and utilization of amino acids for various intracellular processes. Thus, we observed higher uptake rates of these amino acids.

As a cellular functional parameter the consumption rate of the carbon substrate glucose was determined (Figure 6-12a). Stressed old age hepatocytes show consumption of glucose in comparison to control old age hepatocytes (see supplementary table S4). Thus, a negative fold change in glucose consumption was observed. The high standard deviation in this rate is due to variance in glucose consumption rates in the PRH isolated from the three old age rats. This could be due to inhibition of gluconeogenesis or depletion of enzymes related to glycogenolysis in contrast to middle age PRH. This is in line with a study by Sumida *et al.* (Sumida et al., 2005) where decreased hepatic gluconeogenesis and glycogenolysis in old age ethanol treated cells as compared to middle age PRH was observed. On the other hand, middle age PRH exposed to heat and hydrogen peroxide stress produce significantly more glucose during the first 12 hours followed by a significant reduction from 12 – 24 hours. It has been shown in a study by Biljana *et al*. (Biljana, 2013) that glucose is released by liver cells up to 6 h after heat stress isolated from heat stressed rats. An upregulation of enzymes related to glycogenolysis was observed. Then the period from 6 to 24 hours was characterized by intensive rebound of glycogen stores leading to reduced glucose production. Our results show a similar trend in glucose production. These results highlight the differences in carbohydrate metabolism between old and middle age PRH exposed to oxidative stress.

From these results, we could say that hepatocytes isolated from old age rats are more susceptible to metabolite changes due to hydrogen peroxide stress than heat stress. Hydrogen peroxide is a strong inducer of free radicals in cells. Depending on its concentration, it can affect various cellular pathways or cause apoptosis (Giorgio et al., 2007). It can be degraded by cells either via glutathione peroxidase or catalase (Oshino et al., 1975; Jones et al., 1978). Thus, it is possible that the lower intracellular GSH levels in old age PRH were not able to completely eliminate hydrogen peroxide leading to changes in metabolite and enzyme levels. Hepatocytes on the other hand can acclimatize to heat stress via generation of heat shock proteins (Moseley, 1997). Hence, we did not observe metabolic variations due to heat stress in old or middle age hepatocytes. Previous studies have shown reduction in organisms ability to tolerate heat stress with age (Hall et al., 2000; Oberley et al., 2008; Zhang et al., 2003). However, these studies have been done *in vivo* in old age rats. This study shows that hepatocytes from old age rats cultured *in vitro* are more robust to extracellular heat stress.

These metabolism results related to oxidative stress could be used to simulate intracellular fluxes to analyze the deleterious effects of oxidative stress on different metabolic pathways during aging. Measurement of other intracellular metabolites would help to strengthen this model to determine more accurately the intracellular fluxes. Manipulation of these pathways could help in finding therapeutic interventions to counteract the aging related diseases.

7. Quercetin treatment affects metabolite rates in middle age primary rat hepatocytes exposed to oxidative stress

Abstract

The effects of antioxidant quercetin on primary rat hepatocytes (PRH) exposed to oxidative stress were studied. It is one of the most abundant flavonoids in the human diet found in fruits and vegetables. Primary rat hepatocytes from 6 and 24 month old male Sprague-Dawley rats were pre-treated with 50 µM quercetin for 4 hours followed by exposure to oxidative stress via hydrogen peroxide (H_2O_2) (2 mM for 1 h) and heat (HS) (42 °C for 1 h). Various cellular parameters and extracellular metabolites were measured for 0 – 12 h and 12 – 24 h time interval. There was a decrease in intracellular ROS and GSH and increased LDH leakage in quercetin treated middle age hepatocytes. This is due to conversion of quercetin to oxidized quercetin which arylates with GSH causing GSH consumption and LDH leakage in middle age PRH. In a 2-D PCA plot of specific uptake production rates of amino acids, organic acids and urea, HS and H_2O_2 stressed middle age PRH were clearly separated from quercetin pre-treated cells. There was an increase in uptake of amino acids due to quercetin pre-treatment suggesting changes in intracellular metabolism. There was also an increase in glucose production indicating an effect of quercetin on glucose metabolism in cells. Old age hepatocytes showed no distinct changes in metabolite levels due to quercetin. Thus, we could say that, surprisingly, oxidatively stressed middle age PRH are more susceptible to metabolic changes under quercetin treatment in comparison to old age PRH. The results from this study contribute to an improved understanding of the effect of quercetin on differentially aged hepatocytes exposed to oxidative stress.

Introduction

Oxidative stress produced in cells is counteracted by its endogenous anti-oxidant defenses. Two of the most commonly externally supplied anti-oxidants are N-acetylcysteine and Quercetin.

N-acetylcysteine (NAC), containing an acetylated form of the amino acid L-cysteine is widely used as an anti-oxidant *in vivo* and *in vitro*. It functions as a precursor of cysteine, the rate-limiting step in glutathione synthesis (Atkuri et al., 2007). In humans it can be administered orally or by intravenous infusion and can also be inhaled using a nebulizer. Currently it is used as an antioxidant and a mucolytic agent (Dodd et al., 2008). Its clinical applications have been shown in conditions such as HIV infection, cancer, heart disease, kidney and liver diseases (Kelly 1998).

Quercetin (3,3′,4′,5,7-pentahydroxyflavone) is one of the most abundant flavonoids in the human diet, which is found in fruits and vegetables such as blueberries, onions, curly kale, broccoli, and leek (Manach et al., 1999). It has a broad range of activity, such as antioxidative and hypolipidemic properties, ROS scavenging, anti-inflammatory and anti-fibrotic properties (El-Nekeety et al., 2014). Daily intake of quercetin is estimated at up to 25 mg/day in a normal human diet (Dajas et al., 2003). Its chemical structure (as shown below) includes phenolic hydroxyl groups, which imparts its antioxidant properties with significant therapeutic potential against many diseases, including hepatic diseases, ischemic heart disease, atherosclerosis, cancer and kidney damage (Chobot, 2010; Singh et al.,2004; Tokyol et al., 2006)

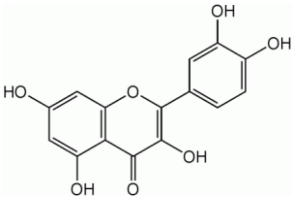

Chemical Structure of quercetin

In one study, quercetin protected rat brain from lipopolysaccharide (LPS)-induced shock by attenuating lipid peroxidation and nitric oxide generation (Gawad et al., 2001). Various *in vitro* and animal studies demonstrated inhibition of degranulation from mast cells, basophils and neutrophils by quercetin. It inhibits Jun amino-terminal kinases (JNK) / Stress-activated

protein kinases (SAPK), its substrate C-Jun (encoded by the JUN gene) and iNOS (inducible nitric oxide synthase) transcription, in part, by suppressing activation of the transcription factor AP-1 (activator protein) (Wadsworth et al., 2001). JNK/SAPK is a member of the mitogen activated protein kinase (MAPK) family which are activated by a variety of environmental stresses, inflammatory cytokines and growth factors (Nishina et al., 2004). It also modulates the activity of inflammatory mediators by inhibiting nuclear factor kappa B (NF-kB) (Rangan et al., 1999; Pilkhwal et al., 2010). Its role in inhibiting oxidative stress in primary hepatocytes has also been extensively studied (El-Nekeety et al., 2014; Li et al., 2013; Pilkhwal et al., 2010; Weina et al., 2009).

NAC at various concentrations did not show any effect on intracellular ROS levels for middle age PRH exposed to heat stress (see Sec 3.2). However, cells pre-treated with quercetin for 4 hours at 50 μM concentration significantly reduced intracellular ROS generation. This concentration was taken based on a previous study (Liu et al. 2010) where quercetin pre-treatment of rat hepatocytes followed by ethanol exposure was able to reduce the cytotoxic effects of ethanol. It was seen that quercetin (50 μM) pre-treatment before ethanol exposure could reduce the release of LDH and AST significantly. However, quercetin (50 μM) co-treatment or post-treatment had very little reversing effect. Pre-treatment was able to consistently restore the GSH, SOD and CAT levels but not co-treatment or post-treatment. Thus, we chose to pre-treat the hepatocytes with quercetin followed by exposure to oxidative stress.

In this work hepatocytes isolated from middle and old age rats were pre-treated for 4 hours with 50 μM quercetin followed by exposure to oxidative stress (through heat and hydrogen peroxide). The effect of quercetin as an anti-oxidant on age related oxidative stress was analyzed via analysis of various cellular parameters like AST (aspartate transaminase), LDH (lactate dehydrogenase), intracellular GSH (glutathione), ROS and CYP450 enzymes, albumin and metabolites like amino acids, glucose, lactate, pyruvate and urea for 0 – 12 h and 12 – 24 h time interval. Sampling was done at 0, 12 and 24 hours. Metabolism is furthest down the line from gene to function and is most characteristic of the entire organism phenotype. Therefore, changes in the metabolism would provide a good overview of the effect of the anti-oxidant with age.

7.1. Experimental Design

Freshly isolated primary rat hepatocytes (PRH) from old (23 months) and middle age (6 months) male Sprague – Dawley rats (N = 3) were enriched with Percoll followed by overnight culture in Williams Medium E. Next day, cells were pre-treated for 4 hours with quercetin followed by exposure to heat and hydrogen peroxide stress. Supernatants were collected at various time points for metabolite analysis and measurement of other end point parameters. The experimental scheme is shown below:

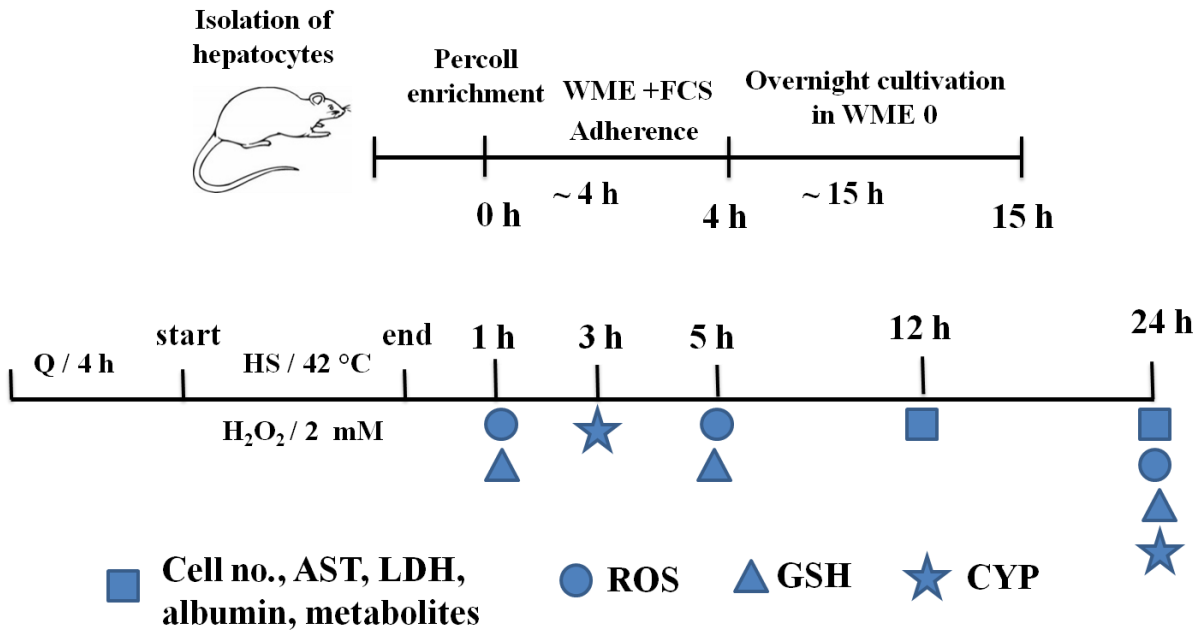

Figure 7-1 Experimental design to study the effect of pre-incubation with quercetin on heat and hydrogen peroxide stress in PRH on various biochemical parameters and metabolite levels in PRH isolated from old (23 months) and middle (6 months) age rats. Symbols indicate time points of sampling. Q – quercetin, HS – heat stress, H_2O_2 – hydrogen peroxide stress. The upper part refers to cell preparation; the lower part refers to stress experiments.

7.2. Calculation of extracellular rates

The following equation was used for the calculation of substrate consumption and product formation rates of amino acids, glucose, lactate, pyruvate, urea, AST, LDH and albumin:

$$r = \frac{(C_{r,t2} - C_{r,t1}) * V_w}{\Delta t * \text{Cell Number}_{t2}} \qquad \text{Eq (4.1)}$$

where, r is the specific consumption or production rate (fmol/cell/h). $C_{r,t2}$ is concentration measured at 12 h and $C_{r,t1}$ is measured at 0 h for 0 -12 h time interval, $C_{r,t2}$ is concentration measured at 24 h and $C_{r,t1}$ measured at 12 h for 12 - 24 h time interval, V_w is the volume of the culture well and Δt is the time difference, Cell Number_{t2} is living cell number at 12 h or 24 h. r > 0 signifies production of a metabolite and r < 0 signifies consumption of the metabolite.

7.3. Statistical analysis

The experiments were carried out in 3 middle and 3 old age rats (N = 3), with 3 biological replicates (n = 9) in each. To observe the effect of quercetin, the results have been presented as fold change of various parameters (metabolite rates, enzyme activities of AST, LDH, CYP450, cell viability, and intracellular ROS, GSH and albumin production) in heat stress (HS+Q) or hydrogen peroxide stress (H_2O_2+Q) hepatocytes pre-treated with quercetin to HS or H_2O_2 stressed hepatocytes from middle and old age rats.

$$R_{HS+Q} = \frac{r_{HS+Q}}{r_{HS}} \qquad \text{Eq 7.1}$$

$$R_{H_2O_2+Q} = \frac{r_{H_2O_2+Q}}{r_{H_2O_2}} \qquad \text{Eq 7.2}$$

where, R is the ratio of the uptake or the production rate of the respective metabolite or cellular parameter of HS+Q (r_{HS+Q}) or H_2O_2+Q ($r_{H_2O_2+Q}$) treated hepatocytes with respect to H_2O_2 stressed ($r_{H_2O_2}$) or HS hepatocytes (r_{HS}). A negative value of R represents change in the direction of the respective metabolic rate for quercetin treated hepatocytes in comparison to non-quercetin treated stressed hepatocytes.

An unpaired Student's t-test and principal component analysis (PCA) was performed using MatLab 2012b (MathWorks, Nattick, MA, USA) ®. Differences between two measurements were considered significant at $p < 0.001$, $p < 0.01$ and $p < 0.05$. Data for uptake or production rate of amino acid, urea, glucose, lactate and pyruvate was normalized by Z-score for PCA analysis (in-built MatLab routine) (See details of PCA analysis in Sec 4.3).

7.4. Results

7.4.1. Effect of quercetin on various cellular parameters

Figure 7-2 shows the changes in cell viability, albumin production and enzymatic activity for middle and old age PRH pre - treated with 50 µM quercetin for 4 hours followed by exposure to heat stress (42 °C / 1 h) and hydrogen peroxide stress (2 mM / 1 h) (as shown by Eq 7.1 and 7.2). No significant effect of quercetin pre-treatment was seen on cell viability for both PRH (Figure 7-2a). A significantly lower albumin production during 0 - 12 and 12 - 24 h was observed for middle age PRH pre-treated with quercetin. No significant changes were seen for old age PRH (Figure 7-2b). Old age PRH pre-treated with quercetin followed by heat and hydrogen peroxide stress showed almost a 20% decrease in AST activity in the first 12 hours of cell culture (Figure 7-2c). 50% increase in LDH activity was observed for middle age PRH pre-treated with quercetin and exposed to heat stress in the first 12 hours. A small increase was also seen for hydrogen peroxide exposed and quercetin pre-treated PRH (Figure 7-2d).

7.4.2. Effect of quercetin on intracellular ROS and GSH

Fold change in intracellular ROS and GSH as markers of oxidative stress were measured after quercetin pre-treatment at 1, 5 and 24 h. A significant decrease in intracellular ROS at 1 h and 5 h was observed for quercetin pre-treated cells in both middle and old age PRH. At 24 hours, the ROS values are comparable to non-quercetin treated hepatocytes. Old age PRH show lower ROS values at 24 hours in comparison to middle age PRH (Figure 7-3a,b). There was almost a 30% decrease in intracellular GSH values at 1 h and 5 h for middle age PRH pre-treated with quercetin. Old age PRH on the other hand showed an increase in GSH for heat stressed cells pre-treated with quercetin. No significant change at 1 h was observed for H_2O_2 exposed cells. A 10% decrease was observed at 5 h (Figure 7-3c,d).

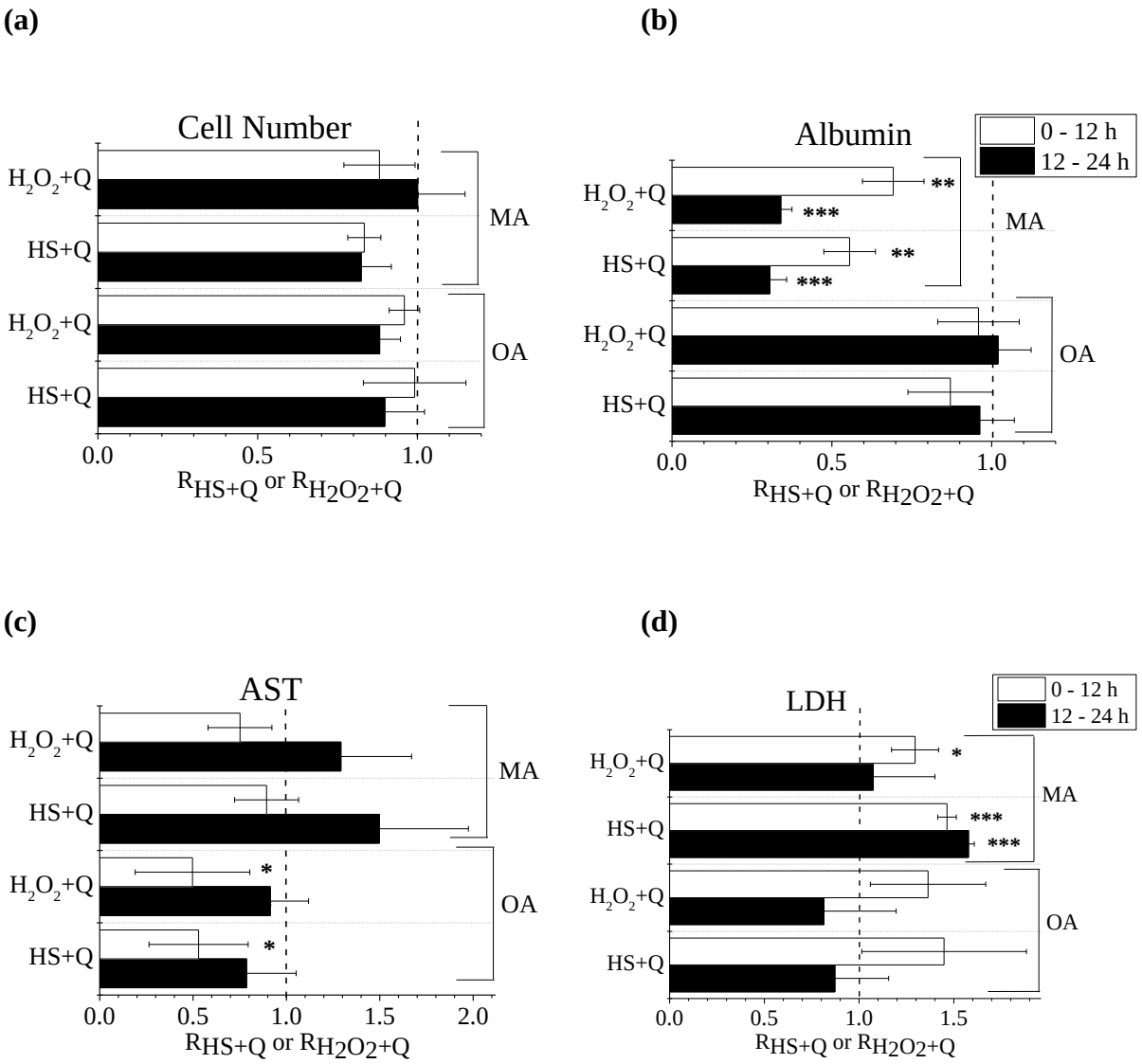

Figure 7-2 Ratio of responses of heat stress with quercetin (HS+Q) ($\mathbf{R_{HS+Q}}$) and hydrogen peroxide stress with quercetin (H_2O_2+Q) ($\mathbf{R_{H_2O_2+Q}}$) to HS or H_2O_2 exposed PRH (calculated according to Eq. 7.1 and 7.2) in (a) cell number at 12 and 24 h (b) albumin production (c) AST (d) LDH activity during 0 – 12 and 12 – 24 h for middle age (MA) and old age (OA) PRH.. *, **, *** indicate significance at $p < 0.05$, $p < 0.01$ and $p < 0.001$ respectively compared to non quercetin pre-treated stressed hepatocytes (R = 1, dashed line). All values are specific ratios related to cell number determined by Calcein AM. Error bars indicate standard deviations (N = 3, n = 9). AST, aspartate transaminase; LDH, lactate dehydrogenase (measured as U/l/cell/h); albumin (measured as fg/cell/h). Original data is shown in supplementary table S5, S6.

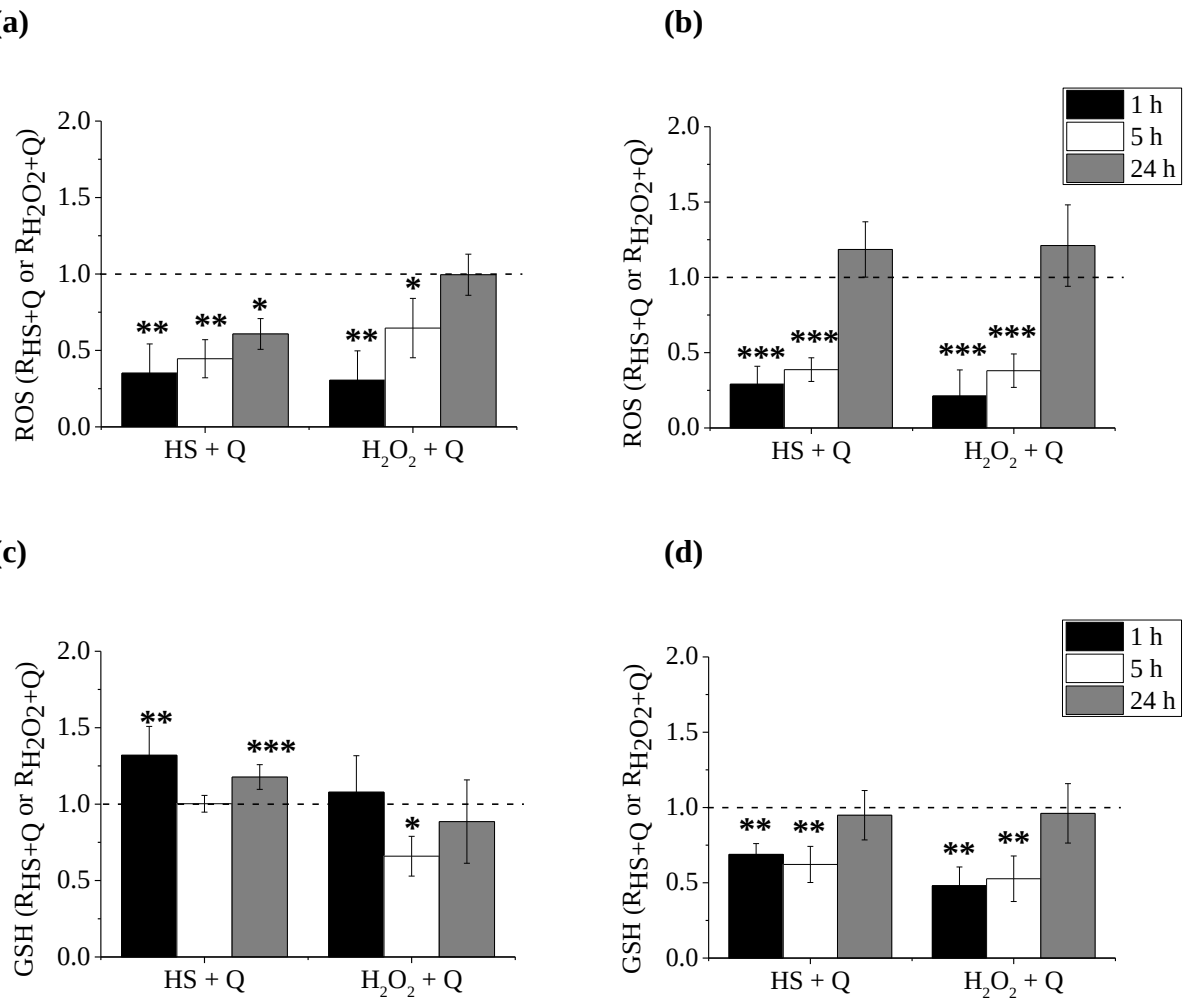

Figure 7-3 Ratio of responses of heat stress with quercetin (HS+Q) ($\mathbf{R_{HS+Q}}$) and hydrogen peroxide stress with quercetin (H_2O_2+Q) ($\mathbf{R_{H_2O_2+Q}}$) to HS or H_2O_2 exposed PRH (calculated according to Eq. 7.1 and 7.2) in (a) ROS (c) GSH for old age PRH (b) ROS (d) GSH for middle age PRH at 1, 5 and 24 h. . *, **, *** indicate significance at $p < 0.05$, $p < 0.01$ and $p < 0.001$ respectively compared to non quercetin pre-treated stressed hepatocytes (R = 1, dashed line). All values are specific ratios related to cell number determined via protein content. Error bars indicate standard deviations (N = 3, n = 9). ROS, reactive oxygen species (measured as RFU/cell); GSH, reduced glutathione (measured as nmol/mg protein). Original data is shown in supplementary Tables S5, S6.

7.4.3. Decrease in CYP 450 activity due to quercetin pre-treatment

To assess liver-specific drug-metabolizing function, a CYP 450 activity assay was performed at 3 h and 24 h of cultivation i.e. metabolizing capacities in the early phase and at the end of the culture were determined. Activities of CYP1A2, CYP2C9, CYP2B6 and CYP3A4 in terms of product formation rates are shown in Figure 7-4. A decrease in activity of CYP isoforms was observed on quercetin pre-treatment for both types of PRH. For CYP2C9 there

was a more significant decrease in activity at 3 h in comparison to 24 hours. For HS+Q old age PRH, the activity at 24 hours was comparable to non-quercetin treated cells.

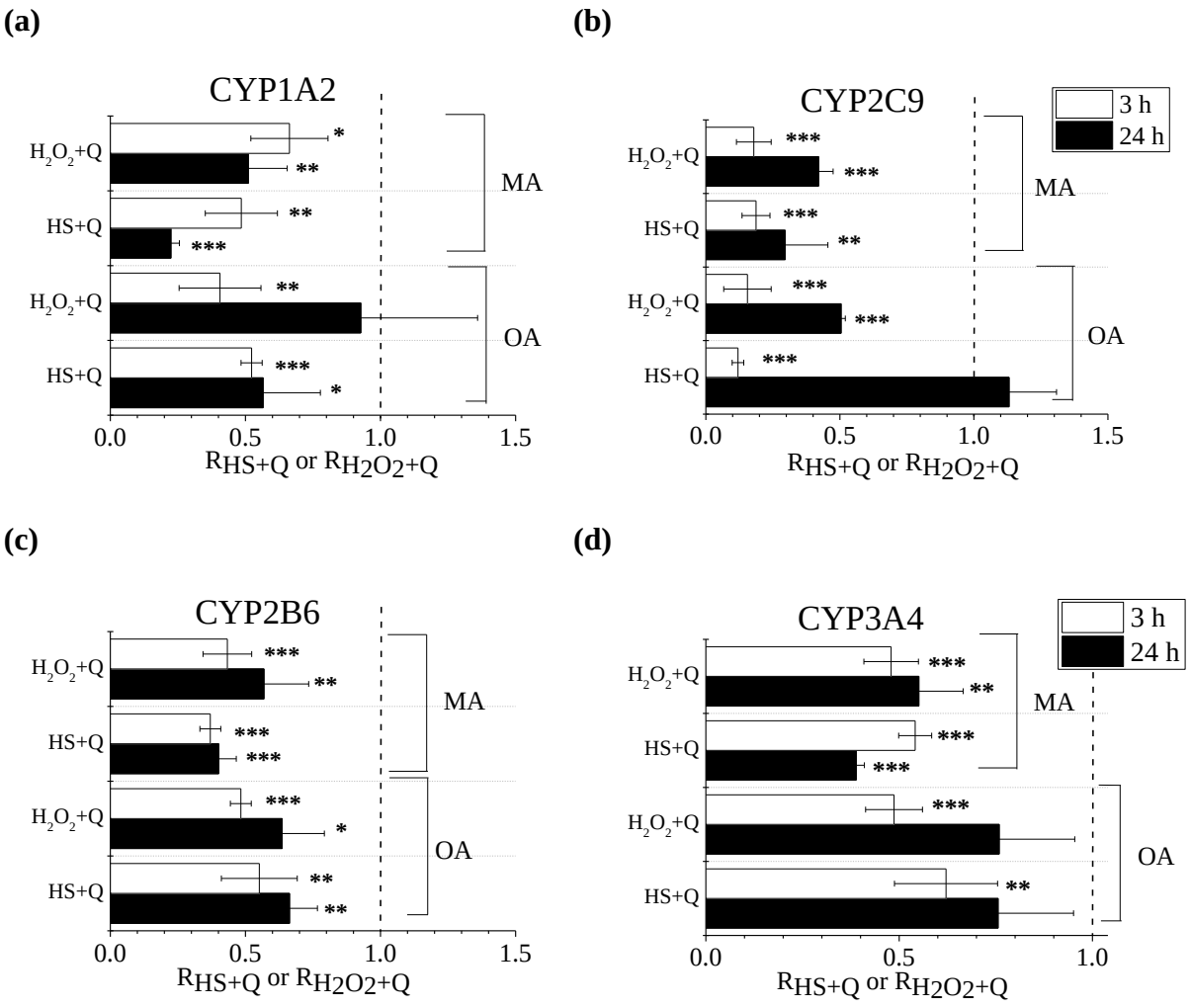

Figure 7-4 Ratio of responses of heat stress with quercetin (HS+Q) ($\mathbf{R_{HS+Q}}$) and hydrogen peroxide stress with quercetin (H_2O_2+Q) ($\mathbf{R_{H_2O_2+Q}}$) to HS or H_2O_2 exposed PRH (calculated according to Eq. 7.1 and 7.2) in CYP enzyme activities (a) CYP1A2 (b) CYP2C9 (c) CYP2B6 (d) CYP3A4 at 3 and 24 h for middle age (MA) and old age (OA) PRH. . *, **, *** indicate significance at $p < 0.05$, $p < 0.01$ and $p < 0.001$ respectively compared to non quercetin pre-treated stressed hepatocytes (R = 1, dashed line). All values are specific ratios related to cell number determined via protein content. Error bars indicate standard deviations (N = 3, n = 9). CYP, cytochrome P450 (measured as pM/cell/h). Original data is shown in supplementary Tables S5, S6.

7.4.4. Susceptibility of heat stressed middle age PRH to quercetin pre-treatment

The uptake or production rates of metabolites were determined (according to Eq. 4.1) for 0 – 12 h and 12 – 24 h for hepatocytes exposed to heat stress with and without quercetin. A 3-D plot of the scores of the three most significant factors of PCA using Z-score is depicted in Figure 7-5a. Hepatocytes from one of the middle age rats exposed to heat stress (HS) and

quercetin (Q) at 24 hours was an outlier in comparison to the hepatocytes from the other two rats (Figure 7-5a). Hence this outlier was removed to obtain another PCA plot (Figure 7-5b). In this plot a clear separation of middle and old age hepatocytes pre-treated with quercetin was observed. For middle age hepatocytes a separation between HS (pink triangle) and HS+Q (blue triangle) groups is observed.

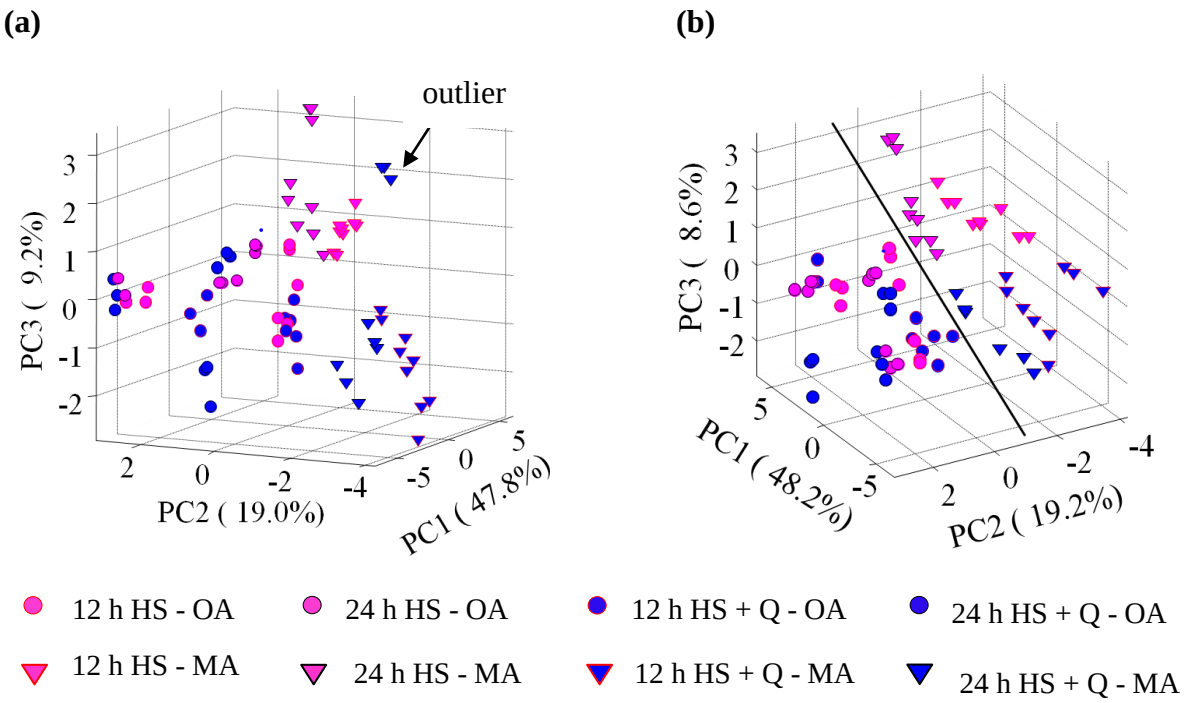

Figure 7-5 PCA of metabolic rates after heat stress and quercetin treatment (a) PCA scores of specific rates of amino acids, glucose, lactate, pyruvate and urea (in fmol/cell/h) measured during 0 – 12 and 12 – 24 h (N = 3, n = 9) of middle (MA) and old age (OA) PRH pre-treated with (HS+Q) and without quercetin (HS). The rates were normalized according to the Z-score (MatLab pca routine). (b) Metabolite rates during 12 - 24 h for one of the HS + Q middle age PRH (n = 3) is an outlier in comparison to other data points. This outlier has been removed to generate a second PCA plot showing separation of middle (triangle) and old (circle) age PRH along PC1, PC2 and PC3**.** Original data is shown in supplementary Tables S1, S2, S3, S4.

PC1 and PC2 scores of a PCA are plotted separately for old and middle age PRH under heat stress and heat stress with quercetin treatment. Hepatocytes from the three middle age rats exposed to heat stress (blue) were clearly separated from the quercetin pre-treated cells (green) at 12 and 24 hours (Figure 7-6b). PC1and PC2 acounted for 41.5% and 26.1% variation in the data. On the other hand, there was no separation due to quercetin pre-treatment for old age hepatocytes (Figure 7-6a).

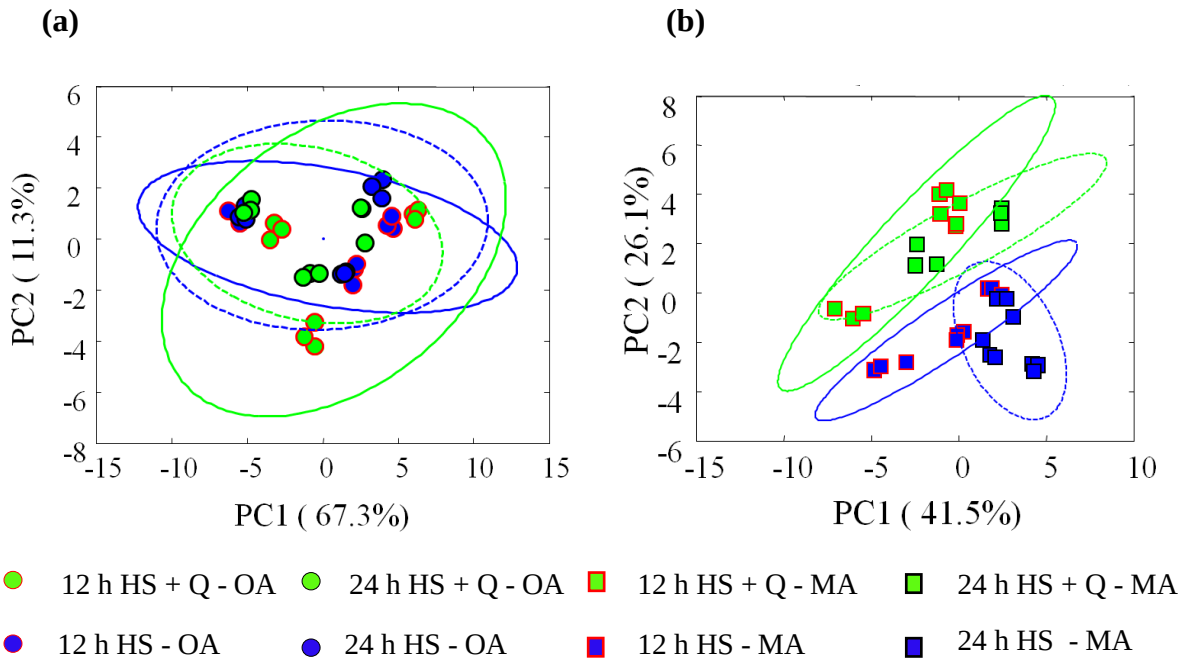

Figure 7-6 PCA scores of specific metabolite rates (measured as fmol/cell/h) for heat stress (HS) with (HS+Q) and without quercetin (HS) in PRH isolated from (a) old age (OA) and (a) middle age (MA) SD rats during 0 – 12 and 12 – 24 h (N = 3, n = 9). The data has been normalized according to the Z-score (MatLab pca routine). 90% confidence ellipses show the clusters of heat stress with and without quercetin during 0 – 12 h (solid line) and 12 – 24 h (dashed line). Outlier for one middle age PRH at 24 h (n = 3) have been left out in this PCA plot. Loadings for the PC1 and PC2 of middle age PRH are shown in supplementary Figure S5.

The loadings with Z-scores for PC1 in supplementary Figure S5 show that all the amino acids except Arg, Leu and Tyr contribute to the separation of heat stress with and without quercetin groups of middle age PRH. Figure 7-9 summarizes the amino acids showing most significant differences in uptake or production rates due to quercetin pre-treatment.

This shows that quercetin pre-treatment effects changes in metabolites for middle age PRH. However, old age PRH are statistically unaffected.

7.4.5. Susceptibility of hydrogen peroxide stressed middle age PRH to quercetin pre-treatment

Significant factors of PCA using normalized metabolite uptake/production rates (Z-score) of old and middle age PRH exposed to hydrogen peroxide (H_2O_2) with and without quercetin (Q) are plotted (Figure 7-7). Hepatocytes from one of the middle age PRH (as seen before in

Chapter 5, Figure 5-5) was a clear outlier in comparison to the hepatocytes isolated from the other two rats (Figure 7-7a). This outlier was removed to plot a second 2-D PCA plot (Figure 7-7b) where a clear separation between old and middle age PRH was observed. PC1 and PC2 accounted now for maximum variation of 42.7% and 20.6% respectively. For middle age PRH a separation between H_2O_2 (pink triangle) and H_2O_2+Q (blue triangle) groups is observed.

A 2-D PCA plot of PC1 and PC2 between hydrogen peroxide with (green) and without quercetin (blue) groups were separated based on their metabolite profiles in middle age PRH (Figure 7-8b). PC1 and PC2 described 34.2% and 21.5% variance in the data. However, old age hepatocytes showed no uniform changes in metabolite profile due to quercetin treatment (Figure 7-8a).

The loadings with Z-scores for PC1 in supplementary Figure S6 show that all the amino acids except Val and Arg contribute to the clustering of hydrogen peroxide stress with and without quercetin groups of middle age PRH. Figure 7-10 summarizes the amino acids showing most significant differences in uptake or production rates due to quercetin pre-treatment.

These results show that middle age PRH are more susceptible to quercetin treatment in terms of metabolite changes in comparison to old age PRH.

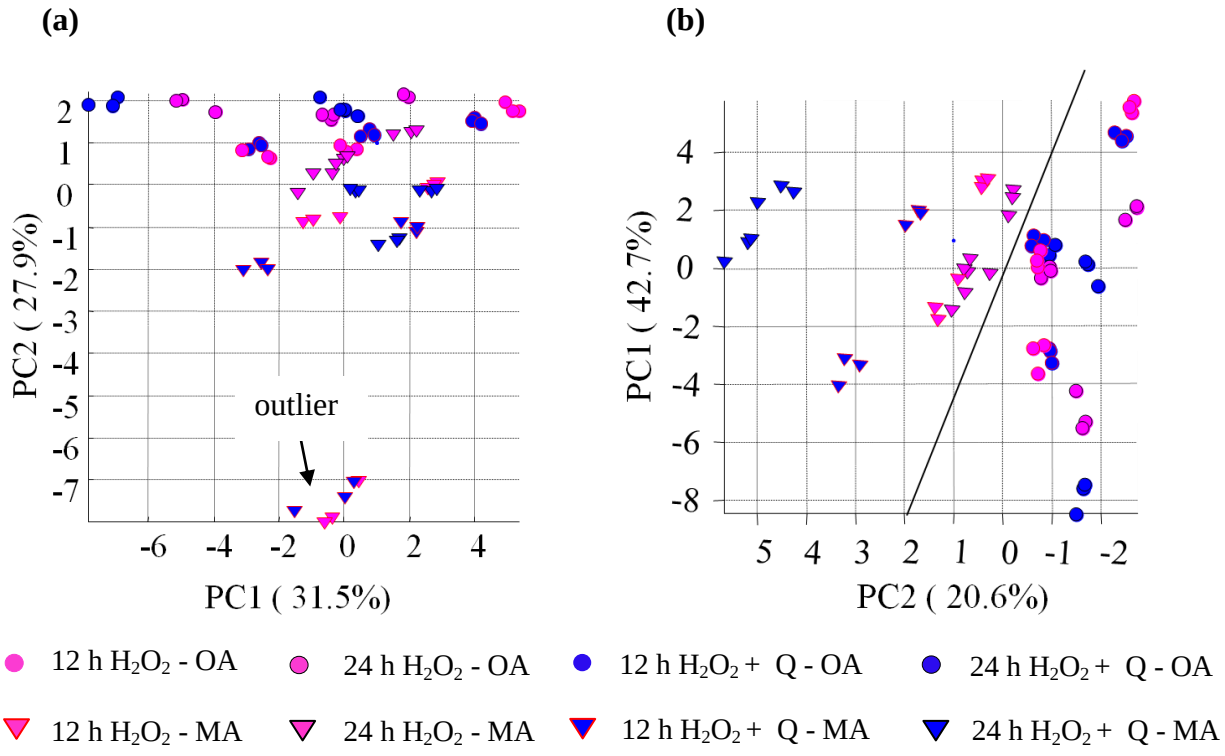

Figure 7-7 PCA of metabolic rates after hydrogen peroxide stress and quercetin treatment (a) PCA scores of specific rates of amino acids, glucose, lactate, pyruvate and urea (in fmol/cell/h) measured during 0 – 12 and 12 – 24 h (N = 3, n = 9) of middle (MA) and old age (OA) PRH pre-treated with (H_2O_2+Q) and without quercetin (H_2O_2). The plot was made with specific rates of amino acids, glucose, lactate, pyruvate and urea (in fmol/cell/h) measured during 0 – 12 and 12 – 24 h (N = 3, n = 9). The data has been normalized according to the Z-score (MatLab pca routine). (b) Metabolite rates during 0 – 12 h and 12 – 24 h of one middle age rat (n = 3) under H_2O_2 and H_2O_2 + Q treatment is an outlier in comparison to other data points. This outlier has been removed to generate a second PCA plot showing separation of middle (triangle) and old (circle) age PRH along PC1, PC2, and PC3. Original data is shown in supplementary Tables S1, S2, S3, S4.

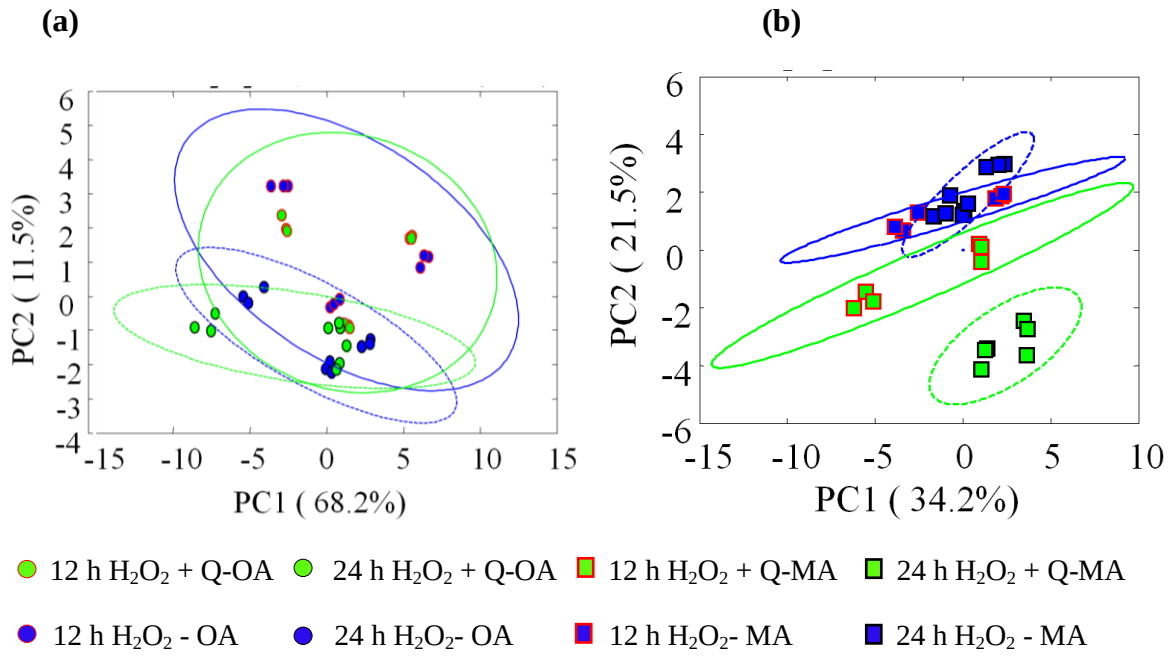

Figure 7-8 PCA scores of specific metabolite rates (measured as fmol/cell/h) for hydrogen peroxide stress with (H_2O_2+Q) and without quercetin (H_2O_2) in PRH isolated from (a) old age (OA) and (a) middle age (MA) SD rats for 0 – 12 and 12 – 24 h (N = 3, n = 9). The data has been normalized according to the Z-score (MatLab pca routine). 90% confidence ellipses show the clusters of hydrogen peroxide stress with and without quercetin for 0 – 12 h (solid line) and 12 – 24 h (dashed line) time interval. Outlier for the middle age PRH have been left out in this PCA plot. Loadings for the PC1 and PC2 of middle age PRH are shown in supplementary Figure S6.

The effect of quercetin on specific uptake and production rates of metabolites were analyzed on middle age PRH exposed to heat and hydrogen peroxide stress. 19 proteinogenic amino acids (contained in the culture medium) were measured at 12 and 24 hours of cultivation. Figure 7-9 summarizes the ratios of specific rates of amino acids for HS+Q to HS exposed PRH (calculated according to Eq. 7.1) for 0 – 12 and 12 – 24 h time interval. Only the amino acids where there is a significant change in rates due to quercetin, i. e. $R_{HS+Q} > 1$ *or* $R_{HS+Q} < 1$, are shown. Essential amino acids like Phe, Met and Thr were significantly taken up throughout 24 hours. Val was taken up in the first 12 hours and then significantly produced from 12 - 24 h by quercetin pretreated hepatocytes. Leu was also produced during 0 - 12 and 12 - 24 h. Non-essential amino acids like Tyr, Gly and Asp showed reduced uptake rates due to quercetin pre-treatment. However, Ala and Asn showed significantly higher uptake rates at 12 h and 24 h. Serine was consumed by HS+Q cells in comparison to HS hepatocytes during

0 - 12 and 12 – 24 h. HS PRH show production of Ser from 12 - 24 hours. Thus, this change in rate leads to a negative fold change.

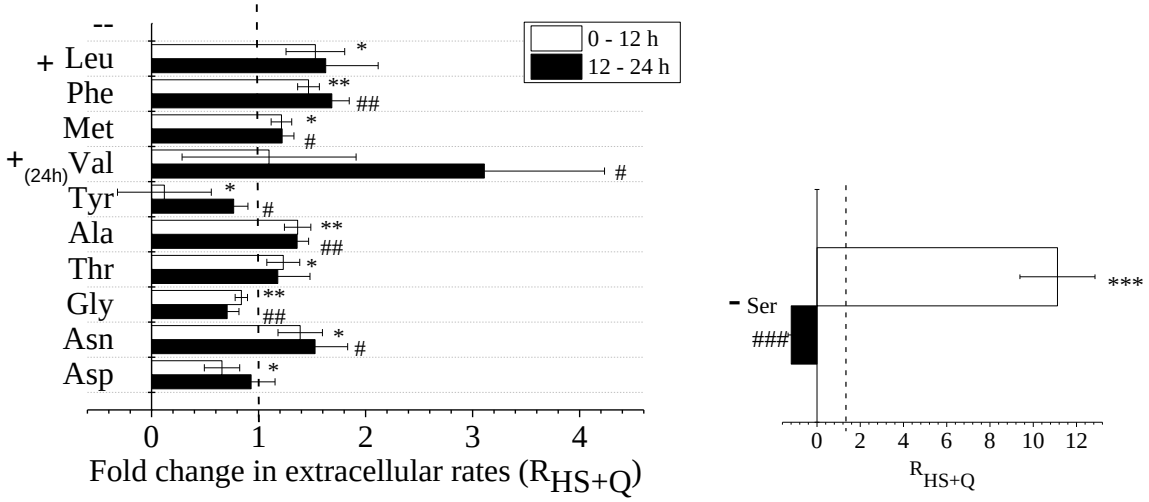

Figure 7-9 Ratio of specific uptake and production rates (measured as fmol/cell/h) of amino acids for heat stress with and without quercetin $\mathbf{R_{HS+Q}}$ (calculated according to Eq. 7.1) measured for 0 – 12 h and 12 – 24 h for middle age (MA) PRH. *, **, *** indicate significance during 0 – 12 h at $p < 0.05$, $p < 0.01$ and $p < 0.001$ respectively compared to non quercetin pre-treated stressed hepatocytes (R = 1, dashed line). # represents significance during 12 – 24 h. The concentration of metabolites was normalized to cell number determined via Calcein AM. Error bars indicate standard deviations (N = 3, n = 9). All amino acids were consumed except for Leu which was produced at 12 h, 24 h and Val which was produced at 24 h by HS+Q cells. Ser was consumed by HS+Q cells at 12 h, 24 h and produced by HS cells at 24 h. Thus the negative fold change from 12 – 24 h. +: production by HS+Q treated PRH, - : consumption by HS+Q treated PRH. Original data is shown in supplementary table S1, S2.

Figure 7-10 summarizes the ratios of specific rates of amino acids for H_2O_2+Q to H_2O_2 exposed PRH (calculated according to Eq. 7.2) for 0 – 12 h and 12 – 24 h time interval. Only the amino acids where there is a significant change due to quercetin, i. e $R_{H_2O_2+Q} > 1$ *or* $R_{H_2O_2+Q} < 1$, are shown. There was a significantly higher uptake of Asn, Ser, Gln, Thr, Ala, Met, Lys and Pro for H_2O_2+Q treated PRH during 0 – 12 h (Figure 7-10). During 12 - 24 h the uptake rates of these amino acids were reduced for H_2O_2 + Q PRH or were comparable to hydrogen peroxide stressed cells. Serine shows significantly lower consumption from 12 – 24 h in H_2O_2+Q treated PRH. It is produced by H_2O_2 stressed cells during 12 - 24 h, thus a negative fold change was observed here. Leu and Ile were produced from 0 - 12 h. However, from 12 - 24 h Leu was consumed and Ile was produced by H_2O_2+Q treated PRH in

comparison to H_2O_2 stressed PRH where, Leu was produced and Ile was consumed. Thus a negative fold change was observed.

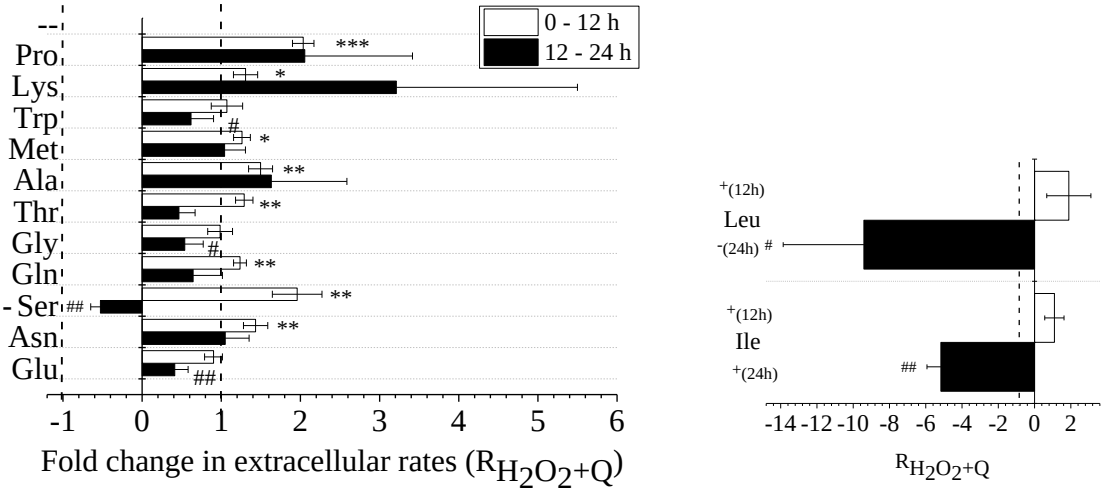

Figure 7-10 Ratio of specific uptake and production rates (measured as fmol/cell/h) of amino acids for hydrogen peroxide stress with quercetin to hydrogen peroxide stress ($\mathbf{R_{H_2O_2+Q}}$) for 0 – 12 h and 12 – 24 h time interval for middle age (MA) PRH. *, **, *** indicate significance during 0 – 12 h at $p < 0.05$, $p < 0.01$ and $p < 0.001$ respectively compared to non quercetin pre-treated stressed hepatocytes (R = 1, dashed line). # represents significance during 12 – 24 h. The concentration of metabolites was normalized to cell number determined via Calcein AM. Error bars indicate standard deviations (N = 3, n = 9). All amino acids were consumed except for Leu which was produced at 12 h and Ile produced at 12 h and 24 h by H_2O_2+Q treated PRH. Ser was consumed by H_2O_2+Q treated PRH at 12 h, 24 h and produced by H_2O_2 stressed PRH at 24 h. Thus the negative fold change from 12 – 24 h. +: production by H_2O_2+Q treated PRH, - : consumption by H_2O_2+Q treated PRH. Original data is shown in supplementary Tables S1, S2.

7.4.6. Effect of quercetin pre-treatment and oxidative stress on glucose, lactate, pyruvate and urea levels

Consumption of glucose was measured during 0 – 12 h and 12 – 24 h (Figure 7-11a). Again, here ratios for HS+Q (R_{HS+Q}) or H_2O_2+Q ($R_{H_2O_2+Q}$) stressed PRH were calculated with respect to HS or H_2O_2 stressed PRH (calculated according to Eq. 7.1 and 7.2). Due to quercetin pre-treatment, there was a significant increase in glucose production for heat stressed middle age PRH at 12 h and 24 h. H_2O_2+Q treated PRH showed significant increase in production from 12 h to 24 h. HS + Q hepatocytes isolated from old age rats showed production from 0 - 12 h and there was both uptake and release seen during 12 - 24 hours. However, HS old age PRH show glucose consumption, thus a negative fold change was observed. H_2O_2 + Q treated old age PRH show both uptake and release of glucose from 0 - 12 h and 12 - 24 h. Due to high standard deviations these changes were not significant.

Lactate was produced throughout 24 hours by both types of PRH. Middle age PRH pre-treated with quercetin and exposed to heat stress showed a 20% increase in lactate production (Figure 7-11b). A corresponding increase in pyruvate consumption was also seen for these cells (Figure 7-11c). There was also high pyruvate consumption for H_2O_2 + Q treated PRH during 0 - 12 hours. No changes for old age PRH were observed. Urea production as a measure of liver function was also determined. HS+Q treated middle age PRH showed significantly higher urea production in comparison to heat stressed PRH (Figure 7-11d). No changes for old age PRH were observed (Figure 7-11d).

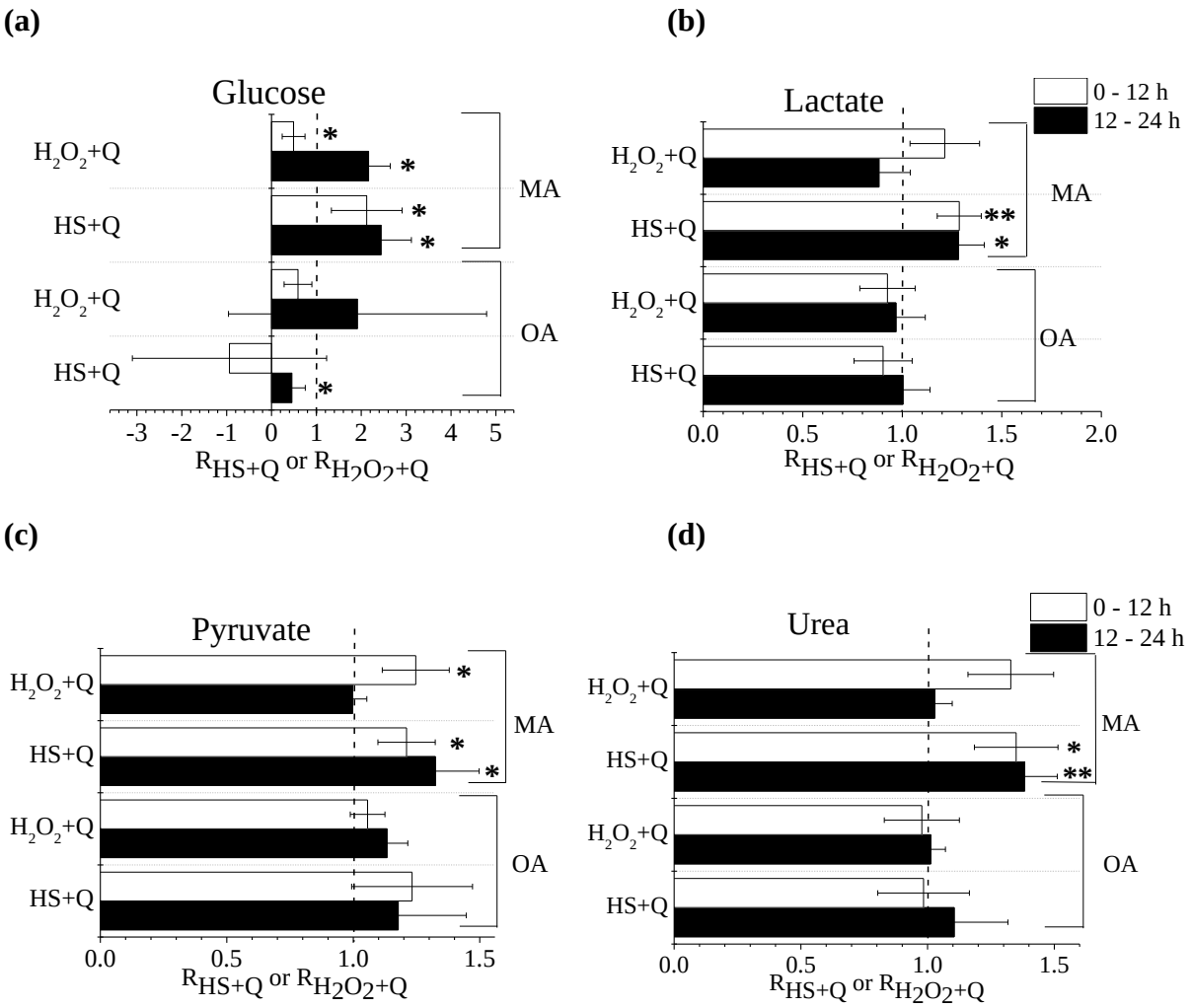

Figure 7-11 Ratio of specific uptake and production rates (measured as fmol/cell/h) of (a) glucose (b) lactate (c) pyruvate and (d) urea for heat stress with quercetin (HS+Q) (R_{HS+Q}) and hydrogen hydrogen peroxide stress with quercetin (H_2O_2+Q) ($R_{H_2O_2+Q}$) to HS or H_2O_2 exposed PRH (calculated according to Eq. 7.1 and 7.2) measured in extracellular supernatants from 0 – 12 h and 12 – 24 h for middle age (MA) and old age (OA) PRH. Negative values for glucose indicate change in direction of glucose production or consumption with respect to non-quercetin treated PRH. The concentration of metabolites was normalized to cell number determined via Calcein AM. Error bars indicate standard deviations (N = 3, n = 9). *, **, *** indicate significance at $p < 0.05$, $p < 0.01$ and $p < 0.001$ respectively compared to non quercetin pre-treated stressed hepatocytes (R = 1, dashed line). Original data is shown in supplementary Tables S1, S2, S3, S4.

7.5. Discussion

In this work, quercetin, a commonly available plant flavonoid, was used to study its potential as an anti-oxidant against heat and hydrogen peroxide stress in hepatocytes. It has been used in various *in vitro* and *in vivo* rat studies (El-Nekeety et al., 2014; Li et al., 2013; Pilkhwal et al., 2010; Weina et al., 2009; Niklas et al. 2012). It acts as a potent free radical scavenger because of its phenolic hydroxyl groups attached to ring structures capable of readily donating electrons to stabilize radical species (Riceo-Evans et al., 1997).

To the best of our knowledge, there has been no study detailing the metabolite changes due to quercetin treatment in primary rat hepatocytes exposed to oxidative stress. In this work, hepatocytes isolated from middle and old age rats were pre-treated with 50 µM quercetin (Q) for 4 hours followed by exposure to heat stress (HS) (42 °C / 1 h) and hydrogen peroxide (H_2O_2) stress (2 mM / 1 h). Extracellular metabolites like amino acids, glucose, lactate, pyruvate, urea and various cellular parameters were measured for a 24 h period (sampling at 0, 12 and 24 h)

AST and LDH are typical markers for liver damage. Quercetin pre-treated HS and H_2O_2 stressed hepatocytes isolated from old age rats initially showed a decrease in AST release (Figure 7-2c). Boulton *et al*. (Boulton et al., 1999) observed that quercetin is rapidly metabolized by cells. This could be the reason that this decrease was observed in the first 12 hours. However, no change was observed for middle age PRH. In the previous experiments it was seen, that HS and H_2O_2 stress does not affect AST levels in middle age PRH (Chapter 6, Figure 6-2). Hence no noticeable effect of quercetin on its release was observed.

An increase in LDH release was observed for HS+Q and H_2O_2+Q treated middle age PRH (Figure 7-2d). Middle age PRH also showed a significant decrease in intracellular GSH (Figure 7-3d) and intracellular ROS (Figure 7-2b). In a study by Boots *et al*. (Boots et al., 2007), a paradox in the action of quercetin is explained. It was observed in *in vitro* culture of lung cells that quercetin efficiently scavenges radicals and protects the cells against oxidative damage. However, during this protection, quercetin is converted into oxidized quercetin. Oxidized quercetin is thiol reactive and will arylate GSH as well as protein thiol groups, leading to GSH consumption (Boots et al., 2003, 2005), an increase in cytosolic free calcium concentration (Ca^{2+}) and LDH leakage (Figure 7-12). Binding of oxidized quercetin to protein

thiols has been shown in isolated membranes and lymphocytes as well as in blood plasma (Yen et al., 2003). Thus, our results of LDH leakage, GSH depletion and reduced intracellular ROS in middle age PRH could be explained by this paradoxical effect of quercetin. However, in old age PRH no significant effect of quercetin on LDH was observed (Figure 7-2d). Due to its easy diffusion in cells and strong free radical scavenger activity (El-Nekeety et al., 2014), a significant decrease in intracellular ROS (Figure 7-3a) was observed for quercetin treated old age PRH. At 24 hours, the ROS values came down to control levels, hence no effect of quercetin was observed. However a slight increase in GSH was observed for quercetin pre-treated heat stressed old age hepatocytes (Figure 7-3c). Old age hepatocytes have significantly lower intracellular GSH (see supplementary table S6, Chapter 5, Figure 5-3) in comparison to middle age hepatocytes. Hence, it is possible that the effect of oxidized quercetin is not so pronounced in old age PRH. Thus, we could observe a differential effect of quercetin on middle and old age hepatocytes in terms of enzymatic activity (AST, LDH), intracellular ROS and GSH.

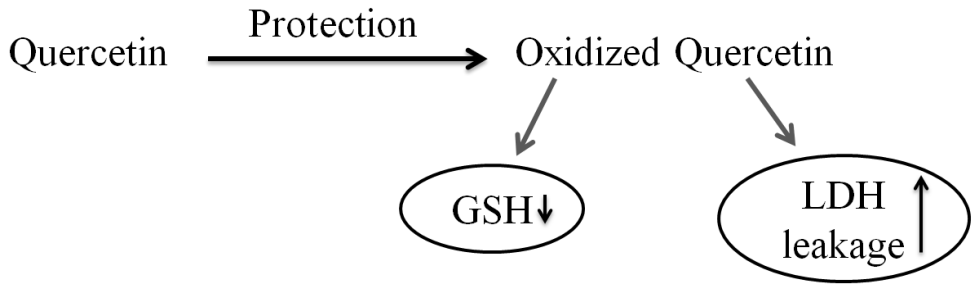

Figure 7-12 Schematic overview of the quercetin paradox. The paradox of quercetin is that, although a highly reactive species is being neutralized, during the same process a thiol-reactive quercetin metabolite is being formed. In this way, the selective toxicity of the highly reactive radical is swapped for a more selective toxicity of the quercetin metabolite. The binding of oxidized quercetin with GSH is reversible. This leads to GSH consumption and LDH leakage

Another marker for liver function, albumin was measured. Significant decrease in albumin production was observed for HS + Q and H_2O_2 + Q treated middle age PRH (Figure 7-2b). Quercetin has a high affinity for serum albumins. It is oxidized in cells and the product can covalently bind to cellular proteins (Boulton et al., 1998). Thus we see lower albumin values. Old age PRH already show very low values of albumin in comparison to middle age PRH (Figure 5-2b), hence the effect of quercetin might not be observed.

The cytochrome P450 (CYP) isoenzymes are a group of heme - containing enzymes found mainly in the lipid bilayer of the endoplasmic reticulum of hepatocytes, responsible for metabolism of drugs (Guengerich, 1992). CYP3A4 and CYP1A2 are the most abundant enzymes present in the liver for drug metabolism. CYP activity was measured during 2 days of cell cultivation. A decrease in CYP activity was seen for both types of PRH (Figure 7-4). The activity of CYP2C9 was significantly lower at 24 h than at 3 h. Hence a stronger reduction due to quercetin is seen at 3 h. This is in agreement with previous studies where quercetin was shown to inhibit P450 enzymes due to its hydroxyl group (Buening et al., 1981).

A PCA scores plot between the most important principal components based on normalized metabolite rates showed a distinct separation of stressed old and middle age hepatocytes pre-treated with quercetin (Figure 7-5, 7-7). When old and middle age PRH were analyzed individually, middle age PRH showed a clear separation in their metabolite profiles due to quercetin treatment for both HS and H_2O_2 stressed hepatocytes (Figure 7-6, 7-8). However, old age PRH showed no such distinction due to quercetin.

Uptake and production rates of metabolites showed significant differences due to quercetin pre-treatment in middle age PRH. HS+Q treated PRH showed higher uptake rates of various amino acids like Phe, Met, Thr, Ala, Ser and Asn at 12 h and 24 h (Figure 7-9). For H_2O_2+Q treated PRH, there was a increased uptake rate of amino acids like Asn, Ser, Gln, Thr, Ala, Met, Lys and Pro from 0 – 12 h and a reduced uptake from 12 – 24 h (Figure 7-10). Boulton et al. (Boulton et al., 1999) found that quercetin is rapidly taken up and metabolized by HepG2 cells. This could be the reason that changes in the extracellular metabolism were observed during the first 12 hours. However, this is true only for H_2O_2+Q treated PRH. In a previous study by Niklas et al. (Niklas et al., 2012) increased fluxes through the TCA cycle were observed due to quercetin treatment of human AGE1.HN cells. In isolated perfused rat liver, it was shown that quercetin is stimulating TCA cycle activity which is probably caused by an increased mitochondrial NAD^+ availability (Buss et al. 2005). This is in line with our results where increased uptake of amino acids was observed which could be diverted towards anaplerotic reactions in cells and hence results in increase in intracellular fluxes. The resulting increase in energy could be used by cells to protect against oxidative stress. This is also in correspondence with a previous study by Weina *et al.* (Weina et al., 2009) where a 24 h pre-

treatment of hydrogen peroxide stressed hepatocytes with quercetin resulted in increased glycolysis and fatty acid oxidation. However, intracellular metabolites have to be measured to confirm this hypothesis.

High glucose production by quercetin treated middle age PRH suggests that quercetin can stimulate glycogenolysis in oxidatively stressed hepatocytes (Figure 7-11). This effect was also shown in a previous isolated rat perfusion model (Gasparin et al., 2003). HS+Q treated middle age PRH show increased pyruvate uptake and a corresponding increase in lactate production from 0 – 12 h and 12 – 24 h. Higher urea production was also observed. However this effect was not seen in old age PRH (Figure 7-11). In case of old age PRH there was both uptake and release of glucose due to quercetin treatment in oxidatively stressed PRH. Due to huge variation in glucose data in PRH from the three old age rats, no uniform action of quercetin on glucose values could be observed.

Thus it can be concluded that, middle age PRH show significant changes in metabolite levels due to quercetin pre-treatment.

In summary, it can be stated that quercetin is a potent free radical scavenger in hepatocytes isolated from middle and old age rats. However its effect on metabolite levels under oxidative stress conditions is more pronounced in middle age PRH. The results from this study contribute to an improved understanding of the effect of quercetin on the level of metabolic activity in primary rat hepatocytes. The action of quercetin on middle age PRH is summarized in Figure 7-13. Quercetin pre-treated stressed middle age PRH show significantly higher consumption of amino acids in comparison to old age hepatocytes. These amino acids could be used for anaplerotic reactions or protein synthesis by hepatocytes. Increased glucose production was also observed due to quercetin pre-treatment in middle age hepatocytes. It could be possible that higher uptake of amino acids due to quercetin pre-treatment is utilized by cells to provide for more energy in order to protect against oxidative stress. Quercetin clearly has a distinct effect on metabolism of differentially aged hepatocytes. It could significantly reduce intracellular ROS levels in both old and middle age stressed hepatocytes suggesting its strong free radical scavenging activity. Protection by quercetin results in generation of oxidized quercetin which arylates with GSH leading to GSH consumption. Hence, lower intracellular GSH was observed for middle age hepatocytes.

In future studies, intracellular metabolites can be measured after quercetin treatment. The combination of the extra and intracellular data can help in building of a metabolic flux model for hepatocytes to determine various intracellular fluxes. This could help in determining the effect of quercetin with age. Thus its usage could be optimized for a healthier aging process.

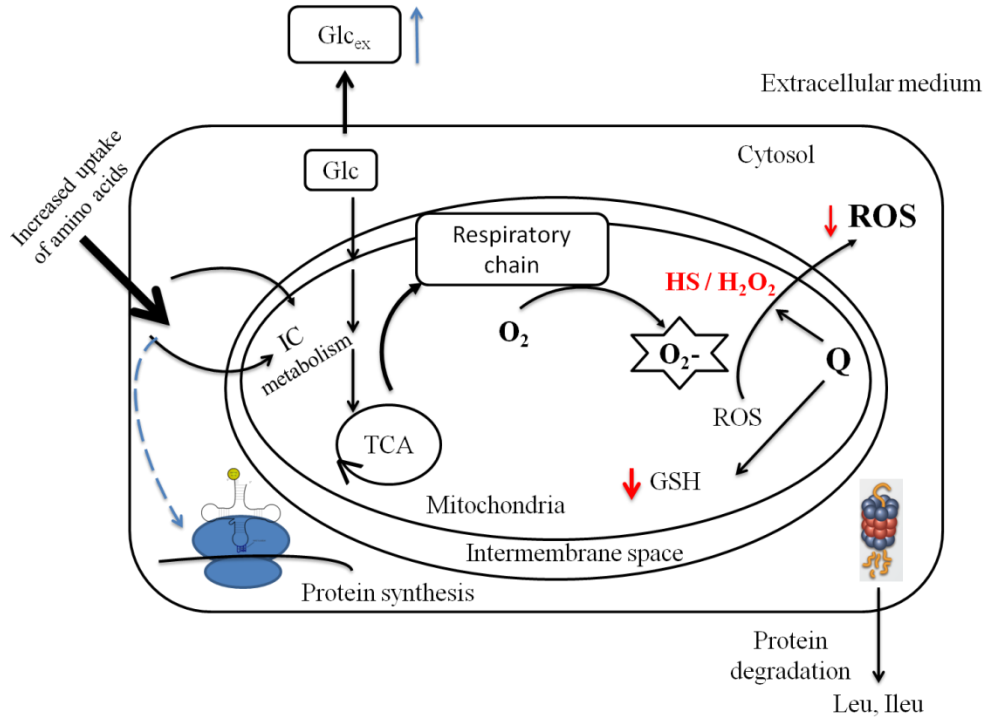

Higher consumption of amino acids by quercetin treated stressed middle age PRH in comparison to old age PRH.

Increased glucose production by quercetin treated stressed middle age PRH in comparison to old age PRH.

Significant decrease in intracellular ROS and GSH due to quercetin.

Figure 7-13 Schematic diagram showing increased uptake of amino acids by quercetin (Q) pre-treated stressed middle age PRH: These amino acids can contribute to anaplerotic reactions in intracellular metabolism (IC) or cellular protein synthesis. Increased production of glucose was seen for HS+Q and H_2O_2+Q middle age hepatocytes. Quercetin leads to reduced intracellular ROS and GSH values. GSH is consumed due to formation of the oxidized quercetin.

8. Summary and future prospects

Aging research is important in our society, where healthcare costs for the elderly increase dramatically at a rapid and highly detrimental pace. Apart from cancer, various other diseases such as dementia, heart disease and diabetes are closely linked to old age. Aging is often regarded as a complex multifaceted process, and well over 300 theories have been proposed to describe its cause and mechanisms (Viña et al., 2007). However, a complete theoretical framework for understanding the aging process is lacking. It was proposed in the 1950´s that oxidative stress plays an important role in the aging process. (Harman, 1956). Since then, it has been the most popular view to describe deleterious changes associated with aging. However, the underlying mechanisms of the response to oxidative stress and its implication for the aging process are not yet fully understood. A deeper understanding of ROS-induced alterations at a systems level, i.e. at the metabolic level would not only help to expand the knowledge about progression of aging, but also to identify potential therapeutic targets for manipulation of aging processes.

The first part of this project focuses on identification of differences in metabolic activities due to aging in freshly isolated rat hepatocytes. It is a known fact that physiological functions decline with the increasing age. This loss in functionality has been mostly ascribed to increases in reactive oxygen species (ROS) which accompany aging and lead to functional alterations. This formed the basis for the second part of our project. Middle (6 months) and old age (24 months) rat hepatocytes were exposed to oxidative stress via heat and hydrogen peroxide to analyze changes in uptake or production rates of extracellular metabolites. Thus, we could investigate the metabolite changes associated with oxidative stress during aging. The third aim of this project was to study the metabolite changes due to administration of anti-oxidant to cells. Flavonoids are a group of plant metabolites thought to provide health benefits through cell signaling pathways and antioxidant effects. Quercetin is one of the most abundant flavonoids in the human diet, which is found in fruits and vegetables such as blueberries, onions, curly kale, broccoli, and leek (Manach et al., 1999). It has a broad range of activity, such as antioxidative, ROS scavenging, anti-inflammatory and anti-fibrotic properties (El-Nekeety et al., 2014). The action of quercetin given extracellularly in the medium on metabolic rates of middle and old age hepatocytes was investigated. Since

metabolism is furthest down the line from gene to function, it is the most embracing of all the physiological states of the organism. Aging in liver is associated with many changes at physiological levels. It is also sensitive to oxidative stress injury (Hall et al., 2000; Yen et al., 1994). Thus, hepatocytes were chosen for this study.

Principal component analysis (PCA) is a commonly used technique to emphasize variation and bring out patterns in a data set. It is commonly used for analyzing large sets of metabolite data. We have mainly used this tool for analyzing the dataset of metabolic rate or fluxes of different experimental groups. Uptake and production rates of amino acids, glucose, lactate, pyruvate and urea normalized to Z-scores through MatLab (MathWorks, Nattick, MA, USA) was used to make the PCA plot.

This project was started with characterizing metabolic activity of two most commonly used starins of experimental rats: Sprague-Dawley (SD) and Wistar. Strain differences between SD and Wistar rats are already known to exist regarding food intake, growth rate, hormone levels (Kühn et al., 1983), metabolic differences in urinary samples, expression of CYP 450 1A and 3A enzymes (Kishida et al., 2008). Previous studies have shown that strain variations can lead to differences in experimental results related to drug toxicity and antibiotic responses (Garcia-Lopez et al., 1996; Hart et al., 1982; Riley et al., 2000). Thus, we decided to firstly study the extracellular metabolism by determination of extracellular rates of middle and old age hepatocytes from both these rats. We could identify distinct clusters of Wistar and SD rats via PCA and the major metabolites that contribute to this separation were glucose, lactate, pyruvate urea and amino acids like leucine, arginine, methionine, phenylalanine, glycine, asparagine, alanine, tyrosine, tryptophan histidine, lysine threonine, glutamine and serine. These differences were apparent for both middle and old age groups. These amino acids were consumed at higher rates by hepatocytes isolated from SD rats. These amino acids are utilized by cells for various intracellular metabolic pathways and protein synthesis. This suggests hypermetabolic state of SD rat hepatocytes in comparison to Wistar rat cells. The next experiments in this work were done with hepatocytes isolated from Sprague Dawley rats. We could not get old Wistar rats within Europe. Thus, we had to use hepatocytes from SD rats for this study. But from these results we can say that results from different rat strains are not inter-changeable in case of aging associated studies.

Next part of this work was to characterize metabolic changes in hepatocytes due to aging. Aging studies have been done previously in rats to identify metabolite differences associated

with age (Nevedomskaya et al., 2010; Williams et al., 2005; Yan et al. 2009; Houtkooper et al. 2011). However these studies have been done using urine or plasma from rats which are easily available in a non-life threatening manner. A direct study on metabolite changes in freshly isolated hepatocytes in a 2-D monolayer culture has not been done before. In this work, we were able to successfully establish a 2-D monolayer system to study age associated changes in metabolites and various liver specific parameters in rat hepatocytes. The hepatocytes from middle and old age rats were cultivated for 48 hours. Experiments were started 12 hours after cell adherence. Metabolites were analyzed during two phases: 0 – 12 h and 12 – 24 h. We observed a reduction in CYP activity, intracellular GSH and cell viability, accompanied with an increase in AST and LDH release for old age hepatocytes suggesting the sensitivity of old age hepatocytes to stress related to cell isolation and *in vitro* cultivation in comparison to middle age hepatocytes. Middle and old age hepatocytes showed distinct separation on a 2-D PCA plot based on their metabolite rates. The consumption rates of various essential and non-essential amino acids like Lys, Met, Phe, His Thr, Gln, Tyr, Ala, Asn, Gly and Pro were higher for middle age rat hepatocytes in comparison to old age ones. These results suggest that middle age hepatocytes metabolize amino acids at faster rates than old age hepatocytes. Significant differences in carbohydrate metabolism were also observed between the two age groups. Old age hepatocytes tend to produce more glucose and lactate than middle age hepatocytes suggesting probably higher rates of glycogen degradation and glycolysis. Thus, we were able to successfully investigate metabolite patterns in middle and old age hepatocytes.

In the second part of this study, effect of heat (42 °C for 1 h) and hydrogen peroxide stress (2 mM for 1 h) on aged hepatocytes was investigated. Old age hepatocytes showed reduced cell viability, CYP activity and significant increase in AST and LDH values due to hydrogen peroxide and heat stress. Middle age hepatocytes showed no changes in these cellular parameters. Old age hepatocytes showed an increase in intracellular ROS and GSH due to hydrogen peroxide stress. No significant change in ROS or GSH was observed due to heat stress. However, in our previous experiments we observed that intracellular ROS increases during heat stress and reduces to control levels as soon as cells come back to control temperatures. This suggests that free radicals are generated due to heat stress but they have lower life time in *in vitro* hepatocyte culture as compared to *in vivo* studies where rats are heated followed by liver isolation (as seen in an *in vivo* study by Zhang et al., 2003).

Control and hydrogen peroxide stressed hepatocytes from the individual old age rats were clearly separated in a 2-D PCA scores plot based on their metabolite profiles. However, no significant differences in metabolic profile among individual old age rat hepatocytes were observed due to heat stress. However, in previous *in vivo* studies, old age liver cells showed many changes due to heat stress like apoptosis, expression of heat shock proteins, hepatocellular vacuolization and necrosis (Hall et al., 2000; Oberley et al., 2008; Zhang et al., 2003). These results highlight that in *in vitro* culture old age hepatocytes can better acclimatize to heat stress and thus no significant changes in metabolite levels are observed. Hydrogen peroxide stressed old age hepatocytes showed increased consumption of various amino acids like Lys, Met, Phe, His, Tyr, Ala, Gln, Asn. This suggests increased cellular demands under hydrogen peroxide stress by old age hepatocytes. Middle age hepatocytes were robust to any changes in their extracellular metabolite rates due to heat and hydrogen peroxide stress. However, a combined PCA scores plot based on the metabolite profiles of stressed old and middle age hepatocytes showed clear separation among the two age groups.

There were also significant differences in glucose utilization between stressed old and middle age hepatocytes. Old age hepatocytes from two of the rats exposed to heat or hydrogen peroxide stress showed glucose consumption in comparison to control cells. This could be due to inhibition of gluconeogenesis or depletion of enzymes related to glycogenolysis in contrast to middle age PRH. They could also be taking up more glucose to compensate for increased energy demand of cells due to oxidative stress. Stressed middle age PRH produce significantly higher glucose during first 12 hours followed by a significant reduction from 12 – 24 hours. Our results show a similar trend in glucose production as observed by Biljana *et al*. (Biljana, 2013). They observed glucose release during the first 6 h after heat stress due to up regulation of enzymes related to glycogenolysis. Then the period from 6 to 24 hours was characterized by intensive rebound of glycogen stores leading to reduced glucose production.

From these results we could say that, firstly old age hepatocytes are more susceptible to changes in metabolism due to oxidative stress generated via hydrogen peroxide. Secondly, oxidative stress during aging leads to increased utilization of amino acids for various intracellular processes. Thirdly, hepatocytes *in vitro* are robust to heat stress irrespective of the age of rats.

In the third part of this study, the effect of quercetin was studied on extracellular metabolites in stressed old and middle age hepatocytes. Hepatocytes were pre-treated with 50 µM quercetin for 4 hours followed by exposure to oxidative stress via hydrogen peroxide and heat. Quercetin significantly decreased intracellular ROS generation due to stress in both middle and old age hepatocytes. This could be attributed to its easy diffusion in cells and strong free radical scavenger activity (El-Nekeety et al., 2014). However middle age hepatocytes showed decrease in GSH and increased LDH leakage due to quercetin treatment. This is a paradoxical action of quercetin and may be due to formation of a oxidized quercetin product (Boots et al., 2003, 2005). This has not been previously seen in hepatocytes. Significantly high glucose production by quercetin treated middle age PRH was observed suggesting that quercetin can stimulate glycogenolysis in oxidative stress hepatocytes. Glucose production was also observed in a previous isolated rat perfusion model (Gasparin et al., 2003).

A PCA plot between the most important principal components based on normalized metabolite rates showed a distinct separation of stressed old and middle age hepatocytes pre-treated with quercetin. When old and middle age rats were analyzed individually, middle age PRH showed distinct separation in their metabolite profiles due to quercetin treatment for both HS and H_2O_2 stress cells. However, old age hepatocytes showed no distinct changes in metabolite levels due to quercetin.

Stressed middle age hepatocytes showed increased uptake of amino acids due to quercetin pre-treatment. These amino acids could be used in various intracellular anapleurotic reactions as seen in a previous study by Niklas et al. (Niklas et al., 2012). They observed increased fluxes through TCA cycle due to quercetin treatment of human AGE1.HN cells. The resulting increase in energy could be used by cells to protect against oxidative stress as seen in a previous study by Weina *et al.* (Weina et al., 2009) where a 24 h pre-treatment of hydrogen peroxide stressed hepatocytes with quercetin resulted in increased glycolysis and fatty acid oxidation. However, intracellular metabolites need to be measured to confirm this hypothesis.

Thus, we could say that stressed middle age hepatocytes are more susceptible to metabolic changes under quercetin treatment in comparison to old age hepatocytes. The results from this study contribute to an improved understanding of the effect of quercetin on metabolic activities e.g. fluxes in differentially aged hepatocytes.

The results from this study gave a detailed overview of changes in extracellular metabolism due to oxidative stress in aged hepatocytes. We also investigated the effects of anti-oxidant quercetin on metabolite profiles in differentially aged hepatocytes. In future studies, intracellular metabolites could be measured for all these conditions. The integration of the extracellular and intracellular data could help to build a valid metabolic flux model to determine variations in intracellular fluxes due to oxidative stress and anti-oxidant treatment. We can identify pathways that are altered due to aging and oxidative stress. These pathways could be used for identification of metabolite markers to develop targeted drugs for ROS induced alterations during aging. Quercetin concentrations could be adjusted to target specific cellular pathways to lead to a healthier aging process or to target cancer cells.

Moreover the metabolic and flux data could be integrated with gene and protein expression data, to decribe, simulate and predict more accurately the aging processes in liver. This could later serve as a physiological model for human-predictive studies to analyze hepatic aging and oxidative stress effects on hepatic metabolism.

9. Bibliography

Abd El-Gawad HM, Khalifa AE. 2001. "Quercetin, Coenzyme Q10, and L-Canavanine as Protective Agents against Lipid Peroxidation and Nitric Oxide Generation in Endotoxin-Induced Shock in Rat Brain." *Pharmacological research : the official journal of the Italian Pharmacological Society* 43(3): 257–63.

Abdoli N, Azarmi Y, Eghbal MA. 2014. "Protective Effects of N-Acetylcysteine against the Statins Cytotoxicity in Freshly Isolated Rat Hepatocytes." *Advanced Pharmaceutical Bulletin* 4(3): 249–54.

Aggarwal S and Gupta S. 1999. "Increased Activity of Caspase 3 and Caspase 8 in Anti-Fas-Induced Apoptosis in Lymphocytes from Ageing Humans." *Clinical and Experimental Immunology* 117(2): 285–90.

Alía M, Ramos S, Mateos R, Bravo L, Goya L. 2005. "Response of the Antioxidant Defense System Totert-Butyl Hydroperoxide and Hydrogen Peroxide in a Human Hepatoma Cell Line (HepG2)." *Journal of Biochemical and Molecular Toxicology* 19(2): 119–28.

Ames B N, Shigenaga M K, and Hagen T M. 1993. "Oxidants, Antioxidants, and the Degenerative Diseases of Aging." *Proceedings of the National Academy of Sciences of the United States of America* 90(17): 7915–22.

Ando M, Katagiri K, Yamamoto S, Wakamatsu K, Kawahara I, Asanuma S, Usuda M, Sasaki K. 1997. "Age-Related Effects of Heat Stress on Protective Enzymes for Peroxides and Microsomal Monooxygenase in Rat Liver." *Environmental Health Perspectives* 105(7): 726–33.

Atkuri KR, Mantovani JJ, Herzenberg LA, and Herzenberg LA. 2007. "N-Acetylcysteine-a Safe Antidote for Cysteine/glutathione Deficiency." *Current Opinion in Pharmacology* 7(4): 355–59.

Bae YS, Kang SW, Seo MS, Baines IC, Tekle E, Chock PB, Rhee SG. 1997. "Epidermal Growth Factor (EGF)-Induced Generation of Hydrogen Peroxide." *Journal of Biological Chemistry* 272(1): 217–21.

Bai J, Rodriguez AM, Melendez JA, and Cederbaum AI. 1999. "Overexpression of Catalase in Cytosolic or Mitochondrial Compartment Protects HepG2 Cells against Oxidative Injury." *The Journal of biological chemistry* 274(37): 26217–24.

Bajt ML. 2004. "Acetaminophen-Induced Oxidant Stress and Cell Injury in Cultured Mouse Hepatocytes: Protection by N-Acetyl Cysteine." *Toxicological Sciences* 80(2): 343–49.

Bar-Or D, Thomas GW, Rael LT, Lau EP, Winkler JV. 2001. "Asp-Ala-His-Lys (DAHK) Inhibits Copper-Induced Oxidative DNA Double Strand Breaks and Telomere Shortening." *Biochemical and biophysical research communications* 282(1): 356–60.

Barzilai A and Ken IY. 2004. “DNA Damage Responses to Oxidative Stress.” *DNA Repair* 3(8-9): 1109–15.

Beauséjour CM, Krtolica A, Galimi F, Narita M, Lowe SW, Yaswen P, Campisi J. 2003. “Reversal of Human Cellular Senescence: Roles of the p53 and p16 Pathways.” *EMBO Journal* 22(16): 4212–22.

Becker SA, Feist AM, Mo ML, Hannum G, Palsson BØ, Herrgard MJ. 2007. “Quantitative Prediction of Cellular Metabolism with Constraint-Based Models: The COBRA Toolbox.” *Nature protocols* 2(3): 727–38.

Bejma J, Ramires P, Ji LL. 2000. “Free Radical Generation and Oxidative Stress with Ageing and Exercise: Differential Effects in the Myocardium and Liver.” *Acta Physiologica Scandinavica* 169(4): 343–51.

Berger A, Milgram E, Mitchell M, Lawton K, Hanson R, Kalhan S, and Milburn M. 2007. “The Metabolomics of Aging.” *Faseb Journal* 21(6): A1040.

Berlett BS. 1997. “Protein Oxidation in Aging, Disease, and Oxidative Stress.” *Journal of Biological Chemistry* 272(33): 20313–16.

Miova B et al. 2013. “Liver Carbohydrate Metabolism in Rats in the Period of Recovery.” *Macedonian Journal of Medical Sciences* 6(1): 16–23.

Bissell DM, Stamatoglou SC, Nermut MV, Hughes RC. 1986. “Interactions of Rat Hepatocytes with Type IV Collagen, Fibronectin and Laminin Matrices. Distinct Matrix-Controlled Modes of Attachment and Spreading.” *European journal of cell biology* 40(1): 72–78.

Blander G, de Oliveira RM, Conboy CM, Haigis M, Guarente L. 2003. “Superoxide Dismutase 1 Knock-down Induces Senescence in Human Fibroblasts.” *The Journal of biological chemistry* 278(40): 38966–69.

Blomgren K, Hagberg H. 2006. “Free Radicals, Mitochondria, and Hypoxia-Ischemia in the Developing Brain.” *Free Radical Biology and Medicine* 40(3): 388–97.

Bokov A, Chaudhuri A, Richardson A. 2004. “The Role of Oxidative Damage and Stress in Aging.” *Mechanisms of Ageing and Development* 125(10-11): 811–26.

Boots AW, Balk JM, Bast A, Haenen GR. 2005. “The Reversibility of the Glutathionyl-Quercetin Adduct Spreads Oxidized Quercetin-Induced Toxicity.” *Biochemical and Biophysical Research Communications* 338(2): 923–29.

Boots AW, Kubben N, Haenen GR, Bast A. 2003. “Oxidized Quercetin Reacts with Thiols rather than with Ascorbate: Implication for Quercetin Supplementation.” *Biochemical and Biophysical Research Communications* 308(3): 560–65.

Boots AW, Li H, Schins RP, Duffin R, Heemskerk JW, Bast A, Haenen GR. 2007. The quercetin paradox. *Toxicology and Applied Pharmacology, 222*(1), 89–96.

Boulton DW, Walle UK and Walle T. 1998. "Extensive Binding of the Bioflavonoid Quercetin to Human Plasma Proteins." *The Journal of pharmacy and pharmacology* 50(2): 243–49.

Boulton DW, Walle UK and Walle T. 1999. "Fate of the Flavonoid Quercetin in Human Cell Lines: Chemical Instability and Metabolism." *The Journal of pharmacy and pharmacology* 51(3): 353–59.

Boveris A, Oshino N, Chance B. 1972. "The Cellular Production of Hydrogen Peroxide." *Biochemical Journal* 128(3): 617–30.

C Bowler, MV Montagu, and D Inze. 1992. "Superoxide Dismutase and Stress Tolerance." *Annu Rev Plant Physiol Plant Mol Biol* 43: 83–116.

MM Bradford,. 1976. "A Rapid and Sensitive Method for the Quantitation of Microgram Quantities of Protein Utilizing the Principle of Protein-Dye Binding." *Analytical biochemistry* 72: 248–54.

Bratosin D, Mitrofan L, Palii C, Estaquier J, Montreuil J. 2005. "Novel Fluorescence Assay Using Calcein-AM for the Determination of Human Erythrocyte Viability and Aging." *Cytometry Part A* 66(1): 78–84.

Brosnan ME, Brosnan JT. 2009. "Hepatic Glutamate Metabolism: A Tale of 2 Hepatocytes." *American Journal of Clinical Nutrition* 90(3).

Brys K, Vanfleteren JR, Braeckman BP. 2007. "Testing the Rate-of-Living/oxidative Damage Theory of Aging in the Nematode Model Caenorhabditis Elegans." *Experimental gerontology* 42(9): 845–51.

Buening MK, Chang RL, Huang MT, Fortner JG, Wood AW, Conney AH. 1981. "Activation and Inhibition of Benzo(a)pyrene and Aflatoxin B1 Metabolism in Human Liver Microsomes by Naturally Occurring Flavonoids." *Cancer research* 41: 67–72.

Butler D, Bahr BA. 2006. "Oxidative Stress and Lysosomes: CNS-Related Consequences and Implications for Lysosomal Enhancement Strategies and Induction of Autophagy." *Antioxidants & redox signaling* 8(1-2): 185–96.

Campisi J. 2000. "Cancer, Aging and Cellular Senescence." *In Vivo* 14(1): 183–88.

Carriere R. 1967. "Polyploid Cell Reproduction in Normal Adult Rat Liver." *Experimental cell research* 46(3): 533–40.

Carvalho M, Remião F, Milhazes N, Borges F, Fernandes E, Carvalho F, Bastos ML. 2004. "The Toxicity of N-Methyl-A-Methyldopamine to Freshly Isolated Rat Hepatocytes Is Prevented by Ascorbic Acid and N-Acetylcysteine." *Toxicology* 200(2-3): 193–203.

Castro L, and Freeman BA. 2001. "Reactive Oxygen Species in Human Health and Disease." *Nutrition* 17(2): 161–65.

Chance B, Sies H, Boveris A. 1979. “Hydroperoxide Metabolism in Mammalian Organs.” *Physiological reviews* 59(3): 527–605.

Q Chen, A Fischer, J D Reagan, L J Yan, and B N Ames. 1995. “Oxidative DNA Damage and Senescence of Human Diploid Fibroblast Cells.” *Proceedings of the National Academy of Sciences of the United States of America* 92(10): 4337–41.

Chokkathukalam A, Kim DH, Barrett MP, Breitling R, Creek DJ. 2014. “Stable Isotope-Labeling Studies in Metabolomics: New Insights into Structure and Dynamics of Metabolic Networks.” *Bioanalysis* 6(4): 511–24.

Christensen B, and Nielsen J. 1999. “Isotopomer Analysis Using GC-MS.” *Metabolic engineering* 1(4): 282–90.

Chung HY, Sung B, Jung KJ, Zou Y, Yu BP. 2006. “The Molecular Inflammatory Process in Aging.” *Antioxidants & redox signaling* 8(3-4): 572–81.

Ciechanover A. 2005. “Proteolysis: From the Lysosome to Ubiquitin and the Proteasome.” *Nature reviews. Molecular cell biology* 6(1): 79–87.

Clark S, Francis PS, Conlan XA, Barnett NW. 2007. “Determination of Urea Using High-Performance Liquid Chromatography with Fluorescence Detection after automated derivatisation with xanthydrol. J Chromatogr A 1161(1-2):207-13.

Commoner B, Townsend J and Pake GE. 1954. “Free Radicals in Biological Materials.” *Nature* 174(4432): 689–91.

Conconi M, Szweda LI, Levine RL, Stadtman ER, and Friguet B. 1996. “Age-Related Decline of Rat Liver Multicatalytic Proteinase Activity and Protection from Oxidative Inactivation by Heat-Shock Protein 90.” *Archives of biochemistry and biophysics* 331(2): 232–40.

Conde de la Rosa L, Schoemaker MH, Vrenken TE, Buist-Homan M, Havinga R, Jansen PL, Moshage H. 2006. “Superoxide Anions and Hydrogen Peroxide Induce Hepatocyte Death by Different Mechanisms: Involvement of JNK and ERK MAP Kinases.” *Journal of Hepatology* 44(5): 918–29.

Cornelius E. 1972. “Increased Incidence of Lymphomas in Thymectomized Mice--Evidence for an Immunological Theory of Aging.” *Experientia* 28(4): 459.

Crane LJ, and Miller DL. 1977. “Plasma Protein Synthesis by Isolated Rat Hepatocytes.” *The Journal of cell biology* 72(1): 11–25.

Dajas F, Rivera-Megret F, Blasina F, Arredondo F, Abin-Carriquiry JA, Costa G, Echeverry C, Lafon L, Heizen H, Ferreira M, Morquio A. 2003. “Neuroprotection by Flavonoids.” *Brazilian Journal of Medical and Biological Research* 36(12): 1613–20.

Mueller D, Tascher G, Müller-Vieira U, Knobeloch D, Nuessler AK, Zeilinger K, Heinzle E, Noor F. 2011. “In-Depth Physiological Characterization of Primary Human Hepatocytes

in a 3D Hollow-Fiber Bioreactor." *Journal of tissue engineering and regenerative medicine*.

Davidovic M, Goran S, Petar S, Dragoslav PM, Nebojsa D, and Predrag E. 2010. "Old Age as a Privilege of the 'Selfish Ones'." *Aging and disease* 1(2): 139–46.

Davidson JF, and Schiestl RH. 2001. "Mitochondrial Respiratory Electron Carriers Are Involved in Oxidative Stress during Heat Stress in Saccharomyces Cerevisiae." *Molecular and cellular biology* 21(24): 8483–89.

Wu D, Cederbaum AI. 2004. "Alcohol, Oxidative Stress, and Free Radical Damage." *National Institute on Alcohol Abuse and Alcoholism*.

DeLeve LD, Kaplowitz N. 1991. "Glutathione Metabolism and Its Role in Hepatotoxicity." *Pharmacology and Therapeutics* 52(3): 287–305.

Diggs J. 2008. "The Cross-Linkage Theory of Aging." *Encyclopedia of Aging and Public Health*: 250–52.

Ding Q, Dimayuga E, Keller JN. 2006. "Proteasome Regulation of Oxidative Stress in Aging and Age-Related Diseases of the CNS." *Antioxidants & redox signaling* 8(1-2): 163–72.

Woodhouse K. 1992. "Drugs and the Liver:Ageing of the Liver and the Metabolism." *Biopharmaceutics & Drug Disposition* 13: 311-320

Dodd SO, Dean DLC, Malhi GS, and Berk M. 2008. "N-Acetylcysteine for Antioxidant Therapy: Pharmacology and Clinical Utility." *Expert Opinion on Biological Therapy* 8(12): 1955–62.

Dröge W. 2002. "Free Radicals in the Physiological Control of Cell Function." *Physiol Rev* 82: 47–95.

El-Nekeety AA, Sekena HAA, Aziza MH, Nabila SH, Soher EA, and Mosaad AW. 2014. "Quercetin Inhibits the Cytotoxicity and Oxidative Stress in Liver of Rats Fed Aflatoxin-Contaminated Diet." *Toxicology Reports* 1(0): 319–29.

Abeer H.**,** Sally SA**,** Amira AER. 2012. "Genetic and Biochemical Studies on Hepatocytes of Young and Old Heat-Stressed Rats." *Journal of the Arab Society for Medical Research* 7: 78–85.

Ermak G, Davies KJ. 2002. "Calcium and Oxidative Stress: From Cell Signaling to Cell Death." *Molecular immunology* 38(10): 713–21.

Estrela JM, Saez GT, Such, L, and Vina J. 1983. "The Effect of Cysteine and N-Acetyl Cysteine on Rat Liver Glutathione (GSH)." *Biochemical pharmacology* 32(22): 3483–85.

Fabrizio P, Pozza F, Pletcher SD, Gendron CM, and Longo VD. 2001. "Regulation of Longevity and Stress Resistance by Sch9 in Yeast." *Science (New York, N.Y.)* 292(5515): 288–90.

Fenton HJH. 1894. "Oxidation of Tartaric Acid in Presence of Iron." *J. Chem. Soc. Proc.* 10: 157–58.

Festing MF, Diamanti P, and Turton JA. 2001. "Strain Differences in Haematological Response to Chloroamphenicol Succinate in Mice: Implications for Toxicological Research." *Food and Chemical Toxicology* 39(4): 375–83.

Toren F. 2000. "Redox-Dependent Signal Transduction." *FEBS Letters* 476(1-2): 52–54.

Fortun J, Go JC, Li J, Amici SA, Dunn WA Jr, Notterpek L. 2006. "Alterations in Degradative Pathways and Protein Aggregation in a Neuropathy Model Based on PMP22 Overexpression." *Neurobiology of Disease* 22(1): 153–64.

Fridman E' Pichersky E. 2005. "Metabolomics, Genomics, Proteomics, and the Identification of Enzymes and Their Substrates and Products." *Current Opinion in Plant Biology* 8(3 SPEC. ISS.): 242–48.

Frith J, Jones D, Newton JL. 2009. "Chronic Liver Disease in an Ageing Population." *Age and Ageing* 38(1): 11–18.

Gao X, Zhao A, Zhou M, Lin J, Qiu Y, Su M and Jia W. 2011. "GC/MS-Based Urinary Metabolomics Reveals Systematic Differences in Metabolism and Ethanol Response between Sprague-Dawley and Wistar Rats." *Metabolomics* 7(3): 363–74.

García-López P, Pérez-Urizar J, Ibarra A, Grijalva I, Madrazo I, Flores-Murrieta F, Castañeda-Hernández G, Guízar-Sahagún G. 1996. "Comparison between Sprague-Dawley and Wistar Rats as an Experimental Model of Pharmacokinetic Alterations Induced by Spinal Cord Injury." *Arch Med Res* 27(4): 453–57.

Gasparin FR, Salgueiro-Pagadigorria CL, Bracht L, Ishii-Iwamoto EL, Bracht A, Constantin J. 2003. "Action of Quercetin on Glycogen Catabolism in the Rat Liver." *Xenobiotica* 33(6): 587–602.

Gasparin, FRS, Spitzner FL, Ishii-Iwamoto EL, Bracht A, and Constantin J. 2003. "Actions of Quercetin on Gluconeogenesis and Glycolysis in Rat Liver." *Xenobiotica* 33(9): 903–11.

Giorgio M, Trinei M, Migliaccio E, Pelicci PG. 2007. "Hydrogen Peroxide: A Metabolic by-Product or a Common Mediator of Ageing Signals?" *Nature reviews. Molecular cell biology* 8(9): 722–28.

Gire V and Wynford-Thomas D. 1998. "Reinitiation of DNA Synthesis and Cell Division in Senescent Human Fibroblasts by Microinjection of Anti-p53 Antibodies." *Molecular and cellular biology* 18(3): 1611–21.

Gomes A, Eduarda F and José LFCL. 2005. “Fluorescence Probes Used for Detection of Reactive Oxygen Species.” *Journal of Biochemical and Biophysical Methods* 65(2-3): 45–80.

Goswami A, Dikshit P, Mishra A, Mulherkar S, Nukina N, Jana NR. 2006. “Oxidative Stress Promotes Mutant Huntingtin Aggregation and Mutant Huntingtin-Dependent Cell Death by Mimicking Proteasomal Malfunction.” *Biochemical and Biophysical Research Communications* 342(1): 184–90.

Guengerich FP. 1992. “Characterization of Human Cytochrome P450 Enzymes.” *FASEB Journal* 6: 745–48.

Hagen JL, Krause DJ, Baker DJ, Fu MH, Tarnopolsky MA, Hepple RT. 2004. “Skeletal Muscle Aging in F344BN F1-Hybrid Rats: I. Mitochondrial Dysfunction Contributes to the Age-Associated Reduction in VO2max.” *The journals of gerontology. Series A, Biological sciences and medical sciences* 59(11): 1099–1110.

Hagen TM. 2005. “Oxidative Stress, Redox Imbalance, and the Aging Process.” *Antioxidant & Redox Signaling* 5(5): 503–6.

Hall DM, Xu L, Drake VJ, Oberley LW, Oberley TD, Moseley PL, Kregel KC. 2000. “Aging Reduces Adaptive Capacity and Stress Protein Expression in the Liver after Heat Stress.” *Journal of applied physiology (Bethesda, Md. : 1985)* 89(2): 749–59.

Harman D. 1956. “Aging: A Theory Based on Free Radical and Radiation Chemistry.” : 298–300.

Hart S J, Calder IC, and Tange JD. 1982. “The Metabolism and Toxicity of Paracetamol in Sprague-Dawley and Wistar Rats.” *European journal of drug metabolism and pharmacokinetics* 7(3): 203–22.

Hayes GR, and Lockwood DH. 1987. “Role of Insulin Receptor Phosphorylation in the Insulinomimetic Effects of Hydrogen Peroxide.” *Proc Natl Acad Sci U S A* 84: 8115–19.

Heemst DV. 2010. “Insulin, IGF-1 and Longevity.” *Aging and Disease* 1: 147–57.

Hempelmann LH, and Hoffman JG. 1953. “Practical Aspects of Radiation Injury.” *Annual Review of Nuclear Science* 3(1): 369–92.

Herbig U, Ferreira M, Condel L, Carey D, Sedivy JM. 2006. “Cellular Senescence in Aging Primates.” *Science (New York, N.Y.)* 311(5765): 1257.

Heydari AR, You S, Takahashi R, Gutsmann-Conrad A, Sarge KD, Richardson A. 2000. “Age-Related Alterations in the Activation of Heat Shock Transcription Factor 1 in Rat Hepatocytes.” *Exp Cell Res* 256(1): 83–93.

Holmström KM, Finkel T. 2014. “Cellular Mechanisms and Physiological Consequences of Redox-Dependent Signalling.” *Nature reviews. Molecular cell biology* 15(6): 411–21.

Holzenberger M, Dupont J, Ducos B, Leneuve P, Géloën A, Even PC, Cervera P, Le Bouc Y. 2003. "IGF-1 Receptor Regulates Lifespan and Resistance to Oxidative Stress in Mice." *Nature* 421(6919): 182–87.

Hood L, Heath JR, Phelps ME, and Lin B. 2004. "Systems Biology and New Technologies Enable Predictive and Preventative Medicine." *Science (New York, N.Y.)* 306(5696): 640–43.

Horowitz M. 1998. "Do Cellular Heat Acclimation Responses Modulate Central Thermoregulatory Activity ?" *Physiology* 13: 218–25.

Houtkooper RH, Argmann C, Houten SM, Cantó C, Jeninga EH, Andreux PA, Thomas C, Doenlen R, Schoonjans K, Auwerx J. 2011a. "The Metabolic Footprint of Aging in Mice." *Scientific reports* 1: 134.

Hursting SD, Lavigne JA, Berrigan D, Perkins SN, Barrett JC. 2003. "Calorie Restriction, Aging, and Cancer Prevention: Mechanisms of Action and Applicability to Humans." *Annual review of medicine* 54: 131–52.

Hwan C, Sinskey AJ and Lodish HF. 1992. "Oxidized Redox State of Glutathione in the Endoplasmic Reticulum." *Science (New York, N.Y.)* 257(5076): 1496–1502.

Imlay JA and Linn S. 1988. "DNA Damage and Oxygen Radical Toxicity." *Science (New York, N.Y.)* 240: 1302–9.

Ippolito DL, Lewis JA, Yu C, Leon LR, and Stallings JD. 2014. "Alteration in Circulating Metabolites during and after Heat Stress in the Conscious Rat: Potential Biomarkers of Exposure and Organ-Specific Injury." *BMC Physiology* 14(1): 1–17.

Jones DP, Thor H, Andersson B and Orrenius S. 1978. "Detoxification Reactions in Isolated Hepatocytes. Role of Glutathione Peroxidase, Catalase, and Formaldehyde Dehydrogenase in Reactions Relating to N-Demethylation by the Cytochrome P-450 System." *Journal of Biological Chemistry* 253(17): 6031–37.

Judah JD and Nicholls MR. 1971. "Biosynthesis of Rat Serum Albumin." *Biochemical Journal* 123(4): 649–55.

Katschinski DM, Boos K, Schindler SG and Fandrey J. 2000. "Pivotal Role of Reactive Oxygen Species as Intracellular Mediators of Hyperthermia-Induced Apoptosis." *Journal of Biological Chemistry* 275(28): 21094–98.

Kell DB, Brown M, Davey HM, Warwick BD, Spasic I and Oliver SG. 2005. "Metabolic Footprinting and Systems Biology: The Medium Is the Message." *Nature reviews. Microbiology* 3(7): 557–65.

Kelleher JK. 1999. "Estimating Gluconeogenesis with [U-13C]glucose: Molecular Condensation Requires a Molecular Approach." *The American journal of physiology* 277(3 Pt 1): E395–400.

Kelly GS. 1998. “Clinical Applications of N-Acetylcysteine.” *Alternative Medicine Review* 3(2): 114–27.

Kenyon CJ. 2010. “The Genetics of Ageing.” *Nature* 464(7288): 504–12.

Kirkwood TB and Austad SN. 2000. “Why Do We Age?” *Nature* 408(6809): 233–38.

Kishida T, Muto S, Hayashi M, Tsutsui M, Tanaka S, Murakami M, Kuroda J. 2008. “Strain Differences in Hepatic Cytochrome P450 1A and 3A Expression between Sprague-Dawley and Wistar Rats.” *The Journal of toxicological sciences* 33(4): 447–57.

Kitani K. 1992. “Liver and Aging.” *Gastroenterologia Japonica* 27(2): 276–85.

Kourtis N, Tavernarakis N. 2011. “Cellular Stress Response Pathways and Ageing: Intricate Molecular Relationships.” *The EMBO journal* 30(13): 2520–31.

Kregel KC, Zhang HJ. 2007. “An Integrated View of Oxidative Stress in Aging : Basic Mechanisms , Functional Effects , and Pathological Considerations.” *American Journal of Integrative Comp Physiology* 292: 18–36.

Krömer JO, Fritz M, Heinzle E, Wittmann C. 2005. “In Vivo Quantification of Intracellular Amino Acids and Intermediates of the Methionine Pathway in Corynebacterium Glutamicum.” *Analytical Biochemistry* 340(1): 171–73.

Kubatka P, Ahlersová E, Ahlers I, Bojková B, Kalická K, Adámeková E, Marková M, Chamilová M, Ermáková M. 2002. “Variability of Mammary Carcinogenesis Induction in Female Sprague-Dawley and Wistar:Han Rats: The Effect of Season and Age.” *Physiological research / Academia Scientiarum Bohemoslovaca* 51(6): 633–40.

Kühn ER, Bellon K, Huybrechts L and Heyns W. 1983. “Endocrine Differences between the Wistar and Sprague-Dawley Laboratory Rat: Influence of Cold Adaptation.” *Hormone and metabolic research* 15(10): 491–98.

Kulju KS and Lehman JM. 1995. “Increased p53 Protein Associated with Aging in Human Diploid Fibroblasts.” *Exp Cell Res* 217(2): 336–45.

Laine RA and Sweeley CC. 1971. “Analysis of Trimethylsilyl O-Methyloximes of Carbohydrates by Combined Gas-Liquid Chromatography-Mass Spectrometry.” *Analytical biochemistry* 43(2): 533–38.

LeBel CP, Ischiropoulos H and Bondy SC. 1992. “Evaluation of the Probe 2’,7'-Dichlorofluorescin as an Indicator of Reactive Oxygen Species Formation and Oxidative Stress.” *Chemical research in toxicology* 5(2): 227–31.

Li SQ, Li RF, Xi SM, Hu S, Jia ZQ, Li SP, Wen XL, Song YK, Li S, Li SP, Wei FB, Chen XL. 2012. “Systematical Analysis of Impacts of Heat Stress on the Proliferation, Apoptosis and Metabolism of Mouse Hepatocyte.” *Journal of Physiological Sciences* 62(1): 29–43.

Li Y, Deng Y, Tang Y, Yu H, Gao C, Liu L and Yao P. 2013. "Quercetin Protects Rat Hepatocytes from Oxidative Damage Induced by Ethanol and Iron by Maintaining Intercellular Liable Iron Pool." *Human & experimental toxicology* 33: 534.

Liu S, Hou W, Yao P, Zhang B, Sun S, Nüssler AK, Liu L. 2010. "Quercetin Protects against Ethanol-Induced Oxidative Damage in Rat Primary Hepatocytes." *Toxicology in vitro : an international journal published in association with BIBRA* 24(2): 516–22.

Lu SC. 1999. "Regulation of Hepatic Glutathione Synthesis: Current Concepts and Controversies." *FASEB journal : official publication of the Federation of American Societies for Experimental Biology* 13(10): 1169–83.

Lu SC, Sun WM, Yi J, Ookhtens M, Sze G and Kaplowitz N. 1996. "Role of Two Recently Cloned Rat Liver GSH Transporters in the Ubiquitous Transport of GSH in Mammalian Cells." *Journal of Clinical Investigation* 97(6): 1488–96.

Lu Y, A J, Wang G, Hao H, Huang Q, Yan B, Zha W, Gu S, Ren H, Zhang Y, Fan X, Zhang M, Hao K. 2008. "Gas Chromatography/time-of-Flight Mass Spectrometry Based Metabonomic Approach to Differentiating Hypertension- and Age-Related Metabolic Variation in Spontaneously Hypertensive Rats." *Rapid Communications in Mass Spectrometry* 22(18): 2882–88.

Malarkey DE, Johnson K, Ryan L, Boorman G and Maronpot RR. 2005. "New Insights into Functional Aspects of Liver Morphology." *Toxicologic pathology* 33(1): 27–34.

Manach C, Texier O, Morand C, Crespy V, Régérat F, Demigné C, Rémésy C.. 1999. "Comparison of the Bioavailability of Quercetin and Catechin in Rats." *Free Radical Biology and Medicine* 27(11-12): 1259–66.

Martin DE, Soulard A, Hall MN. 2004. "TOR Regulates Ribosomal Protein Gene Expression via PKA and the Forkhead Transcription Factor FHL1." *Cell* 119(7): 969–79.

Matés JM, Pérez-Gómez C, Núñez de Castro I. 1999. "Antioxidant Enzymes and Human Diseases." *Clinical biochemistry* 32(8): 595–603.

Matsuzawa A, Ichijo H. 2005. "Stress-Responsive Protein Kinases in Redox-Regulated Apoptosis Signaling." *Antioxidants & redox signaling* 7(3-4): 472–81.

Michiels C, Raes M, Toussaint O, Remacle J. 1994. "Importance of Se-Glutathione Peroxidase, Catalase, and Cu/Zn-SOD for Cell Survival against Oxidative Stress." *Free Radical Biology and Medicine* 17(3): 235–48.

Middleton E Jr, Kandaswami C, Theoharides TC.. 2000. "The Effects of Plant Flavonoids on Mammalian Cells : Implications for Inflammation , Heart Disease , and Cancer." *Pharmacol Rev* 52(4): 673–751.

Mishur RJ, Rea SL.. 2012. "Applications of Mass Spectrometry to Metabolomics and Metabonomics: Detection of Biomarkers of Aging and of Age-Related Diseases." *Mass Spectrometry Reviews* 31(1): 70–95.

Berry MN, Grivell AR, and Grivell MB. 1997. “Isolated Hepatocytes--Past, Present and Future.” *Cell Biol Toxicol.* 13(4-5): 223–33.

Mo ML, Palsson BO, Herrgård MJ. 2009. “Connecting Extracellular Metabolomic Measurements to Intracellular Flux States in Yeast.” *BMC Systems Biology*.

Morimoto RI. 2008. “Proteotoxic Stress and Inducible Chaperone Networks in Neurodegenerative Disease and Aging.” *Genes and Development* 22(11): 1427–38.

Mortimore GE, and Pösö AR. 1987. “Intracellular Protein Catabolism and Its Control during Nutrient Deprivation and Supply.” *Annual review of nutrition* 7: 539–64.

Moseley PL. 1997. “Heat Shock Proteins and Heat Adaptation of the Whole Organism.” *Journal of applied physiology (Bethesda, Md. : 1985)* 83(5): 1413–17.

Mueller D, Tascher G, Müller-Vieira U, Knobeloch D, Nuessler AK, Zeilinger K, Heinzle E, Noor F. 2011. “In-Depth Physiological Characterization of Primary Human Hepatocytes in a 3D Hollow-Fiber Bioreactor.” *Journal of Tissue Engineering and Regenerative Medicine* 5(8).

Muller FL, Lustgarten MS, Jang Y, Richardson A, Van Remmen H. 2007. “Trends in Oxidative Aging Theories.” *Free Radical Biology and Medicine* 43(4): 477–503.

Murphy MP. 2009. “How Mitochondria Produce Reactive Oxygen Species.” *The Biochemical journal* 417(1): 1–13.

Nevedomskaya E, Meissner A, Goraler S, De Waard M, Ridwan Y, Zondag G, Pluijm IVD, Deelder AM, and Mayboroda OA. 2010. “Metabolic Profiling of Accelerated Aging ERCC1d/- Mice.” *Journal of Proteome Research* 9(7): 3680–87.

Nicholson JK, Wilson ID. 2003. “Opinion: Understanding ‘Global’ Systems Biology: Metabonomics and the Continuum of Metabolism.” *Nat. Rev. Drug Discovery.* 2(August): 668–76.

Nicolae A, Wahrheit J, Bahnemann J, Zeng AP, Heinzle E. 2014. “Non-Stationary 13C Metabolic Flux Analysis of Chinese Hamster Ovary Cells in Batch Culture Using Extracellular Labeling Highlights Metabolic Reversibility and Compartmentation.” *BMC systems biology* 8(1): 50.

Niki, Etsuo, Yasukazu Yoshida, Yoshiro Saito, and Noriko Noguchi. 2005. “Lipid Peroxidation: Mechanisms, Inhibition, and Biological Effects.” *Biochemical and Biophysical Research Communications* 338(1): 668–76.

Niklas J, Nonnenmacher Y, Rose T, Sandig V, Heinzle E. 2012. “Quercetin Treatment Changes Fluxes in the Primary Metabolism and Increases Culture Longevity and Recombinant α1-Antitrypsin Production in Human AGE1.HN Cells.” *Applied Microbiology and Biotechnology* 94(1): 57–67.

Nishina H, Wada T, Katada T. 2004. "Physiological Roles of SAPK/JNK Signaling Pathway." *Journal of Biochemistry* 136(2): 123–26.

Noor F, Niklas J, Müller-Vieira U, Heinzle E. 2009. "An Integrated Approach to Improved Toxicity Prediction for the Safety Assessment during Preclinical Drug Development Using Hep G2 Cells." *Toxicology and Applied Pharmacology* 237(2): 221–31.

North S, Moenner M, Bikfalvi A. 2005. "Recent Developments in the Regulation of the Angiogenic Switch by Cellular Stress Factors in Tumors." *Cancer Letters* 218(1): 1–14.

O'Donnell VB, Spycher S and Azzi A. 1995. "Involvement of Oxidants and Oxidant-Generating Enzyme(s) in Tumour-Necrosis-Factor-Alpha-Mediated Apoptosis: Role for Lipoxygenase Pathway but Not Mitochondrial Respiratory Chain." *The Biochemical journal* 310 (Pt 1: 133–41.

Oberley TD, Swanlund JM, Zhang HJ, Kregel KC. 2008. "Aging Results in Increased Autophagy of Mitochondria and Protein Nitration in Rat Hepatocytes Following Heat Stress." *The journal of histochemistry and cytochemistry : official journal of the Histochemistry Society* 56(6): 615–27.

Oliver CN, Ahn BW, Moerman EJ, Goldstein S and Stadtman ER.. 1987. "Age-Related Changes in Oxidized Proteins." *Journal of Biological Chemistry* 262(12): 5488–91.

Oshino NDJ and Chance B. 1975. "The Properties of Hydrogen Peroxide Production under Hyperoxic and Hypoxic Conditions of Perfused Rat Liver." *Biochemical Journal* 146(1): 53–65.

Pawłowska-Góral K, Kurzeja E, Stec M. 2013. "N-Acetylcysteine Protects against Fluoride-Induced Oxidative Damage in Primary Rat Hepatocytes." *Toxicology in Vitro* 27(8): 2279–82.

Perry J J P, Shin DS, Getzoff ED and Tainer JA. 2010. "The Structural Biochemistry of the Superoxide Dismutases." *Biochimica et Biophysica Acta - Proteins and Proteomics* 1804(2): 245–62.

Pilkhwal S, Tirkey N, Kuhad A and Chopra K. 2010. "Effect of Bioflavonoid Quercetin on Endotoxin- Induced Hepatotoxicity and Oxidative Stress in Rat Liver." *Iranian Journal of Pharmacology & Therapeutics* 9(2): 47–53.

Plumb RS, Granger JH, Stumpf CL, Johnson KA, Smith BW, Gaulitz S, Wilson ID, Castro-Perez J. 2005. "A Rapid Screening Approach to Metabonomics Using UPLC and Oa-TOF Mass Spectrometry: Application to Age, Gender and Diurnal Variation in normal/Zucker Obese Rats and Black, White and Nude Mice." *The Analyst* 130(6): 844–49.

Priesnitz C, Sperber S, Garg R, Orsini M and Noor F. 2016. "Fluorescence Based Cell Counting in Collagen Monolayer Cultures of Primary Hepatocytes." *Cytotechnology* 68(4):1647-53.

Rahman I, Kode A, and Biswas SK. 2006. "Assay for Quantitative Determination of Glutathione and Glutathione Disulfide Levels Using Enzymatic Recycling Method." *Nature protocols* 1(6): 3159–65.

Rangan GK, Wang Y, Tay YC, Harris DC. 1999. "Inhibition of NF Kappa B Activation with Antioxidants Is Correlated with Reduced Cytokine Transcription in PTC." *Renal Physiology* 277: 779–89.

Rattan SI. 2008. "Hormesis in Aging." *Ageing Research Reviews* 7(1): 63–78.

Riceo-Evans C., Miller NJ, Paganga G. 1997. "Antioxidant Properties of Phenolic Compounds." *Trends in Plant Science* 2(4): 152–59.

Richardson A, Liu F, Adamo ML, Van Remmen H, Nelson JF. 2004. "The Role of Insulin and Insulin-like Growth Factor-I in Mammalian Ageing." *Best practice & research. Clinical endocrinology & metabolism* 18(3): 393–406.

Richter CJWP and Ames BN. 1988. "Normal Oxidative Damage to Mitochondrial and Nuclear DNA Is Extensive." *Proceedings of the National Academy of Sciences of the United States of America* 85(17): 6465–67.

Rikans LE and Hornbrook KR. 1997. "Lipid Peroxidation, Antioxidant Protection and Aging." *Biochimica et biophysica acta* 1362(2-3): 116–27.

Riley MG, Castelli MC, Paehler EA.. 2000. "Subchronic Oral Toxicity of Salcaprozate Sodium (SNAC) in Sprague-Dawley and Wistar Rats." *International journal of toxicology* 28(4): 278–93.

Riley PA. 1994. "Free Radicals in Biology : Oxidative Stress and the Effects of Ionizing Radiation."

Roberts LJ and Reckelhoff JF. 2001. "Measurement of F(2)-Isoprostanes Unveils Profound Oxidative Stress in Aged Rats." *Biochemical and biophysical research communications* 287(1): 254–56.

Rose MR. 1988. "Modern Biological Theories of Aging." *American journal of human genetics* 43(2): 220–21.

Roy S, Sen CK, Packer L. 1998. "Determination of Cell-Cell Adhesion in Response to Oxidants and Antioxidants." *Methods in Enzymology* 300: 395–401.

Sastre J, Pallardó FV, Plá R, Pellín A, Juan G, O'Connor JE, Estrela JM, Miquel J, Viña J. 1996. "Aging of the Liver: Age-Associated Mitochondrial Damage in Intact Hepatocytes." *Hepatology* 24(5): 1199–1205.

Schamhart DH, Berendsen W, van Rijn J, and van Wijk R. 1984. "Comparative Studies of Heat Sensitivity of Several Rat Hepatoma Cell Lines and Hepatocytes in Primary Culture." *Cancer research* 44(10): 4507–16.

Schmucker DL. 1998. “Aging and the Liver: An Update.” *The journals of gerontology. Series A, Biological sciences and medical sciences* 53(5): B315–20.

Schmucker DL. 2005. “Age-Related Changes in Liver Structure and Function: Implications for Disease?” *Experimental Gerontology* 40(8-9): 650–59.

Schmucker DL and Sanchez H. 2011. “Liver Regeneration and Aging: A Current Perspective.” *Current Gerontology and Geriatrics Research* 2011.

Schnackenberg LK, Sun J, Espandiari P, Holland RD, Hanig J and Beger RD. 2007. “Metabonomics Evaluations of Age-Related Changes in the Urinary Compositions of Male Sprague Dawley Rats and Effects of Data Normalization Methods on Statistical and Quantitative Analysis.” *BMC bioinformatics* 8 Suppl 7: S3.

Schrader M, Fahimi HD.. 2006. “Peroxisomes and Oxidative Stress.” *Biochimica et Biophysica Acta - Molecular Cell Research* 1763(12): 1755–66.

Seglen PO. 1976. “Preparation of Isolated Rat Liver Cells.” *Methods Cell Biol.* 13: 29–83.

Shellabarger CJ, Stone JP and Holtzman S. 1978. “Rat Differences in Mammary Tumor Induction with Estrogen and Neutron Radiation.” *Journal of the National Cancer Institute* 61(6): 1505–8. .

Shenvi SV, Dixon BM, Shay KP and Hagen TM. 2008. “A Rat Primary Hepatocyte Culture Model for Aging Studies.” *Current Protocols in Toxicology* (Suppl. 37).

Shirai T, Nakamura A, Fukushima S, Yamamoto A, Tada M and Ito N. 1990. “Different Carcinogenic Responses in a Variety of Organs, Including the Prostate, of Five Different Rat Strains given 3,2’-Dimethyl-4-Aminobiphenyl.” *Carcinogenesis* 11(5): 793–97.

Ikeyama S, Kokkonen G, Shack S, Wang XT, Holbrook NJ. 2002. “Loss in Oxidative Stress Tolerance with Aging Linked to Reduced Extracellular Signal-Regulated Kinase and Akt Kinase Activities.” *The FASEB journal : official publication of the Federation of American Societies for Experimental Biology* 16(1): 93–95.

Singh D, Ghander V and Chopra K. 2004. “The Effect of Quercetin, a Bioflavonoid on Ischemia/reperfusion Induced Renal Injury in Rats.” *Archives of Medical Research* 35(6): 484–94.

Soltow QA, Jones DP and Promislow DEL. 2010. “A Network Perspective on Metabolism and Aging.” *Integrative and Comparative Biology* 50(5): 844–54.

Son N, Hur HJ, Sung MJ, Kim MS, Hwang JT, Park JH, Yang HJ, Kwon DY, Yoon SH, Chung HY, Kim HJ. 2012. “Liquid Chromatography-Mass Spectrometry-Based Metabolomic Analysis of Livers from Aged Rats.” *Journal of Proteome Research* 11(4): 2551–58.

Sotaniemi EA, Arranto AJ, Pelkonen O, Pasanen M.. 1997. "Age and Cytochrome P450-Linked Drug Metabolism in Humans: An Analysis of 226 Subjects with Equal Histopathologic Conditions." *Clinical Pharmacology and Therapeutics* 61(3): 331–39.

Stadtman, ER. 1992. "Protein Oxidation and Aging." *Science* 257(5074): 1220–24.

Starke PE, and Farbee JL. 1985. "Endogenous Defenses against the Cytotoxicity of Hydrogen Peroxide in Cultured Rat Hepatocytes." *Journal of Biological Chemistry* 260(1): 86–92.

Stell D , Frcs G, William JW, and Frcs C. 2003. "The Impact of Aging on the Liver." *Biology of Aging* 6(March).

Sumida KD, Crandall SC, Chadha PL, Qureshi T. 2005. "Differential Effects of Alcohol upon Gluconeogenesis from Lactate in Young and Old Hepatocytes." *Experimental gerontology* 40(4): 324–29.

Suzukawa K[1], Miura K, Mitsushita J, Resau J, Hirose K, Crystal R, Kamata T. 2000. "Nerve Growth Factor-Induced Neuronal Differentiation Requires Generation of Rac1-Regulated Reactive Oxygen Species." *Journal of Biological Chemistry* 275(18): 13175–78.

Tokyol C, Yilmaz S, Kahraman A, Cakar H, Polat C. 2006. "The Effects of Desferrioxamine and Quercetin on Liver Injury Induced by Hepatic Ischaemia-Reperfusion in Rats." *Acta chirurgica Belgica* 106(1): 68–72.

Toussaint O, Royer V, Salmon M, Remacle J. 2002. "Stress-Induced Premature Senescence and Tissue Ageing." *Biochemical Pharmacology* 64(5-6): 1007–9.

Uchida K, Nomura Y, Kadowaki M, Takase H, Takano K, Takeuchi N. 1978. "Age-Related Changes in Cholesterol and Bile Acid Metabolism in Rats." *Journal of lipid research* 19(5): 544–52.

Uri N. 1952. "Inorganic Free Radicals in Solution." *Chem. Rev* 40: 375–454.

Valde MA 2013. "Metabolomic Markers of Aging." *Oxford University press*.

Vichai V, Kirtikara K. 2006. "Sulforhodamine B Colorimetric Assay for Cytotoxicity Screening." *Nature Protocols* 1(3): 1112–16.

Villas-Boas SG, Roessner U, Hansen MAE, Smedsgaard J and Nielsen J. 2007. *Metabolome Analysis: An Introduction* ,. 2007th ed. John Wiley & Sons, Inc.

Viña J, Borrás C and Miquel J. 2007. "Theories of Ageing." *IUBMB life* 59(4-5): 249–54.

Wadsworth TL, McDonald TL and Koop DR. 2001. "Effects of Ginkgo Biloba Extract (EGb 761) and Quercetin on Lipopolysaccharide-Induced Signaling Pathways Involved in the Release of Tumor Necrosis Factor-Alpha." *Biochem Pharmacol* 62(7): 963–74.

Wallace DC. 2005. “A Mitochondrial Paradigm of Metabolic and Degenerative Diseases, Aging, and Cancer: A Dawn for Evolutionary Medicine.” *Annu Rev Genet. 2005 ; 39: 359. d* 39: 359–407.

Wanders RJA, and Waterham HR. 2006. “Peroxisomal Disorders: The Single Peroxisomal Enzyme Deficiencies.” *Biochimica et Biophysica Acta - Molecular Cell Research* 1763(12): 1707–20.

Wang X, Su M, Qiu Y, Ni Y, Zhao T, Zhou M, Zhao A, Yang S, Zhao L, Jia W. 2007. “Metabolic Regulatory Network Alterations in Response to Acute Cold Stress and Ginsenoside Intervention.” *J Proteome Res* 6(9): 3449–55.

Wang X, Zhao T, Qiu Y, Su M, Jiang T, Zhou M, Zhao A, Jia W. 2009. “Metabonomics Approach to Understanding Acute and Chronic Stress in Rat Models.” *Journal of proteome research* 8(5): 2511–18.

Weina G, Changjiang G and Jianquan W. 2009. “The Protective Effects of Quercetin on Rat Hepatocytes Against Oxidative Stress in Metabolomics.” *Annals of Nutrition and Metabolism* 55(Suppl. 1): 431.

Westervelt BP and Timothy JL. 1999. “Inside the Neutrophil Phagosome: Oxidants, Myeloperoxidase, and Bacterial Killing.” *The American Society of Hematology* 93(7): 2143–48.

Wikoff WR, Anfora AT, Liu J, Schultz PG, Lesley SA, Peters EC and Siuzdak G. 2009. “Metabolomics Analysis Reveals Large Effects of Gut Microflora on Mammalian Blood Metabolites.” *Proceedings of the National Academy of Sciences of the United States of America* 106(10): 3698–3703.

Williams RE, Lenz EM, Lowden JS, Rantalainen M and Wilson ID. 2005. “The Metabonomics of Aging and Development in the Rat: An Investigation into the Effect of Age on the Profile of Endogenous Metabolites in the Urine of Male Rats Using 1H NMR and HPLC-TOF MS.” *Molecular bioSystems* 1(2): 166–75.

Wittmann C. 2007. “Fluxome Analysis Using GC-MS.” *Microbial cell factories* 6: 6.

Wittmann C, Hans M and Heinzle E. 2002. “In Vivo Analysis of Intracellular Amino Acid Labelings by GC/MS.” *Analytical Biochemistry* 307(2): 379–82.

Wolkow CA, Kimura KD, Lee MS, Ruvkun G.. 2000. “Regulation of C. Elegans Life-Span by Insulinlike Signaling in the Nervous System.” *Science (New York, N.Y.)* 290(5489): 147–50.

Wullschleger S, Loewith R, Hall MN.. 2006. “TOR Signaling in Growth and Metabolism.” *Cell* 124(3): 471–84.

Wynne HA, Cope LH, Mutch E, Rawlins MD, Woodhouse KW, James OF.. 1989. “The Effect of Age upon Liver Volume and Apparent Liver Blood Flow in Healthy Man.” *Hepatology (Baltimore, Md.)* 9(2): 297–301.

Wallace DC. 2005. “A Mitochondrial Paradigm of Metabolic and Degenerative Diseases, Aging, and Cancer: A Dawn for Evolutionary Medicine.” *Annu Rev Genet. 2005 ; 39: 359. d* 39: 359–407.

Wanders RJA, and Waterham HR. 2006. “Peroxisomal Disorders: The Single Peroxisomal Enzyme Deficiencies.” *Biochimica et Biophysica Acta - Molecular Cell Research* 1763(12): 1707–20.

Wang X, Su M, Qiu Y, Ni Y, Zhao T, Zhou M, Zhao A, Yang S, Zhao L, Jia W. 2007. “Metabolic Regulatory Network Alterations in Response to Acute Cold Stress and Ginsenoside Intervention.” *J Proteome Res* 6(9): 3449–55.

Wang X, Zhao T, Qiu Y, Su M, Jiang T, Zhou M, Zhao A, Jia W. 2009. “Metabonomics Approach to Understanding Acute and Chronic Stress in Rat Models.” *Journal of proteome research* 8(5): 2511–18.

Weina G, Changjiang G and Jianquan W. 2009. “The Protective Effects of Quercetin on Rat Hepatocytes Against Oxidative Stress in Metabolomics.” *Annals of Nutrition and Metabolism* 55(Suppl. 1): 431.

Westervelt BP and Timothy JL. 1999. “Inside the Neutrophil Phagosome: Oxidants, Myeloperoxidase, and Bacterial Killing.” *The American Society of Hematology* 93(7): 2143–48.

Wikoff WR, Anfora AT, Liu J, Schultz PG, Lesley SA, Peters EC and Siuzdak G. 2009. “Metabolomics Analysis Reveals Large Effects of Gut Microflora on Mammalian Blood Metabolites.” *Proceedings of the National Academy of Sciences of the United States of America* 106(10): 3698–3703.

Williams RE, Lenz EM, Lowden JS, Rantalainen M and Wilson ID. 2005. “The Metabonomics of Aging and Development in the Rat: An Investigation into the Effect of Age on the Profile of Endogenous Metabolites in the Urine of Male Rats Using 1H NMR and HPLC-TOF MS.” *Molecular bioSystems* 1(2): 166–75.

Wittmann C. 2007. “Fluxome Analysis Using GC-MS.” *Microbial cell factories* 6: 6.

Wittmann C, Hans M and Heinzle E. 2002. “In Vivo Analysis of Intracellular Amino Acid Labelings by GC/MS.” *Analytical Biochemistry* 307(2): 379–82.

Wolkow CA, Kimura KD, Lee MS, Ruvkun G.. 2000. “Regulation of C. Elegans Life-Span by Insulinlike Signaling in the Nervous System.” *Science (New York, N.Y.)* 290(5489): 147–50.

Wullschleger S, Loewith R, Hall MN.. 2006. “TOR Signaling in Growth and Metabolism.” *Cell* 124(3): 471–84.

Wynne HA, Cope LH, Mutch E, Rawlins MD, Woodhouse KW, James OF.. 1989. “The Effect of Age upon Liver Volume and Apparent Liver Blood Flow in Healthy Man.” *Hepatology (Baltimore, Md.)* 9(2): 297–301.

Yang TH, Bolten CJ, Coppi MV, Sun J, Heinzle E.. 2009. “Numerical Bias Estimation for Mass Spectrometric Mass Isotopomer Analysis.” *Analytical Biochemistry* 388(2): 192–203.

Yen GC, Duh PD, Tsai HL, Huang SL.. 2003. “Pro-Oxidative Properties of Flavonoids in Human Lymphocytes.” *Bioscience, biotechnology, and biochemistry* 67(6): 1215–22.

Yen TC, King KL, Lee HC, Yeh SH, Wei YH. 1994. “Age-Dependent Increase of Mitochondrial DNA Deletions Together with Lipid Peroxides and Superoxide Dismutase in Human Liver Mitochondria.” *Free radical biology & medicine* 16(2): 207–14.

Zainal TA, Oberley TD, Allison DB, Szweda LI, Weindruch R.. 2000. “Caloric Restriction of Rhesus Monkeys Lowers Oxidative Damage in Skeletal Muscle.” *The FASEB journal : official publication of the Federation of American Societies for Experimental Biology* 14(12): 1825–36.

Zangar RC, Davydov DR, Verma S. 2004. “Mechanisms That Regulate Production of Reactive Oxygen Species by Cytochrome P450.” *Toxicology and Applied Pharmacology* 199(3): 316–31.

Zhang A, Sun H, Wang P, Han Y, Wang X.. 2012. “Modern Analytical Techniques in Metabolomics Analysis.” *The Analyst* 137(2): 293.

Zhang HJ, Xu L, Drake VJ, Xie L, Oberley LW, Kregel KC.. 2003a. “Heat-Induced Liver Injury in Old Rats Is Associated with Exaggerated Oxidative Stress and Altered Transcription Factor Activation.” *The FASEB journal : official publication of the Federation of American Societies for Experimental Biology* 17(15): 2293–95.

Zhao QL, Fujiwara Y, Kondo T. 2006. “Mechanism of Cell Death Induction by Nitroxide and Hyperthermia.” *Free Radical Biology and Medicine* 40(7): 1131–43.

Zmarowski A, Beekhuijzen M, Lensen J, Emmen H. 2012. “Differential Performance of Wistar Han and Sprague Dawley Rats in Behavioral Tests: Differences in Baseline Behavior and Reactivity to Positive Control Agents.” *Reprod Toxicol* 34(2): 192–203.

Supplementary Material

Table S1: Extracellular Metabolite fluxes of 19 amino acids, glucose, lactate, pyruvate and urea measured in fmol / cell / h for control (C), heat stress (HS), hydrogen peroxide (H_2O_2), heat stress pre-treated with quercetin (HS + Q) and hydrogen peroxide stress cells pre-treated with quercetin (H_2O_2 + Q) in Sprague Dawley **middle age (MA) PRH** measured during **0 - 12 h**. The values represent average (Avg) and standard deviation (SD) from 3 technical replicates of the three middle age rats (a) middle age rat 1 (MA 1) (b) middle age rat 2 (MA 2) (c) middle age rat 3 (MA 3) (n = 3). Standard 3 letter code is used for amino acids.

(a) Middle age rat 1 (MA 1) 0 – 12 h

MA 1	Avg	SD	Avg	SD	Avg	SD	Avg	SD	Avg	SD
	C	C	HS	HS	H_2O_2	H_2O_2	HS+Q	HS+Q	H_2O_2 + Q	H_2O_2+Q
Asp	-3.80	0.35	-17.93	0.23	-12.92	0.06	-13.78	0.01	-19.42	0.14
Glu	27.30	4.22	22.62	1.92	7.64	2.22	12.78	1.05	6.31	1.86
Asn	-26.48	1.14	-41.11	1.18	-35.20	3.15	-45.59	1.98	-48.33	1.95
Ser	3.42	0.55	-1.77	0.18	-13.12	0.37	-23.26	1.34	-23.80	1.71
Gln	-180.73	4.68	-341.69	6.98	-294.39	18.48	-360.74	26.97	-367.72	19.92
His	-10.55	0.35	-18.34	0.16	-15.60	1.24	-18.39	0.70	-20.50	0.99
Gly	-131.51	2.49	-195.21	6.40	-160.08	13.19	-158.72	3.69	-184.55	7.04
Thr	-33.43	0.51	-62.75	1.77	-51.81	3.50	-65.85	3.87	-69.82	3.17
Arg	-144.05	8.50	-178.21	3.08	-166.47	15.49	-195.88	1.24	-212.17	7.92
Ala	-168.41	8.70	-269.99	13.35	-235.34	3.84	-302.75	13.68	-318.66	17.82
Tyr	-14.15	0.17	-38.93	0.82	-31.25	2.23	-26.33	0.04	-33.06	0.35
Val	2.27	0.71	-23.75	0.99	-21.07	0.27	-22.68	2.05	9.05	0.81
Met	-20.19	0.98	-29.70	0.64	-25.71	2.36	-31.33	0.65	-34.11	1.47
Trp	-9.76	0.17	-14.03	0.30	-13.02	1.18	-14.68	0.47	-16.65	0.46
Phe	-33.23	1.76	-47.37	1.02	-52.90	5.49	-61.25	0.47	-70.09	2.73
Ile	-22.86	1.66	10.59	0.54	6.50	2.14	13.49	2.57	9.85	1.19
Leu	10.46	0.46	15.50	1.24	5.89	2.48	22.49	3.75	15.42	3.49
Lys	-56.10	2.74	-89.04	3.00	-86.81	7.69	-91.67	2.86	-114.51	6.52
Pro	-43.82	2.58	-71.99	6.08	-38.72	1.75	-93.14	5.88	-77.01	2.74
Glc	343.45	61.15	239.82	9.58	384.08	7.99	368.99	49.05	105.91	3.22
Lac	239.27	5.33	293.70	9.48	273.02	13.71	356.73	6.98	368.09	8.58
Pyr	-53.87	3.11	-77.03	1.32	-70.64	5.26	-84.88	0.33	-93.75	1.66
Urea	507.87	33.20	705.71	7.20	602.76	56.85	807.65	20.67	875.88	14.24

(b) Middle age rat 2 (MA 2) 0 – 12 h

MA 2	Avg	SD	Avg	SD	Avg	SD	Avg	SD	Avg	SD
	C	C	HS	HS	H_2O_2	H_2O_2	HS+Q	HS+Q	H_2O_2 + Q	H_2O_2+Q
Asp	-14.72	2.96	-19.68	0.68	-22.39	0.07	-11.02	0.30	-24.84	11.39
Glu	42.92	5.67	35.34	2.19	17.29	3.10	42.11	0.91	27.55	18.86
Asn	-75.45	1.43	-29.80	0.04	-91.60	0.43	-41.80	0.16	-80.06	0.43
Ser	-34.56	1.37	-0.99	0.00	-46.69	1.40	-9.70	0.40	-42.84	1.33
Gln	261.25	23.20	-171.37	1.87	359.65	26.64	-151.85	1.40	243.79	49.04
His	-3.09	1.01	-9.00	0.27	-6.74	0.94	-8.77	0.18	-7.94	2.51
Gly	-127.30	0.89	-158.44	3.25	-101.38	0.29	-134.96	0.11	-107.70	24.40
Thr	-22.09	3.36	-26.37	0.78	-23.65	0.03	-29.46	1.42	-37.07	13.88
Arg	-160.56	1.37	-176.15	2.32	-179.64	16.83	-213.93	9.47	-168.01	0.47
Ala	-560.87	8.84	-320.11	0.84	-629.74	55.20	-445.08	5.12	-594.41	1.73
Tyr	-18.07	1.21	-22.96	0.96	-10.99	2.36	2.23	0.28	-9.50	6.34
Val	9.30	4.70	-12.21	1.15	-1.26	0.17	-3.03	0.06	15.23	21.07
Met	-22.15	0.94	-24.22	0.48	-20.37	1.08	-29.60	0.42	-23.40	4.09
Trp	-1.79	0.45	-3.31	0.01	-2.38	0.09	-2.55	0.32	-2.33	1.41
Phe	-33.51	2.63	-31.61	0.45	-52.64	2.62	-52.99	0.95	-54.68	6.79
Ile	-189.39	4.70	-13.48	0.17	-217.59	19.99	-7.33	0.34	-202.22	1.56
Leu	-285.72	7.49	4.35	0.33	-326.75	30.06	23.48	4.53	-303.18	2.46
Lys	-238.94	4.83	-51.79	1.46	-271.47	24.91	-62.72	1.26	-253.93	0.90
Pro	-47.76	7.97	-70.35	0.82	-60.59	3.29	-11.95	7.82	-77.66	12.00
Glc	542.96	3.36	200.23	91.00	239.89	26.35	472.96	15.48	75.63	8.59
Lac	179.98	6.53	385.36	11.56	200.28	17.49	566.69	26.76	188.42	1.38
Pyr	-68.92	0.57	-75.54	1.03	-77.05	7.22	-91.84	3.97	-72.15	0.00
Urea	494.40	11.25	786.39	7.04	476.72	49.72	1179.94	45.20	530.82	30.35

(c) Middle age rat 3 (MA 3) 0 – 12 h

MA 3	Avg	SD	Avg	SD	Avg	SD	Avg	SD	Avg	SD
	C	C	HS	HS	H_2O_2	H_2O_2	HS+Q	HS+Q	H_2O_2 + Q	H_2O_2+Q
Asp	-13.84	3.42	-7.33	2.18	-6.54	0.55	-4.04	1.89	-4.84	0.51
Glu	44.05	1.01	41.23	0.89	20.92	1.68	26.40	8.18	20.35	1.91
Asn	-25.93	3.06	-19.50	1.83	-16.41	0.10	-29.88	0.48	-25.45	1.18
Ser	1.35	0.41	-0.27	0.04	-8.66	0.52	-24.65	2.29	-19.90	2.47
Gln	-176.64	24.37	-201.65	13.28	-119.32	5.74	-201.23	7.20	-145.32	0.20
His	-5.23	0.93	-3.22	0.59	-6.37	0.27	-8.09	0.23	-6.16	0.25
Gly	-148.04	13.01	-122.16	9.49	-94.26	3.63	-97.80	6.62	-82.29	0.14
Thr	-31.46	4.32	-23.16	3.21	-16.58	0.00	-34.39	1.37	-21.04	1.59
Arg	-184.47	6.72	-158.20	15.73	-184.75	1.38	-228.30	15.28	-179.93	2.81
Ala	-308.11	5.46	-239.49	18.04	-183.13	5.63	-335.83	10.52	-288.07	13.02
Tyr	-25.07	3.60	-21.80	1.94	-14.36	1.10	5.37	1.41	0.54	0.14
Val	0.59	0.00	-2.54	0.75	-2.84	0.74	-5.05	0.00	3.41	1.82
Met	-20.24	1.87	-16.99	1.39	-14.34	0.09	-20.83	0.18	-18.01	0.78
Trp	-2.57	0.42	-1.37	0.31	-3.90	0.03	-4.69	0.05	-3.13	0.40
Phe	-28.71	2.53	-27.30	1.86	-38.54	0.14	-37.12	1.62	-34.44	0.57
Ile	-13.44	8.21	8.03	1.42	4.82	2.18	11.34	5.74	2.92	0.52
Leu	19.59	5.11	34.56	0.56	31.22	3.00	44.32	10.10	23.25	11.74
Lys	-58.61	8.43	-37.39	6.22	-30.23	1.59	-44.04	2.66	-42.30	1.73
Pro	-42.31	3.25	-43.71	14.97	-4.23	0.42	-14.42	0.79	-58.44	1.20
Glc	313.74	24.81	634.88	37.19	649.65	41.53	791.56	54.69	447.90	7.77
Lac	442.09	6.67	376.14	27.45	391.90	0.16	444.42	35.38	386.17	48.84
Pyr	-82.43	3.89	-74.52	3.26	-63.25	0.29	-81.10	1.01	-80.51	11.30
Urea	765.95	32.15	671.28	2.18	654.11	18.01	931.57	86.82	845.17	65.99

Table S2: Extracellular Metabolite fluxes of 19 amino acids, glucose, lactate, pyruvate and urea measured in fmol / cell / h for control (C), heat stress (HS), hydrogen peroxide (H_2O_2), heat stress pre-treated with quercetin (HS + Que) and hydrogen peroxide stress cells pre-treated with quercetin (H_2O_2 + Que) in Sprague Dawley **middle age (MA) PRH** measured during **12 – 24 h**. The values represent average (Avg) and standard deviation (SD) from 3 technical replicates of the three middle age rats (a) middle age rat 1 (MA 1) (b) middle age rat 2 (MA 2) (c) middle age rat 3 (MA 3) (n = 3). Standard 3 letter code is used for amino acids.

(a) Middle age rat 1 (MA 1) 12 – 24 h

MA 1	Avg	SD	Avg	SD	Avg	SD	Avg	SD	Avg	SD
	C	C	HS	HS	H_2O_2	H_2O_2	HS+Q	HS+Q	H_2O_2 + Q	H_2O_2+Q
Asp	-8.18	5.10	-16.86	0.69	-18.53	0.46	-17.56	0.11	-20.91	0.91
Glu	44.32	2.71	45.77	1.40	76.52	2.55	52.74	3.08	20.08	0.08
Asn	-10.91	2.78	-10.61	0.41	-11.48	0.75	-12.77	0.11	-15.80	0.01
Ser	38.13	2.43	12.58	0.82	21.19	0.69	-15.51	1.04	-13.45	0.27
Gln	-71.75	34.59	-167.36	2.73	-215.73	17.70	-157.54	4.33	-196.87	1.31
His	-1.05	0.00	-4.66	0.43	-4.18	0.34	-2.73	0.08	-4.13	0.06
Gly	-135.66	19.67	-102.44	7.87	-123.26	6.87	-62.42	3.12	-99.30	2.34
Thr	15.10	3.41	-8.61	1.89	-9.57	0.69	-3.40	0.98	-6.46	0.12
Arg	-177.40	19.01	-134.80	6.58	-188.82	0.44	-154.62	0.35	-176.84	0.63
Ala	-192.08	21.96	-185.62	11.74	-119.45	13.01	-228.70	0.40	-291.76	1.11
Tyr	-31.53	7.22	-14.39	1.08	-14.06	1.80	-11.16	1.80	-19.85	0.62
Val	5.46	0.44	2.71	0.86	-28.86	1.41	9.17	2.08	11.91	0.84
Met	-11.15	1.37	-11.36	0.87	-14.98	0.81	-12.91	0.14	-16.26	0.17
Trp	-8.67	1.80	-7.53	0.17	-9.81	1.02	-8.96	0.28	-10.37	0.03
Phe	-13.16	3.38	-16.72	1.21	-19.33	0.35	-27.85	0.06	152.02	0.68
Ile	7.37	5.86	-19.07	1.57	-19.48	0.45	9.10	1.93	104.84	0.82
Leu	10.34	0.83	6.21	2.40	8.38	2.24	15.59	3.63	-129.02	0.30
Lys	11.05	5.08	-14.89	1.38	-18.98	4.09	-13.08	3.70	-116.14	3.70
Pro	-16.14	3.81	-32.16	0.56	-19.52	0.25	-43.14	0.12	-54.71	3.70
Glc	324.81	0.00	252.77	8.98	228.70	15.80	282.25	17.70	425.64	27.38
Lac	323.63	34.98	203.78	8.13	305.93	2.45	255.32	5.13	295.38	2.74
Pyr	-103.31	5.77	-85.39	3.50	-120.31	0.00	-99.27	2.20	-114.45	0.00
Urea	745.96	35.93	532.56	22.49	771.03	18.29	694.60	0.60	821.35	1.57

(b) Middle age rat 2 (MA 2) 12 – 24 h

MA 2	Avg	SD	Avg	SD	Avg	SD	Avg	SD	Avg	SD
	C	C	HS	HS	H_2O_2	H_2O_2	HS+Q	HS+Q	H_2O_2 + Q	H_2O_2+Q
Asp	-13.65	1.16	-15.38	0.33	-18.41	4.20	-17.79	0.16	-9.35	0.25
Glu	54.11	2.42	46.32	0.02	27.96	1.43	37.67	2.36	15.45	0.23
Asn	-16.58	1.43	-17.83	0.68	-20.86	0.29	-34.58	0.07	-25.19	0.72
Ser	33.34	2.53	32.85	0.09	18.14	1.29	-1.22	0.00	0.73	0.00
Gln	-81.14	4.31	-109.55	6.76	-163.45	5.11	-200.73	0.81	-177.13	3.62
His	-4.88	0.79	-7.50	0.33	-9.26	0.49	-12.21	1.33	-10.37	0.09
Gly	-209.42	17.92	-211.11	3.27	-224.20	9.29	-171.50	2.23	-105.66	6.80
Thr	-14.55	1.36	-18.44	0.85	-23.50	0.46	-28.48	0.72	-24.16	1.31
Arg	-190.25	12.64	-206.68	14.53	-230.81	2.16	-292.44	12.84	-206.23	0.27
Ala	-260.63	22.80	-262.85	14.95	-298.96	12.66	-407.45	5.60	-286.96	6.26
Tyr	-37.24	2.66	-42.53	2.03	-37.12	2.90	-33.20	0.86	-23.46	0.15
Val	-2.71	0.23	-7.32	0.05	-18.86	4.11	-16.07	2.82	-17.87	1.27
Met	-21.41	1.75	-22.46	1.44	-21.76	2.01	-31.34	0.24	-22.43	1.08
Trp	-2.66	0.26	-3.20	0.25	-4.16	0.03	-3.99	0.41	-1.85	0.19
Phe	-28.67	1.98	-31.41	0.11	-36.22	0.54	-57.88	1.83	-41.78	1.59
Ile	-1.81	0.19	-5.31	0.26	-15.43	4.39	-14.53	2.95	-15.35	0.98
Leu	26.41	0.93	22.01	2.35	7.32	8.88	21.01	2.36	24.02	10.49
Lys	-32.42	2.08	-37.02	4.64	-45.44	1.17	-61.11	0.18	-45.26	1.16
Pro	-52.42	2.56	-60.05	13.75	-74.32	3.36	-77.12	9.13	-48.42	6.89
Glc	190.98	14.98	98.33	0.00	43.75	3.76	304.83	23.63	91.61	25.73
Lac	359.00	11.11	376.34	22.48	395.95	29.28	543.52	21.26	400.08	20.39
Pyr	-80.98	5.07	-87.82	6.10	-95.39	6.55	-124.04	5.57	-87.56	0.00
Urea	732.81	23.68	776.70	55.21	781.93	3.37	1105.18	54.72	818.70	16.30

(c) Middle age rat 3 (MA 3) 12 – 24 h

MA 3	Avg	SD	Avg	SD	Avg	SD	Avg	SD	Avg	SD
	C	C	HS	HS	H_2O_2	H_2O_2	HS+Q	HS+Q	H_2O_2 + Q	H_2O_2+Q
Asp	-4.34	0.63	-7.03	0.13	-11.08	2.04	-3.39	2.31	-2.90	1.14
Glu	62.96	8.16	40.16	0.02	63.78	0.79	35.20	7.02	35.92	4.58
Asn	-13.26	1.12	-15.09	0.41	-22.70	3.38	-21.98	1.55	-16.42	0.62
Ser	34.90	0.29	11.29	0.88	22.59	2.95	-12.56	0.87	-9.43	1.52
Gln	-56.26	0.06	-107.88	56.42	-130.05	6.93	-65.89	10.03	-49.00	2.07
His	-1.97	0.20	-5.48	0.07	-8.49	0.83	-4.78	0.70	-3.16	0.25
Gly	-175.58	12.79	-135.48	21.69	-188.83	10.67	-85.16	3.47	-65.61	2.64
Thr	-14.22	0.48	-16.37	0.11	-29.05	4.01	-15.53	0.07	-9.18	1.09
Arg	-187.21	10.97	-227.08	19.41	-250.11	8.81	-269.28	0.85	-251.44	29.83
Ala	-233.02	14.95	-208.22	1.77	-244.69	5.20	-275.79	26.47	-223.22	14.02
Tyr	-36.27	4.02	-38.16	2.41	-41.39	1.33	-22.26	2.72	-25.09	2.28
Val	8.67	0.65	2.45	0.19	-6.52	2.38	7.83	1.77	12.76	1.30
Met	-17.91	1.56	-18.06	1.00	-19.22	0.63	-20.10	1.94	-16.39	1.26
Trp	-3.49	0.05	-4.76	1.04	-7.00	0.18	-4.03	0.04	-2.90	0.33
Phe	-24.08	2.63	-25.46	3.37	-33.91	0.98	-37.82	0.71	185.18	17.30
Ile	2.98	0.80	-0.81	0.52	-9.93	1.22	3.61	2.63	183.09	19.39
Leu	32.31	1.99	26.77	2.77	19.87	4.70	42.70	2.82	-122.59	10.97
Lys	-45.20	0.60	-41.85	4.52	-56.14	9.20	-42.43	1.20	-71.48	48.28
Pro	-20.65	4.90	-15.64	2.14	-43.33	53.10	26.45	0.21	-36.15	8.57
Glc	222.21	21.32	146.18	19.96	116.11	4.59	307.65	43.45	264.93	124.00
Lac	350.73	27.83	312.99	26.14	477.32	91.81	367.07	13.19	353.75	12.28
Pyr	-93.47	5.49	-91.30	8.09	-109.97	9.61	-114.61	3.92	-99.99	0.02
Urea	723.80	26.05	727.92	10.23	829.03	20.06	961.53	22.85	827.73	27.34

Table S3: Extracellular Metabolite fluxes of 19 amino acids, glucose, lactate, pyruvate and urea measured in fmol / cell / h for control (C), heat stress (HS), hydrogen peroxide (H_2O_2), heat stress pre-treated with quercetin (HS + Q) and hydrogen peroxide stress cells pre-treated with quercetin (H_2O_2 + Q) in Sprague Dawley **old age (OA) PRH** measured during **0 – 12 h**. The values represent average (Avg) and standard deviation (SD) from 3 technical replicates of the three old age rats (a) old age rat 1 (OA 1) (b) old age rat 2 (OA 2) (c) old age rat 3 (OA 3) (n = 3). Standard 3 letter code is used for amino acids.

(a) Old age rat 1 (OA 1) 0 – 12 h

OA 1	Avg	SD	Avg	SD	Avg	SD	Avg	SD	Avg	SD
	C	C	HS	HS	H_2O_2	H_2O_2	HS+Q	HS+Q	H_2O_2 + Q	H_2O_2+Q
Asp	-3.40	11.81	0.00	0.12	13.25	0.65	19.38	0.46	9.57	0.17
Glu	47.25	63.67	2.50	0.18	54.84	2.97	59.01	1.94	39.32	1.64
Asn	-18.39	-14.80	4.16	0.53	-12.50	0.33	-10.66	0.18	-15.78	0.88
Ser	28.30	22.93	8.29	1.33	23.73	0.56	14.28	0.70	13.00	0.69
Gln	-31.32	-84.63	5.05	0.62	-47.92	0.98	-67.66	1.32	-39.90	1.09
His	-7.00	-12.15	1.53	2.45	-9.76	1.54	-8.65	0.74	-12.94	0.40
Gly	-93.14	-113.02	21.03	6.24	-94.85	4.01	-48.18	2.16	-79.27	0.66
Thr	-8.09	15.05	0.00	0.19	18.39	0.75	19.36	0.81	10.44	1.48
Arg	-173.63	-183.38	7.57	1.28	-159.22	0.04	-189.38	1.52	-148.73	3.17
Ala	-148.46	-190.44	8.01	2.82	-158.97	3.42	-157.82	4.28	-139.94	0.60
Tyr	-12.18	5.16	0.00	0.52	7.74	0.46	11.36	0.77	-0.79	0.97
Val	-36.12	-14.14	22.37	1.22	-2.20	1.09	-9.11	0.04	-34.56	3.28
Met	-15.58	-15.47	2.82	0.06	-11.07	0.83	-10.64	0.08	-12.23	1.02
Trp	-2.23	8.98	0.00	1.32	21.87	0.63	15.07	1.03	-2.94	0.11
Phe	-21.27	-24.46	4.94	0.11	-23.74	0.80	-18.11	0.08	-22.23	1.86
Ile	6.04	7.20	0.40	0.11	5.45	0.57	8.25	1.05	3.81	0.23
Leu	71.84	90.68	9.22	0.61	75.23	2.85	100.34	0.21	51.61	9.12
Lys	-19.13	-1.71	18.47	1.57	-11.04	3.62	6.00	2.62	-25.97	3.02
Pro	-9.64	10.10	0.92	6.74	7.25	1.01	13.29	1.93	20.86	1.47
Glc	680.73	714.09	28.39	9.00	821.58	1.02	738.71	29.57	520.75	71.38
Lac	470.35	572.41	36.11	7.82	514.38	21.29	484.57	2.35	372.54	12.79
Pyr	-61.93	-69.21	6.00	1.18	-58.76	0.18	-74.09	1.17	-60.88	0.59
Urea	523.77	643.62	27.62	39.10	480.14	6.52	565.65	32.75	400.70	21.16

(b) Old age rat 2 (OA 2) 0 – 12 h

OA 2	Avg	SD	Avg	SD	Avg	SD	Avg	SD	Avg	SD
	C	C	HS	HS	H_2O_2	H_2O_2	HS+Q	HS+Q	H_2O_2 + Q	H_2O_2+Q
Asp	-7.62	1.04	-17.48	4.17	-14.30	0.97	-13.48	2.96	-11.65	2.42
Glu	7.14	0.61	1.37	1.44	5.01	0.00	1.44	1.58	5.43	4.25
Asn	-29.10	2.40	-40.75	0.10	-35.22	1.04	-34.48	2.38	-35.75	0.64
Ser	15.25	0.54	19.88	1.28	7.26	0.29	12.82	0.95	13.75	0.17
Gln	-196.38	8.56	-339.01	52.43	-324.77	26.04	-278.47	30.06	-304.09	10.09
His	-17.92	2.02	-26.49	3.44	-25.38	2.04	-23.26	2.71	-23.39	0.21
Gly	-188.86	18.89	-261.65	31.87	-196.80	11.78	-191.34	6.67	-209.02	5.19
Thr	-2.64	0.56	-11.64	0.67	-6.36	0.84	-9.09	4.01	-5.87	0.00
Arg	-210.58	26.11	-278.52	26.85	-284.96	20.99	-274.61	16.38	-278.23	3.92
Ala	-183.04	12.62	-243.53	0.86	-225.50	20.60	-231.69	21.89	-216.76	4.56
Tyr	-30.89	2.30	-37.65	0.96	-28.76	2.64	-32.00	2.67	-21.54	0.19
Val	-21.06	0.31	-38.78	5.84	-34.36	4.75	-25.59	4.93	-24.65	0.60
Met	-21.49	1.61	-29.92	0.58	-25.88	2.41	-24.74	1.15	-25.10	0.39
Trp	-5.44	0.40	-7.93	1.03	-5.82	0.01	-5.18	1.00	-3.50	0.59
Phe	-40.38	3.15	-55.80	0.76	-53.18	1.58	-44.93	1.00	-55.13	2.06
Ile	-20.87	0.74	-36.93	5.57	-35.48	3.55	-25.27	4.55	-26.29	1.50
Leu	-16.61	0.79	-30.80	3.50	-27.98	3.10	-15.08	4.63	-14.72	1.35
Lys	-86.17	5.66	-111.38	1.63	-120.94	9.10	-95.57	3.97	-104.16	0.46
Pro	-2.31	1.46	-77.11	1.64	-81.43	1.53	-62.32	2.46	-81.38	3.88
Glc	2996.77	109.00	-496.40	31.95	1467.32	228.05	1447.51	235.23	168.60	2.47
Lac	1849.51	157.71	1819.28	33.37	1263.53	96.71	1486.48	62.41	1267.36	9.07
Pyr	-59.15	2.30	-77.89	4.85	-104.94	5.36	-94.89	2.68	-108.75	4.11
Urea	472.34	44.49	552.68	45.74	547.41	50.87	487.72	21.38	544.18	37.69

(c) Old age rat 3 (OA 3) 0 – 12 h

OA 3	Avg	SD	Avg	SD	Avg	SD	Avg	SD	Avg	SD
	C	C	HS	HS	H_2O_2	H_2O_2	HS+Q	HS+Q	H_2O_2 + Q	H_2O_2+Q
Asp	-2.59	1.49	-3.19	0.99	-11.07	1.39	-11.36	5.52	-5.26	0.00
Glu	32.29	3.33	39.02	6.57	12.67	1.21	32.55	18.97	23.38	0.12
Asn	-19.63	2.81	-20.83	0.07	-24.55	0.61	-26.81	4.47	-22.17	0.34
Ser	14.40	1.58	10.74	0.57	10.89	0.68	5.55	2.22	14.90	0.55
Gln	-84.77	17.67	-112.32	4.41	-198.81	1.03	-224.92	35.62	-182.03	11.45
His	-10.85	1.49	-9.37	0.34	-14.43	0.23	-11.58	0.73	-8.82	4.33
Gly	-110.53	13.96	-107.53	7.93	-122.68	0.83	-122.52	10.91	-98.57	24.76
Thr	-5.64	1.12	-2.37	1.45	-14.68	0.21	-20.16	7.42	-8.58	0.29
Arg	-199.85	26.28	-220.75	14.57	-210.75	11.52	-249.72	7.57	-216.38	0.39
Ala	-144.61	22.84	-211.82	15.38	-212.24	7.42	-294.73	17.17	-203.09	3.81
Tyr	-23.27	2.94	-21.23	0.83	-24.98	0.16	-26.85	2.54	-22.88	0.92
Val	-2.32	1.11	-4.43	5.48	-21.73	0.87	-23.43	9.35	-11.09	0.77
Met	-14.46	1.76	-16.07	0.14	-16.78	0.49	-22.20	1.45	-15.62	0.48
Trp	-4.78	0.51	-4.91	0.22	-6.34	0.08	-7.73	1.14	-4.18	0.41
Phe	-26.56	3.19	-31.50	0.99	-40.87	0.97	-41.95	2.77	-32.64	1.47
Ile	1.21	0.49	9.35	2.87	-16.32	1.61	-13.72	8.85	-6.00	0.16
Leu	32.02	7.22	49.00	5.49	8.06	1.35	54.46	35.19	20.41	1.33
Lys	-30.10	1.33	-22.17	2.57	-43.31	1.06	-46.66	8.30	-41.14	5.22
Pro	-8.87	0.96	-13.51	0.57	-13.77	0.13	-29.31	2.94	-15.97	15.51
Glc	542.58	179.04	-35.85	8.82	-526.21	59.45	396.86	76.96	-444.55	1.85
Lac	771.54	68.50	700.14	66.04	696.79	28.61	786.68	45.63	709.50	1.02
Pyr	-94.08	13.61	-109.00	6.98	-103.93	5.45	-158.00	9.41	-119.82	5.93
Urea	578.12	74.89	607.45	50.39	541.43	14.40	723.67	53.85	603.75	29.66

Table S4: Extracellular Metabolite fluxes of 19 amino acids, glucose, lactate, pyruvate and urea measured in fmol / cell / h for control (C), heat stress (HS), hydrogen peroxide (H_2O_2), heat stress pre-treated with quercetin (HS + Q) and hydrogen peroxide stress cells pre-treated with quercetin (H_2O_2 + Q) in Sprague Dawley **old age (OA) PRH** measured during **12 - 24 h**. The values represent average (Avg) and standard deviation (SD) from 3 technical replicates of the three old age rats (a) old age rat 1 (OA 1) (b) old age rat 2 (OA 2) (c) old age rat 3 (OA 3) (n = 3). Standard 3 letter code is used for amino acids.

(a) Old age rat 1 (OA 1) 12 – 24 h

OA 1	Avg	SD	Avg	SD	Avg	SD	Avg	SD	Avg	SD
	C	C	HS	HS	H_2O_2	H_2O_2	HS+Q	HS+Q	H_2O_2 + Q	H_2O_2+Q
Asp	-2.10	-2.22	0.16	0.00	-4.51	1.04	8.22	0.99	-4.50	0.28
Glu	43.94	62.54	1.18	4.18	55.18	1.41	54.17	7.65	26.72	0.53
Asn	-11.90	-8.36	0.61	1.96	-17.68	0.85	-15.28	1.43	-22.47	0.94
Ser	38.24	55.57	1.90	5.78	48.66	4.21	42.94	3.63	32.27	0.59
Gln	-81.22	-60.76	5.28	26.52	-147.41	29.12	-166.63	11.33	-208.68	5.47
His	-7.17	-7.53	0.61	0.13	-12.94	1.06	-15.15	1.08	-11.81	0.95
Gly	-143.77	-154.18	0.49	1.97	-186.36	13.65	-166.74	6.95	-204.20	2.61
Thr	2.86	20.12	0.48	8.34	-4.69	0.00	7.76	2.64	-12.09	0.20
Arg	-185.37	-217.57	1.86	0.62	-221.71	1.00	-246.34	1.12	-223.02	1.85
Ala	-170.53	-184.51	0.99	13.04	-225.68	3.63	-200.19	1.76	-226.64	2.68
Tyr	-12.31	-11.68	0.41	2.12	-15.81	1.40	-9.12	2.38	-18.94	0.25
Val	-30.39	-18.97	2.04	7.12	-27.07	6.08	-32.79	2.23	-61.31	0.52
Met	-15.86	-17.96	0.16	1.38	-19.66	0.51	-18.12	0.19	-22.66	0.26
Trp	-0.22	13.63	0.00	0.63	30.37	0.08	25.98	0.67	-7.82	0.03
Phe	-22.32	-26.54	0.46	1.91	-29.56	0.28	-24.35	1.15	-30.91	0.23
Ile	5.23	6.78	0.64	0.16	6.80	0.47	14.02	1.84	4.52	0.37
Leu	44.43	62.22	2.62	7.30	39.20	8.00	58.11	5.81	17.66	1.01
Lys	-16.76	-15.99	0.87	3.79	-43.21	4.00	-27.09	0.97	-56.84	1.17
Pro	66.33	10.56	0.99	8.35	-4.33	0.00	-6.87	0.00	-4.70	0.00
Glc	206.29	443.96	10.38	67.62	147.49	19.29	323.21	55.54	-60.68	6.63
Lac	418.82	408.18	0.12	18.45	501.04	39.45	429.29	46.88	401.36	61.16
Pyr	-76.16	-84.60	3.32	0.03	-89.30	4.59	-110.51	0.00	-102.47	0.00
Urea	460.16	482.05	27.00	1.65	480.88	17.62	590.41	19.57	514.73	9.80

(b) Old age rat 2 (OA 2) 12 – 24 h

OA 2	Avg	SD	Avg	SD	Avg	SD	Avg	SD	Avg	SD
	C	C	HS	HS	H_2O_2	H_2O_2	HS+Q	HS+Q	H_2O_2 + Q	H_2O_2+Q
Asp	-7.56	0.60	-7.79	1.78	-9.74	1.62	-11.77	0.74	-16.05	4.96
Glu	10.74	0.71	13.23	6.14	7.27	0.00	5.84	1.28	7.05	18.02
Asn	-33.38	0.91	-37.49	0.23	-39.71	1.24	-35.72	0.70	-47.25	2.52
Ser	45.30	3.23	54.39	3.51	45.58	3.15	44.71	0.36	48.90	2.85
Gln	-260.23	7.63	-294.35	6.78	-366.02	26.33	-343.07	4.78	-453.82	32.26
His	-18.93	0.03	-22.65	1.35	-23.58	1.50	-22.58	1.17	-28.51	1.21
Gly	-261.61	7.81	-304.09	10.16	-298.78	23.26	-279.71	6.18	-353.86	7.81
Thr	-5.03	1.02	-13.58	4.20	-8.64	0.01	-9.62	0.03	-17.23	8.54
Arg	-260.09	7.46	-279.80	12.04	-299.75	25.39	-283.88	3.46	-348.69	0.51
Ala	-229.45	4.08	-273.43	6.61	-270.03	15.51	-221.91	3.08	-328.59	8.13
Tyr	-42.80	0.13	-50.19	0.66	-46.45	1.19	-37.10	1.08	-53.28	5.30
Val	-27.58	0.04	-31.96	2.74	-37.70	2.28	-36.88	1.56	-52.72	8.71
Met	-26.32	0.46	-30.49	0.87	-30.73	2.30	-27.39	0.87	-36.45	1.31
Trp	-6.65	0.50	-12.02	0.26	-6.99	0.79	-9.31	0.97	-10.00	0.94
Phe	-44.97	1.19	-50.66	0.58	-57.24	0.61	-47.45	1.10	-65.22	4.12
Ile	-29.80	0.55	-33.89	3.94	-40.16	2.86	-38.29	0.81	-52.78	7.88
Leu	-22.64	1.13	-27.17	5.46	-36.83	1.70	-32.96	1.15	-51.53	11.23
Lys	-87.57	6.32	-96.36	1.48	-110.38	6.00	-105.71	0.99	-134.66	3.96
Pro	18.25	3.83	-60.39	1.35	-66.81	2.15	-59.87	7.22	-84.44	1.57
Glc	2225.39	343.71	-711.46	15.44	-185.77	12.49	-391.31	84.30	-1278.00	134.17
Lac	1447.27	63.35	1227.47	38.63	1266.24	77.23	1301.31	41.29	1332.64	93.98
Pyr	-98.07	5.48	-108.67	3.71	-129.85	8.75	-108.67	1.62	-151.01	1.20
Urea	470.33	17.73	475.55	0.74	594.29	10.72	497.68	49.76	610.25	15.83

(c) Old age rat 3 (OA 3) 12 – 24 h

OA 3	Avg C	SD C	Avg HS	SD HS	Avg H_2O_2	SD H_2O_2	Avg HS+Q	SD HS+Q	Avg H_2O_2 + Q	SD H_2O_2+Q
Asp	-5.98	1.42	-11.83	0.56	-15.62	1.00	-12.46	2.03	-6.99	2.26
Glu	44.55	5.41	37.23	7.03	37.50	2.75	20.37	5.83	31.27	1.89
Asn	-12.33	1.37	-16.74	0.22	-20.98	0.43	-24.64	1.29	-18.43	2.03
Ser	35.08	0.79	30.12	3.40	36.01	2.23	29.38	1.87	32.98	4.01
Gln	-94.74	13.57	-149.43	13.49	-207.54	4.94	-220.77	18.38	-175.63	10.82
His	-5.42	0.51	-8.35	0.85	-12.40	0.42	-14.44	0.66	-10.76	0.15
Gly	-113.74	6.90	-144.20	2.65	-157.98	3.53	-168.67	2.77	-180.96	12.92
Thr	-4.97	0.00	-10.09	4.89	-16.15	1.80	-20.62	3.43	-8.71	0.99
Arg	-223.49	14.79	-244.35	4.30	-243.17	0.72	-251.44	5.56	-203.58	1.40
Ala	-169.87	3.47	-195.39	3.94	-219.85	0.43	-228.74	1.15	-226.02	6.75
Tyr	-23.95	2.14	-29.83	0.18	-31.46	0.42	-32.02	1.17	-29.12	0.61
Val	-2.62	0.00	-8.21	3.93	-18.85	1.80	-23.76	5.38	-7.64	2.99
Met	-13.16	1.10	-15.46	0.15	-18.35	0.49	-19.56	0.03	-18.19	0.38
Trp	-3.06	0.20	-3.51	0.20	-4.58	0.16	-5.45	0.54	-2.58	0.22
Phe	-22.55	0.26	-29.09	0.53	-34.72	0.63	-33.57	0.00	-32.45	0.68
Ile	10.47	4.82	-3.57	3.93	-13.20	3.22	-18.70	5.59	-3.51	3.33
Leu	53.55	7.66	32.95	6.96	23.44	2.74	9.78	7.17	23.21	5.02
Lys	-4.85	0.76	-14.83	3.22	-24.63	3.70	-30.48	7.39	-21.17	2.31
Pro	23.90	17.35	-11.10	2.56	-30.12	2.70	-29.37	1.95	-23.65	10.95
Glc	339.07	15.32	428.64	9.29	-59.94	2.94	35.30	2.29	42.20	0.00
Lac	724.44	26.41	668.45	18.85	708.80	42.60	586.22	88.13	779.93	23.00
Pyr	-122.91	6.99	-131.14	3.98	-135.65	4.64	-140.31	4.68	-148.69	0.94
Urea	614.22	64.46	570.08	2.73	619.36	33.26	561.14	43.34	642.71	41.07

Table S5: Various biochemical parameters measured for control (C), heat stress (HS), hydrogen peroxide (H_2O_2), heat stress pre-treated with quercetin (HS + Q) and hydrogen peroxide stress cells pre-treated with quercetin (H_2O_2 + Q) in Sprague Dawley **middle age (MA) PRH** measured during **0 -12 h and 12 – 24 h**. The values represent average (Avg) and standard deviation (SD) from 3 technical replicates of the three middle age rats (a) middle age rat 1 (MA 1) (b) middle age rat 2 (MA 2) (c) middle age rat 3 (MA 3) (n = 3). Standard 3 letter code is used for amino acids.

(a) Middle age rat 1 (MA 1)

MA 1	Avg	SD	Avg	SD	Avg	SD	Avg	SD	Avg	SD
Cell Number	C	C	HS	HS	H_2O_2	H_2O_2	HS+Q	HS+Q	H_2O_2+Q	H_2O_2+Q
12 h	494095	29779	415900	30106	427313	38139	342672	33116	325987	7035
24 h	296180	31256	385294	16152	313736	57380	323501	14215	268808	25930
AST (U/cell/h)										
0-12h	1.07E-05	6.15E-07	1.3E-05	5E-07	1.21E-05	2E-06	2.14E-05	6.1E-06	1.35E-05	1.46E-06
12-24h	5.64E-06	2.28E-06	6.2E-06	5E-07	8.73E-06	2E-07	1.08E-05	2E-06	1.19E-05	3.31E-07
LDH (U/cell/h)										
0-12h	1.49E-07	1.65E-08	1.6E-07	1E-08	1.6E-07	4E-08	2.46E-07	2.9E-08	1.66E-07	1.87E-08
12-24h	1.39E-07	1.61E-08	9.4E-08	1E-08	1.3E-07	4E-08	1.5E-07	3.1E-09	1.37E-07	9.72E-09
Abumin (fg/cell/h)										
0-12h	1864.03	121.64	2212.26	183.21	2292.24	186.61	1355.43	247.41	1430.11	166.96
12-24h	5670.83	1432.70	2580.29	327.00	3762.89	332.66	671.66	157.94	2810.20	141.51
GSH nmol/mg protein)										
1h	285.15	34.93	497.61	102.49	306.75	34.39	308.39	10.28	190.58	10.66
5h	270.96	21.31	356.41	72.05	328.25	2.27	207.90	7.70	230.17	41.90
24h	306.68	8.08	374.16	44.77	311.79	17.67	425.91	54.49	365.79	29.82
ROS (RFU/cell)										
1h	0.1107	0.0074	0.0728	0.0040	0.1097	0.0084	0.0229	0.0001	0.0234	0.0015
5h	0.0980	0.0051	0.0766	0.0082	0.0659	0.0031	0.0288	0.0016	0.0252	0.0008
24h	0.0182	0.0006	0.0136	0.0015	0.0190	0.0024	0.0257	0.0041	0.0273	0.0013
CYP1A2 (pmol/cell/h)										
Day 1	1.47	0.35	0.90	0.16	1.08	0.15	0.52	0.11	0.54	0.14
Day 2	1.25	0.11	0.68	0.01	0.74	0.14	0.17	0.03	0.30	0.01
CYP3A4 (pmol/cell/h)										
Day 1	0.14	0.03	0.13	0.02	0.14	0.01	0.07	0.02	0.07	0.01
Day 2	0.12	0.01	0.09	0.03	0.10	0.01	0.03	0.01	0.06	0.02
CYP2C9 (pmol/cell/h)										
Day 1	1.59	0.17	0.86	0.12	0.99	0.04	0.17	0.06	0.12	0.00
Day 2	0.27	0.03	0.17	0.03	0.09	0.03	0.02	0.00	0.04	0.02
CYP2B6 (pmol/cell/h)										
Day 1	0.38	0.09	0.29	0.04	0.31	0.01	0.11	0.02	0.13	0.01
Day 2	0.22	0.02	0.15	0.03	0.16	0.02	0.05	0.00	0.12	0.01

(b) Middle age rat 2 (MA 2)

MA 2	Avg	SD	Avg	SD	Avg	SD	Avg	SD	Avg	SD
Cell Number	C	C	HS	HS	H_2O_2	H_2O_2	HS+Q	HS+Q	H_2O_2+Q	H_2O_2+Q
12 h	367150	3043	332393	5564	329854	30920	261731	25759	324653	36872
24 h	293486	34987	303846	31068	270746	23243	219918	29125	268890	27096
AST (U/cell/h)										
0-12h	9.22E-06	8E-07	1.21E-05	1E-06	1.29E-05	2E-06	6.65E-06	1.9E-06	7.25E-06	2.372E-06
12-24h	9.7E-06	9E-07	9.11E-06	6E-07	7.35E-06	1E-06	1.63E-05	3E-06	1.32E-05	2.825E-08
LDH (U/cell/h)										
0-12h	1.81E-07	2E-08	2.13E-07	9E-09	3.72E-07	2E-08	5.2E-07	7.2E-08	5.06E-07	7.228E-08
12-24h	2.45E-07	4E-09	3.79E-07	1E-07	2.79E-07	3E-09	8.06E-07	1.9E-07	3.93E-07	5.698E-08
Abumin (fg/cell/h)										
0-12h	2297.46	179.53	3493.66	415.95	746.47	108.89	1741.35	85.06	567.47	57.44
12-24h	4980.58	601.38	5429.43	184.68	2696.39	411.80	1790.07	30.05	984.75	72.45
GSH nmol/mg protein)										
1h	571.73	8.88	331.36	62.26	589.10	53.70	225.91	63.30	255.93	2.95
5h	332.75	57.74	500.74	106.61	1226.14	118.85	263.45	30.13	542.02	24.80
24h	493.76	64.64	489.38	45.22	483.74	18.74	418.35	0.00	378.48	85.03
ROS (RFU/cell)										
1h	0.0794	0.0037	0.0746	0.0028	0.1130	0.0196	0.0228	0.0012	0.0233	0.0024
5h	0.0567	0.0044	0.0550	0.0051	0.0615	0.0031	0.0212	0.0014	0.0219	0.0027
24h	0.0227	0.0014	0.0236	0.0014	0.0249	0.0014	0.0227	0.0014	0.0235	0.0028
CYP1A2 (pmol/cell/h)										
Day 1	0.96	0.17	0.78	0.17	0.72	0.25	0.30	0.04	0.54	0.09
Day 2	0.64	0.08	0.53	0.12	0.44	0.12	0.11	0.01	0.27	0.10
CYP3A4 (pmol/cell/h)										
Day 1	0.16	0.04	0.17	0.02	0.15	0.01	0.08	0.01	0.10	0.01
Day 2	0.12	0.01	0.10	0.02	0.09	0.02	0.04	0.01	0.05	0.01
CYP2C9 (pmol/cell/h)										
Day 1	1.30	0.43	1.03	0.24	1.13	0.17	0.24	0.00	0.28	0.04
Day 2	0.18	0.03	0.19	0.04	0.19	0.00	0.09	0.01	0.09	0.03
CYP2B6 (pmol/cell/h)										
Day 1	0.36	0.05	0.34	0.02	0.33	0.02	0.14	0.00	0.17	0.01
Day 2	0.23	0.02	0.17	0.03	0.19	0.01	0.08	0.01	0.11	0.03

(c) Middle age rat 3 (MA 3)

MA 3	Avg	SD	Avg	SD	Avg	SD	Avg	SD	Avg	SD
Cell Number	C	C	HS	HS	H_2O_2	H_2O_2	HS+Q	HS+Q	H_2O_2+Q	H_2O_2+Q
12 h	321316	12607	372746	49381	396584	3637	331656	18673	355605	55906
24 h	333698	52139	293899	46700	242328	49008	267460	3751	279393	26862
AST (U/cell/h)										
0-12h	1.71E-05	8E-07	1.5E-05	2E-06	1.45E-05	9E-07	1E-05	2.2E-06	7.84E-06	9.504E-07
12-24h	1.42E-05	2E-06	1.54E-05	1E-06	1.33E-05	2E-06	1E-05	2.3E-06	1.63E-05	3.941E-06
LDH (U/cell/h)										
0-12h	3.07E-07	9E-09	3.21E-07	8E-08	2.35E-07	2E-08	5E-07	1E-07	3.07E-07	2.259E-08
12-24h	3.45E-07	5E-08	2.91E-07	3E-08	6.17E-07	7E-08	5E-07	5.6E-08	4.68E-07	5.84E-08
Abumin (fg/cell/h)										
0-12h	3235.32	227.75	2906.95	501.22	1766.92	27.50	952.32	53.67	795.43	51.35
12-24h	4440.71	991.81	3652.81	729.99	2920.83	680.23	1081.04	71.32	922.81	95.95
GSH nmol/mg protein)										
1h	316.02	57.50	305.97	16.61	403.31	17.31	233.50	8.36	155.70	14.66
5h	326.09	11.43	315.33	15.58	567.69	132.28	238.41	8.19	247.96	72.16
24h	363.72	20.34	343.56	20.89	426.68	33.63	293.29	13.73	201.66	12.22
ROS (RFU/cell)										
1h	0.0684	0.0037	0.0907	0.0060	0.1083	0.0273	0.0226	0.0007	0.0208	0.0004
5h	0.0429	0.0037	0.0554	0.0015	0.0468	0.0021	0.0220	0.0025	0.0187	0.0011
24h	0.0169	0.0001	0.0174	0.0013	0.0200	0.0011	0.0235	0.0016	0.0293	0.0050
CYP1A2 (pmol/cell/h)										
Day 1	1.00	0.21	0.75	0.09	0.74	0.09	0.55	0.09	0.55	0.04
Day 2	1.31	0.27	1.22	0.34	1.46	0.07	0.16	0.00	0.28	0.06
CYP3A4 (pmol/cell/h)										
Day 1	0.21	0.03	0.18	0.02	0.20	0.02	0.10	0.01	0.09	0.01
Day 2	0.13	0.00	0.11	0.03	0.13	0.01	0.04	0.00	0.06	0.00
CYP2C9 (pmol/cell/h)										
Day 1	1.19	0.22	0.85	0.28	0.84	0.29	0.11	0.02	0.14	0.03
Day 2	0.47	0.15	0.36	0.08	0.31	0.07	0.11	0.03	0.11	0.02
CYP2B6 (pmol/cell/h)										
Day 1	0.38	0.06	0.32	0.05	0.30	0.04	0.10	0.01	0.11	0.01
Day 2	0.31	0.03	0.24	0.04	0.29	0.03	0.10	0.02	0.12	0.01

Table S6: Various biochemical parameters measured for control (C), heat stress (HS), hydrogen peroxide (H_2O_2), heat stress pre-treated with quercetin (HS + Q) and hydrogen peroxide stress cells pre-treated with quercetin (H_2O_2 + Q) in Sprague Dawley **old age (MA) PRH** measured during **0 -12 h and 12 – 24 h**. The values represent average (Avg) and standard deviation (SD) from 3 technical replicates of the three middle age rats (a) old age rat 1 (OA 1) (b) old age rat 2 (OA 2) (c) old age rat 3 (OA 3) (n = 3). Standard 3 letter code is used for amino acids.

(a) Old age rat 1 (OA 1)

OA 1	Avg	SD	Avg	SD	Avg	SD	Avg	SD	Avg	SD
Cell Number	C	C	HS	HS	H_2O_2	H_2O_2	HS+Q	HS+Q	H_2O_2 + Q	H_2O_2 + Q
12 h	304739	26872	267609	12486	302755	17479	281854	25976	293656	43267
24 h	281178	4178	238902	706	248213	21599	181490	41033	206762	28671
AST (U/cell/h)										
0-12h	9E-06	3E-07	1E-05	5E-07	7E-06	2E-06	8.52E-06	2.003E-06	4.905E-06	3.72E-07
12-24h	7E-06	2E-06	6E-06	5E-07	6E-06	3E-07	1.17E-05	9.282E-07	4.71E-06	1.08E-06
LDH (U/cell/h)										
0-12h	2E-06	2E-07	3E-06	2E-07	1E-06	3E-07	1.55E-06	2.687E-07	1.55E-06	2.64E-07
12-24h	2E-06	0	3E-06	3E-07	2E-06	5E-07	2.62E-06	3.973E-07	3.097E-06	3.02E-08
Abumin (fg/cell/h)										
0-12h	703.63	39.20	804.15	31.56	600.70	5.34	624.72	41.65	521.75	97.35
12-24h	714.75	44.94	851.32	37.06	890.60	75.16	754.77	91.92	843.33	20.82
GSH nmol/mg protein)										
1h	140.31	0.00	117.63	0.00	188.05	7.39	167.05	27.39	101.63	11.83
5h	146.39	2.28	170.57	28.50	243.55	32.47	180.84	26.78	138.20	26.58
24h	186.73	15.91	148.56	19.33	115.06	5.00	183.92	34.16	138.02	13.85
ROS (RFU/cell)										
1h	0.0184	0.0030	0.0335	0.0028	0.0343	0.0014	0.0119	0.0017	0.0053	0.0006
5h	0.0226	0.0024	0.0487	0.0037	0.0299	0.0007	0.0192	0.0022	0.0121	0.0002
24h	0.0061	0.0009	0.0094	0.0007	0.0055	0.0004	0.0060	0.0010	0.0056	0.0002
CYP1A2 (pmol/cell/h)										
Day 1	0.47	0.04	0.52	0.04	0.19	0.03	0.28	0.01	0.07	0.01
Day 2	0.27	0.03	0.14	0.00	0.12	0.02	0.10	0.00	0.05	0.01
CYP3A4 (pmol/cell/h)										
Day 1	0.11	0.01	0.11	0.02	0.08	0.01	0.08	0.01	0.04	0.00
Day 2	0.04	0.01	0.04	0.00	0.04	0.00	0.02	0.00	0.02	0.01
CYP2C9 (pmol/cell/h)										
Day 1	1.02	0.14	1.25	0.50	0.42	0.04	0.18	0.06	0.10	0.04
Day 2	0.10	0.02	0.08	0.01	0.13	0.01	0.10	0.06	0.06	0.01
CYP2B6 (pmol/cell/h)										
Day 1	0.15	0.01	0.14	0.02	0.10	0.01	0.10	0.03	0.05	0.01
Day 2	0.07	0.00	0.03	0.01	0.04	0.02	0.02	0.00	0.02	0.01

(b) Old age rat 2 (OA 2)

OA 2	Avg	SD	Avg	SD	Avg	SD	Avg	SD	Avg	SD
Cell Number	C	C	HS	HS	H_2O_2	H_2O_2	HS+Q	HS+Q	H_2O_2 + Q	H_2O_2 + Q
12 h	283413	34875	202302	22875	208998	15307	224997	19034	209198	3065
24 h	232375	14914	209788	6300	192609	12948	196462	9017	165209	2629
AST (U/cell/h)										
0-12h	2.6E-05	5E-06	3E-05	2E-06	2E-05	4E-06	7.6E-06	8.4E-07	7.44348E-06	1.048E-06
12-24h	2.3E-05	6E-06	3E-05	3E-06	2E-05	0	4.8E-06	1E-06	1.35806E-05	4.8368E-06
LDH (U/cell/h)										
0-12h	1.9E-06	6E-07	3E-06	1E-07	2E-06	8E-07	3.4E-06	5.4E-07	3.28162E-06	8.5367E-07
12-24h	1.8E-06	8E-07	3E-06	6E-07	3E-06	2E-07	1.7E-06	3.2E-07	1.85682E-06	8.1919E-07
Abumin (fg/cell/h)										
0-12h	213.84	0.00	107.28	0.00	-627.39	68.23	103.70	0.00	-577.53	54.38
12-24h	1210.39	140.65	770.29	539.52	642.79	213.39	810.72	43.52	1117.44	420.68
GSH nmol/mg protein)										
1h	123.59	10.40	111.99	6.29	76.58	4.67	123.29	6.97	95.48	11.84
5h	87.57	3.41	122.83	6.68	161.36	37.94	116.80	10.16	121.26	30.28
24h	126.16	22.89	98.15	7.02	86.25	0.00	118.56	10.68	60.85	6.74
ROS (RFU/cell)										
1h	0.0172	0.0003	0.0181	0.0017	0.0419	0.0031	0.0073	0.0007	0.0127	0.0004
5h	0.0125	0.0018	0.0126	0.0008	0.0094	0.0009	0.0061	0.0008	0.0070	0.0002
24h	0.0061	0.0009	0.0094	0.0007	0.0055	0.0004	0.0060	0.0010	0.0056	0.0002
CYP1A2 (pmol/cell/h)										
Day 1	0.63	0.05	0.57	0.04	0.33	0.04	0.28	0.05	0.19	0.02
Day 2	0.31	0.03	0.20	0.00	0.15	0.02	0.08	0.04	0.18	0.01
CYP3A4 (pmol/cell/h)										
Day 1	0.08	0.00	0.09	0.00	0.06	0.00	0.06	0.01	0.06	0.01
Day 2	0.07	0.00	0.06	0.01	0.06	0.00	0.05	0.01	0.06	0.00
CYP2C9 (pmol/cell/h)										
Day 1	0.44	0.06	0.52	0.11	0.33	0.08	0.06	0.01	0.05	0.00
Day 2	0.09	0.03	0.07	0.01	0.11	0.05	0.06	0.00	0.05	0.00
CYP2B6 (pmol/cell/h)										
Day 1	0.07	0.01	0.05	0.00	0.06	0.01	0.02	0.00	0.03	0.00
Day 2	0.03	0.01	0.03	0.01	0.02	0.00	0.02	0.01	0.02	0.00

(c) Old age rat 3 (OA 3)

OA 3	Avg	SD	Avg	SD	Avg	SD	Avg	SD	Avg	SD
Cell Number	C	C	HS	HS	H_2O_2	H_2O_2	HS+Q	HS+Q	H_2O_2 + Q	H_2O_2 + Q
12 h	320818	43366	302840	29015	297309	20121	245054	16206	269724	10910
24 h	274279	11483	250013	7268	243336	11951	249735	11597	232538	20818
AST (U/cell/h)										
0-12h	2.8E-05	1.98E-06	2.04E-05	2E-06	2.27E-05	2E-06	1.31E-05	1.09E-06	7.109E-06	7.08E-07
12-24h	1.8E-05	2.58E-06	2.4E-05	2E-06	1.99E-05	3E-06	6.45E-06	3.35E-07	2.279E-05	1.802E-06
LDH (U/cell/h)										
0-12h	2.3E-06	4.49E-07	1.61E-06	7E-07	2.46E-06	7E-07	2.97E-06	1.61E-07	2.653E-06	3.489E-07
12-24h	2E-06	2.18E-07	1.79E-06	3E-07	3.31E-06	7E-08	2.24E-06	2.53E-07	1.821E-06	3.224E-08
Abumin (fg/cell/h)										
0-12h	1373.72	11.44	995.40	49.23	1172.32	15.25	960.45	32.50	1229.71	79.82
12-24h	1345.75	50.75	1056.48	102.30	1279.61	10.42	1097.83	17.52	1398.72	128.84
GSH nmol/mg protein)										
1h	173.13	25.29	121.54	4.08	276.17	16.30	174.67	32.85	75.17	2.84
5h	189.46	4.86	155.32	44.30	316.07	102.07	154.70	28.48	127.31	48.32
24h	216.82	2.75	154.12	2.36	81.30	9.37	167.28	23.59	61.16	0.19
ROS (RFU/cell)										
1h	0.0480	0.0017	0.0470	0.0010	0.0580	0.0022	0.0138	0.0015	0.0148	0.0002
5h	0.0449	0.0019	0.0262	0.0014	0.0403	0.0035	0.0109	0.0005	0.0217	0.0004
24h	0.0109	0.0007	0.0069	0.0004	0.0110	0.0009	0.0041	0.0005	0.0097	0.0008
CYP1A2 (pmol/cell/h)										
Day 1	0.68	0.07	0.66	0.04	0.63	0.02	0.18	0.02	0.18	0.01
Day 2	0.29	0.04	0.19	0.03	0.33	0.02	0.38	0.09	0.37	0.03
CYP3A4 (pmol/cell/h)										
Day 1	0.18	0.02	0.16	0.00	0.14	0.01	0.07	0.01	0.06	0.01
Day 2	0.06	0.01	0.05	0.00	0.04	0.01	0.09	0.00	0.07	0.01
CYP2C9 (pmol/cell/h)										
Day 1	1.48	0.26	1.23	0.15	0.96	0.29	0.13	0.05	0.07	0.00
Day 2	0.08	0.01	0.11	0.02	0.04	0.01	0.12	0.02	0.20	0.04
CYP2B6 (pmol/cell/h)										
Day 1	0.18	0.02	0.15	0.00	0.16	0.01	0.07	0.01	0.07	0.01
Day 2	0.05	0.01	0.05	0.02	0.05	0.00	0.09	0.01	0.07	0.01

Table S7: Mass isotopomer distribution of the analyzed fragment of isoleucine, leucine and valine as measured by GC-MS and calculated mass isotopomer distribution calculated for natural abundant fragments of isoleucine, leucine and valine. (unlabeled fragment (*m* + 0), one carbon labeled fragment (*m* + 1), two carbon labeled fragment (*m* + 2), three carbon labeled (*m* + 3)).

	^{13}C - Labeling with GC-MS	**Calculated ^{13}C - abundance**
Ile (m/z)		
302 (m+0)	100	100
303 (m+1)	25.822	26.46
304 (m+2)	9.94	10.28
305 (m+3)	1.72	1.7
Leu (m/z)		
302 (m+0)	100	100
303 (m+1)	26.84	26.46
304 (m+2)	10.56	10.28
305 (m+3)	1.92	1.7
Val(m/z)		
288 (m+0)	100	100
289 (m+1)	27.9	25.33
290 (m+2)	11.0	9.99
291 (m+3)	1.9	1.65

(a)

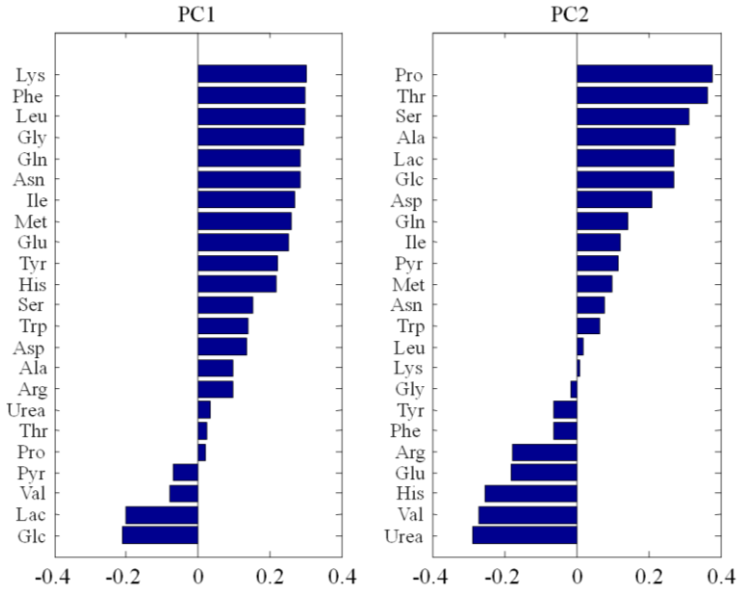

(b)

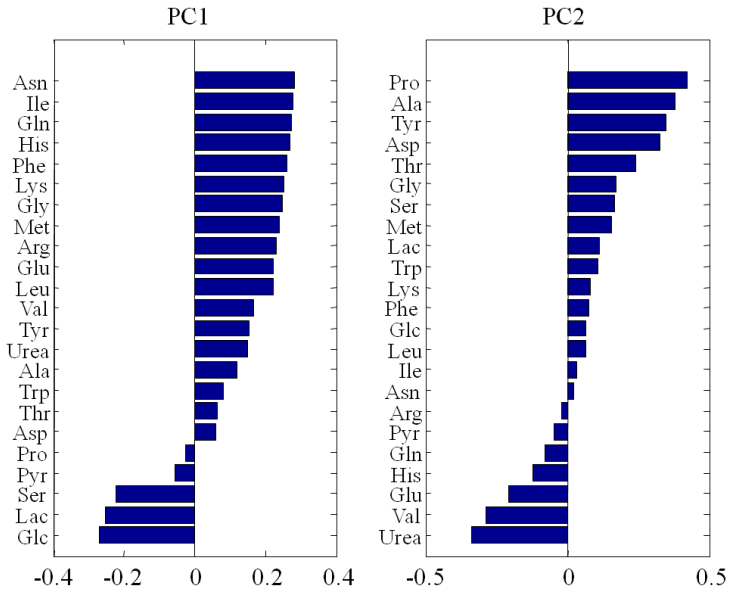

Fig S1. Loadings for PC1 and PC2 for middle and old age Sprague Dawley rat PRH at (a) 0 – 12 h (b) 12 – 24 h.

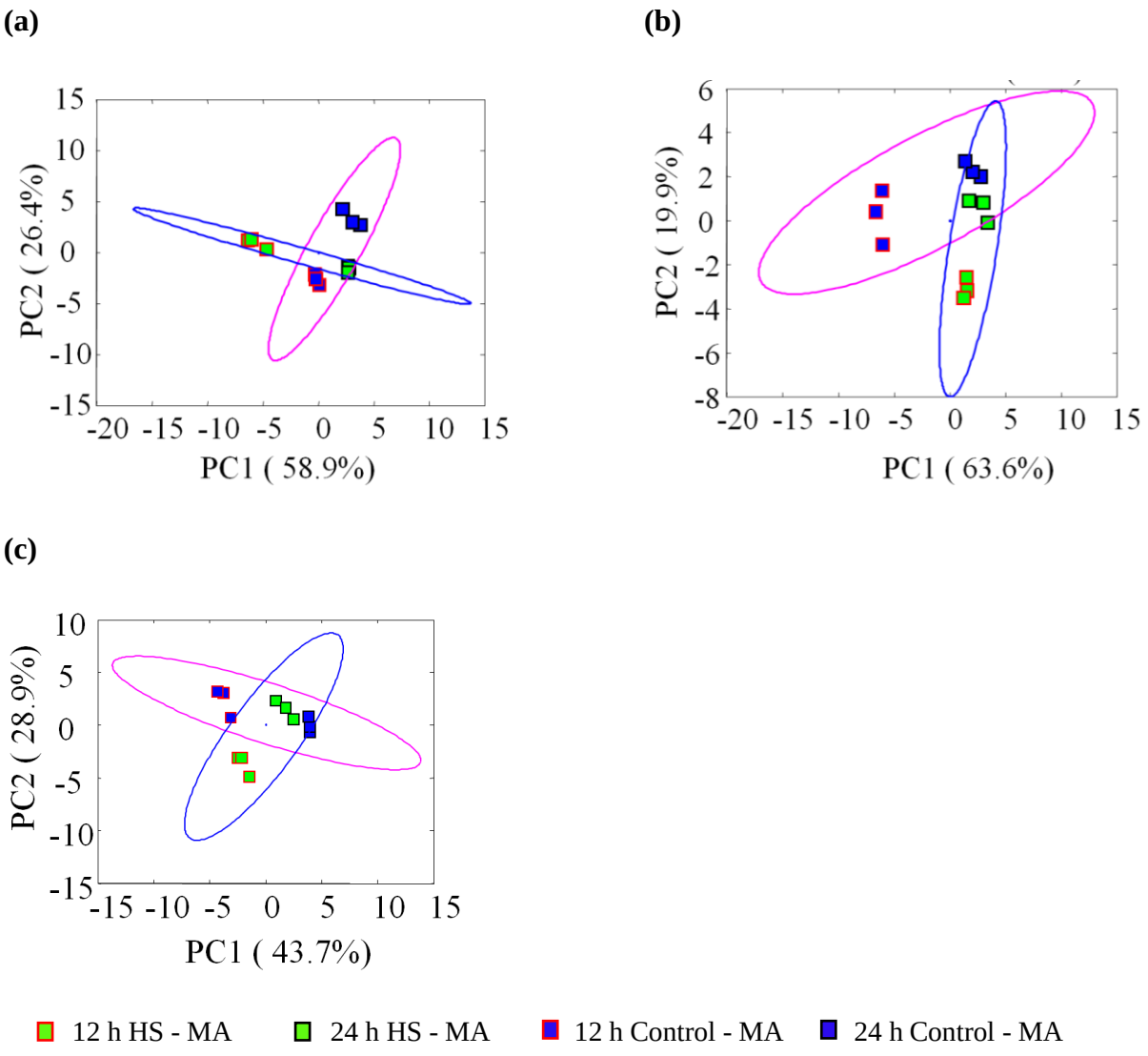

Fig S2 PCA scores of heat stress (HS) and control (C) for Sprague Dawley (a) middle age (MA) rat 1 (b) middle age (MA) rat 2 and (c) middle age (OA) rat 3 during 0 – 12 and 12 – 24 hour. The data has been normalized according to the Z-score. 90% confidence ellipses show the clusters for control (pink line) and heat stress stress (blue line) cells

(a) **(b)**

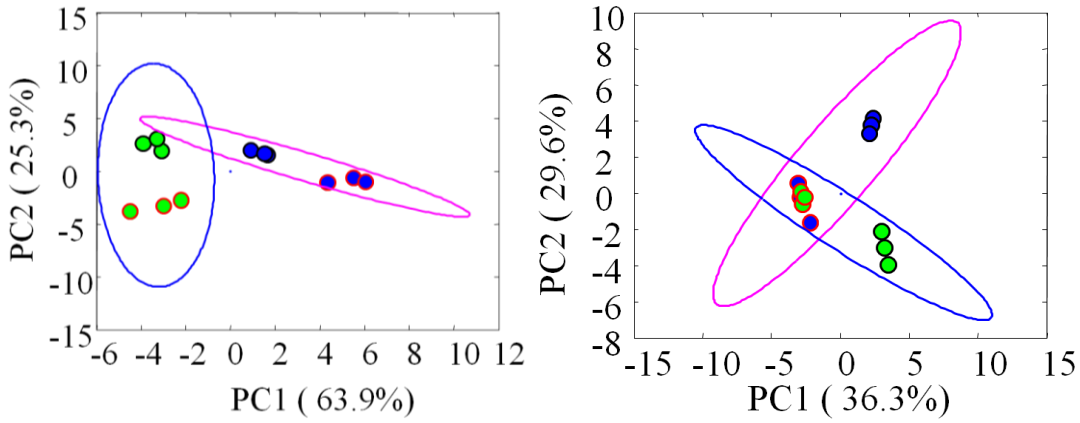

(c)

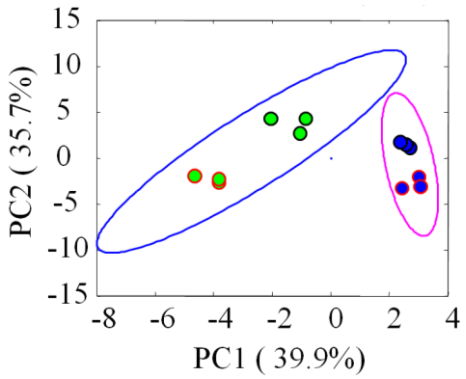

12 h HS - OA 24 h HS - OA 12 h Control - OA 24 h Control - OA

Fig S3 PCA scores of heat stress (HS) and control (C) for (a) old age (OA) rat 1 (b) old age (OA) rat 2 and (c) old age (OA) rat 3 during 0 – 12 and 12 – 24 hour. The data has been normalized according to the Z-score. 90% confidence ellipses show the clusters for control (pink line) and heat stress stress (blue line) cells

(a)

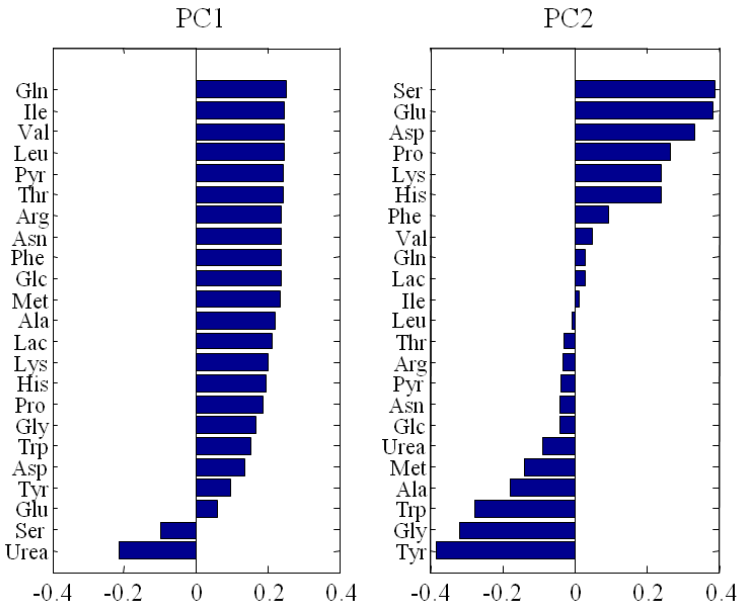
PC1
PC2
Gln
Ile
Val
Leu
Pyr
Thr
Arg
Asn
Phe
Glc
Met
Ala
Lac
Lys
His
Pro
Gly
Trp
Asp
Tyr
Glu
Ser
Urea
Ser
Glu
Asp
Pro
Lys
His
Phe
Val
Gln
Lac
Ile
Leu
Thr
Arg
Pyr
Asn
Glc
Urea
Met
Ala
Trp
Gly
Tyr
-0.4
-0.2
0
0.2
0.4

(b)

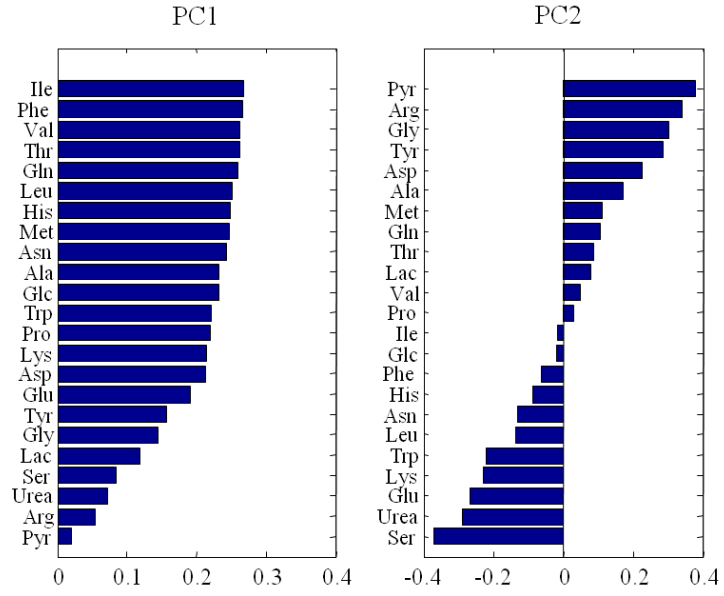
PC1
PC2
Ile
Phe
Val
Thr
Gln
Leu
His
Met
Asn
Ala
Glc
Trp
Pro
Lys
Asp
Glu
Tyr
Gly
Lac
Ser
Urea
Arg
Pyr
Pyr
Arg
Gly
Tyr
Asp
Ala
Met
Gln
Thr
Lac
Val
Pro
Ile
Glc
Phe
His
Asn
Leu
Trp
Lys
Glu
Urea
Ser
0
0.1
0.2
0.3
0.4
-0.4
-0.2
0
0.2
0.4

(c)

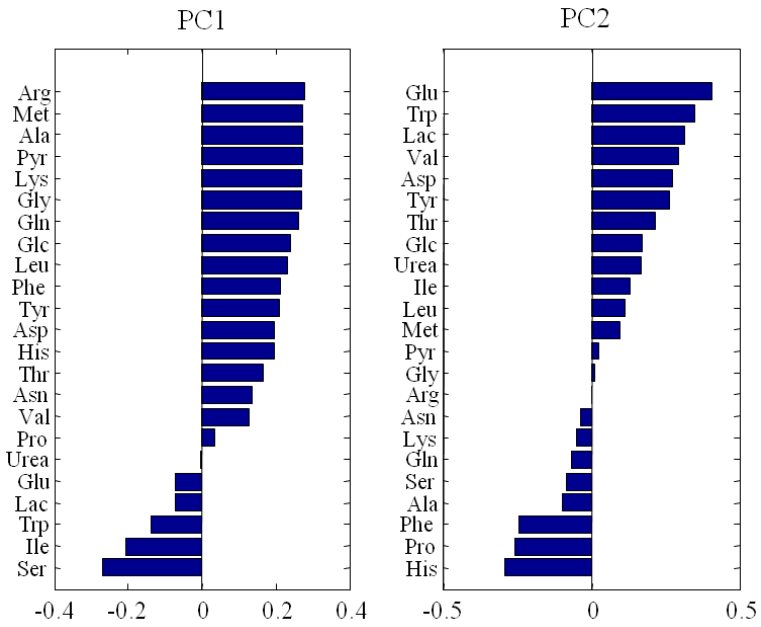

Fig S4: PC1 and PC2 loadings of metabolites at 0 – 12 h and 12 – 24 h for control and hydrogen peroxide stress old age PRH in (a) old age rat 1 (b) old age rat 2 (c) old age rat 3

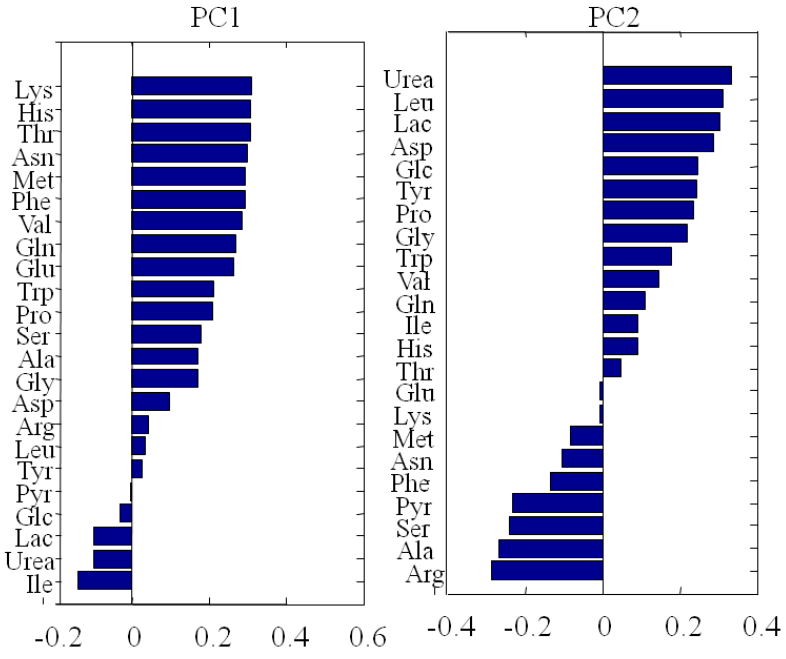

Fig S5: PC1 and PC2 loadings of metabolites at 0 – 12 h and 12 – 24 h for heat stress (HS) with and without quercetin (Q) middle age (MA) PRH.

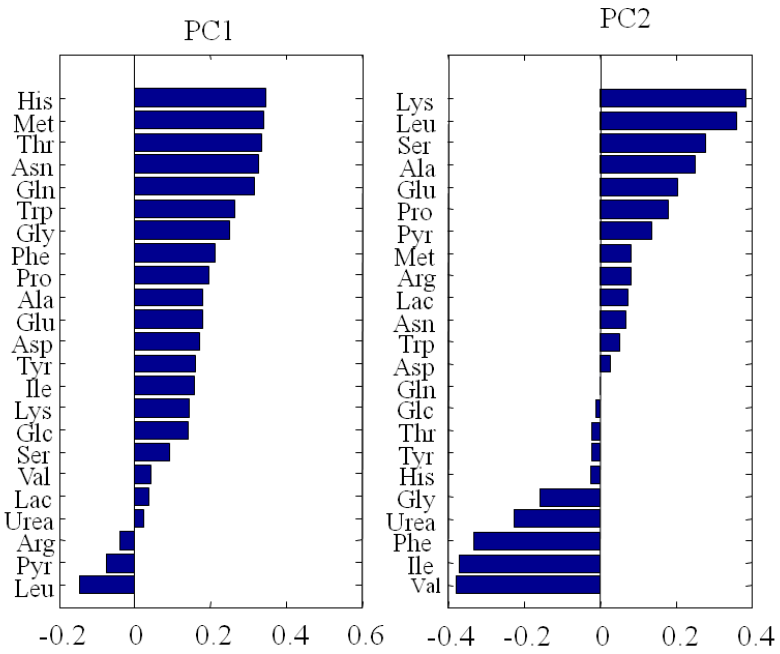

Fig S6: PC1 and PC2 loadings of metabolites at 0 – 12 h and 12 – 24 h for hydrogen peroxide stress (H_2O_2) with and without quercetin (Q) middle age (MA) PRH.

Table S8 Extracellular metabolite rates of 19 amino acids, glucose, lactate, pyruvate and urea measured in fmol / cell / h for Sprague Dawley (SD) middle age (MA) hepatocytes measured during 0 - 12 h (12 h) and 12 – 24 h (24 h). The values are given for experimental replicates from 2 rats (r1, r2, r3). One replicate for 12 – 24 h was removed as it was an outlier. Standard 3 letter code is used for amino acids.

	SD	SD	SD	SD	SD	SD	SD	SD	SD	SD	SD
	rat 1	rat 1	rat 1	rat 2	rat 2	rat 2	rat 1	rat 1	rat 2	rat 2	rat 2
	MA	MA	MA	MA	MA	MA	MA	MA	MA	MA	MA
Metabolites	12h	12h	12h	12h	12h	12h	24h	24h	24h	24h	24h
(fmol/cell/h)	r1	r2	r3	r1	r2	r3	r2	r3	r1	r2	r3
Asp	-3.6	-3.8	-4.0	-11.4	-16.3	-13.8	-4.6	-8.2	-4.8	-4.3	-3.9
Glu	30.7	22.6	28.6	44.8	44.0	43.3	46.2	44.3	57.2	63.0	68.7
Asn	-27.7	-25.4	-26.4	-27.3	-28.1	-22.4	-8.9	-10.9	-12.9	-12.4	-14.5
Ser	3.1	3.2	4.0	1.1	1.3	1.6	36.4	38.1	35.1	34.9	34.7
Gln	-182.7	-184.1	-175.4	-193.9	-176.6	-159.4	-47.3	-71.8	-56.2	-56.3	-56.3
His	-10.7	-10.8	-10.1	-5.9	-5.2	-4.6	-1.0	-1.0	-1.8	-2.0	-2.1
Gly	-134.0	-129.0	-131.5	-161.3	-147.4	-135.3	-121.7	-135.7	-166.5	-175.6	-184.6
Thr	-33.5	-33.9	-32.9	-28.4	-34.5	-31.5	-9.5	-9.5	-13.7	-14.7	-14.3
Arg	-151.7	-134.9	-145.6	-188.0	-188.7	-176.7	-175.0	-159.7	-179.5	-187.2	-195.0
Ala	-176.7	-159.3	-169.2	-312.0	-304.2	-308.1	-176.6	-192.1	-222.5	-233.0	-243.6
Tyr	-14.2	-14.3	-14.0	-29.2	-22.9	-23.1	-26.4	-31.5	-33.4	-36.3	-39.1
Val	2.8	2.3	1.8	0.6	0.6	0.6	5.2	5.5	8.2	8.7	9.1
Met	-21.2	-19.3	-20.1	-21.6	-21.0	-18.1	-10.2	-11.1	-16.8	-17.9	-19.0
Trp	-9.7	-9.6	-10.0	-2.9	-3.8	-2.3	-7.4	-8.7	-3.5	-3.5	-3.5
Phe	-34.7	-31.3	-33.7	-31.4	-28.3	-26.4	-10.8	-13.2	-22.2	-24.1	-25.9
Ile	-22.0	-24.8	-21.8	-7.6	-19.2	-13.4	11.5	7.4	2.4	3.0	3.5
Leu	10.8	10.5	10.1	16.0	19.6	23.2	9.8	10.3	30.9	32.3	33.7
Lys	-58.4	-56.8	-53.1	-58.7	-67.0	-50.1	14.6	11.1	-44.8	-45.2	-45.6
Pro	-42.0	-43.8	-45.6	-40.0	-44.6	-42.3	-13.4	-16.1	-20.6	-17.2	-24.1
Glc	386.7	300.2	343.5	296.2	331.3	313.7	324.8	324.8	237.3	207.1	222.2
Lac	242.6	233.1	242.1	440.5	436.4	449.4	298.9	323.6	331.0	370.4	350.7
Pyr	-65.6	-51.7	-56.1	-85.2	-99.5	-79.7	-99.5	-100.4	-89.6	-83.9	-97.3
Urea	540.4	474.0	509.2	800.0	736.1	761.7	720.6	746.0	705.4	742.2	723.8

Table S9 Extracellular metabolite rates of 19 amino acids, glucose, lactate, pyruvate and urea measured in fmol / cell / h for Wistar (W) middle age (MA) hepatocytes measured during 0 - 12 h (12 h) and 12 – 24 h (24 h). The values are given for experimental replicates from 2 rats (r1, r2, r3). Standard 3 letter code is used for amino acids.

	W	W	W	W	W	W	W	W	W	W	W	W
	rat 1	rat 1	rat 1	rat 2	rat 2	rat 2	rat 1	rat 1	rat 1	rat 2	rat 2	rat 2
	MA	MA	MA	MA	MA	MA	MA	MA	MA	MA	MA	MA
Metabolites	12h	12h	12h	12h	12h	12h	24h	24h	24h	24h	24h	24h
(fmol/cell/h)	r1	r2	r3	r1	r2	r3	r1	r2	r3	r1	r2	r3
Asp	-4.2	-3.5	-5.0	-1.8	-1.7	-1.8	-6.7	-4.7	-5.7	-4.5	-5.2	-4.9
Glu	11.6	15.0	13.3	28.9	28.0	28.1	10.9	11.6	11.2	55.3	55.1	55.5
Asn	-8.8	-8.7	-8.9	-14.0	-15.4	-15.7	-5.2	-4.0	-4.6	-16.6	-15.3	-12.9
Ser	-2.2	-2.0	-1.7	-1.2	-1.4	-1.8	6.3	5.4	5.9	8.6	8.7	8.5
Gln	-74.3	-68.9	-79.6	-67.2	-71.0	-66.1	-55.6	-39.7	-47.6	-57.5	-51.8	-46.2
His	-2.7	-2.4	-3.0	-1.0	-0.9	-1.1	-1.8	-0.9	-1.3	-1.4	-1.5	-1.5
Gly	-44.8	-45.3	-44.4	-45.2	-41.1	-42.0	-55.2	-44.9	-50.1	-84.0	-89.6	-78.3
Thr	-7.5	-6.4	-8.6	-7.6	-7.0	-6.5	-7.9	-5.2	-6.6	-15.5	-14.8	-10.3
Arg	-63.6	-67.5	-59.7	-104.7	-104.7	-107.5	-67.5	-54.8	-61.2	-83.5	-87.6	-79.4
Ala	-134.3	-100.8	-117.5	-177.4	-182.8	-186.8	-72.1	-61.7	-66.9	-249.4	-206.7	-228.1
Tyr	-6.5	-5.9	-7.2	-8.6	-6.6	-7.8	-9.7	-6.2	-7.9	-17.8	-19.0	-16.6
Val	-10.0	-7.7	-5.5	-2.2	-1.0	-1.6	-5.5	-2.7	-4.1	-1.3	-4.9	-3.1
Met	-8.6	-8.7	-8.5	-7.3	-8.2	-8.5	-6.9	-5.9	-6.4	-13.9	-11.4	-10.3
Trp	-1.6	-1.5	-1.7	-0.8	-0.7	-0.9	-1.3	-0.8	-1.1	-0.8	-0.9	-0.9
Phe	-9.1	-9.0	-9.3	-9.8	-8.6	-10.5	-7.9	-5.3	-6.6	-12.1	-12.6	-11.6
Ile	-10.1	-8.0	-5.9	-0.6	-0.9	-0.2	-5.5	-2.6	-4.0	-2.6	-7.1	-4.9
Leu	-16.8	-13.4	-10.1	-1.7	-2.1	-1.3	-8.5	-4.3	-6.4	-5.5	-3.9	-2.3
Lys	-28.9	-27.8	-30.1	-4.8	-3.2	-6.5	-12.2	-7.5	-9.8	-21.4	-21.5	-21.4
Pro	-9.2	-8.6	-8.0	-19.5	-12.1	-13.2	-10.7	-10.5	-10.6	-29.7	-22.7	-21.1
Glc	124.1	102.5	99.3	187.0	62.5	121.0	94.9	35.2	65.0	174.6	182.5	178.5
Lac	265.2	219.2	198.6	187.0	189.1	171.4	221.5	167.3	180.5	393.6	293.9	285.2
Pyr	-39.5	-32.6	-29.0	-12.5	-13.1	-13.1	-36.9	-30.8	-34.2	-5.3	-4.3	-4.1
Urea	290.9	232.4	205.0	300.0	311.6	314.1	186.7	166.4	149.0	485.2	382.9	385.8

Table S10 Extracellular metabolite rates of 19 amino acids, glucose, lactate, pyruvate and urea measured in fmol / cell / h for Sprague Dawley (SD) old age (OA) hepatocytes measured during 0 - 12 h (12 h) and 12 – 24 h (24 h). The values are given for experimental replicates from 2 rats (r1, r2, r3). Standard 3 letter code is used for amino acids.

	SD	SD	SD	SD	SD	SD	SD	SD	SD	SD	SD	SD
	rat 1	rat 1	rat 1	rat 2	rat 2	rat 2	rat 1	rat 1	rat 1	rat 2	rat 2	rat 2
	OA	OA	OA	OA	OA	OA	OA	OA	OA	OA	OA	OA
Metabolites	12h	12h	12h	12h	12h	12h	24h	24h	24h	24h	24h	24h
(fmol/cell/h)	r1	r2	r3	r1	r2	r3	r1	r2	r3	r1	r2	r3
Asp	-3.6	-2.6	-1.5	-3.4	-3.4	-3.4	-6.0	-5.0	-7.0	-2.2	-2.0	-2.1
Glu	34.6	32.3	29.9	49.0	47.3	45.5	44.5	48.4	40.7	43.1	44.8	43.9
Asn	-21.6	-19.6	-17.6	-15.4	-21.3	-18.4	-10.8	-13.3	-12.9	-12.5	-12.0	-11.3
Ser	15.5	14.4	13.3	22.4	28.3	34.2	35.6	34.5	35.1	36.1	38.8	39.8
Gln	-84.8	-84.8	-84.8	-34.9	-31.3	-27.7	-94.7	-85.1	-104.3	-85.2	-75.2	-83.3
His	-11.9	-10.9	-9.8	-5.9	-7.0	-8.1	-4.9	-5.9	-5.5	-7.6	-6.7	-7.2
Gly	-120.4	-110.5	-100.7	-108.0	-93.1	-78.3	-121.7	-110.4	-109.1	-143.6	-143.4	-144.3
Thr	-6.4	-5.6	-4.9	-8.1	-8.1	-8.1	-5.0	-5.0	-5.0	2.5	3.2	2.9
Arg	-225.1	-199.8	-172.7	-168.3	-179.0	-173.6	-234.8	-228.9	-206.8	-183.3	-186.9	-185.9
Ala	-193.4	-144.6	-161.1	-154.1	-148.5	-142.8	-169.9	-167.4	-172.3	-169.4	-171.1	-171.1
Tyr	-25.4	-23.3	-21.2	-12.2	-12.2	-12.2	-21.5	-25.4	-25.0	-12.3	-12.7	-11.9
Val	-3.1	-2.3	-1.5	-20.3	-51.9	-36.1	-2.6	-2.6	-2.6	-32.3	-30.6	-28.3
Met	-15.7	-14.5	-13.2	-13.6	-17.6	-15.6	-11.9	-13.9	-13.6	-15.9	-15.7	-16.0
Trp	-5.1	-4.8	-4.4	-2.2	-2.2	-2.2	-3.1	-2.9	-3.2	-0.2	-0.2	-0.2
Phe	-28.8	-26.6	-24.3	-17.8	-24.8	-21.3	-19.8	-22.7	-22.4	-22.8	-22.1	-22.0
Ile	0.9	1.2	1.6	5.8	6.3	6.0	13.9	7.1	10.5	4.6	5.2	5.9
Leu	37.1	32.0	26.9	65.3	71.8	78.4	59.0	48.1	53.5	41.4	46.1	45.8
Lys	-31.0	-30.1	-29.2	-6.1	-32.2	-19.1	-4.3	-5.4	-4.9	-17.2	-15.8	-17.3
Pro	-9.6	-8.9	-8.2	-9.0	-9.6	-10.3	11.6	36.2	23.9	67.0	65.6	66.3
Glc	669.2	416.0	542.6	700.8	660.7	680.7	814.9	328.2	571.5	213.6	198.9	206.3
Lac	865.4	820.0	723.1	483.1	498.4	429.6	743.1	705.8	630.3	395.8	418.9	418.7
Pyr	-106.9	-95.6	-79.8	-62.7	-67.5	-55.6	-118.8	-119.0	-131.0	-72.3	-78.3	-77.9
Urea	631.1	525.2	454.9	555.0	502.6	513.7	568.6	659.8	485.2	487.7	459.2	433.7

Table S11 Extracellular metabolite rates of 19 amino acids, glucose, lactate, pyruvate and urea measured in fmol / cell / h for Wistar (W) old age (OA) hepatocytes measured during 0 - 12 h (12 h) and 12 – 24 h (24 h). The values are given for experimental replicates from 2 rats (r1, r2, r3). Standard 3 letter code is used for amino acids.

	W	W	W	W	W	W	W	W	W	W	W	W
	rat 1	rat 1	rat 1	rat 2	rat 2	rat 2	rat 1	rat 1	rat 1	rat 2	rat 2	rat 2
	OA	OA	OA	OA	OA	OA	OA	OA	OA	OA	OA	OA
Metabolites	12h	12h	12h	12h	12h	12h	24h	24h	24h	24h	24h	24h
(fmol/cell/h)	r1	r2	r3	r1	r2	r3	r1	r2	r3	r1	r2	r3
Asp	-10.8	-10.8	-13.7	-3.6	-3.5	-4.1	-9.8	-9.8	-9.2	-3.7	-3.7	-2.3
Glu	-10.5	-13.4	-14.7	10.6	11.7	10.3	-12.5	-13.0	-11.7	14.5	13.6	15.4
Asn	-8.8	-9.4	-9.1	-10.4	-10.9	-10.8	-7.2	-6.7	-7.0	-6.9	-7.8	-7.3
Ser	4.5	3.3	3.9	7.1	7.0	6.6	12.6	12.7	12.7	28.4	25.1	25.4
Gln	-142.1	-123.0	-161.3	-58.6	-60.3	-63.9	-122.9	-113.2	-123.8	-29.8	-38.5	-27.5
His	-7.1	-7.1	-7.1	-2.9	-3.0	-3.4	-6.7	-6.5	-6.5	-1.5	-1.8	-1.5
Gly	-45.0	-49.6	-47.3	-52.6	-50.7	-50.8	-59.5	-58.4	-57.4	-93.4	-88.0	-83.9
Thr	-17.8	-13.9	-15.8	-4.3	-4.2	-4.9	-11.8	-14.2	-12.1	-2.5	-3.2	-1.5
Arg	-78.8	-84.7	-81.7	-54.3	-55.9	-55.7	-97.4	-98.6	-99.7	-85.8	-80.6	-79.2
Ala	-66.1	-74.8	-70.4	-94.5	-97.4	-96.8	-74.6	-65.5	-75.4	-91.5	-96.2	-93.2
Tyr	-20.2	-22.4	-21.3	-3.6	-2.9	-3.6	-21.6	-18.7	-20.9	-8.4	-7.3	-5.5
Val	-17.6	-18.9	-18.3	-1.8	-1.3	-1.6	-17.6	-17.6	-17.4	-0.8	-1.5	-1.1
Met	-6.4	-7.3	-6.9	-7.6	-7.6	-7.8	-7.9	-6.6	-7.7	-9.7	-9.6	-9.2
Trp	-3.1	-3.6	-3.3	-1.2	-1.1	-1.1	-3.4	-3.0	-3.3	-0.6	-0.5	-0.6
Phe	-15.3	-16.4	-15.9	-4.4	-4.0	-4.7	-17.1	-14.1	-16.4	-5.9	-5.1	-4.4
Ile	-16.1	-18.4	-17.3	-1.4	-1.1	-1.9	-18.3	-17.8	-17.6	-0.3	-0.9	-0.6
Leu	-28.1	-25.6	-30.5	-3.3	-2.7	-3.7	-25.3	-23.7	-24.4	-2.4	-3.4	-2.9
Lys	-34.4	-41.5	-58.1	-2.9	-0.9	-1.9	-39.9	-37.0	-35.6	-2.9	-1.9	-2.4
Pro	2.6	3.4	3.0	-8.0	-5.8	-8.7	2.8	4.5	1.1	-5.9	-6.3	-4.3
Glc	14.2	152.9	83.6	81.9	40.2	44.0	-157.0	-112.0	-173.8	-65.3	-72.3	-68.8
Lac	383.0	423.9	423.9	202.4	199.3	182.0	279.4	215.1	266.1	227.4	211.8	224.1
Pyr	-18.6	-20.9	-36.6	-4.7	-5.5	-4.9	-30.2	-24.8	-31.9	-7.3	-7.0	-7.6
Urea	139.2	140.3	217.7	177.7	186.9	199.6	131.7	127.3	152.0	228.2	219.0	211.9

Poster Presentations

- Age-dependent differences in the metabolome of primary rat hepatocytes. **Richa Garg**, Elmar Heinzle and Fozia Noor. Systems Biology of Human Diseases conference (SBHD) in Heidelberg (June 12 – 14, 2013).

- Effect of heat stress on primary rat hepatocytes from middle age and old age rats**.** **Richa Garg**, Sophia Bongard, Anne Bonin, Jens Niklas, Julia Prizibilla, Ursula Mueller-Vieira, Elmar Heinzle and Fozia Noor. Systems Biology of Mammalian cells (SBMC) in Berlin (May 12 – May 14, 2014).

- Primary rat hepatocytes of different age show only few changes in metabolic flux distribution. **Richa Garg**, Sophia Bongard, Anne Bonin, Jens Niklas, Julia Prizibilla, Ursula Mueller-Vieira, Elmar Heinzle and Fozia Noor. International conferences of Systems Biology (ICSB), in Melbourne, Australia (September 14 – 18, 2014)

Publications

- Fluorescence based cell counting in collagen monolayer cultures of primary hepatocytes.
  Priesnitz, C., Sperber, S., **Garg R.,** Orsini, M. and Noor, F. *Cytotechnology*, 2014

- Hepatocytes of Wistar and Sprague Dawley rats differ significantly in their central metabolism
  Garg, R., Noor, F., Heinzle, E. *J Cellular Biochem*, DOI: 10.1002/jcb.26255

- Comparison of oxidative stress effects in primary rat hepatocytes from 6 and 24 month old rats
  Garg, R., Noor, F., Heinzle, E. (Manuscript in preparation)